

**Development of A closed Loop Control System for Vibration
Assisted Grinding**

HEISUM EWAD

**A thesis Submitted in Partial Fulfilment of the Requirement of Liverpool
John Moores University for the Degree of Doctor of Philosophy**

November 2015

Abstract

Increasing demand for components made of hard and brittle materials such as glasses, steel alloys and advanced ceramics is such that conventional grinding and polishing techniques can no longer meet the requirements of today's precision manufacturing community.

However, it is essential and much needed to undertake such processes based on a scientific approach, i.e. the process to be quantitatively controlled and optimized rather than carried out in a trial-and-error manner.

Vibration assisted machining has been demonstrated to reduce the amount of forces, pattern definition on a finished surface. Axial oscillation (parallel to the wheel axis) allows the grains to cut with two more faces. With vibration in two directions, the wheel exposes four times more cutting edges (two edges per oscillation) than in continuous cutting which uses only one edge, which is a great advantage over continuous cutting, Axial oscillation induces an elliptic motion leading to a lapping process, which improves the cutting efficiency as well as the quality of the finished surface. Oscillation greatly reduces the load per grain, reduces wheel wear and induces a chip-breaking effect, which is a great advantage for prevention of wheel loading.

In this research, theory modelling and instrumentation for vibration assisted grinding are presented and discussed in depth. The modelling is focused on control of the amplitude of oscillation in the cutting zone which is the fulcrum of this investigation. The control system was developed using Labview 8.5 and Matlab.

It was found that the application of vibration reduces the forces, increases the material removal rate and increases the G-Ratio compared to conventional grinding. The superimposition of vibration in axial direction secured better process outcomes in terms of grinding forces (average 25% improvement), surface finish quality and power consumption. In terms of frequencies it was identified that superimposing vibration at 100 Hz in this study provided the lowest forces. In addition, it was shown that at 100 Hz the desired amplitude of oscillation was achieved at the lowest driving voltage, i.e. 4V.

Comparing the techniques of control systems, which were open loop, closed loop and conventional grinding, applying vibration always gave better results than with no vibration. The closed loop control in most cases was the best. Comparing oscillating in axial direction and tangential direction, the Axial gave on additional 9% reduction in grinding forces. In general the grinding with vibration assisted secured a greater depth of cut. The oscillating in Axial direction provided an additional 16 % in actual depth of cut, so Applying oscillating in axial direction showed that a significant improvement of quality could be achieved.

Acknowledgements

I would like to express my thankfulness to my Director of Studies, Dr Andre D. L. Batako for his appreciated advice, guidance, support, motivation and encouragement in developing research successfully, and research supervisor who have given me hope and accepted me under his supervision Dr. Ahmad Abass from Liverpool university, and my special thanks go to Professor Xun Chen and Professor Dingle-Li Yu.

Moreover, I would like to thanks my family. Specially my mother and my wife and brother and also my son Mohamad and two daughter Maab and Malaz,

Exceptional thanks to Mr Peter Moran for his support for helping in my experiment,

Nevertheless, I'm also grateful to Liverpool John Moores University represented by staff in general.

Finally, my heart and mind go to my beloved Country Sudan in this difficult time hopping that peace and development would sooner prevail, and peace surrounding all over the world.

Nomenclature

Symbol	Meaning	Units
a	Applied depth of cut	m
a_e	Real depth of cut	m
b_s	Grinding width	m
b_w	Contact width	m
C_s	Spindle compliance	m/N
d_e	Mean diameter of wheel	m
e_c	Specific energy	J/mm ³
$F(t)$	Excitation force	N
F'_n	Specific normal force	N/mm
F'_t	Specific tangential force	N/mm
F_n	Normal grinding force	N
F_t	Tangential grinding force	N
F_a	Force Across wheel Width	N/m
K	stiffness	N/m
l_g	Geometric contact length	m
m	Mass	Kg
P	Grinding power	W
Q	Material removal rate	m ³ /s
Q'	Specific material removal rate	m ³ /s
R_a	Surface roughness	m
V_s	Wheel speed	m/s
V_w	Work speed	mm/s
μ	Coefficient of grinding	-

Abbreviations

ARMAX	Auto Regressive Moving eXogenous
ARX	Auto Regressive eXogenous
AC	Alternating Current
B(s)	Primary Feedback Signal
C(s)	Control Output
CBN	Cubic Boron Nitride
DAQ	Data Acquisition
DC	Direct Current
DDS	Dynamic Data System
DOE	Design Of Experimental
E(s)	Actual Signal
FEM	Finite Element Method
FRF	Frequency Response Function
Gc	Transfer function
HRC	Hardness Rockwell Cone
ID	Internal Diameter
Kp	Proportional Gain
Kd	Derivative Gain
Ki	Integral Gain
KD	Derivative Controller
Ki	Integral Controller
LDVT	Linear different variable transformer
MIMO	Multi Input Multi Output

Abbreviations

Mp	Maximum Peak
NI	National Instrument
OD	Outer Diameter
PID	Proportional- Integral- Derivative
PI	Proportional Integral
PD	Proportional Derivative
PI	Physik Instrument
PZT	Piezoelectric Lead Zirconate Titanate
PRBS	Pseudorandom Binary Sequence
R(s)	Reference Input
RPM	Revolution Per Minute
SISO	Single Input Single Output
tp	Peak time
ts	Setting time
tr	Rise time
Tp1	Compensated system
Tp2	uncompensated system
Ti	Integral time
Tp1	Compensated system
Td	Derivative Time
UAG	Ultrasonic Assisted Grinding
U(s)	Disturbance
VAM	Vibration assisted machine
VI	Virtual Instruments

Table of Contents

Abstract	I
Acknowledgement	III
Nomenclature	IV
Abbreviations	V
List of Figures	XIII
List of Table	VXII
Chapter 1: Introduction	
1.1 Introduction	1-2
1.2 Novelty of the Grinding in General	1-4
1.3 Research Aim	1-5
1.3.1 Research Objectives	1-5
1.4 Thesis Outline	1-6
Chapter 2: Literature Review	
2.1 Introduction	2-2
2.2 Overview of Vibration Assisted Grinding	2-3
2.3 Advance Grinding Methods	2-12
2.4 Problems in Grinding	2-13
2.5 Styles of Grinding	2-14
Chapter 3: Control Engineering Background	
3.1 Introduction	3.2
3.13 Controller Design	3-20
3.14 Experimental Validation	3-21
3.15 Main Experiments	3-21
3.16 Excitation	3-22
3.17 Data Examination	3.22
3.18 Design of Experiments	3.23

Chapter 4: Equipment

4.1 Introduction	4-2
4.2 Abwood 5025 grinding machine	4-2
4.3 The Oscillating Stage	4-3
4.4 Piezoelectric Actuators	4-4
4.4.1 Features of Piezoelectric Actuators	4-4
4.5 Identification of Suitable Displacement Sensor	4.6
4.6 Power Amplifier	4-8
4.7 Accelerometer	4-8
4.8 Data Acquisition	4-9
4.8.1 Data Acquisition Hardware (DAQ)	4-9
4.8.2 Output DAQ NI9263	4-10
4.9 Kistler Charge Amplifier Type 5073	4-11
4.10 Force Measurement Using the Dynamometer	4-11
4.11 The Force Results	4-12
4.12 Grinding Wheel	4-14
4.12.1 The Main Components of Grinding Wheel	4-14
4.13 Function Generator	4-15
4.14 Brukker GTK surface texture system	4-16
4.14.1 Superior imaging and resolution	4-16
4.15 Work Piece Materials	4-17
4.16 Software	4-18
4.17 Identification of Optimum Driving Voltage and Frequency	4-18
4.18 Remarks	4-20

Chapter 5: Grinding Wheel Head Response

5.1 Introduction	5-2
5.2 Spindle unit Static stiffness and Compliance	5-5
5.3 Natural Frequency of the Spindle Unit	5-8
5.4 Dynamic Stiffness of the Spindle Unit	5-10
5.5 Frequency Response of the Spindle Unit – Rotating Mode	5-11
5.6 Observation	5-12

Chapter 6: Controller Design

6.1 Introduction of mathematical Model	6-2
6.2 Mathematical Model for Oscillating Jig	6-3
6.3 Design of Controller	6-4
6.4 Modelling & Simulation	6-5
6.5 Simulation and Analysis the Model with the PID Controller	6-6
6.6 The Experimental System	6-7
6.7 The Labview Code	6-8
6.8 Basic Idea and Design Consideration	6-9
6.9 Experimental Implementation	6-9
6.9.1 Model Identification from the Data	6-9
6.9.2 Validation Result	6-10
6.10 Experimental Result	6-12

Chapter 7: Preliminary Studies

7.1 Introduction	7-2
7.2 Experimental Configuration	7-2
7.3 experimental Setup	7-4
7.4 Results	7-6
7.4.1 Process Performance as Function of Frequency	7-7
7.4.2 Conventional grinding and Vibration Assistance	7-9
7.4.3 Grinding Force Ratio	7-13
7.4.4 Surface Roughness	7-14
7.4.5 Specific Grinding Energy	7-16
7.5 Remarks	7-17

Chapter 8: Effect of Vibration Grinding Process

8.1 Introduction	8-2
8.2 Vibration Frequency Effect	8-2
8.3 Result of all Forces	8-4

Table of Contents

8.4 Normal and Tangential Forces	8-8
8.5 Grinding Power	8-11
8.6 Specific Grinding Energy	8-12
8.7 Surface Roughness	8-13
8.8 Grinding Coefficient	8-14
8.9 Remarks	8-15

Chapter 9: Performance of the developed controller

9.1 Introduction	9-2
9.2 Grinding Forces	9-3
9.3 Surface Roughness	9-6
9.4 Performance of the Developed Controller	9-7
9.5 Surface Roughness	9-8
9.6 Specific Grinding	9-10
9.7 Remarks	9-12

Chapter 10: Discussion and Conclusion

10.1 Discussion	10-2
10.2 Conclusion	10-5
10.3 Recommendation for Future Work	10-7

References

Appendices

A-B-C-D-E-F-G-H

List of Figures

Figure 2.1: Micro-Vibration Device	2-7
Figure 2.2: Fraunhofer servo design	2-8
Figure 2. 3: First Concept Vibrating System Configuration	2-13
Figure 2.4: Surface Grinding	2-14
Figure 2.5: Outer- Diameter	2-15
Figure 2.6: ID Grinding	2-15
Figure 3. 1: Control Design	3-5
Figure 3.2: Functional Block Diagram of an Open-Loop Control System	3-7
Figure 3.3: System Set up In Open Loop Control	3-7
Figure 3.4: Control System with PD/PI/PID Controller	3-10
Figure 3.5: Flow Chart illustrating the System Identification Process	3-14
Figure 3.6: Identification Signal	3-20
Figure 3.7: Estimation & Validation Data Set for Vibration System	3-22
Figure 4.1: Abwood Surface Grinding Machine Tool	4-3
Figure 4.2: Self Contained Vibration System	4-4
Figure 4.3: Piezoelectric Actuator	4-5
Figure 4.4: Response of the LDVT Sensor in Static Mode	4-6
Figure 4.5: Displacement Sensors Response	4-7
Figure 4.6: Input NI 9215 DAQ, Input DAQ NI 9233	4-10
Figure 4.7: Output NI 9263 DAQ	4-10
Figure 4.8: Experimental Calibration Setup	4-12
Figure 4.9: Force Response in Tangential Direction (X-Axis)	4-13
Figure 4.10: Force Response in Normal Direction (Y-Axis)	4-13
Figure 4.11: Force Response in Axial Direction Z-Axis	4-13
Figure 4.17: Work Piece Materials	4-17
Figure 4.18: Displacement envelop	4-20

Figure 5.1: Set-Up for Measuring the Static Stiffness	5-7
Figure 5.2: Static Stiffness of the Spindle Unit	5-8
Figure 5.3: Experimental Configuration for Sweep-Sine Test	5-9
Figure 5.4: Frequency-Amplitude Characteristics	5-9
Figure 5.5: Dynamic Stiffness of the Spindle Unit	5-10
Figure 5.6: Dynamic Compliance of the Spindle Unit	5-11
Figure 5.7: Frequency Response of the Wheel	5-12
Figure 6.1: Flow Chart Illustrating the System Controlling Strategy	6-2
Figure 6.2a: Applying Open Loop Control Strategy	6-5
Figure 6.2b: Result of Applying Open Loop Control Strategy	6-5
Figure 6.3a: Applying Closed Loop Control Strategy System Identification	6-6
Figure 6.3b: Result of Applying Closed Loop Control Strategy System Identification	6-7
Figure 6.4: Code from the Labview	6-8
Figure 6.5: Front Panel of Data Acquisition in Labview	6-8
Figure 6.6: Time Domain Representation	6-10
Figure 6.7: The Input and the Output Signals	6-10
Figure 6.8: Model Parameter	6-11
Figure 6.9: Validation	6-12
Figure 6.10: PI Controller Selection from Parameter Space	6-13
Figure 7.1: Experimental Configuration.	7-2
Figure 7.2: Experimental Setup	7-3
Figure 7.3: Experimental Configuration	7-3
Figure 7.4: Actual Experimental Setup	7-4
Figure 7.5: Typical Cutting Forces	7-5
Figure 7.6: Actual depth of Cut	7-8
Figure 7.7: Cutting Forces A) Tangential (F_t); b) Normal (F_n)	7-8
Figure 7.8a: Hard Steel as a Function of Depth of Cut at 100Hz	7-10
Figure 7.8b: Hard Steel as a Function of Depth of Cut No Vibration	7-10
Figure 7.9a: Grinding Forces in Different Depth of Cut for Normal Forces	7-11
Figure 7.9b: Grinding in Different Depth of Cut for Tangential Forces	7-11

Figure 7.10a: Specific Normal Force	7-12
Figure 7.10b: Specific Tangential Force	7-13
Figure 7.11: Grinding Force Ratio	7-14
Figure 7.12: Surface Roughness	7-14
Figure 7.13: Power Consumption- Preliminary Studies	7-15
Figure 7.14: Specific Grinding Energies	7-16
Figure 8.1: Vibration Frequency Effect: a) -Normal; b) – Tangential	8-3
Figure 8.2: Schematic Representation of Grit Motion	8-4
Figure 8.3: Grinding Forces for Hard Steel:	8-5
Figure 8.4: Grinding Forces for Soft Steel:	8-6
Figure 8.5: System Response under Actual Grinding	8-8
Figure 8.6: Grinding Force For Hard Steel	8-9
Figure 8.7: Grinding Forces for Soft Steel:	8-10
Figure 8.8: Power Consumption: a) – Hard Steel; b) – Soft Steel	8-11
Figure 8.9: Specific Grinding Energy: a) – Hard Steel; b) – Soft Steel	8-12
Figure 8.10: Surface Roughness: a) – Hard Steel; b) – Soft Steel	8-13
Figure 8.11: Grinding Force Ratio: a) – Hard Steel; b) – Soft Steel	8-14
Figure 9.1: Normal Forces in Axial and Tangential	9-4
Figure 9.2: Tangential Forces in Axial and Tangential	9-4
Figure 9.3: Preliminary Experiment Actual Depth of Cut	9-5
Figure 9.4: Surface Roughness for Mild Steel in Open Loop	9-6
Figure 9.5: Normal Force for Hard Steel	9-7
Figure 9.6: Tangential Force for Hard Steel	9-8
Figure 9.7: Surface Roughness a) Mild Steel b) Hard Steel	9-9
Figure 9.8: Specific Energy in Hard Steel	9-10
Figure 9.8b: Specific Energy in Mild Steel	9-10
Figure 9.9a: Specific Energy in Mild Steel	9-11
Figure 9.9b: Specific Energy in Hard Steel	9-11

List of Tables

Table 3.1: Description of System Performance Parameter	3-9
Table 3.2: Function of PD, PI and PID Controller	3-12
Table 4.1: Specification of – Abwood 5025 Machine	4-2
Table 4.2: Specification of Piezoelectric Actuators Type P212.8	4-5
Table 4.3: Specification of Power Amplifier E-472.2	4-8
Table 4.4: Accelerometer Specification Kistler 8704B100	4-9
Table 4.5: Important Characteristic for Input NI 9233 DAQ and NI 9215	4-10
Table 4.6: Important Characteristic for Output NI 9263 DAQ	4-10
Table 4.7: Important Characteristic Kistler Charge Amplifier Type 5073	4-11
Table 4.8: Specification for the Function Generator	4-15
Table 4.9: Specification for Brukker GTK surface texture system	4-16
Table 4.10: Measured Hardness of Work piece Materials	4-17
Table 5.1: Recorded Amplitude	4-19
Table 7.1: Grinding Parameters for Experimental Studies	7-6
Table 8.1: Grinding Parameter for Experimental Studies	8-2
Table 11.1 Preliminary Experiment-Grinding Parameters	9-3

|

Chapter 1
INTRODUCTION

1. 1 Introduction

Grinding is known as one of the most environmentally hostile manufacturing processes, and usually is the last finishing operation to be complete on the workpiece and hence any deviations in quality such as geometrical error and surface finish cannot be passed onto the next operation (Walsh et al, 2004). Historically been considered a complex domain by the Manufacturing researchers and practitioners because of the complex domain (Palanna and Bukapatanam, 2002)

Manufacturing makes ever-increasing demands for higher machining speeds. This is particularly true in car and aircraft production but also for cutting tools. Abrasive machining processes cover a great part (20-25%) of all manufacturing processes. Vibration is used in various technological processes to improve the performance of the machines by exploiting intelligently the synergy of the oscillations. Classic examples are vibration conveyers, ultrasonic assisted turning of aerospace materials, ultrasonic grinding and vibro-impact drilling in offshore technology. Vibration provides several benefits for various technologies, such as manufacturing, medical, communications, transport, industries, etc. Vibration assisted machining techniques have recently become an attraction for many engineering applications. In machining processes, vibration can lead to improvements when applied in a controlled manner. Vibration assisted machining is a technique in which a certain frequency of vibration is applied to the cutting tool or the workpiece (besides the original relative motion between these two) to achieve better cutting performance (Shamoto et al, 2006). There are a number of different experimental setups to simplify the process, but the tendency is to give a wide range of machining processes for hard and brittle materials (Milos and Milutinovic, 2009).

However grinding technology does not generally exploit the positive aspects of superimposed vibration. The avoidance of vibration (chatter) is the main concern due to its effect on accuracy. However, chatter is a persisting problem regardless of the measures taken and a list of techniques is provided to reduce vibration in Marinescu (2005). A self-excited vibration that leads to an undulation of the cutting force, with subsequent uneven wear of the wheel, causes wheel-regenerative chatter.

Chapter1. Introduction

A possible solution to this type of chatter is to apply a periodic disengagement of the wheel from the workpiece, and periodic variation of the work speed, this has been reported to increase the grinding ratio up to 40% and the productivity up to 300%, by extending the time between wheel sharpening (Gallemaers et al, 1986).

The basic element of vibration assisted machining is the oscillation that can be generated using a series of methods; however, piezo-actuators are commonly used. Different designs of actuators have been developed for various applications such as vibration assisted turning, milling, drilling, grinding, and, recently, the combination of electric discharge micro-milling with vibration assisted machining has been reported (Brehl, 2008).

The fundamental feature of vibration assisted machining is that the tool face is separated from the workpiece repeatedly. This technique was first employed in the precision drilling of wood and low carbon steel (Cerniway, 2005).

There are a number of processes with vibration devices for cutting purposes using diamond tools. However, the existing vibration machining process does not effectively cut in to hard and brittle materials because of excessive wear of the diamond tool due to high chemical activity with iron (Bonifacio et al, 1994).

Chern et al (2006) applied vibration in ultra-precision micro drilling at higher frequencies and observed a direct effect on tool life with the amplitude having the highest influence on the interaction between the cutting tool and workpiece.

In vibration assisted machining, the intermittent gap during cutting was identified as an important mechanism in vibrational cutting. Increasing the vibration amplitude means an enlargement of the gap that allows cutting fluid to extract the heat from the cutting process. This enhances the tool's life and reduces production cost.

In Vibration Assisted machining, the following advantages were reported in processing hard-to-machine material. Considerable extended tool life was observed in diamond machining of CBN, cemented carbide tools and glass compared to conventional machining, (Shamoto and Moriwaki, 1999).

Weber et al, (1984) showed that 2D vibration provides longer tool life for the same machining configuration. Using superimposed vibration it is possible to machine

brittle materials as if they were ductile. This was reported by (Xiao, Sato and Karube, (2003) where in precision machining a small depth in the order of 1 μm was used. Parts machined with vibration assistance are burr free (Zhou, Eow, Ngoi and Lim, 2003).

Surface roughness in vibratory machining is better than the quality achieved by conventional machining and can reach the nanometres range depending on process configuration. In large part machining, the superimposed vibration secures a degree of precision with limited tool wear and provides surface roughness about 10 μm RMS with 1mm depth of cut (Shamoto et al, 2005).

In precision diamond turning Rubenach, (2003) achieved surface finishes in the range of 10-30 nm RMS, where Brehl and Dow (2006) reported some economical machining distances of hundreds to several thousand meters in hardened steels.

When depth of cut is kept to a small value and the frequency carefully controlled, many brittle materials are machined as if they were ductile, producing chips by means of plastic deformation and with minimal sub surface cracking (Xiao et al, 2003).

Tsiakoumis (2011) showed that the application of vibration to grinding improved the surface finish quality due to the lapping effect; a reduction of cutting force and reduction of grinding power; interrupted contact allowed for better coolant delivery over the entire contact zone with trapped coolant between successive oscillations which is impossible in continuous grinding and self-sharpening process because grains operate in two directions securing longer wheel life.

1. 2 Novel Approach to Grinding

In order to maintain process stability and precision, the vibration is introduced into the grinding process and needs to be monitored and controlled to achieve an optimum disengagement between the tool and a workpiece.

The required periodic disengagement of the tool from the workpiece and the variation of work speed lead to the subject of the current study. Most of the reported works do not control the actual amplitude of tool-workpiece disengagement. The magnitude of the oscillation is set at the actuator, however, the action of the cutting forces, the compliance and the damping in the system lead to reduced amplitudes of vibration

and at times to variable magnitudes. The intent of the work presented here is to control intelligently the superimposed oscillations to grinding technology more generally. This was achieved through a closed loop control of the vibration generators i.e. piezo- actuators. During the cutting process, machine tool structure dynamics, and a set of feedback from the interaction between the cutting process and structural dynamics were used as controlling parameters.

1. 3 Research Aim

The key aim of this project is to design, model and build a control piezo actuator in grinding operation. Here the control of the amplitude of oscillation in the actual cutting is the fulcrum of this investigation as it is the intrinsic parameter allowing controlled and prescribed motion to achieve efficiency and pattern generation on the machined surface. This programme of work will proceed through several stages as illustrated in the objectives.

1.3 1 Research Objectives

To achieve the aim of this programme of work, the investigation will progress through a series of tasks and objectives designed to facilitate an effective delivery of the project. The key objectives of this study are as follows:

- ❖ Study of control system and design of PID controllers.
- ❖ Data/signal acquisition and processing
 - Matlab / Simulink
 - Labview
- ❖ Initial Development of a controller for one axis - (phase & magnitude)
 - Analytical work/computer simulation – control axis with no load.
 - Acquire data in Labview and link to Matlab
 - Experimental work in controlling a real jig in machining condition.
- ❖ Implement control strategy within Matlab & Labview to control the jig.
- ❖ Full experimental work for grinding/milling

1.4 Anticipated Benefits of Vibration-Assisted Grinding

At this point, the hypothesis put forward is that the introduction of vibration should provide the following benefits:

- I. Reduction in cutting forces.
- II. Better coolant delivery over the entire contact zone. The periodic disengagement of the wheel and the workpiece allows the coolant to reach this critical zone.
- III. Better heat removal from the grinding zone.
- IV. The oscillations of the workpiece allow the grains to cut with more than one edge which can be beneficial to the shelf-sharpening process of the grinding wheel.
- V. Reduction of the load per grain and therefore, therefore reduced wheel wear.
- VI. Better surface finish due to lapping/polishing effect.

1.5 Thesis Outline

The work undertaken in this investigation is presented in thirteen chapters as follow,

Chapter 2

Presents the introduction, literature review of grinding process and especially the work of researchers on the subject of vibration assisted grinding, the main problems in grinding, types of grinding, and applying vibration to grinding.

Chapter 3

Gives the background of control systems, information about the Proportional-Integral-Derivative (PID) controller, objective of a control System, design and implementation of a control system, classification of control systems, types of Control system and some information about Control strategy and Time Domain Specification Definition. Describes the system identification process, the Objectives of System Identification, flowchart of the process and the steps undertaken to design the controller.

Chapter 4

Covers the equipment employed during the experimental work. This includes the Abwood 5025 grinding machine, the vibration system, Data Acquisitions, Piezo actuators, accelerometer, amplifier, workpiece material, Kistler dynamometer, grinding wheel, Function generator and the software used in this study. Introduces the calibration process, Calibration Setup, the force results for all three different axes, Displacement Response of different sensors, Frequency, voltage and Displacement response is also illustrated here.

Chapter 5

In chapter 5 the static and dynamic response of the machine tool is described along with its natural frequencies.

Chapter 6

Focuses on the design of the controller. This includes the mathematical model, Flow Chart illustrating, Modelling and Simulation. the Simulation Results and the response of the PID controller along with, the labview code and Experimental implementation, Collecting Data, and Phase Angle measurement is documented here.

Chapter 7

Presents the result of preliminary tests of the vibration assisted grinding process. This chapter describes the experimental configuration, Process Performance as Function of Frequency, the relationship between the three forces involved in axial vibration assisted grinding, Grinding force Ratio, the surface roughness, power consumption and specific grinding energy,

Chapter 8

Focuses on a new controller method for grinding control measurement and further utilized to experimentally investigate the surface roughness, energy and forces under dry and wet conditions.

Chapter 9

Introduces a closed loop method (PID). The model was develop better results in grinding. The effect of depth of cut and cooling conditions were investegated. It was further applied in the grinding experiments to estimate the energy and surface roughness, and comparing the result in Axial and tangential directions.

Chapter 10

Provides a detailed discussion of all the experimental work, and derives key conclusions and contribution to scientific knowledge and gives some recommendations for future work.

Chapter 2: LITERATURE REVIEW

2.1 Introduction

Precision metal cutting is defined as a cutting technique, which allows the manufacture of mechanical, electronic and optical components with micrometre from accuracy and surface roughness to within a very few micrometres (Ikawa, N., Dondson, R, 1991).

In an attempt to pass the material limitations of diamond machining, a new machining process called vibration assisted machining (VAM) has been developed. And started in early sixties when the technology achieved excellent performance in drilling wood. The hydrostatic bearing with its sub-micrometre rotational precision was the first component of accuracy metal cutting to advantage from the research drive. Along with the modification of conventional machine components (frames, metrology, spindle, metrology etc.).

Vibration assisted machining involves oscillating the diamond tool, bringing it into and out of contact with material in rapid succession. Vibration assisted machining can either be 1 dimensional (1D), oscillation in a single direction, or 2-dimensional (2D), a summation of two independent tool motions. Machining with diamond tool, whether turning or milling has proven itself as the manufacturing process that produces the highest quality surface finish, with the least amount of form error in the minimum amount of time. This new technique was one in which the cutting tool underwent a cyclic displacement independent to the x, y and z- axis displacement of the lathe's slide ways. This class of machining was referred to as vibration cutting. Early experiments were primarily carried out at frequencies greater than 20 KHz. And finally in early 90's, research into vibration cutting at both low and high frequency produced results sufficient for industrial applications (Moriwaki, T., Shamoto, E., 1991).

due to tool wear and the amount of force generated during conventional machine, diamond tools cannot be used on carbon containing materials such as steel and brittle materials such as silicates. Regardless of which manufacturing process is used, an additional polishing step is sometimes required to meet the ever increasing demand of industry of better surface finish and higher form accuracy, (Klocke, F and Rubenach, O, 1998).

Grinding is material removal processing in which the tool consists of hard abrasive particles contained in a bonded grinding wheel. Being a major manufacturing process, grinding accounts for about 20-25% of the total expenditure on machining operation in industrialized countries, Malkin and Stephen (1989). Grinding is often used as a finishing machining process which requires smooth surface and fine tolerances (Oberg, E and Franklin D, 2000).

The developing of precision metal cutting equipment in recent years has not only been focused on better surface finished, but also in expanding the manufacturing sphere of application. Machining of micro-scale parts is one such area. With the diminishing size and increasing complexity of audio/ visual products, the demand for high-presenting micro machining is only going to increase (Jung et al, 1999).

Companies not associated with aerospace or optical component are considering diamond turning to achieve garter performance. Diamond turning is a process that uses a precision ground diamond cutting implement mounted on a lathe capable of nanometre positioning to produce nearly error free shapes (with micrometre of desired) with high quality surface finishes (roughness on nanometres scale).

2.2 Overview of Vibration Assisted Grinding

It has been reported by Adachi et al, (1997) that, unlike ultrasonic vibration cutting low frequency vibration cutting has been found to prolong tool life and help reduce burr size in drilling. They developed an electro-hydraulic servo system to generate vibration of 1 KHz in spindle of an NC machine. Through their experimental studies on drilling aluminium, they found that burr size could be reduced considerably with the assistance of vibration in low frequency.

Moreover, in the case of light materials, the conventional diamond turning method cannot achieve precise surface finish Kim and Choi, (1997). Similarly, glass and ceramics require secondary finish processes such as polishing, grinding, honing and lapping for final finishing which increase the manufacturing time and cost and decrease the productivity (Shamoto et al, 1997)

Another very important consequence of vibration during grinding process is chatters. Mannan et al, (1999) presented a time domain model of plunge grinding operation and

Chapter 2: Literature Review

allowed for the effects of three models of vibration. The simulation result confirmed that torsion could be very significant. However, the torsion mode involving the workpiece showed that the build-up of vibration was affected but not stopped.

Syoji (1999) described very low wheel wear in grinding mild steel a speed of 200m/s or higher. Mild steel are difficult to grind material which usually wear the grinding wheel out at a rate of over 15 times higher than tool steel when ground with a CBN wheel at conventional speeds.

According to Bianchi et al, (1999) the grinding process is known as one of the most complex tooling processes, payable to the great number of variables complicated, while such process should be employed in finishing setups, in which good final excellence, low roughness errors of grinding wheel should always be reserved for costs of the process.

Wang et al, (2002) proved by their experiments they could cut hard and brittle materials in high critical depth of cut. By applying an ultrasonic diamond tool tip a surface roughness of 100nm was achieved.

The material cut was a fused silica with cutting conditions: vibration amplitude 4 μ m, vibration frequency 40 KHz, and spindle speed 90rpm, the principle of the developed vibration is based on the displacement curve of the tool tip through a cycle of vibration on the tool tip.

Due to the demand of machining small objects Kuriyagawa et al, (2002) developed a micro ultrasonic abrasive machining system. This system had an aerostatic vibration spindle, 3- axis NC sliding tables. Dynamometer for machining pressure control and on machining shaping system for small diameter tools, however, the use of smaller tool caused new problem such as tool wear and breakage and maintaining adequate supply of abrasive practices between the tool and the workpiece. In their test they developed an ultrasonic vibration spindle supported by an aerostatic bearing and minimizing eccentricity due to tool mounting error by shaping the tool on the machine. Applying a 25 KHz vibration frequency with 20 μ m tip amplitude and a 1000 rpm rotational speed, they managed to double the machining speed without increasing over time. In the conventional cutting method, these intractable materials almost always cause machining troubles such as chatter vibration, building-up-edge, shipping, and

Chapter 2: Literature Review

unusual and faster tool wear due to their hardness, brittle fractures on finished surface, high mechanical and chemical strength and poor thermal conductivity (Liu et al., 2002; Suzuki, et al 2007) which do not fulfil the main objectives of machining processes.

Previous studies have shown using one dimensional vibration assistance can extend tool life, lead to economic in machining, and also improvement in surface roughness compared to conventional machining (Wu et al, 2003).

However, two dimensional vibration assistance is much more effective, reliable and beneficial to the cutting process. The additional of vertical harmonic motion will bring the tool edge motion into a circle or ellipse that impose an up feed motion related to workpiece,

Experimental studies in previous research the tool forces in two dimensional vibration assistance are consistently small than one dimensional, even with the same tool geometry and machining conditions (Skelton, 1968).

Average tool forces were reduce to 20% by one dimensional machining and addition 2% more for two dimensional machining when compared with conventional machining.

Zhang's piezo was driven by a piezoelectric actuator embedded underneath the top platform of the table and elastic hinges were used to support the platform. The actuator had a maximum table displacement of 16 μ m at 5 KHz. The final results showed that with presence of vibration the normal grinding force was reduced as well as the surface roughness. These two variables increased with increase of depth of cut regardless of the vibration assistance. For example the grinding normal force reduced from 50 N to 25 N for 30 μ m depth of cut. This reduction in normal force also lead to improve surface integrity and reduced subsurface damage to ceramic materials since increase normal grinding force may initiate and propagate median cracks (Zhang and Meng, 2003).

Zhang and Miller (2003) examined the loading of the wheel by applying vibration at different frequencies with various amplitudes during dry grinding. They adopted a simple approach for quantifying wheel loading that utilized microscope images and analysis software. A microscope was used to capture wheel surface images along the wheel circumference. With the help of the software thy determined the percentage of chip loading.

Chapter 2: Literature Review

Suring Zahng and Millers experiment two different types of aluminium oxide wheel were used at different grinding conditions. The amplitude of vibration was set at 5 μ m while the frequency was increased from 500 Hz to 2 KHz. The depth of cut was set at 2 and 20 mm while the feed rate was set at 65mm/s and 50mm/s respectively for each wheel.

Wu and Fan (2003) developed a centreless grinding technique called the ultrasonic elliptic vibration shoe centreless grinding. This few method employs an ultrasonic elliptic-vibration shoe the support the workpiece and control the workpiece rotational motion instead of using a regulating wheel such as that employed in conventional centreless grinding. The vibration ellipse is applied into shoe or bed of the workpiece with frequency of 20 KHz. The shoe is given an intermitted force in micro scale to push the cylindrical towards a spot between the bed and the grinding wheel.

Orynski and Bechinski (2003) in their attempt to avoid wave regeneration effect in plane surface grinding, introduced a high frequency external forced vibration on the spindle of the machine in parallel direction to the cutting speed, their aim was to determine the influence of force vibration with a different parameters on workpiece surface roughness and waviness. The frequency vibration was 100 Hz for 20 μ m depth of cut. The amplitude of vibration was set to 30 μ m and the work speed velocity was 166.6mm/s. the study consist of measurement of roughness and waviness of surface in grinding with and without sparking out.

The obtained result did not show any major different in surface roughness wand waviness during grinding with spark out. However, with spark out grinding, the application of vibration had been beneficial for the surface waviness which was decreased half.

In 2004, Zhong and Yang also establish a device that might create micro-vibration to the workpiece throughout a grinding process. It comprised of two mechanical system generating micro vibration in the vertical direction and horizontal direction. The vertical vibration system had a trial plate and a base plate that was driven by three piezoelectric actuators. The horizontal vibration system required a moving platform was secure on the movable blocks of three linear motion leaders and it could vibrate horizontally.

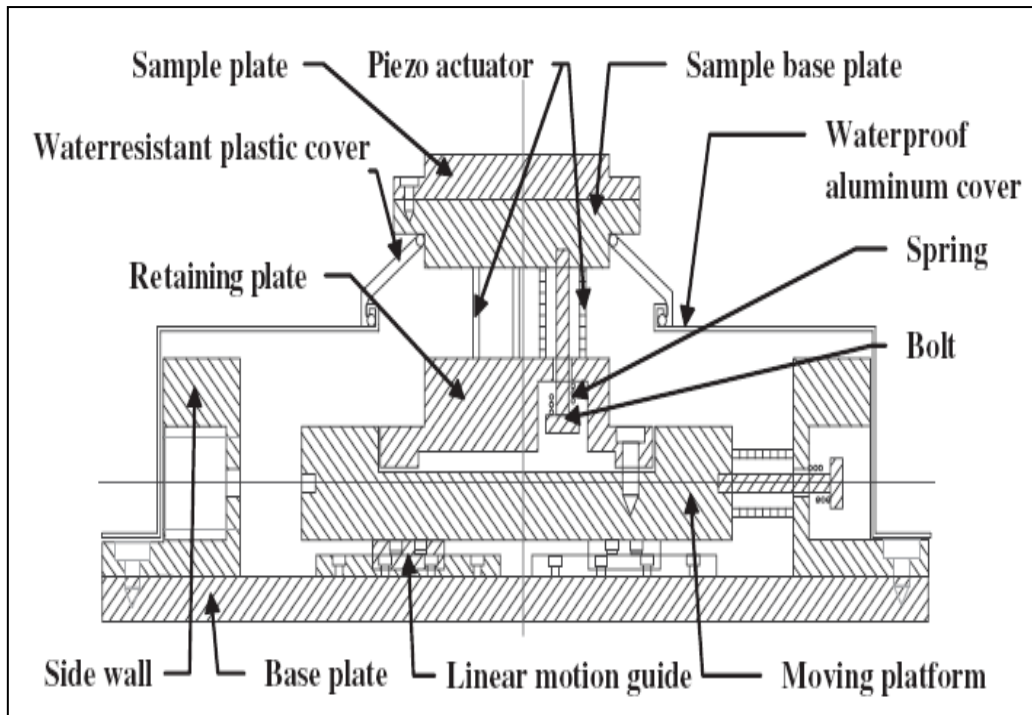


Figure 2.1: Micro- Vibration Device (Zhong & Yang, 2004)

In their investigation of cutting aerospace materials (Babitsky and Kalanishikov, 2003) made an experiment with a turning machine. The ultrasonic vibration process has a common problem when the load applied to the cutting tip and in results the loss of cutting efficiency. Through their experiment, the reduction with the workpiece, so the upper limit on surface speed is further reduced.

Mitrofanov et al, (2003) created a finite element model and induced a high frequency vibration of 20 KHz with amplitude of 10 μm in order to simulate ultrasonic vibration during turning process. The main aim of their study was to improve and decrease the cutting forces, heat and noise radiation. The developed finite element model showed the formation of the chip and the noise-misses stress along the surface of the workpiece during conventional and ultrasonic vibration.

The evaluation and market trending for vibration cutting changed rapidly when more researchers enhanced the piezo-electric in their machine design and on the shop floor.

Developed 1 D actuation servo in this early research on a turning machine at the Fraunhofer institute, as shown in figure 2.2. His investigation focused on the vibration assisted turning using a diamond cutting tool on hard and brittle steel and glass (Klocke, 1998).

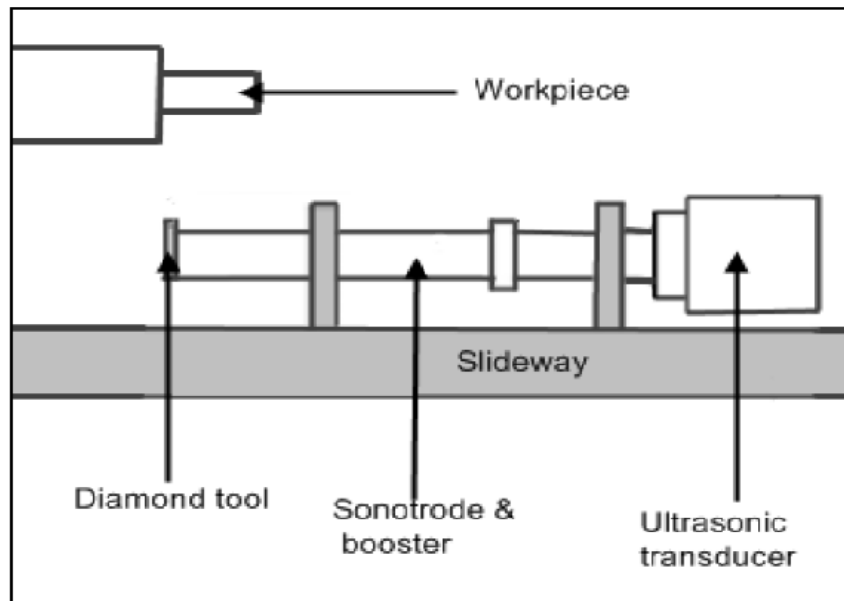


Figure 2.2 Fraunhofer servo design (Klocke, 1998)

Chern and Lee (2005) developed a milling machine with vibration table, which vibrates the table holding a workpiece. They found that hole oversize, displacement of the hole center and surface roughness of the drill wall could be improved with increase of vibrating frequency and amplitude. The result has demonstrated the potential of vibration technology to be developed into a useful tool for enhancing the drilling technology.

Here is a number of different experimental setups to simplify the process, but the tendency is to give a wide range of machining processes to machine hard and brittle materials (Matsumura, 2005).

Many researchers try to machine hard and brittle materials such as glass, stainless steel, and steel alloys to mirror surface finish in different types of machining applications. There are a number of machines equipped with vibration devices for cutting purposes.

Vibration-assisted cutting is a cutting method in which periodic or oscillating cycles are imposed on the cutting tool and the workpiece, besides the original relative motion between these two, so as to get improvement in cutting performance. The fundamental feature of vibration-assisted cutting is that the tool face is separated from the workpiece repeatedly. Historically, this technique was first employed in the precision drilling of wood and low carbon steel (Cerniway, 2005).

Chapter 2: Literature Review

A simulation study to investigate vibration assisted machining was carried out by Cerniway (2005). This was achieved by using a computer technique which simulates the effect of horizontal speed ratio produced from kinematic tool tip surfaces, where a percentage of tool cycling between touched and untouched areas on the workpiece surface was calculated. The author proposed an initial attempt to evolve an application of the cycling or oscillating assessment technology by investigating how frequency and amplitude of machining tool tip location compared simulation.

Vibration assisted machine has proved beneficial in machining metal and ceramics, with special applications being applied to steel (Berhl and Dow, 2006).

Vibration leads to improvements when applied in the correct manner. The same occurs in manufacturing technology. Vibration assisted machining is applied to cutting tool or the workpiece to achieve cutting performance (Shamoto et al, 1999).

Zhang et al, (2006) designed and made up a piezo-table that contained a rectangular and a piezo-electric actuator and used the piezo-table for vibration assisted grinding of ceramics. The key aim of their work was to study the problem affected by wheel loading and the rise of the temperature in the grinding zone. To prevent the loading phenomenon two techniques were used: a) high speed grinding and b) vibration assisted grinding which tends to stop wheel loading and the formation of micro-welding phenomena, reduces friction and facilitates a better coolant delivery to the grinding zone so as to reduce sliding and enhance cooling effect.

An example of how this method can improve surface roughness and extend the cutting life is the work of Chern and Chang (2006) where applied two-dimensional vibration during micro-milling. They combined two piezoelectric actuators with linear guide way in order to vibrate the worktable along with workpiece. The applied of frequency ranged from 500 Hz to 10 KHz. After a number of micro-milling tests they found that the slot centre and slot surface roughness was improved, and vibration at high frequencies did not extend the tool life.

In Centreless grinding, Albizuri et al, (2006) present a method to reduce vibrations which cause the instability for the machine process, bad surface quality and serious wheel wear. They developed a system using piezoelectric actuators which gives a fast

response in the presence of cutting force variation during the process. After several tests it was concluded that the active control system could be used to modify the dynamic characteristics of the machine increasing the table operating range and reducing the vibration.

Chern and Lee (2006) design and developed a vibration worktable in their drilling machine to create a vibration during the process; the design was named the ultra-precision micro-drilling worktable.

Chern and Chang (2006) present another design for a vibration worktable using a piezo-electric affixed to a milling machine centre; the vibration worktable used a piezo-actuator, two dimensional XY axis, a maximum operation frequency of 16 KHz and maximum travelling distance was 10 μm . it operate with a 2 channel high power amplifier to create the desired vibration to cut a slot in aluminium alloy. Through the experiment, they found that slot of oversize about 20 μm . displacement of slot centre and slot surface roughness could be improved: employment of vibration cutting increase the number of slots produced within tolerance when high amplitude and proper frequency were imposed. However, high frequency has a negative effect on tool life, according to previous study, Chern et al, (2006) even through higher frequencies affected tool life, the amplitude in vibration cutting had the highest influence on the interaction between the cutting and workpiece.

The negative vibration (Chatter) in cylindrical grinding is caused by the rational motion of the workpiece. The generated waves on the workpiece surface care caused by the relative vibration of the wheel and the workpiece. This phenomenon leads to the change in depth of cut after one revolution of the workpiece and also can make the process critically unstable Marinescu et al, (2007). A number of authors have tried to detect analyse and suppress these types of vibration with satisfying results.

An increase in the vibration frequency from 10 to 30 KHz results in 47% drop in the level of average cutting forces, which could be attributed to an increased velocity of the tool vibration. Hence, an increase in either vibration frequency or amplitude leads to a decrease in cutting forces, which is beneficial to increase accuracy and improving material removal rate.

Chapter 2: Literature Review

The very basic component of vibration assisted machining is a piezo-actuator. Talking this stage a starting point, many designs of the piezo-actuator have been developed into various application requirements, such as vibration assisted turning, milling and grinding (Endo et al, 2008).

The vibration assisted machining based on the piezo-electric method is improving year by years. In the article by Berhl (2008), the objective was to assess the potential of applying vibration in machining understanding. From this finishing, the process does not allow a complex shape to be made without grinding and polishing.

Surface roughness tool life are very important in the metal removal process focussed on dimensional of ferrous materials. It was found that tool life is extended by 1D and 2D vibration assisted machining. From another point of view, vibration assisted machining experiments in steel, glass, and brittle ceramics confirmed that diamond tool life could be extended to allow economic machining of such materials and also demonstrated improvement in surface finish and ductile cutting when compared to conventional machining. The use of 1D vibration assisted machining led to significantly greater in 2D vibration assisted machining (Brehl, D 2008). In vibration assisted machining, vibration amplitude (normally sine wave) lead to an intermittent gap during cutting and was identified as an important mechanism in vibration cutting.

In order to maintain stability and precision, the vibration within the machining systems need to be monitored so as to achieve the optimum vibration displacement between the tool and a workpiece. Precision metal cutting defined as a cutting technique, which enables the production of optical, mechanical and electronic components with sub-micrometre from accuracy and surface roughness within tens of micrometres (Brehl, D 2008).

In their attempt to apply ultrasonic vibration into grinding process Wu et al, (2003) designed and fabricated a mechanism that could oscillate the spindle of grinding wheel at high frequencies. After a fine element analysis and a number of dynamic experiments of the spindle (driven frequency 23 KHz) they managed to identify all the parameters of the system in order to use it for future works.

Chapter 2: Literature Review

Tawakoli and Azarhoushang (2008) developed an ultrasonic vibration system in order to improve the performance of the grinding process. Their set-up consisted of a transducer with piezo ceramic rings which was driven by an ultrasonic power supply that converted 50 Hz electrical supply to high frequency electrical impulses. These are fed to the transducer and transformed into mechanical vibrations of ultrasonic frequency (23 KHz). The vibration amplitude was amplified by a booster and transmitted to workpiece through a horn. All their experiments were carried out in a dry grinding environment.

The reason was that they intended to decrease the negative environmental impact of the cutting fluid and reducing manufacturing cost. The final results showed 70% reduction in normal force and up to 50% in tangential grinding force. Also, significant improvement in surface roughness and in grinding wheel wear was achieved.

One of the most recent works was carried out by Ling et al, (2010). Where they included two dimensional ultrasonic vibration (22 KHz), in grinding with the purpose of achieving high material removal rate and better quality of the final surface of nanocrystal silicon samples. They combined and synchronised two ultrasonic vibration to accomplish an elliptical motion of the workpiece. Also, when they applied two alternative current voltage with a different phase the system could also, vibrate vertically (bending vibration). The piezoelectric ceramic device they used, were excited at the resonant frequency of the vibrator. They achieved up to 20% reduction in cutting forces with axial ultrasonic assistance and up to 50% decrease in cutting forces with vertical vibration made than conventional grinding. Moreover, the surface roughness was decreased by 10 – 30 % in presence of ultrasonic vibration.

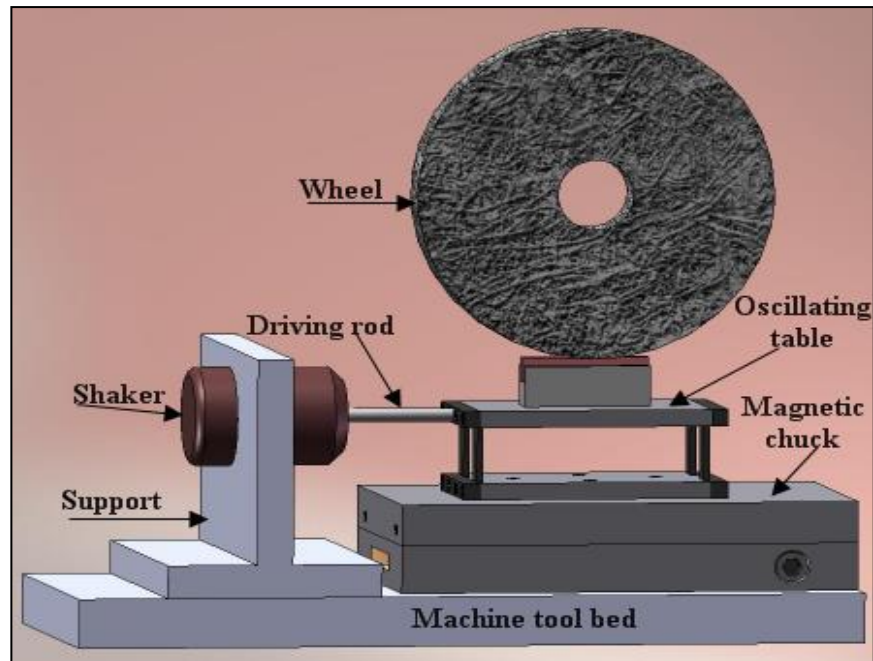


Figure 2. 3: First Concept Vibrating System Configuration, Tsiakoumis (2011).

Tsiakoumis (2011) presented a design of devices that can produce micro-vibration. Figure 2.3 illustrates the concept of the system, the rigs were vibrated at their resonant frequencies in order to achieve high values of amplitude with low voltage input, the dimensional were chosen carefully based on the maximum space between the table and the wheel of the grinding machine. The vibration was produced by piezo actuator. The advantages of this novel method could easily be distinguished as it reduced the grinding forces, power and improved the surface quality of the workpiece. It was observed that for small depths of cut the application of vibration performed as conventional grinding but as the depths of cut increased the reduction of grinding forces and power was obvious. Also, the surface roughness of the workpiece reduced with the application of vibration. Regarding the effect of work speed it could be seen that in most cases vibration-assisted grinding reduced the grinding forces and power. This reduction also became clearer at high work speeds where the load per grain increased. An essential improvement was found while examining the effect of the wheel speed on the process. As the wheel speed increased vibration-assisted grinding outperformed the conventional grinding. Lower forces were recorded for high wheel speed as the travel time of each individual grain was decreased.

2.3 Advance Grinding Methods

High efficiency deep grinding (HEDG) is a novel grinding method which combines very large depth of cut, similar to those of creep-feed grinding, with extremely fast work-speeds and high removal rates. A number of studies have been carried out in this subject area in order to describe this process.

Tawakoli (1993) discussed the technological requirements and theoretical principle for this application. According to the experimental result it was proved that previous practical finding from conventional grinding could not be applied to HEDG because of the complexity of the process.

Batako et al, (2005) employed different methods such as optical, fibres optics and thermocouple techniques with the intention of measuring the temperature during HEDG. Some of these methods proved very accurate when comparing measured and predicted grinding temperature, but others needed further investigation.

An example of how this method can improve surface roughness and extended the cutting tool life is the work of how the methods can improve surface roughness and extend the cutting tool life is the work of Chern and Chang (2006) where they applied two-dimensional vibration during micro-milling, they combined two piezoelectric actuator with linear guideways in order to vibrate the worktable along with the workpiece. The applied frequency ranged from 500 Hz to 100 KHz. After a number of micro-milling tests they found that the slot center and slot surface roughness was improved using mills of 1mm diameter. However, vibration at high frequencies did not extend the tool life.

2.4 Problems in Grinding

In the industrial like manufacturing, the circumstance of precise machine is very significant because the products final outline depend on the efficiency of the cutting and machine tools. Positioning of cutting tool with respect to work piece will affected the precision of the machine (Harris. C. M and Piersol A. G, 2002).

Vibration is a frequent problem that affecting the result of machining and cutting tool life. Vibration can be agreeable and useful, or it can be unpleasant and unsafe.

Chapter 2: Literature Review

Vibration also can interfere with our comfort, damage to structures, and reduction of equipment performance and machinery noise level. Furthermore, a vibration environment can cause malfunction or failure of mechanical systems and may be injury to human beings (Maziah, M 2004).

One of the main problems in grinding is the growing vibration (chatter) between wheel and workpiece during the process. Regenerative vibration is a type of chatter that starts as a slip interaction between wheel and workpiece.

Many studies and tests have been made in order to detect and avoid this dynamic phenomenon which affects a number of parameters including wheel wear and workpiece quality. A possible method to prevent this type of chatter is to apply a periodic disengagement of the wheel from the workpiece and periodic variation of the work speed. These vibrations can be applied to the work-piece by devices such as piezo-electric actuators. Moreover, the temperature rise in the grinding zone and the development of high normal forces are two aspects that must be taken into account. During the process, most of the times the coolant cannot reach the grinding zone. Therefore, there is a high temperature at the contact area, resulting in poor surface quality of the workpiece. Also, due to high grinding forces there is an increase in wheel wear and grinding power.

2.5 Styles of Grinding

There are many forms of grinding, but the most major industrial grinding process is:

- I. **Surface Grinding**
- II. **Cylindrical Grinding**
 - I. Internal and external grinding
 - II. Centreless grinding
- I. **Surface Grinding**

Figure 2.4, shows the most common of the grinding operations. It is a finishing process that uses a rotating abrasive wheel to smooth the flat surface of metallic or non-metallic materials to give them a more refined look or to attain a desired surface for a functional purpose.



Figure 2.4: Surface Grinding: <http://www.dkprecision.co.uk> 12/09/2012)

As the reciprocating table traverses back and forth during a common surface grinding operation, the terms up-grinding and down-grinding become important to understand.

As the reciprocating table traverses back and forth during a common surface grinding operation, the terms up-grinding and down-grinding become important to understand.

- II. **Cylindrical Grinding:** There are Two Types of cylindrical grinding,
 - a) Outer-diameter (OD) grinding is a system in which grinding surfaces are rotated, and a rotating stock piece is introduced next to the abrasive wheel as illustrated in Figure 2.5.



Figure 2.5: Outer- Diameter <http://www.fvht.com/gallmar/i.d-grinding> (12/09/2012)

- b) Internal-diameter (ID) grinding show in Figure 2.6 is another cylindrical style in which an abrasive wheel is inserted into the workpiece along an axis to reshape the inner features.



Figure 2.6: ID Grinding <http://www.fvht.com/gallmar/i.d-grinding> (12/09/2012)

Chapter 3: CONTROL ENGINEERING BACKGROUND

3.1 Introduction

Several industrial processes are controlled using proportional – integral- derivative (PID) controllers Goodwin et al, (2001). The acceptance of the PID controllers can be attributed to their good performance in a varied range in a simple, direct manner and familiarity Astrom et al, (2001) with which it is perceived amongst researchers and practitioners within the process control industries (Pillay and Govender, 2007).

In spite of its widespread use, one of its main short- comings is that there is no efficient tuning method for this type of controller (Astrom and Hagglund, 1995).

Some methods have been proposed for the tuning of PID controllers. Among the conventional PID tuning methods, the Ziegler-Nichols method Ogata K, (1987) may be the most well-known technique. For a wide range of practical processes, this tuning approach works quite well. However, sometimes it does not provide good tuning and tends to produce a big overshoot. Therefore, this method usually needs retuning before applied to control industrial processes. To enhance the capabilities of traditional PID parameter tuning techniques, several intelligent approaches have been suggested PID tuning, such as those using genetic algorithms (GA), (Mahnoy et al, 2000; Wang et al, 2003; Krishna and Goldberg, 1992) and the particle swarm optimization (PSO), (Gaing, (2004); Solihin et al, (2011). It has been asserted that more than half of the industrial controllers in use today utilize PID or modified PID control schemes (Ogata, 2005).

This wide spread acceptance of the controller is largely attributed to their simplicity and robust performance in wide range of operating conditions. One major problem faced in the deployment of PID controllers in the proper tuning of gain values (Visioli, 2001).

Over the years, various heuristic techniques were proposed for tuning the PID controller. Among the earliest methods is the classical Ziegler-Nichols tuning procedure, however, it is difficult to determine optimal or near optimal parameters with this because most industrial plants are often very complex having high order, time delays and nonlinearities (wok et al,1993 ; Krohling et al, 2001).

3.2 Proportional-Integral-Derivative (PID) Controller

Despite all advances in process control over the last 60 years, the PID controller is still the most common controller. The main reasons are the simplicity, robustness and successful application provided by PID-based control structures. The Proportional-Integral-Derivative (PID) controller is widely used in industry (Goodwin et al, 2001; Astrom et al, 1995).

In recent years, considerable research efforts have been concentrated on the computation of the admissible ranges of the coefficient of the PID controllers to maintain stability. The stability domains in a space of the PID controller coefficients were determined for continuous-time PID controllers in several works gathered by Datta (2001) and Soylemez (2003) also gave simple procedures that require less computation. Ackermann and Kaesbaure (2001) presented an additional method in which the results of the parameter space approach in Ackermann (2002), were used to obtain the stability domain of PID controllers. Also the development of (Gryazina and Polyak, (2006) on the parameter space decomposition to stability of the PID control system.

PID controllers are very often implemented digitally using microprocessors, when stability of such system was investigated (Jury and Blanchard 1961, Delansky and Bose 1989). The result of (Xu et al, 2001 and Keel et al, 2003) are generalized to the case of the digital PID controllers. In Keel et al, (2003) an algorithm is presented for computing the stability domain. In Ho and Lin, (2003) the admissible range of PID coefficient to grantee robust performance conditions. Similarly, the industrial PID controllers had many extensions that make them practical tools for operating vibration systems. In addition to the many PID controller-tuning methods, there are some well-known methods. For example, Ziegler-Nichols, (1942) tuning Cohen-coon tuning Cohsen and Coon, (1953) direct synthesis method, internal model control, tuning rules based on the minimization of different error criteria and neural networks based methodologies, all these methods have their own advantages, disadvantages and limitations (Ogata, 2003).

3.3 Objective of Control System

a) Transient Response

Transient response is important for any control system as it is the output primary response to the input signal. Normally, the transitory response of a plant must be appropriate to its components. A control system is designed to achieve a desired transient response by adjusting various design parameters or design components.

b) Steady State Response

This response resembles the input and is usually what remains when transients have decayed to zero. The control system designer should take into account the steady state errors and necessary corrective action to reduce the steady state errors.

c) Stability

Total response of the system is the sum of the natural response and the force response. Natural response describes the way the system dissipates or acquires energy and is dependent only on the system parameters like mass and geometry not the input signal. However, the form of the forced response depends on the input excitation. For a stable and useful control system, the natural response must approach zero or oscillate slightly leaving only the forced response. In some systems, the natural response grows without bound rather than the forced response. This causes instability and may lead to physical destructions if limit stops (saturators) are not part of the control circuit design.

3.4 Control System Design

In order to achieve a good design and implement a control system, some knowledge should be known like:

- I. Knowledge of desired value, (performance specification)
- II. Knowledge of the output value, (feedback sensor, its resolution and dynamic response)
- III. Knowledge of controlling device,
- IV. Knowledge of actuating device,
- V. Knowledge of the plant.

With all this knowledge and information available for the control system. the design steps are shown below in the flow diagram Figure 3.1.

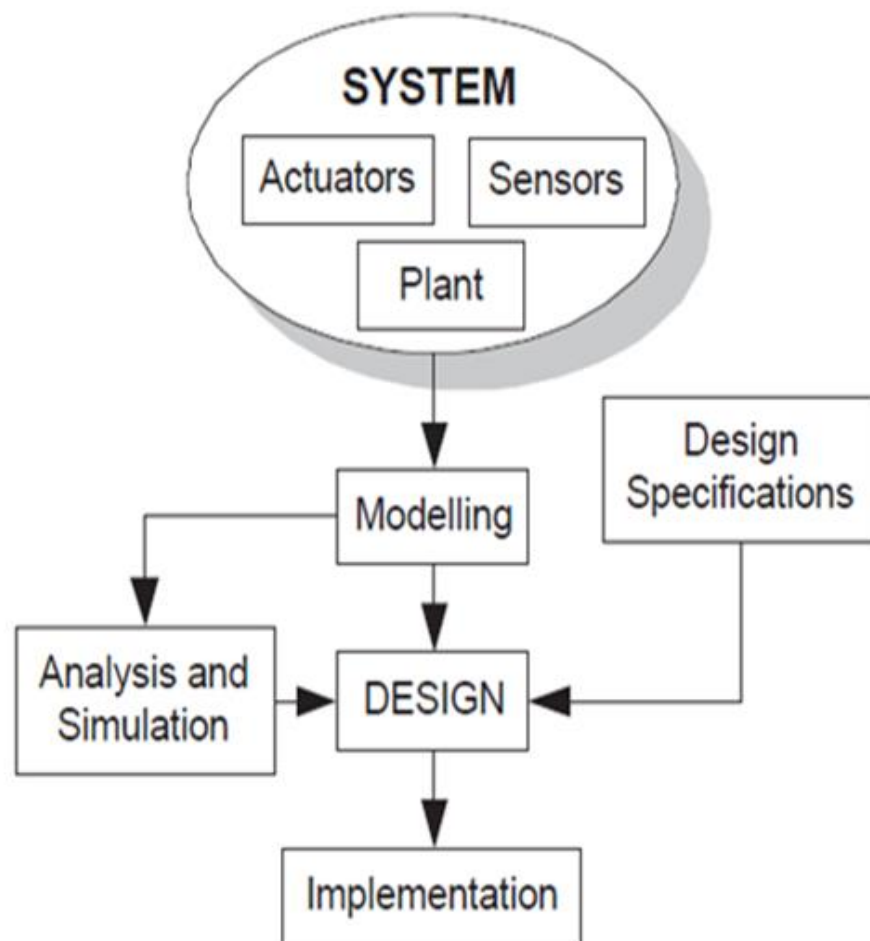


Figure 3.1: Control Design

3.5 Control Systems Classification

Control Systems can be classified as open-loop control and closed-loop control. In the open-loop system, the control action is independent of output and the closed-loop system, control action is somehow dependent on output. The input to the controller is called the reference input. This signal represents the desired system output. Each system has at least two things in common, a controller and an actuator (final control element).

Open-loop control system is used for very simple applications where inputs are known ahead of time and there is no significant disturbance in the controlled output. Here the output is sensitive to the changes in disturbance inputs. Disturbance inputs are undesirable inputs that tend to deflect the plant outputs from their desired values. They must be calibrated and adjusted at regular intervals to ensure proper operation.

Closed-loop systems are also called feedback control systems. Feedback is the property of the closed-loop systems, which permits the output to be compared with the input of the system so that appropriate control action may be formed as a function of inputs and outputs. Feedback systems have the following features:

- Reduced effect of nonlinearities and distortion
- Increased accuracy
- Increased bandwidth
- Less sensitivity to variation of system parameters
- Tendency towards oscillations
- Reduced effects of external disturbances

3.6 Open-Loop Control System

Two outstanding features can characterize open-loop system. First, their ability to perform accurately is determined by their calibration. Second, and most important, they are not generally troubled with the problem of instability. Figure 3.2 show the Block diagram of an Open-Loop control system.

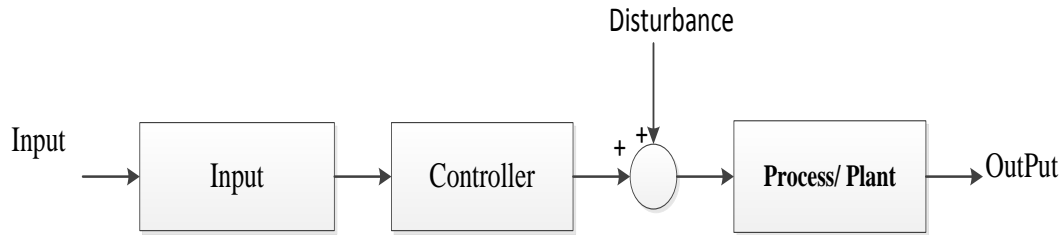


Figure 3.2: Functional Block Diagram of an Open-Loop Control System

3.7 Closed-Loop Control System

A closed-loop system is one in which the control action is dependent on the output system. The closed-loop system is also referred to as the feedback control system. Feedback is the characteristic, which distinguishes the closed-loop system, Feedback is the property which permits the output to the system (or an input to some other internally situated component or subsystem of the system) so that the appropriate control action may be formed as some function of the output and input. The feedback action can be continuous or discontinuous.

Continuous control implies that the output is continuously being fed back, in time, and compared with the reference input, D’Azzo, (1966). In discontinuous feedback control, the input and the output quantities are periodically sampled and compared.

Feedback (closed-loop) control can be used to stabilise systems, speed up the transient response, improve the steady-state characteristics, provide disturbance rejection, and decrease the sensitivity to parameter variations. Figures 3.3 show block diagrams of closed-loop control systems.

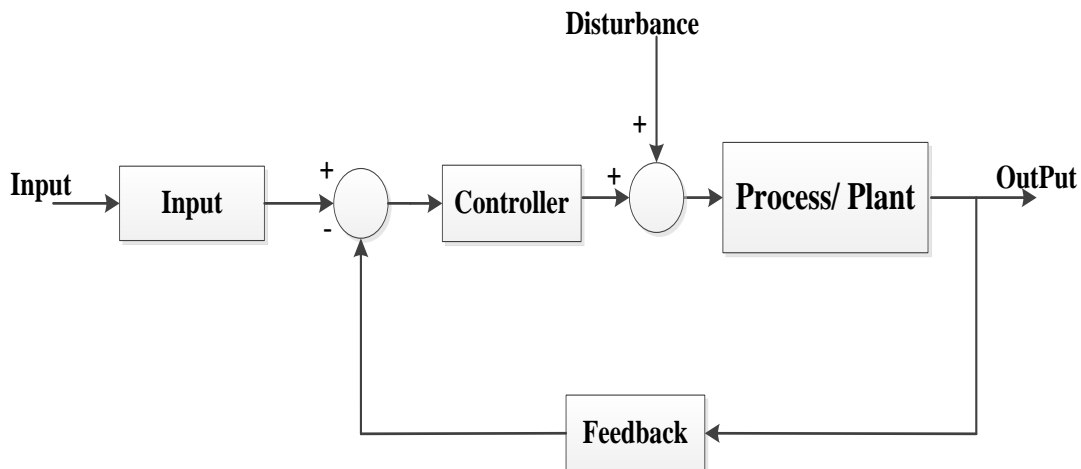


Figure 3.3: Function Block Diagram of a Closed-Loop Control System

As can be seen in Figure 3.3, a closed loop system has a feedback path. The output is delivered at the first summing junction through the feedback path. The output is subtracted from the input signal. The difference between input and output called the actuating signal. The system drives the plant with the signal. If there is no difference and the output has reached the desired response (input), the system will not drive the plant.

For a control system, three main important things have to be considered. The transient response, the steady-state response and the stability. Transient response is related with how well and how fast the system response and the steady state response is more concerned with the final value and differences with the desired value (steady state error). Stability of the system is the core of the control system. If the system is not stable, the transient response and the steady state response will all be negatively affected, (Isaac, 1991).

3.8 Time Response Specification

In many practical cases, the desired performance characteristics of the control system are specified in terms of time domain quantities. Systems with energy storage cannot respond instantaneously. This system will encounter a transient response whenever it is subjected to input or disturbance.

The performance characteristics of a control system are specified in terms of the transient response to a unit step input. The transient response to a unit step input depends on the initial condition. For convenience in comparing various control systems, the initial condition for the various control systems has to be same. Then the transient response characteristic of many systems can be easily compared.

The transient response of a practical system often exhibits damped oscillation before reaching steady state (the desired value). The transient response comprises of the following response characteristics: The stability of the system can be improved by decreasing the overshoot ratio and settle time. PID controller is the most widely used control methods.

Table 3.1: Description of System Performance Parameter

Terms	Description
Max peak, M_p	Maximum peak value
Peak time, t_p	Time require to reach the first, or maximum peak
Settling time, t_s	Time require for transient damped oscillation to reach and stay within $\pm 2\%$ of the steady –state value
Rise time, t_r	Time require for waveform to reach 0.9 of final value from the 0.1 of final value

The input signal for the PID controller is the error signal between reference input and output response. The output signal from the PID controller is then used to control the actuator in order to change the response of dynamic system. The basic equation governing the controller is expressed as follows:

$$m(t) = K_p e(t) + k_i \int e(t) dt + k_d \frac{d}{dt} e(t) \quad (3.1)$$

According to Zhao, (1993) the Transfer function of the PID controller gain can be illustrated as follows:

$$G(s) = k_p + \frac{k_i}{s} + k_d s \quad (3.2)$$

Where $T_i = \frac{K_p}{k_i}$ and $T_d = \frac{k_d}{k_p}$

so the T_i integral time constant and T_d is the derivative, Musa et al, (1996) time constant and the relation between integral time constant and derivative time constant can be expressed as follows:

$$T_i = \alpha T_d, \text{ where } \alpha \text{ is a constant value}$$

$$\frac{K_p}{k_i} = \alpha \frac{k_d}{k_p} \quad (3.3)$$

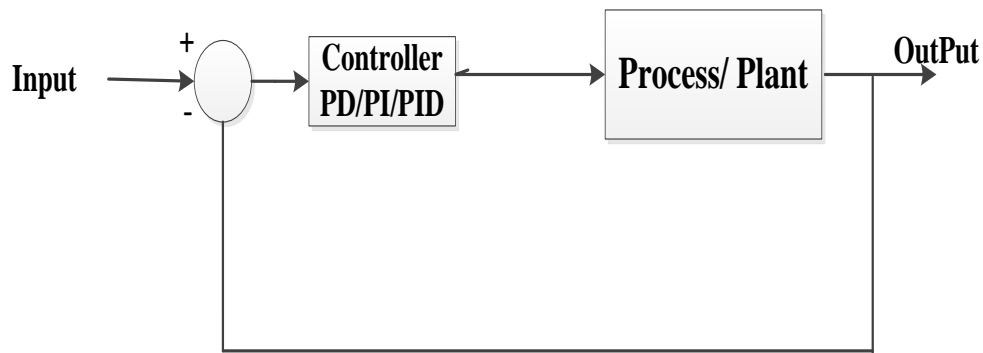


Figure 3.4: Control System with PD/PI/PID Controller

3.9 Proportional Derivative (PD) Controller

Proportional Derivative controller also called as Ideal Derivative Compensation. The function of the PD controller is to improve the transient response.

The yielding information of rise time, settling time and peak time obtained represent the speed of the transient response. In other words, the PD controller can shorten the settling time, rise time and peak time of the system. Therefore, the PD controller will be able to respond faster in the system. The transfer function of the PD controller The gain value is indicated by K_p and K_D :

$$G_c = K_p + k_d s \quad (3.4)$$

3.10 Proportional Integral (PI) Controller

Ideal integral compensator can be called Proportional Integral (PI) controller. This controller is used to improve the steady-state error characteristics. steady state response of a system is when the system approaches to the desired response Ideal integral compensator can be called Proportional Integral (PI) controller. This controller is used to improve the steady-state error characteristics. Steady state response of a system is when the system approaches to the desired response. The steady state response of compensated for the above example is approached to unity and responds with zero steady state error. The transfer function of PI controller, the gain value is indicated by K_P and K_I :

$$G_c = K_p + \frac{K_i}{s} \quad (3.5)$$

The gain value is indicated by K_p and K_i

3.10.1 Proportional Integral Derivative (PID)

The PID controller is effective in a control system in which improvements in both the transient response and the steady-state responses are required. The transfer function of PID looks like the following:

$$G(s) = K_p + \frac{K_i}{s} + K_D s \quad (3.6)$$

Where K_p = Proportional gain, K_i = Integral gain, and K_D = Derivative gain

Proportional controller (K_p) will have effect of reducing the rise time and reducing the steady-state error, but it does not eliminate the error. It tends to increase the overshoot. Integral controller (K_i) will have the effect of decreasing the rise time, and reducing and eliminating the steady-state error. Derivative controller (K_D) will have the effect of decreasing the overshoot and decreasing the settling time.

3.10.2 Controller Effects

- A proportional controller (P) reduces error responses to disturbances, but still allows a steady-state error.
- When the controller includes a term proportional to the integral of the error (I), then the steady state error to a constant input is eliminated, although typically at the cost of deterioration in the dynamic response.
- A derivative controller (d) typically makes the system better damped and more stable.

3.10.3 Summary of the Type of Controller

Table 3.2: Function of PD, PI and PID Controller

Type of controller	Function
PD controller	<ul style="list-style-type: none">• Improving damping• Reducing Maximum overshoot• Reducing rise time• Reducing settling time
PI controller	<ul style="list-style-type: none">• Improving damping• Reducing maximum overshoot• Increasing rise time• Improving steady state error
PID controller	<ul style="list-style-type: none">• Improving settling time• Improving the peak time• Improving rise time• Improving steady state error

3.10.4 System Identification

System identification methods are used to build a mathematical model of dynamic systems based on observed and measured input and output data from the system.

System identification is defined as determination, based on input and output, of a system within a specified class of systems, to which the system under the test is equivalent. In the system control design, the most important consideration is a well-defined model for the plant that should be controlled. The reason is that the entire design will be based on this mathematical model. One way to obtain this model is by using a numerical process known as system identification. This process involves acquiring data from a plant and then numerically analysing stimulus and response data to estimate the parameters of the plant.

3.10.5 Definition of System Identification

System identification is the process of developing or improving the mathematical representation of a physical system using experimental data. There are three types of identification techniques: Modal parameter identification, structural-model parameter identification (used in structural engineering) and control-model identification (used in mechanical and aerospace systems).

The main aim of system identification is to determine a mathematical model of a physical/dynamic system from observed data. Six key steps are involved in system identification, (Soderstrom and Stoica 1989).

1. Develop an approximate analytical model of the structure
2. Establish levels of structural dynamic response which are likely to occur using the analytical model and characteristics of anticipated excitation sources
3. Determine the instrumentation requirements needed to sense the response with prescribed accuracy and spatial resolution
4. Perform experiments and record data,
5. Apply system identification techniques to identify the dynamic characteristics such as system matrices, modal parameters, and excitation and input/output noise characteristics
6. Refine/update the analytical model based on identified results.

Figure 3.5 presents the process for modelling and system identification, (Ljung,1999).

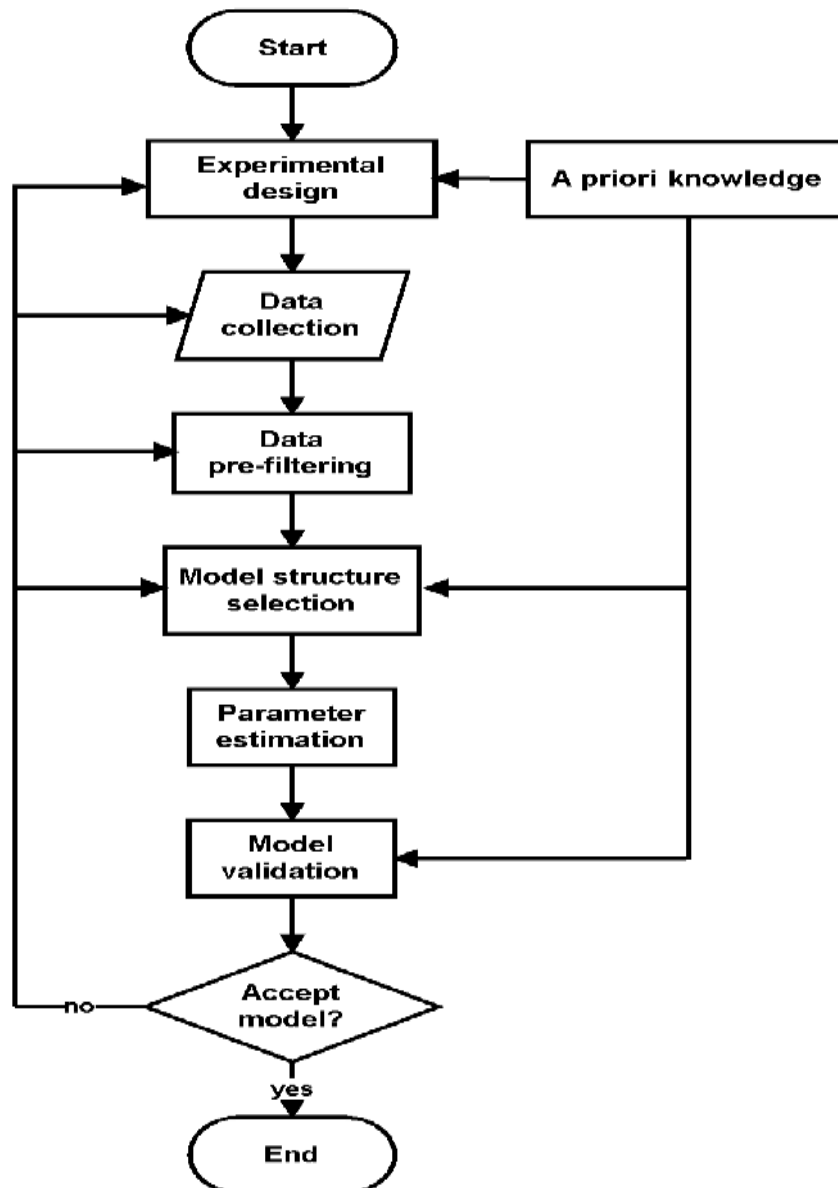


Figure 3.5: Flow Chart illustrating the System Identification Process

3.10.6 Purpose of System Identification

It is important to state the purpose of the model as the first step in the system identification procedure. There is a variety of model applications, for example, the model could be used for control, prediction, signal processing, error detection or simulation. The purpose of the model affects the choice of identification methods and the experimental conditions, and it should therefore be clearly stated. It is important to have an accurate model, if the model is used for control design.

3.10.7 Physical Modelling

It is sometimes possible to derive a model directly from physical laws. However, inherent unknown parameters to have be estimated. If some parameters are known and some are unknown, it is sometimes possible to perform an estimation using the values of the known parameters. Using the procedure illustrated in Figure 3.5, one can derive from the physical model key parameters for the model. These parameters can be in terms of model order, known pole locations (integrator or dominating resonance), static nonlinearities etc. the key problem in system identification is to find a suitable model structure, which a good model is to be found. Fitting a model within a given structure (parameter estimation).

A basic rule in estimation id not to estimate what you already know. In another word, one should utilize prior knowledge and physical insight about the system when selecting the model structure. It is customary to distinguish between three levels of prior knowledge, which have been colour- coded as follows.

3.10.8 White Box Models

A white box model, also known as phenomenological or physical model, is a physical process that describes dynamic system by assembling the low level mathematical representation of it component. This the case when a model is perfectly known; it has been possible to construct it entirely from prior knowledge and physical insight, this approach uses basic scientific principles like newton's laws, kritchhov's laws, thermodynamic laws and reaction kinetics to drive an analytical model (Wellstead, 1979).

And a good phenomenological model should be easily adapted to similar systems, a white box modelling is only necessary where a high level of details in the physical processes is required, and excellent choice for modelling process. Because it's provide more detailed mathematical representation of the physical component, (Hendricks and Sorenson 1990).

3.10.9 Gray-Box Models

This case when some physical insight is available, but several parameters remain to be determined from observed data. It is useful to consider two sub cases:

- Physical modelling: A model structure can be built on physical grounds, which has a certain number of parameters to be estimated from the data.
- Semi-physical model: physical insight is used to suggest certain nonlinear combination of measured data signal. This new signal are then subjected to model structure of black box character.

The Gray box model provides more flexibility than white box models as it Enable the designer to use modelling to optimise a design. In brief, Gray- box Approach attempt to bridge the gap between purely theory based modelling in White box modelling and purely data based modelling in black box modelling, (Atkinson, 1992).

3.10.10 Black-Box Models

Black-box models no physical insight is available or used, but the chosen model structure belong to families that are known to have good flexibility.

This approach is wholly dependent on the use of input and output data collected from the physical system in real time experiments. System identification in this case, is a behaviour approach for developing a model without requirement of physical understanding of the process, (Soderstom and Stoica 1989).

Black box models, the task is really to describe the system's frequency response, the nonlinear black-box situation is much more difficult (Haykin, (1994). The main reason for that is that nothing to excluded, and a very rich spectrum of possible model descriptions must be handled, and most of the real system are non-linear, so in order to achieve an acceptable accuracy of the modelling, it described to use non-linear models, (Sjoberg J., Zhang Q., Ljung L., Benveniste A., Delyon B, (1995).

3.10.11 Model Structure Selection

Selecting a model structure in parametric modelling is hard and should be taken by the designer. To Compare the Auto Regressive eXogenous (ARX), and the Auto Regressive Moving Average eXogenous (ARMAX) and Box Jenkins (BJ) model structures to find out the best model structure for a vibration system, (Ljung, 2010).

The Auto Regressive eXogenous (ARX) model is directly related with a transfer function of the system. This is one of the simple models of transfer function and this is the reason behind its wide use. The Auto Regressive eXogenous (ARX) model is defined as a linear difference equation between input and outputs.

The following approach has been used Billing and Zhu, (1994) Select the parametric model identification technique;

1. Opt for the best model structure among the Auto Regressive eXogenous (ARX), the Auto Regressive Moving Average eXogenous (ARMAX) and Box Jenkins (BJ) model with low order;
2. Apply model estimation and validation techniques and evaluate models
 - a. Performance criteria:
 1. Minimise Final Production error and loss function
 2. Chose a model structure which provides highest percentage of model fit;
 3. Auto-correlation cross-correlation analysis of residual for output shoulder be inside the ideal area ;

ARX model class is a suitable model class for linear control implementations. The parameter estimation problem for both simple single input single output (SISO) system and multi input and multi output (MIMO) system in contrast to ARMAX or State Space model (Triantos. G and Shenon. A, 2004)

3.10.12 ARX Model

For a single input single output (SISO) system. The Auto Regressive eXogenous (ARX) model, (Ljung L, (2007) is expressed as:

$$y(k) = a_1y(k-1) + \dots + a_n y(k-n) + b_1 u(k) + \dots + b_m u(k-m) + e(k) \quad (3.7)$$

Where k = time index,

a and b = constant

$y(k-i)$ = output in previous instant

$u(k-i)$ = input in previous instant

$e(k)$ = residual error

n_a = number of a coefficients

n_b = number of b coefficients

Equation (3.7) can be written as

$$A(q)y(k) = B(q)u(k) + e(k) \quad (3.8)$$

Where the polynomials $A(q)$ and $B(q)$ are defined in terms of the delay operator q^{-1}

$$A(q) = 1 + a_1q^{-1} + \dots + a_{n_a}q^{-n_a}$$

$$B(q) = b_1q^{-1} + \dots + b_{n_b}q^{-n_b}$$

The term $A(q)y(k)$ in equation (3.8) corresponds to the Auto Regressive (AR) parcel of ARX model and the term $B(q)u(k)$ corresponds to the external input.

3.10.13 ARMAX Model

The Auto Regressive Moving Average eXogenous (ARMAX) model is similar to ARX model, which uses a sequence of past inputs that are filtered by the model. However, the Auto Regressive Moving Average eXogenous (ARMAX) model also filters the residual errors aiming at a better disturbance characterization. In analogy with the Auto Regressive eXogenous (ARX) model, the Auto Regressive Moving Average eXogenous (ARMAX) model can be considered as a transfer function of the system that is being identified.

The difference equation of Auto Regressive Moving Average eXogenous (ARMAX) written as for single input single output (SISO) systems, is inscribed as:

$$y(k) + a_1y(k-1) + \dots + a_{n_a}y(k-n_a) = b_1u(k-1) + \dots + b_{n_b}u(k-n_b) + e(k) + c_1e(k-1) + \dots + c_{n_c}e(k-n_c) \quad (3.9)$$

where: $e(k-i)$ = is a White noise in the previous inputs

n_c = is the number of c coefficients

Similarly to The Auto Regressive eXogenous (ARX) model, the Auto Regressive Moving Average eXogenous (ARMAX) model is written as:

$$A(q) y(k) = B(q)u(k) + C(q) e(k) \quad (3.10)$$

Where $A(q)$ and $B(q)$ are the same as defined in The Auto Regressive eXogenous (ARX) model and $C(q)$ is defined as $C(q) = C_1q^{-1} + \dots + C_{nc}q^{-n}$

The ARMAX model incorporates the additional term $C(q)e(k)$ that corresponds to moving average part. Writing Equation (3.11) in transfer function form one obtains similar result to The Auto Regressive eXogenous (ARX) model.

$$y(k) = \frac{B(q)}{A(q)} u(k) + \frac{C(q)}{A(q)} e(k) \quad (3.11)$$

3.10.14 Modelling

Normally, parameter identification is based on models or procedures that are an adequate representation of the physical system under investigation.

There exist several ways to represent a real system. This representation can be performed using differential equations that govern the system, recurrence equations, state-space models, etc. the last two alternatives are commonly known as black-box formalism. This idea comes from the fact that the main goal is to estimate the plant output given the inputs and the previous outputs. In such models, the estimation accuracy is obtained by adjusting the number of previous output to be used or by selecting the system order, in case of state space representation. The choice between models represented by differential equations or by black box models depends exclusively on the requirements to be fulfilled. The models where the parameters have physical meaning are called phenomenological models, and where the parameters do not have physical meaning are called behavioural models.

In this investigation the Matlab software package was used and it included a system identification toolbox. This allowed for the following:

- Import and manipulate input-output test data.
- Estimate various linear models such as transfer functions, process models, state-space, and polynomial models.
- Estimate nonlinear Auto Regressive eXogenous (ARX).
- Validate estimated models on independent data sets.
- Export estimated models to Matlab workspace or to the Linear System Analyser app from Control System Toolbox.

3.10.15 Controller Design

The required system model can be achieved through the system identification method that determines physical characteristics of a plant and presents them in the form of a mathematical expression using real time measurement or experimental data taken directly from the vibration system. After collecting an experimental data, most the essential stages of the model identification process can be summarised as follows,

1. Select between parametric and non-parametric technique.
2. Choose the model structure.
3. Model estimation and validation criteria.

First, the input/output data were collected and uploaded to Matlab workspace simulated using the system identification toolbox. Two vectors and the sampling time were the main variables in the identification process. These vectors were (u) which represented the input signal and vector (y) represented the output signal vector.

Figure 3.6 shows a sample of the input/output data used in the system identification process in this project. The input data Figure 3.6 b has been chosen as pseudorandom binary sequence (PRBS) to make sure that most of the system frequencies are excited during the identification process. The relevant output signals are recorded in Figure 3.6 b.

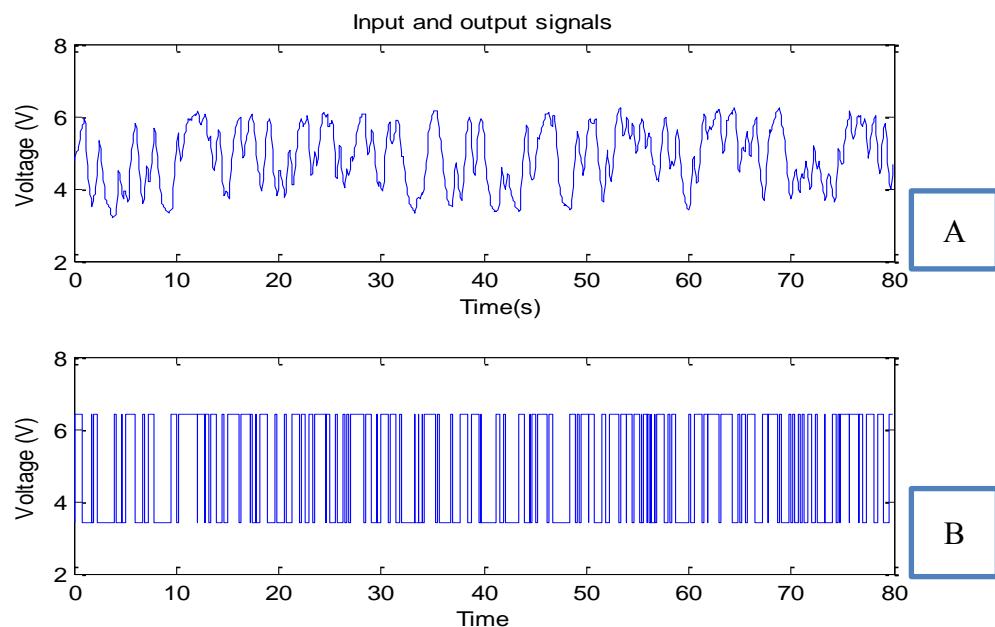


Figure 3.6: Identification Signal

3.10.16 Experimental Validation

Experiments were divided into two steps. The first step was to get a primary knowledge about the most important system characteristics. It was possible to draw a conclusion from these experiments on whether or not the system is linear. The information obtained from the preliminary experiments is then used to determine the appropriate experimental conditions for the main experiment, which gave the data used in the system identification process.

3.10.17 Main Experiments

The main experiments were the trials where data were collected for the system Identification Toolbox after the choice of input signal.

The System Identification Toolbox gave an accurate model at the frequency of 100Hz when the input signal gave the desired displacement at low driving voltage. A pseudo-random binary sequence (PRBS) is a common choice of input signal. A program logger was used to generate of PRBS; a PRBS signal in logger is defined in terms of:

- Sampling interval (h),
- Number of sampling intervals between PRBS shift register updates (M),
- Number of data points collected (N), and
- Amplitude of the excitation signal (A).

A rule of thumb is to let $1/(h \times M)$ assumed to be the bandwidth of the system. To avoid aliasing, M should be at least 2–10. The closed loop system step response should be sampled at 5-10 times during its rise time. The experiment duration has been chosen to get good parameter estimates.

Finally, the entire measured data was divided into two sets keeping the first one reserved for estimation and other for validation. Two-thirds of data is selected of estimation and one-third of data has been reserved for validation.

Figure3.7 shows the estimation and validation data set are black and blue line colours respectively.

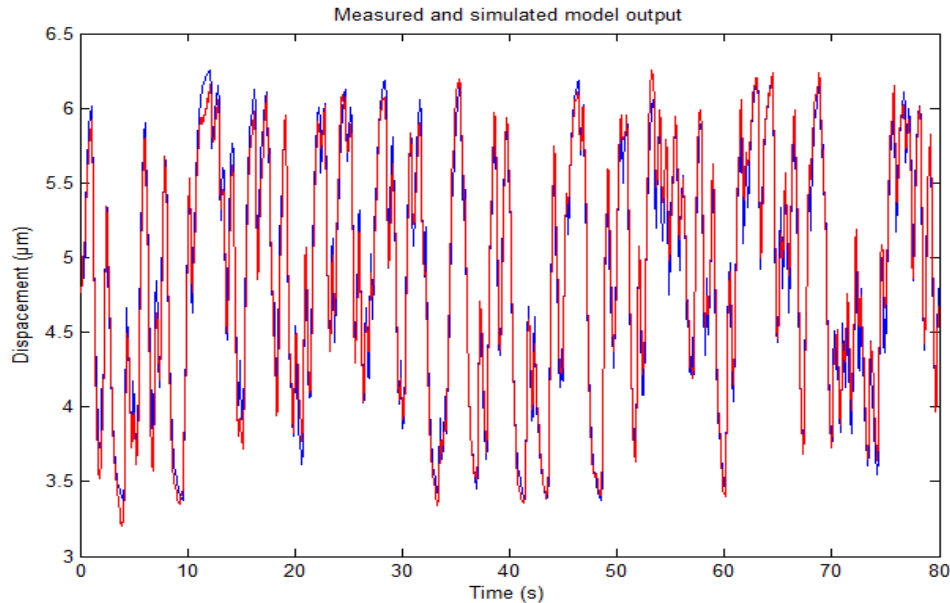


Figure 3.7: Estimation & Validation Data Set for Vibration System

3.10.18 Excitation

The input should provide good excitation in the frequency range where the model needs to be accurate. It can be checked if the input excites the system appropriately by studying the auto spectrum of u and y .

It is possible to concentrate the identification interested frequency ranges by filtering u and y . If the excitation is insufficient after filtering then the experiment must be repeated with new experimental conditions. The Matlab function `spectrum` can be used to plot the auto spectrum and the coherence function.

3.10.19 Data Examination

When an experiment is performed, there is an input sequence and an output sequence represented as column vectors u and y respectively in Matlab. It is appropriate to split the data into two sets, one for identification and one for validation. It is recommended to start by checking the data manually via plots and look for outliers and aliasing.

Outliers should be removed from the data series. If there is aliasing effect in the data, the experiment set-up has to be modified i.e., either the sampling rate should be increased or an appropriate anti-aliasing filter should be used.

3.10.20 Design of Experiments

Design of experiments (DOE) is a body of knowledge and techniques for planning a set of experiments, analysing the resulting data, and drawing conclusions from the analysis.

Here, the experiments were done in two steps. In the first step, preliminary experiments such as impulse and step responses are performed to gain primary knowledge about the important system characteristics such as stationary gain, time delay and dominating time constants.

It is often possible to draw conclusions from these experiments on whether or not the system is linear and time invariant and if there are disturbances acting on the system.

In the second step, the information obtained from the preliminary experiments was then used to determine suitable experimental conditions for the main experiments, which generated the data used in the system identification process.

The element in the design of the experimental setup was the selection of the input and output signals according to the purpose of the identification and control processes.

The idea in this experiment was to work towards designing a controller for the vibration system. This system is a simple single input single output system (SISO).

Firstly, load-vibration amplitude data measurement took place. The input voltage (u) was driven by a function generator with a frequency up to 100Hz and 100 times amplified amplitude by an amplifier. The output acceleration (y) was measured by an accelerometer attached to the system.

Chapter 4: EQUIPMENT

4.1 Introduction

In this investigation a number of pieces of equipment have been used including a grinding machine tool, data acquisition system, oscillating stage with piezo actuator, accelerometer, signal generator, power amplifier and Labview software package to control the system and data recording, and measurement force experiments was the calibration of the equipment. A series of tests were made using the different sensors that will be employed in this study. The outputs of the sensors were calibrated using respective nominal certified scales provided by the manufacturers.

4.2 Abwood 5025 Grinding Machine

The bulk of the experimental work was carried out on the Abwood 5025 grinding machine. It has a 1.5KW motor for the wheel head ensuring rapid stock removal. A self-contained hydraulic pump system built-in operates the fast feed unit. A tank that could hold up to 36 litres of oil is attached to the machine. The unit operates at a maximum pressure of 1MPa and required low pressure pipes was connected to the hydraulic actuators of the machine. The traverse speed could reach 250 mm/s and the wheel speed was controlled through an AC servo motor giving variable control up to 5000 RPM. Figure 4.1 illustrates the actual machine tool and its specification is provided in Table 4.1

Table 4.1: Specification of – Abwood 5025 Machine

Spindle Motor Power	1.5Kw
Spindle Speed	5000RPM
Cross traverse head	260 mm
Resolution	10 μ m
Longitudinal traverse	530 mm
Vertical traverse of head	350 mm
Resolution	1 μ m
Automatic feed	Hydraulic Control x, y, z Axis
Maximum wheel size	400 mm*25 mm



Figure 4.1: Abwood Surface Grinding Machine Tool

4.3 The Oscillating Stage

The system shown in Figure 4.2 below was used in the experimental setup to vibrate the holder-workpiece system. It is linked to a power amplifier which gets a sine wave signal from a function generator. The vibration stage is made of a piezo actuator, a displacement bridge amplifier, the workpiece-holder driving element and the casing. The system operates as follows: a sine wave, the amplitude and frequency of which is set at the function generator is sent to the power amplifier. The wave is magnified by a factor and then sent to the piezo actuator. The piezo crystals in the actuator expand and contract alternately thus producing the oscillations; the amplitude of these oscillations depends on the magnitude of the voltage applied to the piezo.

Figure 4.2 illustrates the content and the external view of the self-contained oscillating stage used in this study. An accelerometer is mounted on the moving workpiece holder to send the system acceleration to a control system that will be described in chapter 9.



Figure 4.2: Self Contained Vibration System

4.4 Piezoelectric Actuators

Piezo actuator is characterized as smart materials and has been widely used in the area of actuators and sensors. The operation principle of a piezo actuator transformer is a combined function of actuator and sensors so that energy can be transform from electrical form to electrical form via mechanical vibration (Rosen, 1956).

4.4.1 Features of Piezoelectric Actuators

- Piezo actuators can perform sub-micrometre motion at high frequencies because they derive their motion from solid-state crystalline effects. They have no rotating or sliding parts to cause friction.
- Piezo actuators can move high loads, up to several tons. Piezo actuators present capacitive loads and dissipate virtually no power in static operation.
- Piezo actuators require no maintenance and are subject to no wear because they have no moving parts.

Figure 4.3 illustrates a typical piezo actuator with typical dimensions from Physik Instrumente.



Figure 4.3: Piezoelectric Actuator (from PI <http://www.piceramic.com/products.html> (11/03/2012))

A full specification of the Piezoelectric actuators used in this study is given in Table 4.2:

Table 4.2: Specification of Piezoelectric Actuators Type P212.8

Technical Data	Value	Units
Length	139	mm
Diameter	18	mm
Translator Diameter	8	mm
Pushing force Capacity	2000	N
Pulling Force Capacity	300	N
Open-Loop Travel	120	μm
Piezoelectric actuators Mass	0.21	Kg

4.4.2 Identification of Suitable Displacement Sensor

In this experiment three sensors namely LDVT macro sensor, laser sensor and Eddy current sensor were tested in measuring the actual amplitude of the oscillation of the workpiece. It was noticed that the LDVT sensor response had some non-linearity, though the calibration was done in static mode as illustrated in Figure 4.4. The LDVT sensor was a spring loaded mechanical sensor and at the application of the oscillation it had a poor signal to noise ratio, therefore its results were discarded.

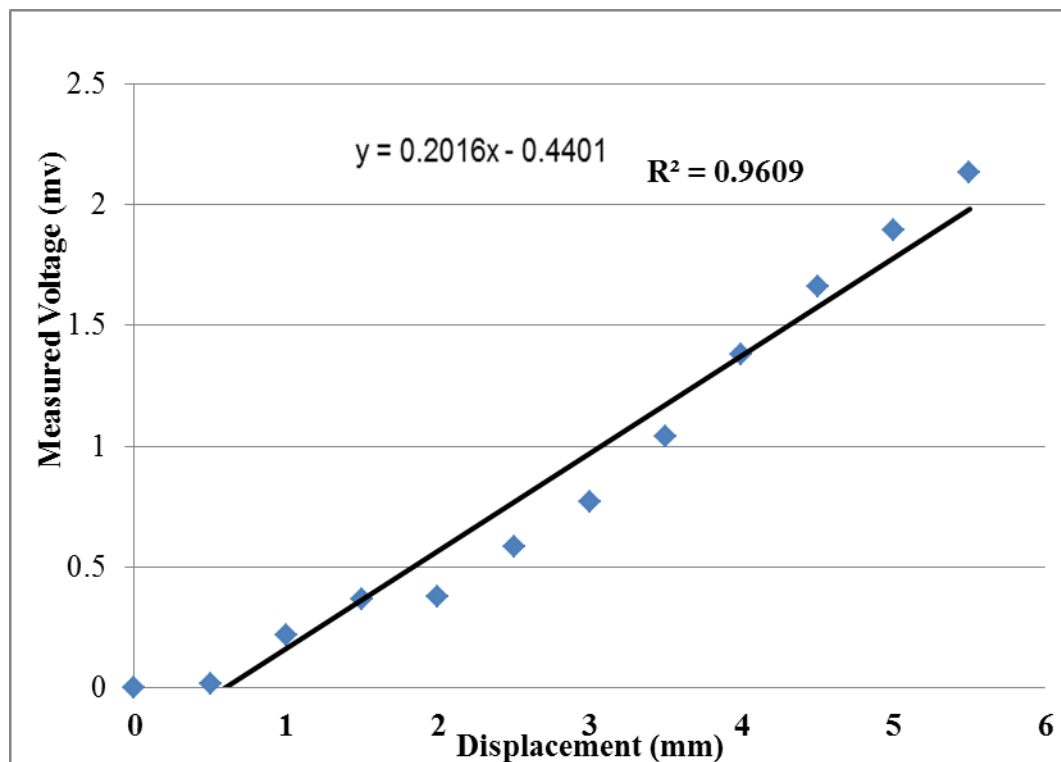


Figure 4.4: Response of the LDVT Sensor in Static Mode (mv)

Figure 4.5, shows the response of the eddy current sensor and laser as a function of frequency. Both sensors responded in a similar way, however, in terms of cost, the Eddy current sensor is smaller, cheaper and has the advantage of being imbedded into the oscillating jig. Thus it could allow for accurate reading and compact design of the oscillatory system. Therefore, the Eddy current sensor was selected for further use.

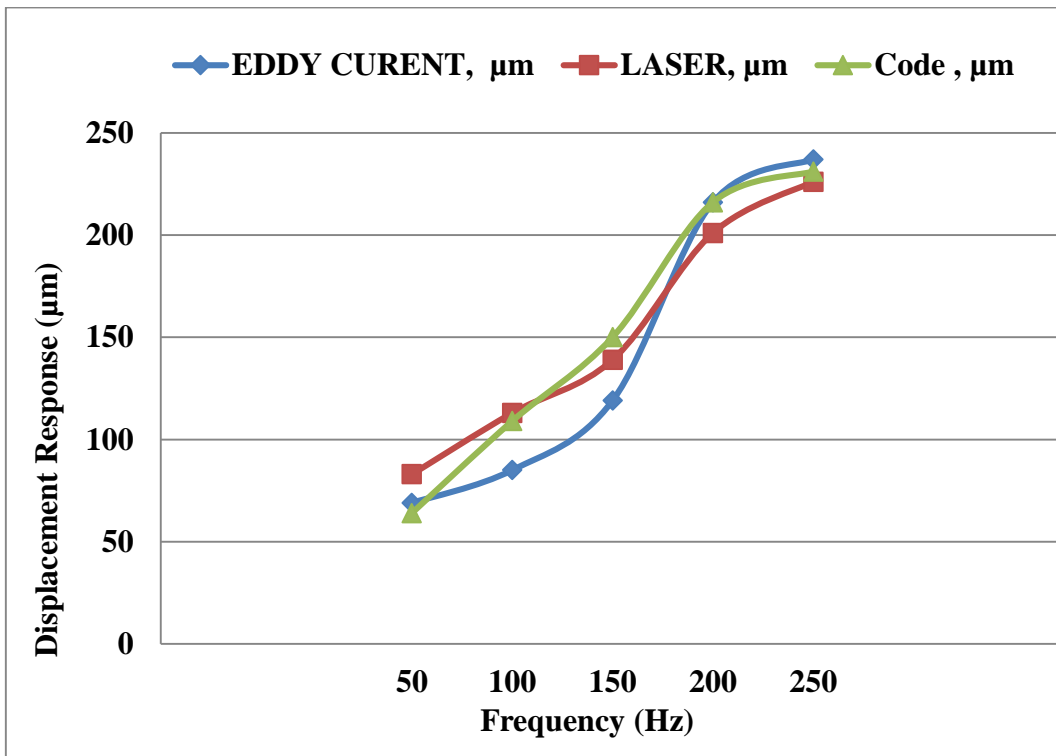
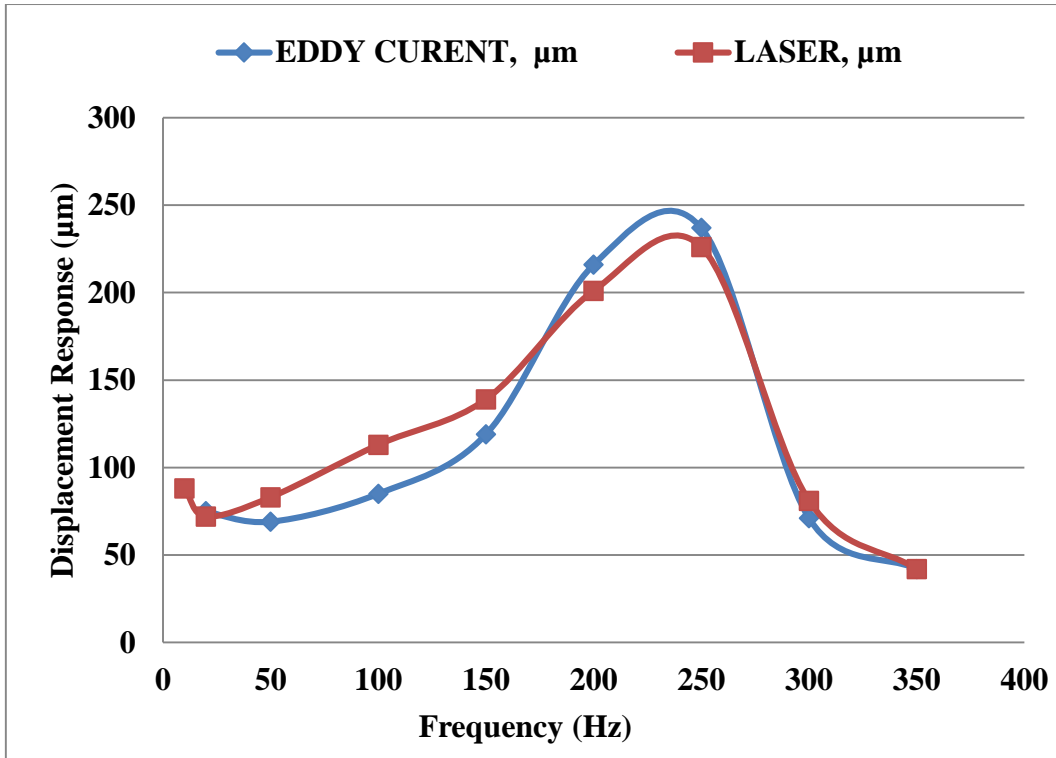


Figure 4.5: Displacement Sensors Response

4.5 Power Amplifier

An amplifier is a device that increases the size or strength of a signal. The E-472.2 series high power amplifier is specially designed to drive high capacitance piezo actuators. The output voltage ranges from -3 to 1100 Volts. The DC offset potentiometer adds a DC bias to the input, allowing continuous shifting of the input range between 0V to +10V and -10V to 0V. Manual closed loop operation displacement of the piezo-actuator can be set by a 10-turn DC offset potentiometer in the range of zero to nominal displacement.

Table 4.3: Specification of Power Amplifier E-472.2

Technical Data	Value	Units
power amplifier total out put	1100	Volts
Number of Channels	2	-
Amplifier average Output Power	110	Watts

4.6 Accelerometer

Accelerometers are the most frequently used transducers to measure vibration responses of structures. The main objective of signal analysis involved in structural vibration test is obtaining information about amplitudes, frequencies, and different phase of the measured accelerations generally the acceleration signal is converted into the velocity and displacement.

The output of accelerometers is g which is the gravitational constant 9.81m/s^2 . Accelerometers are widely used in cars, cell phones, computers, bridges and washing machines to measure their vibration. The accelerometer used for this experiment was a kistler 8704B100 and it has low impedance, voltage mode, low base strain, low thermal transient response and is lightweight. The specification of the accelerometer is given in the Table 4.4:

Table 4.4: Accelerometer Specification Kistler 8704B100

Technical Data	Value	Units
Acceleration Range	± 100	g
Sensitivity $\pm 5\%$	50	mV/g
Operating Temperature	-54	$^{\circ}\text{C}$
Frequency Response $\pm 5\%$	0.5 – 10	KHZ
Housing/Base	Titanium	Material
Weight	8.6	grams

4.7 Data Acquisition

PC-based data acquisition uses a combination of modular hardware, application software, and computer to digitise signals from various sensors and to record these signals on the computer hard disc for further analysis. While each data acquisition system is defined by its application requirements, every system shares a common goal of acquiring, analyzing, and presenting information. Data acquisition systems incorporate signals, sensors, actuators, signal conditioning, data acquisition devices, and application software. So summing up, data acquisition is the process of acquiring signals from real world processes, digitizing the signals, saving the data, analyzing, and presenting the results.

4.7.1 Data Acquisition Hardware (DAQ)

DAQ hardware acts as the interface between the computer and the outside world. It primarily functions as a device that digitizes incoming analogue signals so that the computer can interpret them. Typical DAQ functions are: Analogue input, Analogue output, Digital Input/output and Counter/timer. The system built for this investigation used three specific pieces of hardware manufactured by National Instrument (NI). These were the NI 9233, NI9263 and NI 9215. The DAQ NI 9233 and NI 9215 series is specially designed for multi input



Figure 4.6: Input NI 9233 DAQ and NI 9215 DAQ

Table 4.5: Important Characteristic for Input NI 9233 DAQ and NI 9215

Input Range	+/- 5v
Number Of Channels	4 Analogue input Chanel
Number of Bits	24 bits

4.7.2 Output DAQ NI9263

The Analog output DAQ is national instrument NI9263 series number, important characteristics are found in Table 4.6 as below.



Figure 4.7: Output NI 9263 DAQ

Table 4.6: Important Characteristic for Output NI 9263 DAQ

Output Voltage	+/-10V
Number Of Channels	4 Analogue Output Chanel
Number of Bits	16 bits

4.8 Kistler Charge Amplifier Type 5073

The experimental system is shown schematically in appendix H. The 3- axis Kistler dynamometer is connected to the piezoelectric sensor and charge amplifier, to record the data from the dynamometer national instruments; data acquisition was employed along with the charge amplifier to convert the piezoelectric charge signal from the sensor into an output voltage proportional to the mechanical input quantity. Depending on the version and application, up to four sensors can be connected and integrated into a production machine.

This charge amplifier is suitable for applications with nearly all piezoelectric sensors. The output signals can be used for monitoring, closed loop control and optimization of an industrial measuring process. Its floating-potential digital input for rest /measure and measuring range selection are designed for integration in a machine control system. Table 4.7 below gives the technical data for the Kistler charge amplifier type 5073:

Table 4.7: Important Characteristic Kistler Charge Amplifier Type 5073

Output voltage	V	0...±10
Max. output current	mA	±5
Output impedance	Ω	10
Output voltage limit	V	>±11
Error (transfer factor)	%	<±0,5
Minimum/ maximum temperature	°C	-40/+80

4.9 Force Measurement Using the Dynamometer

The 3-axis Kistler dynamometer type 9257A was used in this investigation therefore it was calibrated to measure the forces during grinding. It has a capacity of measuring loads up to 5 kN. In the grinding contact area there are two major forces acting in normal and tangential directions, however, since in this study the oscillations were applied in the axial direction, the third direction was calibrated. The calibration was done up to 350 N for the tangential direction (X), normal direction (Y) and axial direction (Z).

The dynamometer was connected to charge amplifiers which were set up as follows:

- tangential (X) direction – sensitivity set at 8.015 pC/N with a scale of 50 units/volt
- normal direction (Y) - sensitivity set at 3.755 pC/N with a scale of 50 units/volt
- axial direction (Z) – sensitivity set at 8.15pC/N with a scale of 50 units /volt

The experimental system is shown schematically in Figure 4.8. The 3- axis Kistler dynamometer is connected to the piezoelectric sensor and charge amplifier, to record the data from the dynamometer national instruments, data acquisition was employed along with the charge amplifier to convert the piezoelectric charge signal from the sensor into an output voltage proportional to the mechanical input quantity. Depending on the version and application, up to four sensors can be connected and integrated into a production machine.

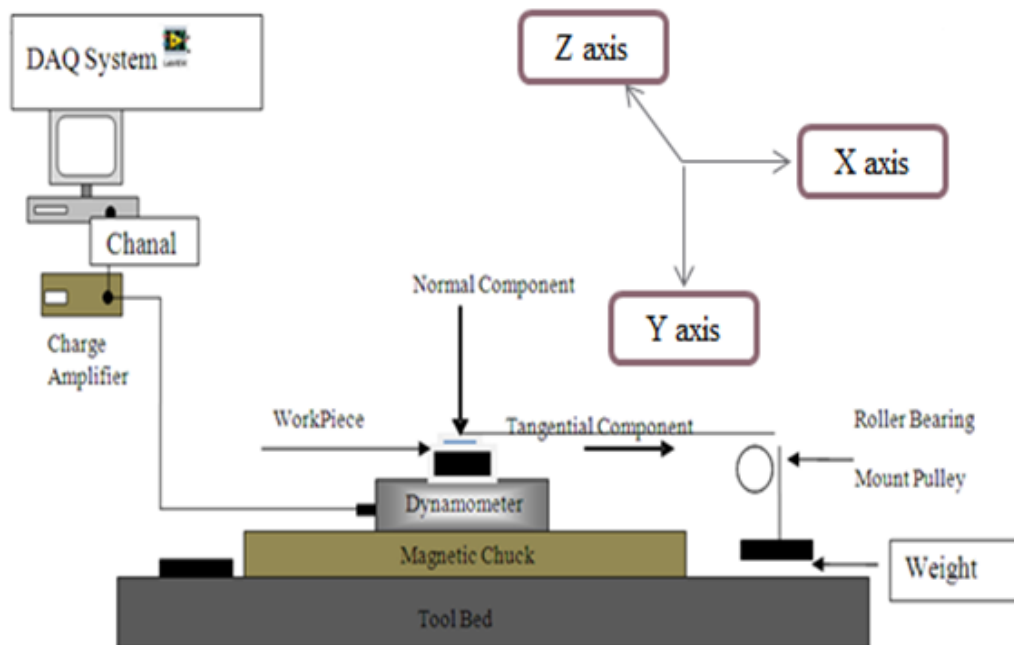


Figure 4.8: Experimental Calibration Setup

4.10 The Force Results

As illustrated in Figure 4.8 LabVIEW data acquisition was used to record all signals from the dynamometer. The calibration was obtained by averaging the results of nine loadings. Figure 4.9, 4.10 and 4.11 give the calibration curves and their first order regression. It is observed that the output dynamometer is linear, therefore during the actual grinding trials; the linear regression obtained from the graphs will be used to estimate the grinding forces.

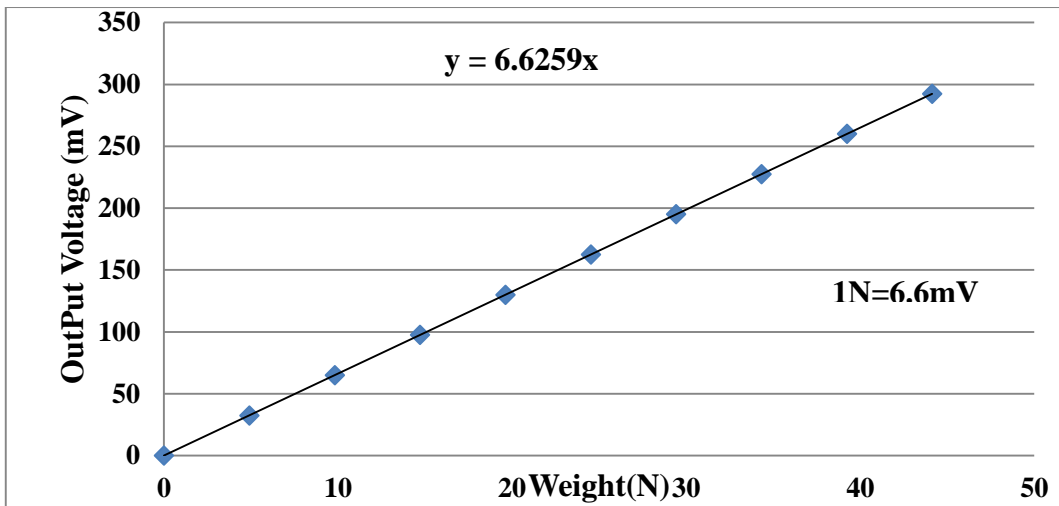


Figure 4.9: Force Response in Tangential Direction (X-Axis)

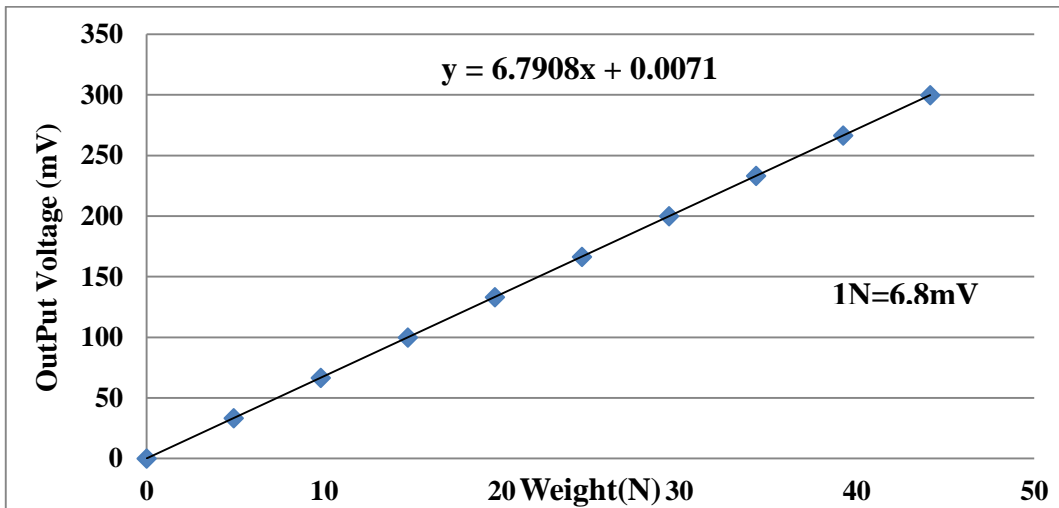


Figure 4.10: Force Response in Normal Direction (Y-Axis)

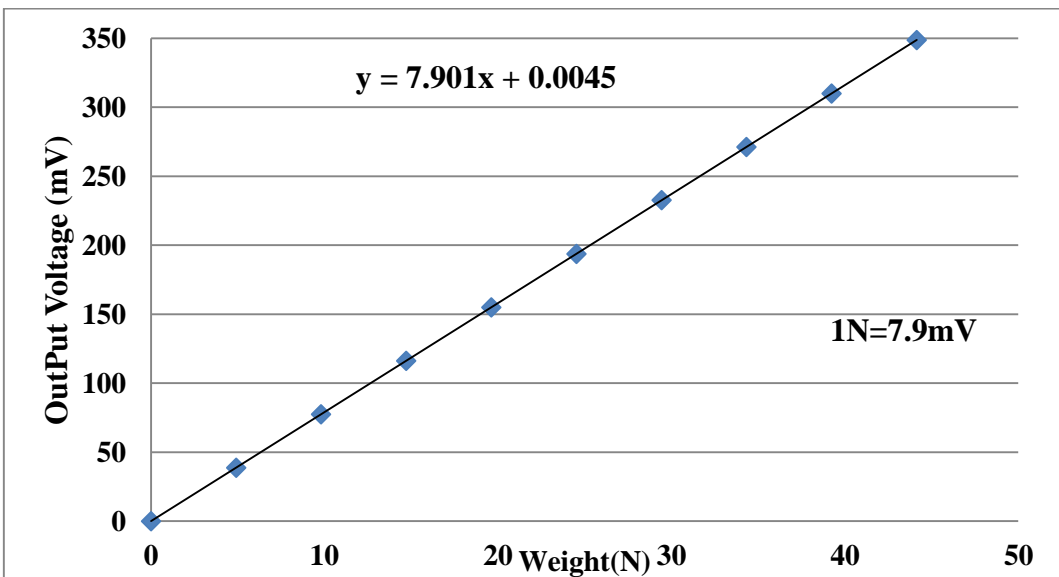


Figure 4.11: Force Response in Axial Direction Z-Axis

4.11 Grinding Wheel

A grinding wheel is a self-sharpening tool composed of discrete abrasive grains held together by bonding agent with much clearance allowance for the cutting edges. The characteristic of a grinding wheel depends upon the combined elements of abrasive, grit size, grade, structure and bond.

4.12 The Main Components of Grinding Wheel

- Abrasive: the abrasive grain is the element that actually performs the cutting activity in the grinding process. And the choice of abrasive grain depends on the materials to be ground.
- Bond: the role of the bond is to hold the individual grains together. The type of the bond depends on the operating and the surface finish required
- Pore: exists between grains and bond. In order to provide chip clearance, air space (pore) must exist between grains and bond. Dense spacing is denoted by low numbers and open spacing by high numbers.

The grinding wheel has been important for all industry. For manufacturing, grinding wheels provide an efficient way to shape and finish metals and other materials. Abrasives are often the only way to create parts with precision dimensions and high-quality surface finishes. Today grinding wheels appear in nearly every manufacturing company in the United States, where they are used to cut steel and masonry blocks; to sharpen knives, drill, and many other tools; or to clean and prepare surfaces for painting or plating. More specifically, the precision of automobile camshafts and jet engine rotors rests upon the use of grinding wheels. To select an optimum grinding wheel, a number of factors must be considered. Including the following parameters:

- Types of materials to be ground
- Kind of abrasive particles used in the wheel
- The amount of stock to be removed
- Wheel speed in operation

4.13 Function Generator

A function generator is a device that can produce various patterns of voltage at a variety of frequencies and amplitudes. It is used to test the response of electronic circuits to common input signals. The electrical leads from the device are attached to the ground and signal input terminals of the device under test. Most function generators allow the user to choose the shape of the output in a form of:

- Square wave
- Sine wave
- Triangle wave
- Random.
- The function generator specification is shown in Table 4.8.

Table 4.8: Specification for the Function Generator

Output function	Sine wave, Square, Triangle, TTL
Frequency range (for sine wave and Square)	0.1Hz – 3MHz
Frequency range (for Triangle)	0.1Hz – 1MHz
Resolution	0.01 Hz maximum
Amplitude range	10 V _{p-p}
Amplitude accuracy	± 20% at maximum position
Impedance	50Ω ± 10%

The amplitude control on a function generator varies the voltage difference between the high and low voltage of the output signal. The direct current (DC) offset control on a function generator varies the average voltage of a signal relative to the ground. The frequency control of a function generator controls the rate at which the output signal oscillates. On some function generators, the frequency control is a combination of different controls. One set of controls chooses the broad frequency range (order of magnitude) and the other selects the precise frequency. This allows the function generator to handle a wide variation in frequency scale needed for signals. In a square wave signal, the duty cycle of a signal refers to the ratio of high voltage to low voltage time, details study will be presented in chapter 8.

4.14 Brukker GTK Surface Texture System

The contour GT-K Optical microscope sets a first-hand industry standard in design and budget of surface metrology performance. With excellent roughness and 2D/3D measurement capability, high resolution imaging.

4.14.1 Superior Imaging and Resolution

- I. Best Z resolution free of magnification
- II. High stability
- III. Great resolution and colour camera choices
- IV. Large field of view
- V. Real time programmed measurement optimization

Table 4.9: Specification for Brukker GTK surface texture system

Max- scan range	Up to 10 mm
Vertical resolution	<0.01 nm
Maximum scan	47 $\mu\text{m}/\text{sec}$ with standard camera
Sample resolution	0.05% - 100%
Maximum sample slope	Up to 40°
Sample height	Up to 10 mm
XY sample stage	150 mm manual or Optional motorized stage
Z focusing	100 mm manual Or Optional motorized stage
Camera	Standard monochrome 640 x 480 High resolution
Software's system	Vision 64 analysis software on windows 7 Automated stitching, scatter and grid
Calibration	Via traceable step standard
System weigh	60 Kg

4.15 Work Piece Materials

The experimental work has been done by two different types of materials hard steel (EN31-64HNC) and mild steel (BS970 080440) as shown in Figure 4.12, the hardness of the two workpiece materials will be presented in Table 4.10 as below.

Table 4.10: Measured Hardness of Workpiece Materials

Workpiece materials	Hardness
hard steel (EN31-64HRC)	64.2 HRC
mild steel (BS970 080440)	90.1 HB

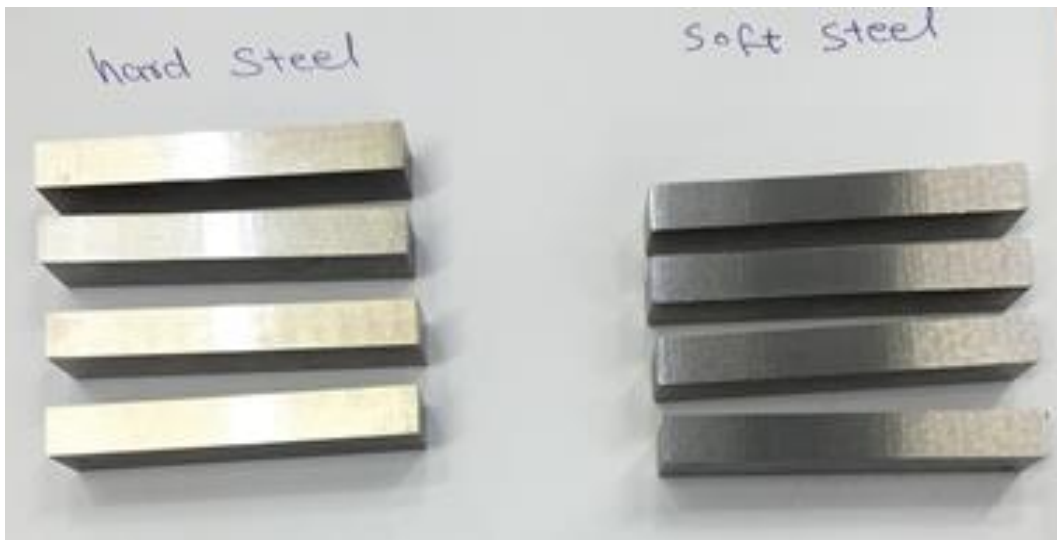


Figure 4.12: Work Piece Materials

The Experiment was done for the Grinding tests with single axis oscillation of the work piece with vibration, and the specification of the materials was as follows:

- The work Piece length was 70 mm.
- The work piece height was 14.9 mm
- width of grinding wheel contact with work $b_w = 8$ mm

4.16 Software

In this study two software packages were used, namely Matlab coupled with Simulink and Labview. Both software packages were key to the success of this investigation. A series of Labview codes (programmes) were developed and were used to test the self-contained oscillating jig in actual grinding and to collect initial experimental data.

Subsequently, Matlab was used to analyse the data and to develop the initial phase of the controller. This was achieved in Simulink and control Toolbox included in the Matlab package. Further development of programming code was undertaken to interlink Matlab and Labview to form a synchronised single system that realised the controller described in chapter 6.

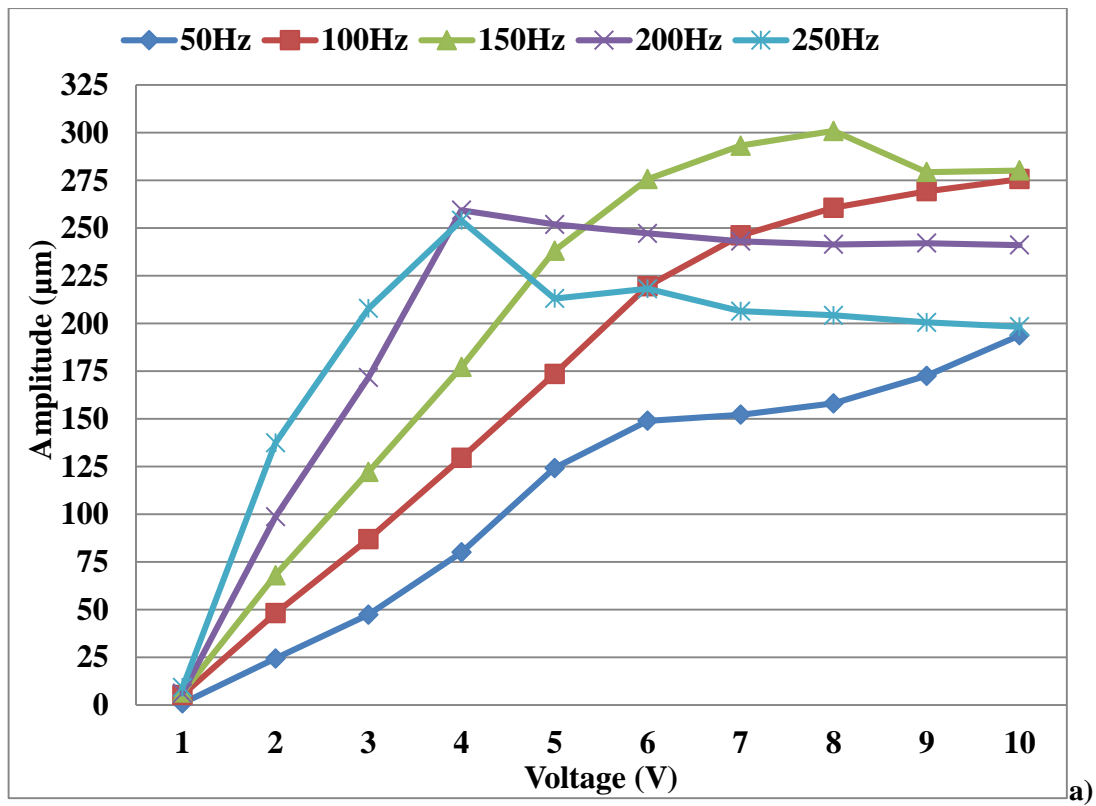
4.17 Identification of Optimum Driving Voltage and Frequency

In this investigation, the hypothesis was to achieve a displacement of the workpiece of at least 130 μm . The piezo actuator can be driven by up to 1000 volts. However, the power amplifier can take up 10 volts maximum at its input. Therefore after the selection of the displacement sensor a series of tests were made to identify the optimum parameter configuration that would provide target displacement at low voltage. The results obtained are illustrated in Table 4.11. Here it is observed that there are a number of combinations that secure a displacement close to the target 130 μm , these are highlighted in light blue. However high excitation voltage is not desired and it was observed that at higher frequency the oscillating jig started ringing at high pitch which was harmful to the operator and to the equipment. Also it was noticed that at higher frequency the grinding process was not performing as desired because of the jig design, which will probably need further modification to resolve these problems. Figure 5.7 illustrates the displacement (δ) performance envelope of the system as a function of frequency (ω) and driving voltage (v); δ , Dirac Delta function (ω , Angular frequency). As 100 Hz secured the target displacement with the lowest excitation, therefore, the system was driven at 4 volts and further experimental work was undertaken at 100 Hz.

Chapter 4. Equipment

Table 4.11: Recorded Amplitude

Excitation Voltage, V										
	1	2	3	4	5	6	7	8	9	10
Frequencies, Hz	Actual Displacement, μm									
50 Hz	1	24	47	80	124	145	152	158	173	194
100Hz	5	48	87	130	174	220	246	261	269	276
150Hz	7	68	122	177	238	276	293	301	279	280
200Hz	6	99	172	259	252	247	243	241	242	241
250Hz	9	137	208	254	213	218	207	204	207	198



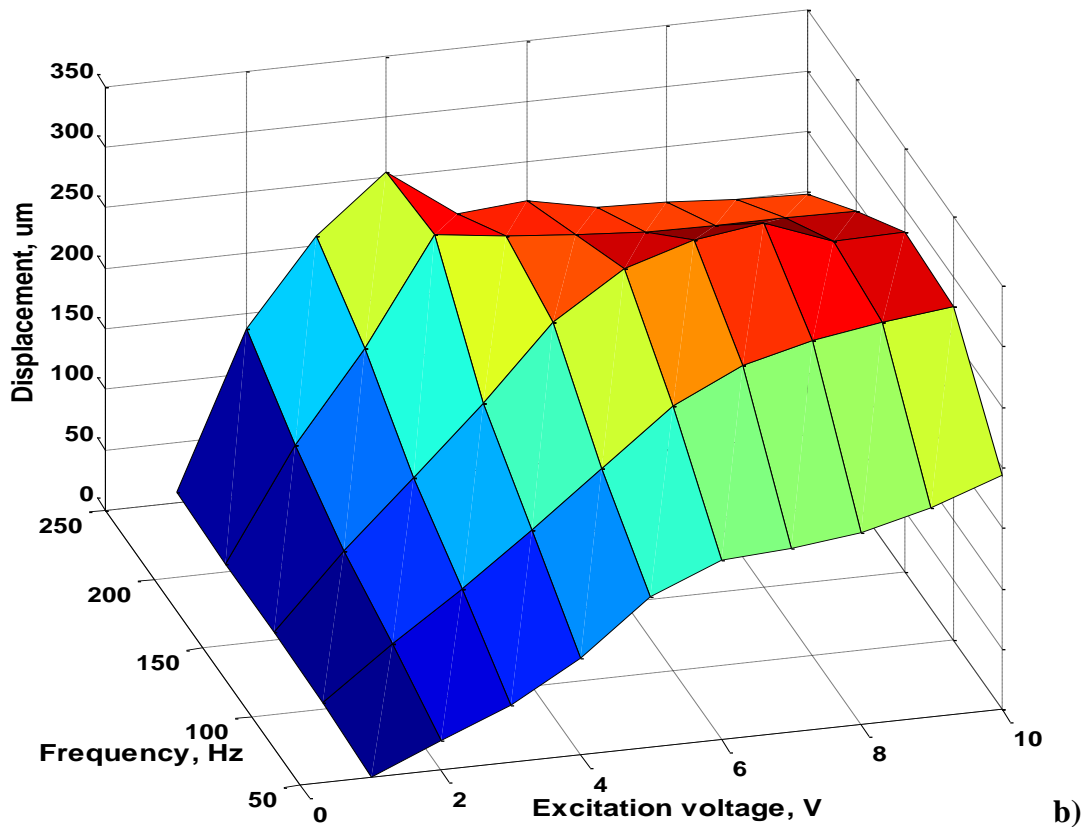


Figure 4.13: Displacement envelop $\delta = f(\omega, v)$

4.18 Remarks

During this calibration process key measurement parameters were adequately identified. This allowed selecting appropriate sensors. It was also revealed that at a certain level higher than 200 Hz, the oscillating was ringing at high pitch. The displacement envelop was produced and allowed for selecting the optimum driving voltage and frequency.

CHAPTER 5: GRINDING WHEEL HEAD RESPONSE

5.1 Introduction

The investigation into vibration assisted grinding is undertaken with five interlinked programmes running concurrently but with a shift in time between the programmes.

This allows the projects to feed one into another. Therefore, the work presented in this chapter was undertaken in the adjacent programme of work and shared across.

A proper and controlled application of vibration to any process requires a fundamental understanding of machine tool response to external excitation. Consequently, it was prudent to explore how the machine tool performed under external dynamic loading conditions. Stiffness and natural frequencies of the grinding wheel head were studied experimentally.

When a workpiece is machined, a high level of accuracy is always required. To achieving this, the machine characteristics and its dynamics must be properly analysed and studied, as machines respond differently to various excitations and inputs. In reviewing work that has been carried out in order to describe and model the dynamic characteristics of different machining processes including milling and drilling; in relation to computational modelling and simulation, (Xiao et al, (1992) were able to develop “Optimization Strategies” for a grinding cycle using intelligent plunge control, whereas Garcia-Gardea et al, (1980) followed a Dynamic Data System (DDS) approach to estimate the dynamic characteristics of the grinding process by analysing the cutting force signal; the work was based on the assumption that, during the grinding process, the cutting force signal should have all the pertinent features of the dynamics of the grinding process. The (DDS) approach also provides better accuracy in terms of grinding dynamics modelling as the modelling was based on real experimental data that was obtained from a grinding operation.

Also Chiu and Malkin, (1993) successfully developed a computational model of a cylindrical plunge grinding wheel; in addition to modelling the behavior of the grinding process itself, the simulation was able to predict failure modes in the process caused by high grinding forces, material removal, thermal expansion, Thermal damages and wheel wear. An interesting feature in this modelling was that, it was able to map a time-dependent grinding process with the finished part quality.

Chapter 5: Grinding Wheel Head Response

The simulation was run by developing a virtual grinding machine that was constructed on a computer; the input parameters for this model were:

- Grinding fluid
- Grinding wheel specification
- Spindle vibration
- Workpiece material specification
- Dressing specification
- System stiffness, and
- Workpiece grinding requirement.

In their work, Kang et al, (2001) used the Finite Element Method (FEM) to model harmonic response of a milling machine. Static, modal and stability analysis were conducted in order to identify the stability margins. The natural frequency of the system was identified, and frequencies and modal shapes allowed them to obtain instability speed threshold.

In order to analyse the dynamic characteristics of the grinding process, and also to examine the effect of parameters such as vibration frequency and amplitude on the grinding performance, a non-linear model was developed by (Kirpitchenko et al, (2002). This model looked into the grinding kinematics by examining the motion of every cutting grain of a grinding wheel relative to a ground component; in this work, the grinding operation was controlled by a control system using two scenarios:

- Minimum bending moment condition at the spindle bearing for both static and dynamic cases; a key benefit for this control scenario is that the control system becomes independent of the input force excitation frequency. The down side of such system is that the relative displacement between the grinding wheel and the workpiece was not maximized.
- Minimum relative deformation at the contact surfaces between the grinding wheel and the workpiece; in this control scenario, it was shown that the proposed control system strongly depended on the input force excitation frequency.

Chapter 5: Grinding Wheel Head Response

As for modelling the grinding tool dynamics, (Orynski and Pawlowski, 2002) developed a model of cylindrical grinding which consisted of a grinding wheel headstock connected to hydrostatic slide ways, a headstock drive system, a grinding wheel and hydrostatic bearings to support the grinding wheel spindle. In this model, the workpiece was mounted on a table with the hydrostatic slide ways dead center. The model analyzed the dynamics of the grinding wheel headstock in idle condition. An experiment was conducted, in which, the table was allowed to vibrate perpendicular to the direction of its hydrostatic slide ways and the grinding process was examined using simulation programs; and they managed to identify a correlation between the vibration and the performance of the grinding process.

Zhang et al, (2005) examined ways of reducing the vibration-caused surface roughness of a workpiece in a grinding process, in doing so, a dynamic analysis of the grinding process was necessary, in which, there was an attempt to determine the frequency-amplitude characteristics of the grinding process. The characteristics of the model used model were as follows:

- Grinding wheel 250 mm made of Synthetic Aluminium oxide
- Grain size 0.4-0.5 mm
- Cutting speed range 30-35 m/s
- Depth of cut range 0.005-0.03 mm
- Vibration Frequency Range 0-120 Hz
- Vibration Amplitude Range 0.001-0.002 mm

The results concluded that, the model was only valid for the considered range of vibration frequency; this is because the machine behavior is a function of the vibration frequency.

Cheng et al, (2007) attempted to model the frequency response of a tool holder of a milling machine. The objective of the modelling was to identify the Frequency Response Function (FRF) of the milling machine; using an impact test while the spindle was stationary. The experiment provided reasonable accuracy in predicting the system response; however, some variations could be identified as the speed increased. The work of Jiang et al, (2007) described the dynamics of a cylindrical grinding machine by utilising modal experimental data. In this work, typical values of the machine-produced vibration were collected and avoided during the grinding process.

In their experiment, 25 measuring points were set on the machines and readings were collected using non-contact displacement sensors and accelerometers. The natural frequency of the machine in static mode was identified in a first experiment, in which the input excitation force was produced by an impact load, whereas, a second experiment identified critical frequencies for wheel rotating speeds ranging from 70-700 RPM. The same test was repeated in a real grinding process in order to reveal critical vibration frequencies that should be avoided during the process. The correlation between the workpiece spindle speed and the surface coarseness concluded that, as the spindle speed increases the surface roughness of the workpiece improves, and that is why grinding speeds are normally high.

A relatively recent work was conducted by Filiz et al, (2009) in which, the frequency response of a tool holder was studied. As for grinding processes, important parameters such as natural frequency, effective grit pass and grinding wheel contact dynamics are normally modelled theoretically, then experimental work is done in order to compare with theoretical modelling.

5.2 Spindle Unit Static Stiffness and Compliance

Dynamic stiffness of a machine tool is a key parameter that affects the quality of machined parts in terms of accuracy. Mainly, spindle units are subjected to various tests to identify their actual stiffness and compliance, which are key characteristics for any given spindle configuration.

Lee and Furukawa, (1988) attempted to define static and dynamic stiffness of a cylindrical grinding machine; considering the contact stiffness between the wheel and the workpiece, they concluded that the stiffness was dependent on the grain size and hardness characteristics of the wheel; and by conducting a number of experiments, a contact stiffness was derived.

Attempting to improve workpiece surface quality (Jenkins and Kurfess, 1996) modelled the dynamic stiffness of a spindle unit of a grinding machine. The model consisted of an excitation input system consisting of an electromagnetic shaker which was used to excite the system at different frequencies (ω) ranging from (30-5000) Hz.

Chapter 5: Grinding Wheel Head Response

In the experiments, the spindle unit response at resonant frequency was observed and monitored and stepped sine sweep tests were performed, with the aid of accelerometers, force sensors and eddy current probes for measurements of actual displacement, a displacement function of the tool-end was successfully obtained in terms of the input applied force frequency. This was due to the fact that the dynamic stiffness is a dependent variable of the input frequency (ω) of the applied force and the system physical constants.

The experimental work considered three different directions, and multiple natural frequencies were identified, each related to the direction considered. Results concluded that, for the spindle unit, several resonance frequencies were identified at which the dynamic stiffness should reduce.

As far as the surface finish effect and the influence of the input force on the system are concerned, different wheel speeds at different work speeds were experimented, and at 160 RPM wheel speed and 4 mm/s and 5.33 mm/s feed rates, larger forces were observed in comparison to 120 RPM wheel speed. In order to maintain the same theoretical surface finish, these two feed rates were kept constants throughout the experiments.

The dynamics of cylindrical grinding were described and modelled by Orynski and Pawlowski, (2002). The distinctive feature of this work was that, it was able to successfully measure the static rigidity of the grinding wheel, the headstock and the workpiece.

Zaruba, (2005) was also able to determine the static stiffness and the compliance matrix of a cylindrical grinding system. In this work, two forces conditions were examined:

- Static forces condition: these forces were related to slow changes of relative position between wheel and workpiece related to a frequency of zero.
- Dynamic forces condition: these were related to the working frequency of the rotating wheel.

Chapter 5: Grinding Wheel Head Response

In cylindrical grinding, this type of chatter is normally caused by the workpiece whereas in cylindrical/surface grinding, it is normally caused by the wheel. In this case, wear resistance in the wheel causes waves to generate rather slowly on the surface of the wheel. As the vibration amplitude started to increase, until it reached a critical limit, the wheel re-dressing end life would have been reached, (Marinescu, 2007). An important conclusion that was drawn out of the experiment was that grinding at the system resonance frequency could improve the surface finish. Additionally, workpiece-tool interaction could cause variations in terms of actual resulting frequencies. However, improving the understanding of the process at resonance frequencies would require taking into consideration the effect of chatter, (Jenkins and Kurfess, 1996).

In this work the Abwood grinding machine tool was used, therefore, the static stiffness and compliance of the spindle unit were identified using the following procedure. A hydraulic jack was placed below the tip of the spindle, and applied a range of forces at the point where the grinding sits. The direction of the external force was parallel to the normal grinding force. The applied force was measured by the dynamometer (KISTLER 9257A) - which was located underneath the jack as illustrated in Figure 5.1. To measure spindle deflection, a dial gauge indicator was positioned on the top of the spindle unit. The applied force was recorded using the aforementioned Data Acquisition System.

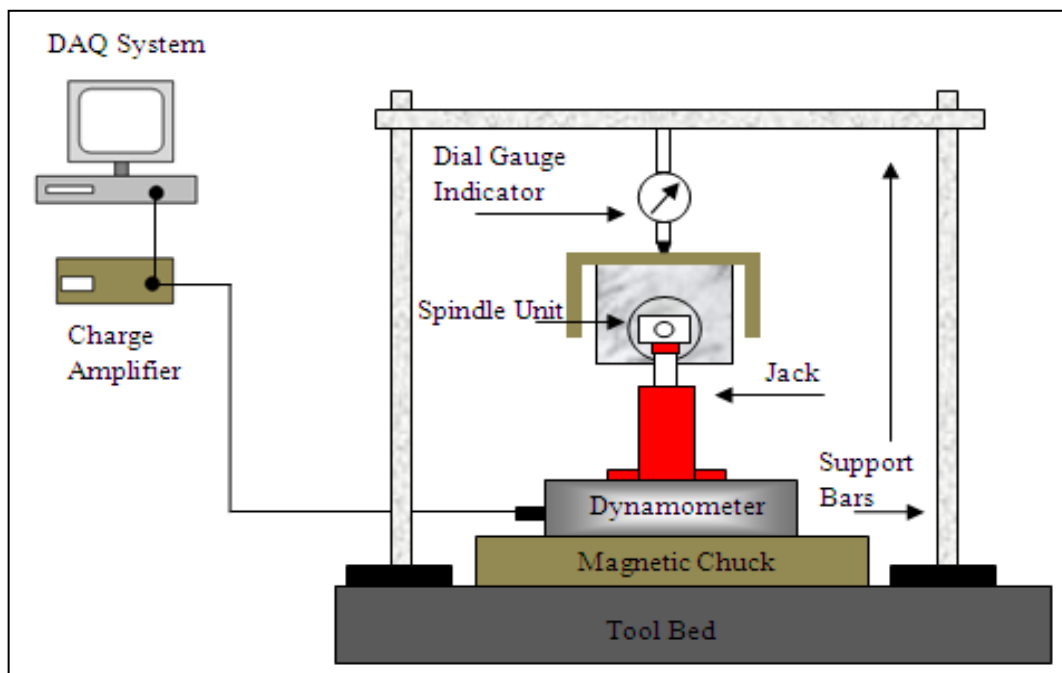


Figure 5.1: Set-Up for Measuring the Static Stiffness of the Spindle Unit

A series of readings were recorded and the force-deflection graph was derived as show in Figure 5.2

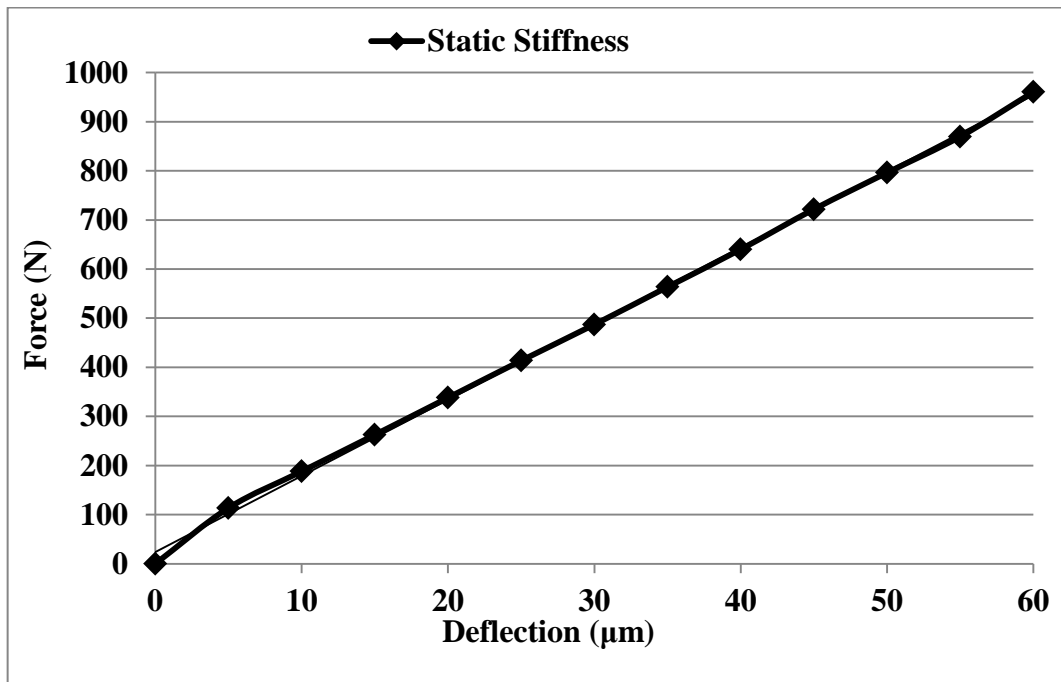


Figure 5.2: Static Stiffness of the Spindle Unit

It is observed that the force-deflection- relationship is linear thus the average stiffness of the spindle unit was defined by linear approximation as $K = 16.67 \text{ N}/\mu\text{m}$. The compliance, being the inverse of the stiffness was defined as $C_s = 1/K = 1/16.67 = 0.059 \mu\text{m}/\text{N}$.

5.3 Natural Frequency of the Spindle Unit

It is well known that system static response differs from dynamic behavior. Therefore, following the static test, the spindle unit in stationary mode was subjected to harmonic excitation using a piezoelectric actuator. A range of frequencies was swept through and a high-resolution displacement sensor recorded the deflection for given frequencies. Figure 5.3 depicts the full configuration of the experiment set up.

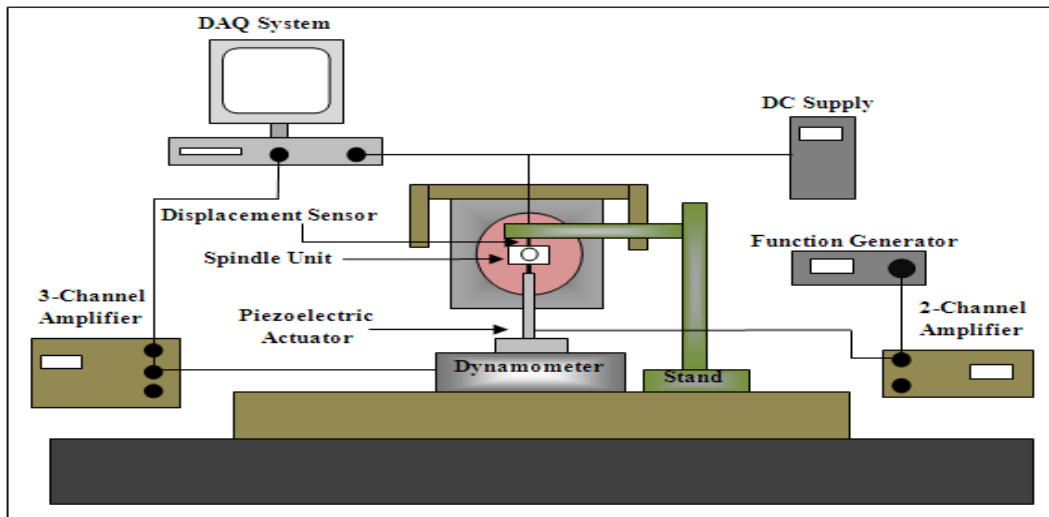


Figure 5.3: Experimental Configuration for Sweep-Sine Test of the Spindle Unit

The vibration was applied in the vertical direction; hence, thus vertical deflection was recorded. The piezoelectric actuator was perpendicular to the magnetic chuck and the wheel spindle. The function generator produced a sine wave, the amplitude and frequency of which was controlled. The displacement sensor was also set perpendicular to the spindle and in line with the piezo actuator. The applied force was kept constant, whilst the frequency varied. The graph in Figure 5.4 shows the amplitude frequency characteristics of the spindle unit for two average force inputs i.e. 44 N and 64 N.

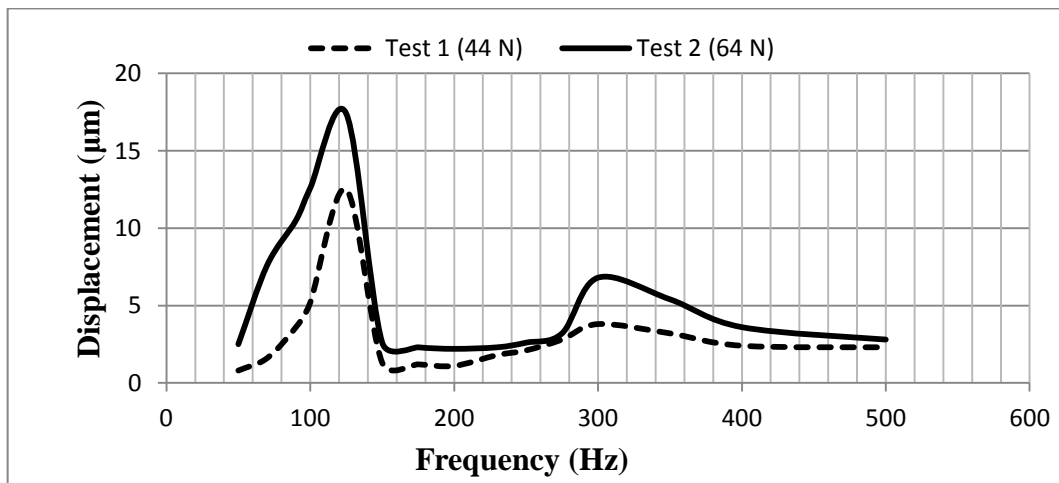


Figure 5.4: Frequency-Amplitude Characteristics of the Machine Tool Spindle Unit Two excitation forces were applied to the spindle unit and with the sweep-sine test, the natural frequency of the spindle was identified as 125 Hz with a maximum deflection at 12.5 μm for 44 N average force and 17.4 μm for 64 N. A second peak was observed at 300 Hz.

5.4 Dynamic Stiffness of the Spindle Unit

The method presented by Jenkins and Kurfess's, (1996) was used to identify the dynamic stiffness of the machine. The spindle unit was excited using a piezoelectric actuator and was considered as a single degree of freedom system with forced vibration and the effect of damping was not taking into account. Here, a sweep-sine test was used to excite the spindle from 50 Hz to 500 Hz at a fixed magnitude. Noting that the spindle resonance frequency was 125 Hz, Figure 5.5 shows the profile of the system dynamic stiffness K which was defined as:

$$K_d(s) = \frac{F(s)}{X(s)} \Big|_{s=j\omega}$$

Where $F(s)$ is the applied force; $X(s)$ is the displacement

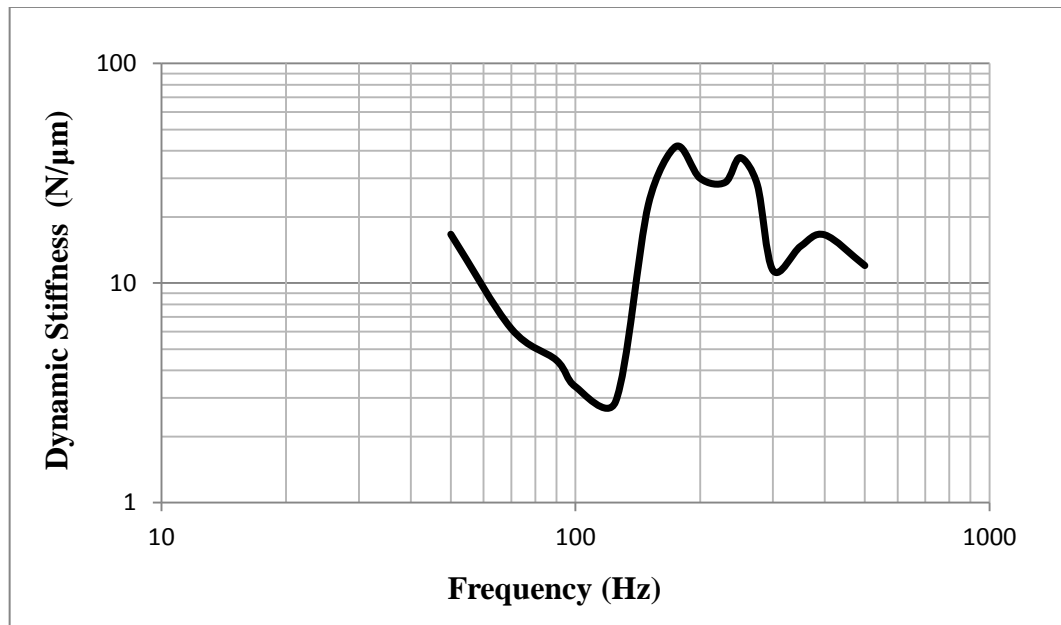


Figure 5.5: Dynamic Stiffness of the Spindle Unit

Figure 5.6 shows that at the resonant frequency (125 Hz), the system has the lowest stiffness. Conversely, at the resonance, the machine tool exhibited the highest compliance. It is seen in this figure that the machine tool has its higher dynamic stiffness between the two resonance peaks. The output of this experimental work was used to design an oscillating jig and to avoid the resonant modes during the grinding process.

The dynamic compliance of the machine tool was defined as the inverse of the stiffness and Figure 6.6 shows the dynamic compliance of the machine tool, where at the resonance (125 Hz) the compliance was $0.36 \mu\text{m}/\text{N}$

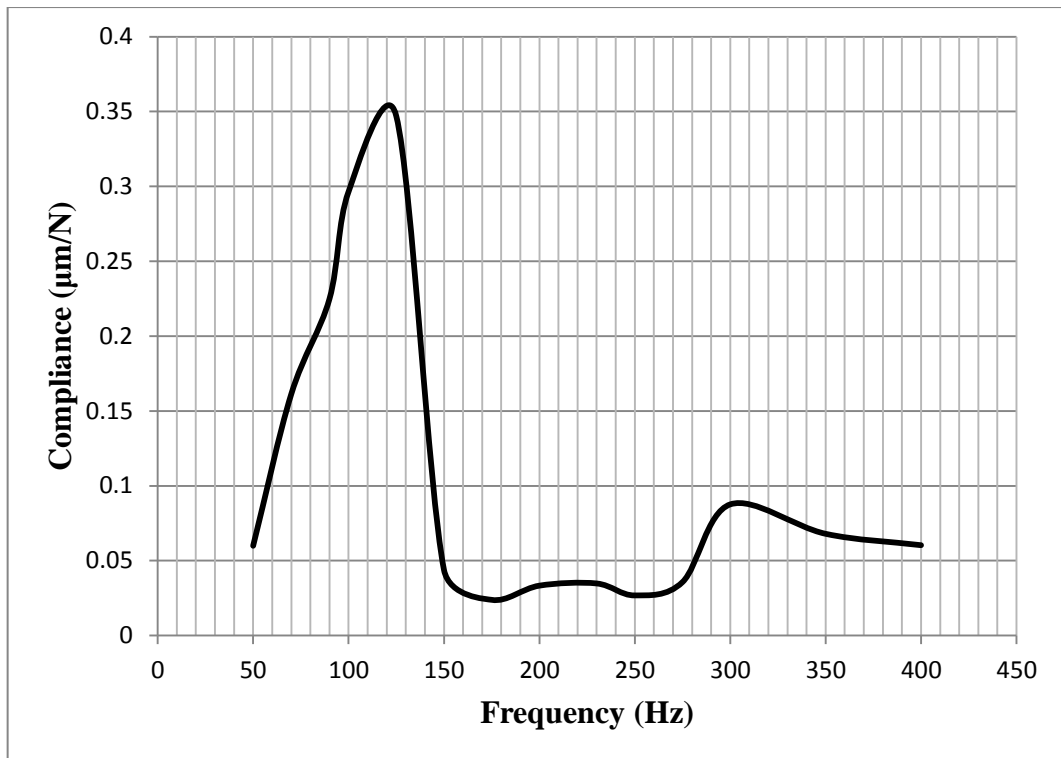


Figure 5.6: Dynamic Compliance of the Spindle Unit

5.5 Frequency Response of the Spindle Unit – Rotating Mode

The aim of this experiment was to obtain the response of the grinding wheel head for the wheel speeds used for actual grinding tests. Here, an accelerometer was mounted on the top of the grinding wheel guard and recorded the vibration of the wheel head while the grinding wheel was spinning. Labview was used to acquire and analyse the data in the frequency domain. The results are illustrated in Figure 5.7; it is observed that at 2400 rpm the wheel head showed a resonance peak at 1350 Hz with acceleration of about 0.014g. Therefore, the bulk of the experiments in this work were carried out at 2660 rpm to avoid this resonance though it has negligible amplitude.

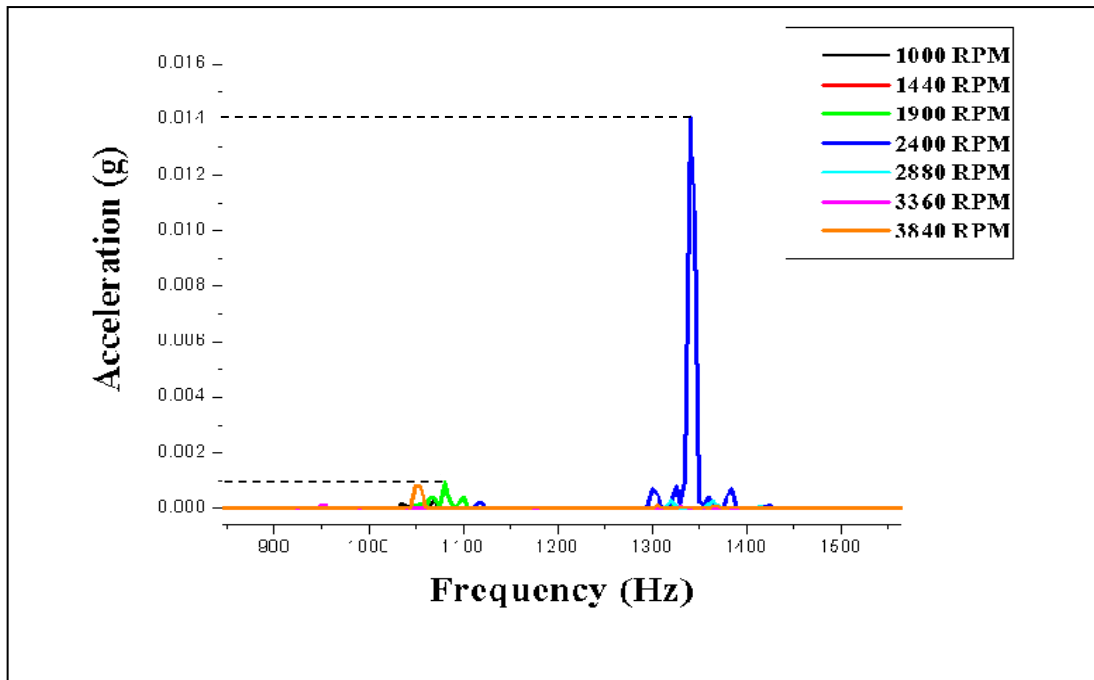


Figure 5. 7: Frequency Response of the Wheel-Spindle System at Various Wheel Speeds

5.6 Observations

The static stiffness of the grinding machine spindle unit was undertaken and the study of the spindle resonance frequencies was used to design the oscillating jig to avoid spindle resonance during machining. The test with the rotating grinding wheel showed that at 2,400 RPM the spindle unit had a kind of resonance peak but at high frequency. Though the amplitude of that peak was small it was prudent to run the experimental work at 2,660 RPM.

Chapter 6: CONTROLLER DESIGN

6.1 Introduction of Mathematical Model

Mathematical models of physical devices are used to design and analyse controllers for these systems. Mathematical models are described by ordinary differential equations. A few generic elements are required in order to design and implement a control system. These elements are the knowledge of the desired value, the knowledge of the outputs, the knowledge of the controlling devices, the knowledge of the actuating devices and knowledge of the main plant Giordano et al, (2008). Figure 6.1 below shows the steps in designing a control system.

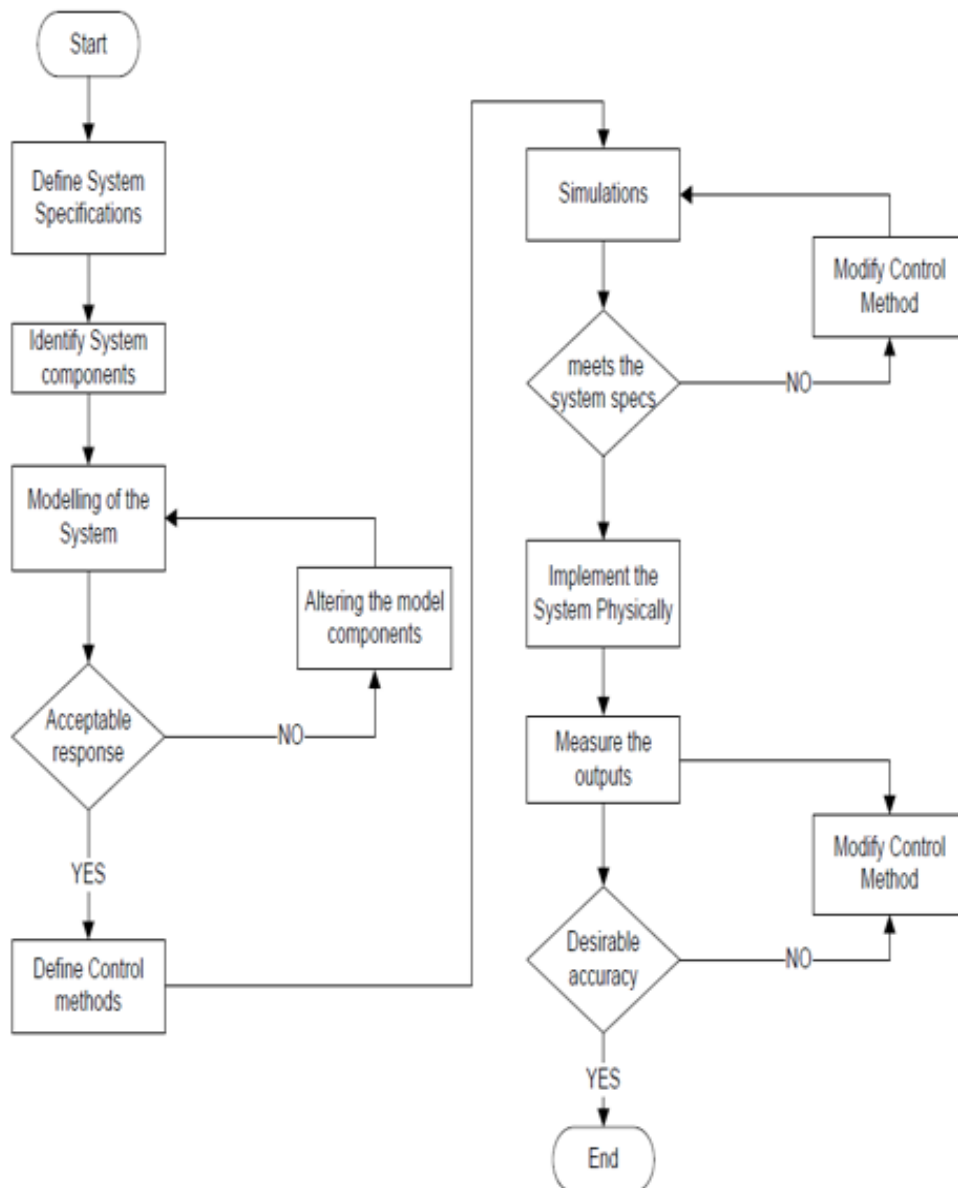


Figure 6.1: Flow Chart Illustrating the System Controlling Strategy

6.2 Mathematical Model for the Oscillating Jig under Grinding Load

The controlled system had an input variable (reference input) and an output variable (controlled value). The system response was described in terms of dependence of the output variable on the input variable. These responses between one or several variables can be described using mathematical equations based on physical laws. Such physical relationships can be determined by experimentation.

A mathematical model was derived from the actual oscillating jig designed for the preliminary investigation in order to design a closed loop control system. Below are key points for the use of mathematical modelling:

- Develop a better understanding of the design system
- Allow to design a controller and test it without any risk
- Low cost production

Most of the work done on the topic of vibratory machining mainly states the amplitude and the frequency generated by the oscillator. However, the actual magnitude to the oscillatory displacement achieved in the cutting zone is rarely reported. Therefore this project was set up to actually control the amplitude of the vibration in the cutting area. A typical mathematical model derived from the actual oscillating jig designed in previous studies was used for the preliminary investigation into the design of a closed loop control system. Below are the equations of motion of the initial jig to be controlled.

$$(m_{pz} + m_r) \frac{dy^2}{dt} + (C_{pz} + C_r) \frac{dy}{dt} + (K_{pz} + K_r) dt = F_{pz}(t) - F_t(t) \quad (6.1)$$

$$\frac{dy^2}{dt} = \frac{F_{pz}(t) - F_t(t) - (C_{pz} + C_r) \frac{dy}{dt} - (K_{pz} + K_r) y}{(m_{pz} + m_m)} \quad (6.2)$$

m_{pz} = equivalent mass of the piezoelectric translator

m_r = Mass of the moving part in the workspace table

C_{pz} = equivalent damping coefficient of the piezoelectric translator

C_r = equivalent damping coefficient of the springs

K_{pz} = stiffness of the piezoelectric translator

K_r = stiffness of the springs for preload

F_{pz} = force generated by the piezoelectric translator

F_t = tangential grinding force

However, the finding at this first stage was used to design more efficient and compact stackable and tuneable oscillators.

In order to apply vibration to machining, an in-depth understanding of grinding/machining technology was required. A sound knowledge of dynamics and control system is a pre-requisite for successful design, modelling and implementation of a two-dimensional oscillation and to control and synchronise the vibration so that the prescribed elliptic motion of the workpiece could be achieved.

A wide range of frequencies of vibrations have been investigated and avoidance of the natural frequencies of the spindle unit was in focus.

The amplitude of the oscillations varied from a few microns to hundreds of microns. However, it is well known that there is an inverse relationship between the amplitude and the frequency, and this has been taken into consideration. Piezo actuators were used to generate oscillations and the effects of saw tooth, sine and square wave was tested.

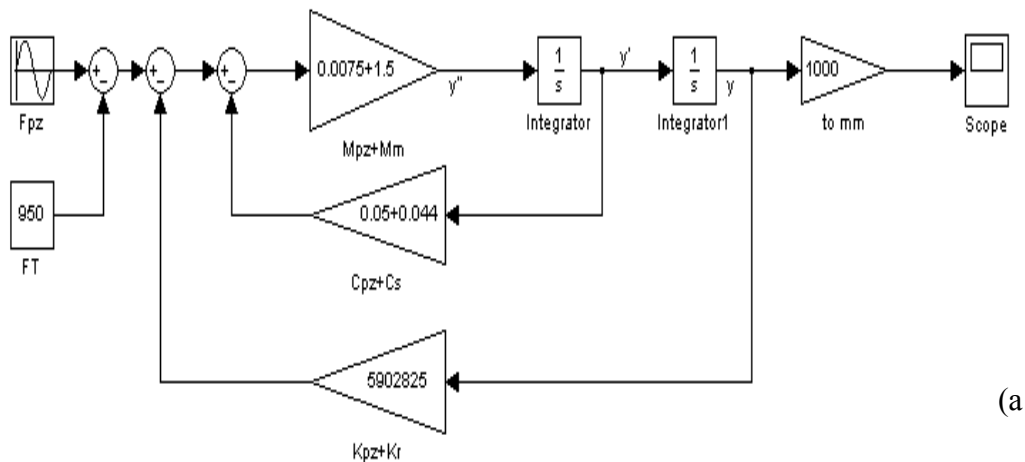
A sound understanding of control systems, sensor, signal, noise and signal to noise ratio and hands-on Matlab & Simulink and LabVIEW are required in order to successfully implement the programme outlined above.

6.3 Design of Controller

To control the amplitude of the vibration of the oscillating jig, a basic PID controller was designed and simulated. The design involves control of the first mode of the vibrating system using a second order model. The controller output is sent to the power amplifier only when the displacement exceeds 130 μm . The Simulink code and the response of the controller signal are shown in the Figure 6.2 (a) and (b) respectively.

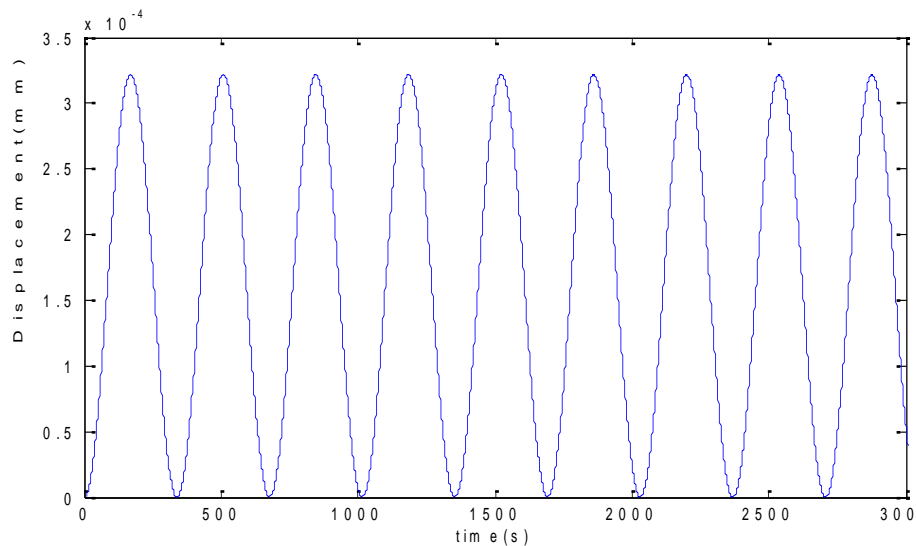
6.4 Modelling & Simulation

The proportional-integral-derivative PID controller was designed to stabilise and control the amplitude of displacement of the vibrating jig. A proper model for the system has been built using a mathematical model. This model was used to find analytical solutions for the problem and to enable the prediction of the system behaviour from a set of parameters and initial conditions.



(a)

Figure 6.2a: Applying Open Loop Control Strategy



(b)

Figure 6.2b: Result of Applying Open Loop Control Strategy

The simulation result in Figure 6.2b showed that the output had uneven amplitude. It meant that the response of the system did not satisfy the requirements. It was also noticed at the start that the oscillation frequency remained stable with time.

It was also observed that the range of the velocity was out of the design criteria. The system settling time was not satisfactory. After some trials are as shown in appendixes G, the PID controller parameters k_p and k_i were corrected.

6.5 Simulation and Analysis the Model With the PID Controller

The simulation of the unity feedback system response was performed using MATLAB that allowed tuning the PID controller parameters. The unit step input response of the system is shown in Figure 6.3a, where the PID controller displayed a good performance. Here the results showed that the rise time, peak time, maximum overshoot and settling times are; 0.45 sec, 1.145 sec, 0.145 sec and 2.49 sec respectively for the unity feedback system. So it can be concluded that the PID controller methods is suitable to control the grinding vibration system, Using this approach, a controller has been designed successfully for closed loop operation of the vibration system and it runs faster and not very close to the reference.

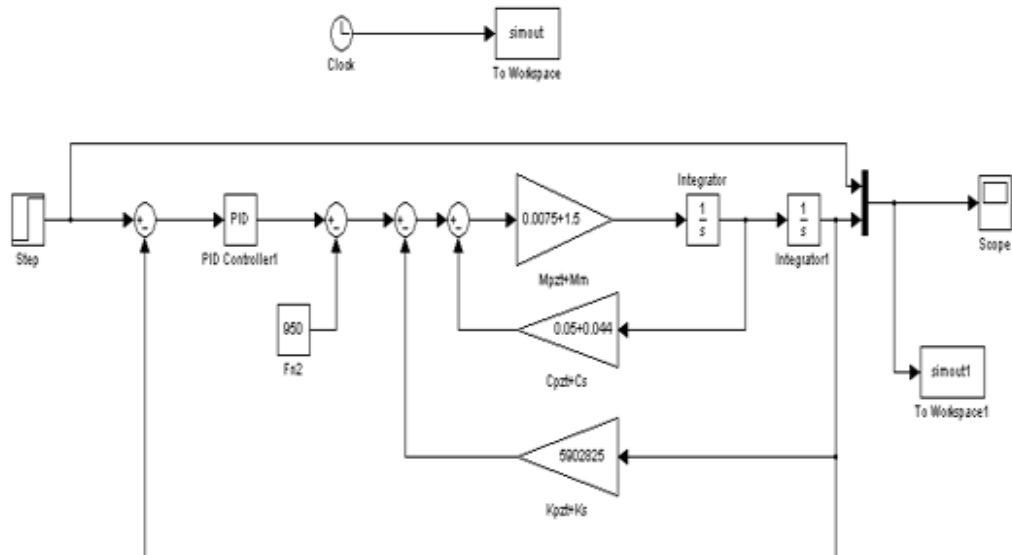


Figure 6.3a: Applying Closed Loop Control Strategy System Identific a)



Figure 6.3b: Result of Applying Closed Loop Control Strategy System Identification

It can be concluded that the closed loop unity feedback and unit step response of the system shown in Figure 6.3b, with the controller in Figure 6.3a were suitable to design a self-tuning system, where the speed of response has significantly increased and the steady state error approached zero.

6.6 The Experimental System

In order to verify the effectiveness of vibration control strategies, Labview was used to set up a data acquisition system (DAQ) that allowed embedding the control into the code as illustrated in Figure 6.4. The setup consisted of the main parts: the software interface, the visuals and the control algorithm to process the measured signal and issue the appropriate control signal. The accelerometer was used to condition the system response. The DAQ had analogue and digital inputs and output (I/O) through the NI 9233, which allowed for controlling the power amplifier that drives the piezo actuator. The LabVIEW code developed for this investigation was the key tool for the experimental work. It collected data from various sensors including the accelerator which was controlling the feedback signal. Based on the numerical value of the latter signal, the control algorithm made the required adjustment and feedback to the power amplifier. By tuning the PID controller a proper control of the actuating displacement of the vibrating system was achieved.

6.8 Basic Idea and Design Consideration

The target of this work was to design a LabVIEW based self-tuning PID controller and to verify its performance in the actual vibration assisted grinding process. At the starting point an existing open loop system configuration was used to identify initial parameters. This was achieved in a series of test grinding, data collection and analysis. This allowed defining sets of parameters for the closed loop controller. In actual grinding tests, the controller reacted adequately to the persistent offset error value as a result of load disturbance or set point change. Practical result showed that such a controller may be adapted to control a variety of industrial processes.

6.9 Experimental Implementation

The evaluation of the performance of the controller through the experiment was an essential part of the design. To substantiate the design and simulation results, the controller designed was incorporated into a full experimental set up which is shown in Figure 9.4 based on initial and calibration results, the grinding trials were undertaken at frequency 100Hz, with a sinusoidal excitation signal of 4 volt peak to peak, which equated to 130 μm oscillation amplitude.

6.9.1 Model Identification from the Data

A set of experimental data was acquired and as stated previously, the input and the output had been divided into two parts i.e. first subset contained 850 data points (1-850) and second subset contained 850 samples (851-1700). The first part of the input and output signals was used to obtain the vibration plant model and the second part of the input and output signals was used to validate the obtained model using the Matlab identification toolbox.

The following procedure was used. First, measurement data such as input voltage, sampling time and output acceleration was loaded in Matlab. Then the input signal (u) vector and output (y) vector were initialized in Matlab work space and the system identification toolbox was activated. The data (input and output data array) were imported and the starting point was set to zero and sampling interval to 0.001sec.

Figure 6.6 shows the time domain representation of observed data, both output acceleration and input voltage plotted with respect to the sampling time period.

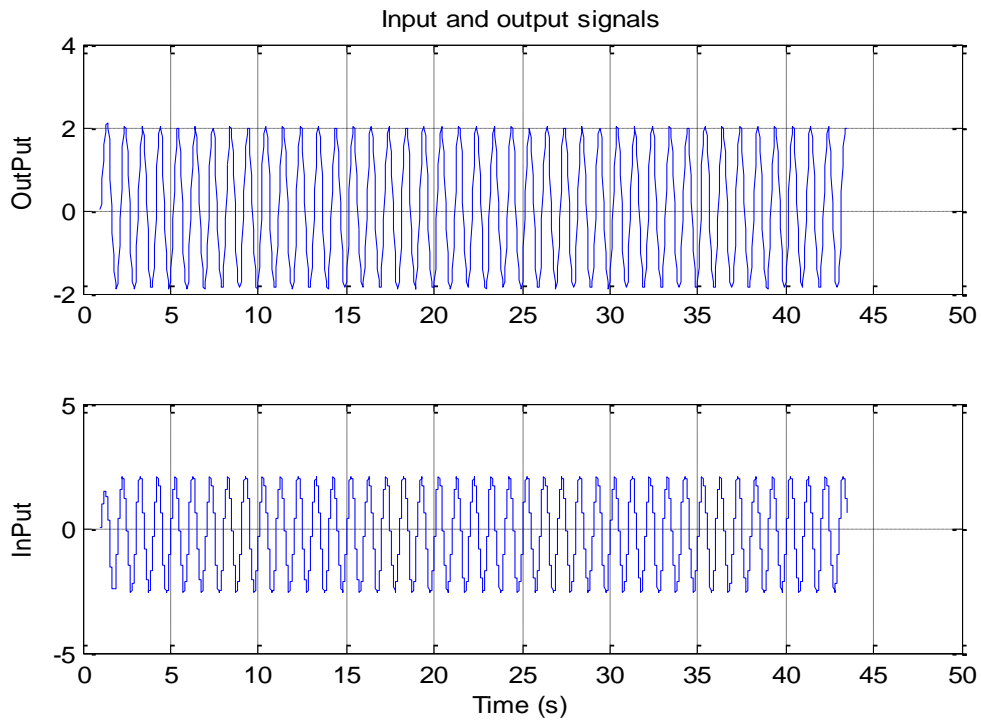


Figure 6.6: Time Domain Representation

In Figure 6.7 show the technique used to measure the phase angle between two periodic signals. The technique works by tracking the location where the signals change from negative to positive. The exact zero crossing of the signals estimation is done by interpolating the negative and positive point.

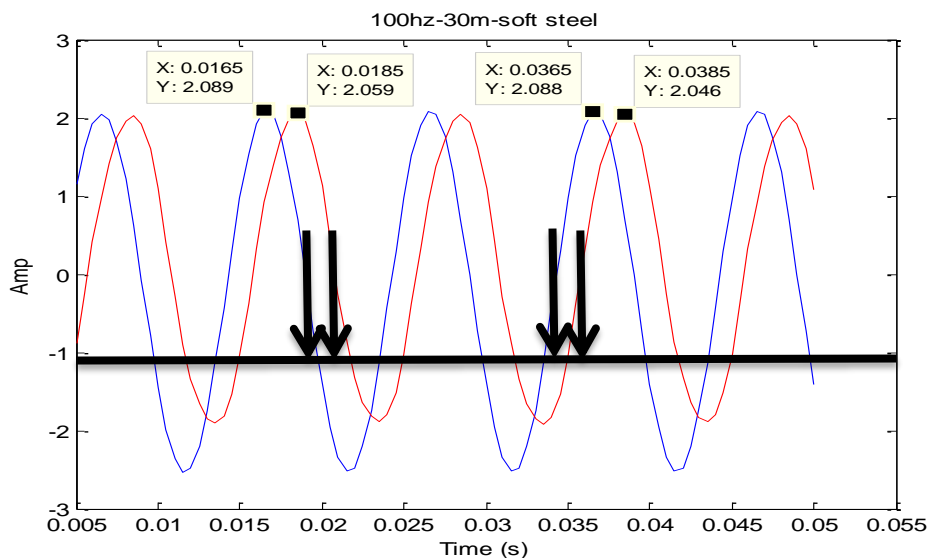


Figure 6.7: The Input and the Output Signals

Chapter 6: Controller Design

Using the ARX approach for identification, the result is compared with the time domain data following as illustrated in Figure 6.8. From this plot it is seen that the hypothesis limits are the red lines and it can be seen that none of the autocorrelations is significant the horizontal axis is the lag for the autocorrelation.

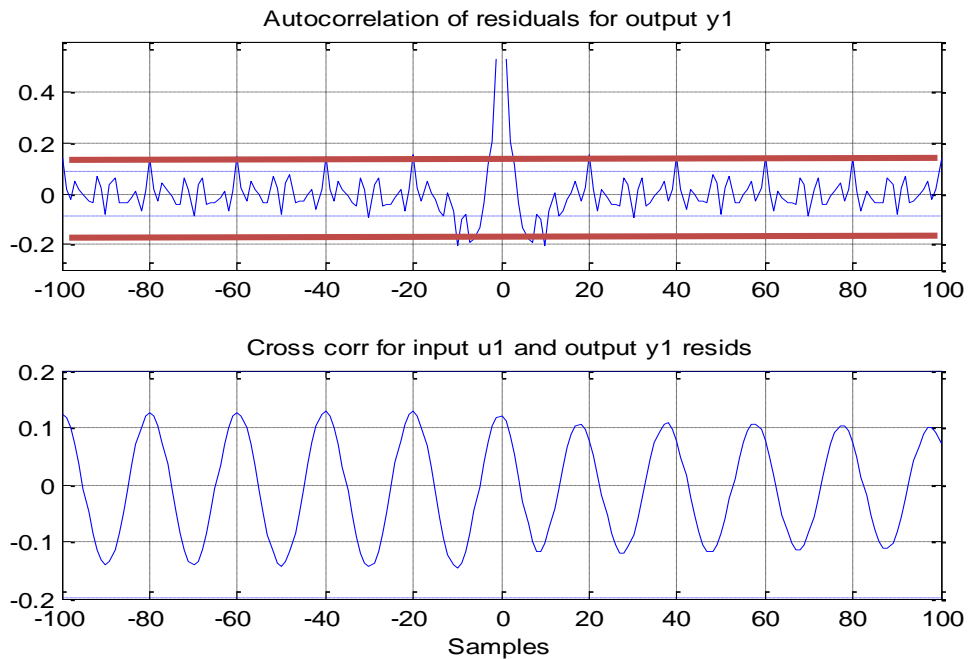


Figure 6.8: Model Parameter

6.9.2 Validation Result

As the data were divided into two groups, the second lot of data was used to validate the correctness of the identified model. Using system identification toolbox, the model was validated and illustrated in Figure 6.9. For a given set of input data, the tool box computes the output of the identified model and by comparing the output with the measured output from the real system. It is found that the mode frequency obtained from the identified model is 91.09 Hz and it's close to the experimentally measured mode frequency 91.08 Hz. This procedure helps avoiding over fitting as depicted in the flowing plot 6.9.

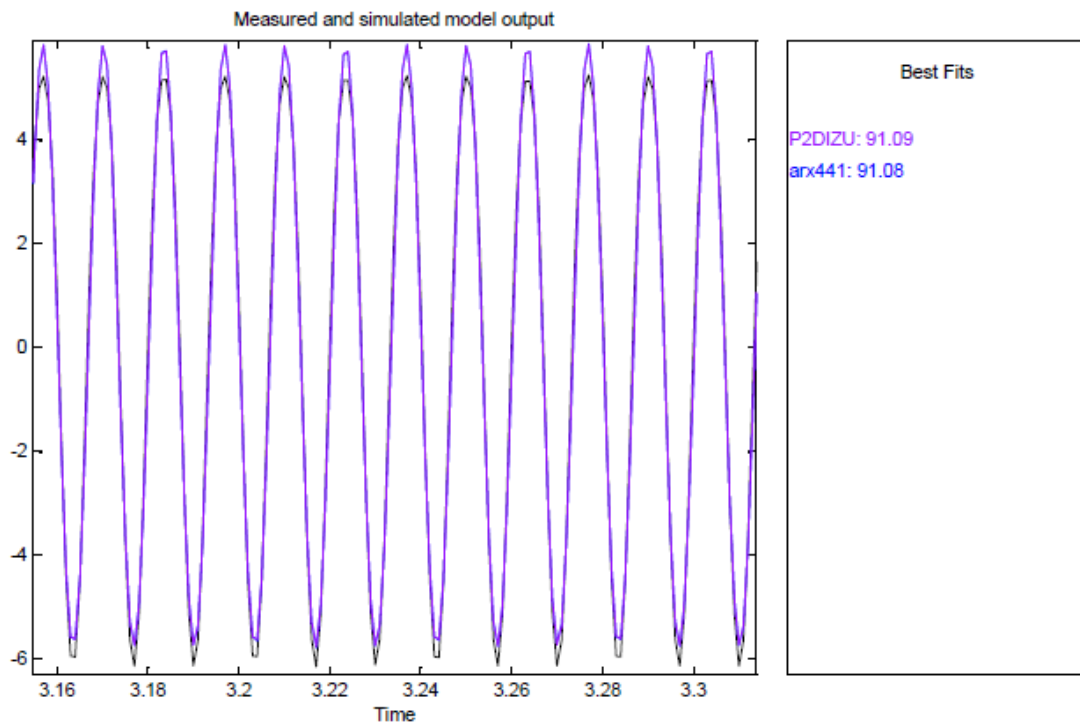


Figure 6.9: Validation

6.10 Experimental Result

The designed PID controller was aimed at reducing the error and eliminating the need for continuous operation attention. A set point is where the measurement is desired to be and the error is defined as the difference between the set point and the measurement. Thus $(error) = (set\ point) - (measurement)$.

The code is inside the M-script, the heart of strategic action and decision making of the controller. The controller outputs pass through gates that limit the outputs between 0 to 4 volts (i.e. 0-130 μm).

The outputs of the blocks are then given to the transfer function model. The controller output as well as output of the transfer function model are stored in the excel sheets during program runtime. The front panel displays the closed loop response with PI control and its control signal obtained through simulation is displayed in Figure 6.10. The designed values are $K_p=800$, $K_i=0.2$ and since K_d has very small action therefore it was opted for a PI controller. The simulation code shows in Appendix G, of the controller with the closed loop response signal obtained through simulation is shown in Figure 6.10.

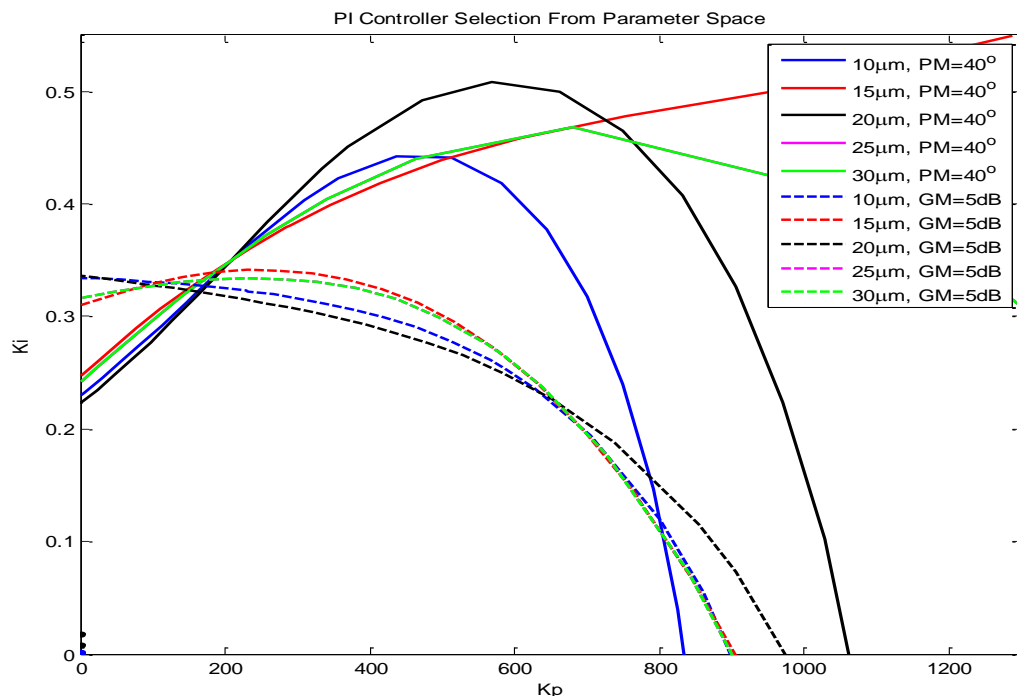


Figure 6.10: PI Controller Selection from Parameter Space

Chapter 7: PRELIMINARY STUDIES

7.1 Introduction

At this early stage, a preliminary study was undertaken to investigate into the performance of vibration-driven grinding. The results of this study would help to refine and fine-tune the design of a closed loop controller for the final full experimental work.

This Experiment presents a real Open Loop system of vibration, which was designed using the LabVIEW software package. A real - time position control of the piezo actuator was realized by using DAQ system, the signal of an accelerometer was used as a feedback to the control system. The system included a displacement amplification bridge, an accelerometer, a charge amplifier, the data acquisition system, a power amplifier for the piezo-actuator and the data acquisition system. The basic idea is to use the vibration generated by the piezo actuator to control the displacement (amplitude) of the vibration in the grinding contact zone. Data acquisition, signal processing and analysis were implemented by virtual instrument based on LabVIEW. In this experiment the materials used were hard steel (EN-31-64HRC) and mild steel (BS970 080440).

7.2 Experimental Configuration

The open loop framework is illustrated in Figure 7.1 in terms of configuration. Here a sine wave generated by a function generator is fed into the power amplifier, which drives the piezo-actuator installed within the displacement bridge that is enclosed in a self-contained oscillating jig.

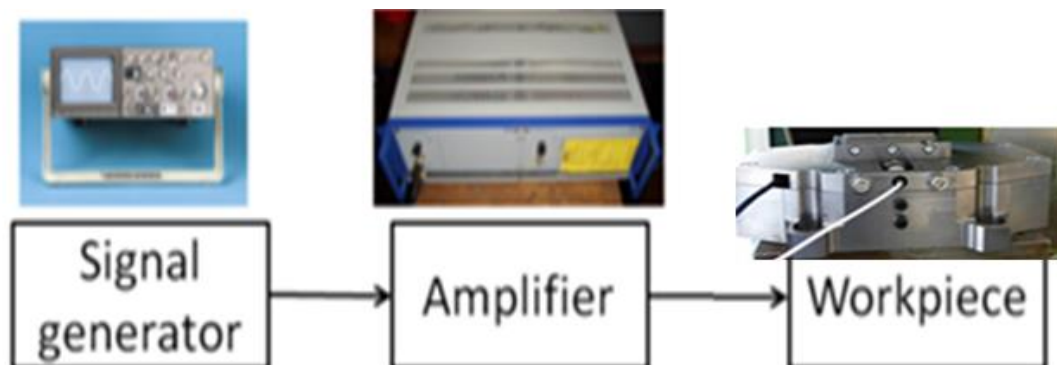


Figure 7.1: Experimental Configuration

Chapter 7. Preliminary Studies

The self-contained oscillating jig is mounted on a 3-axis forces measurement dynamometer as depicted in Figure 7.2, where the signal of the accelerometer is used for feedback to the control system.

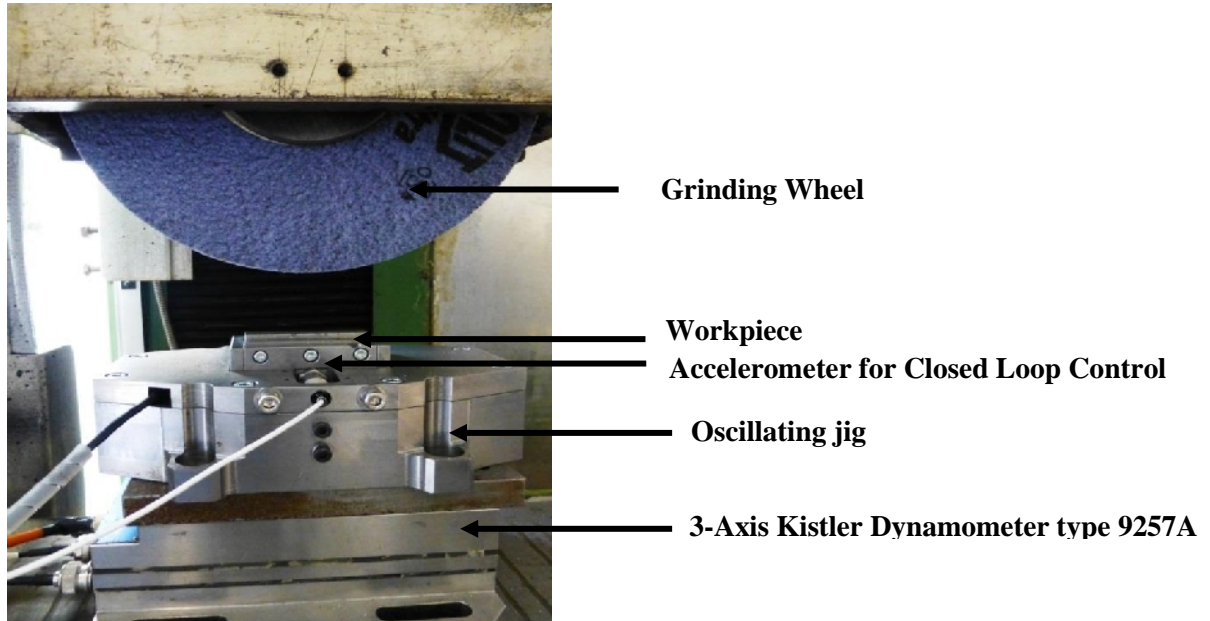


Figure 7.2: Experimental Setup

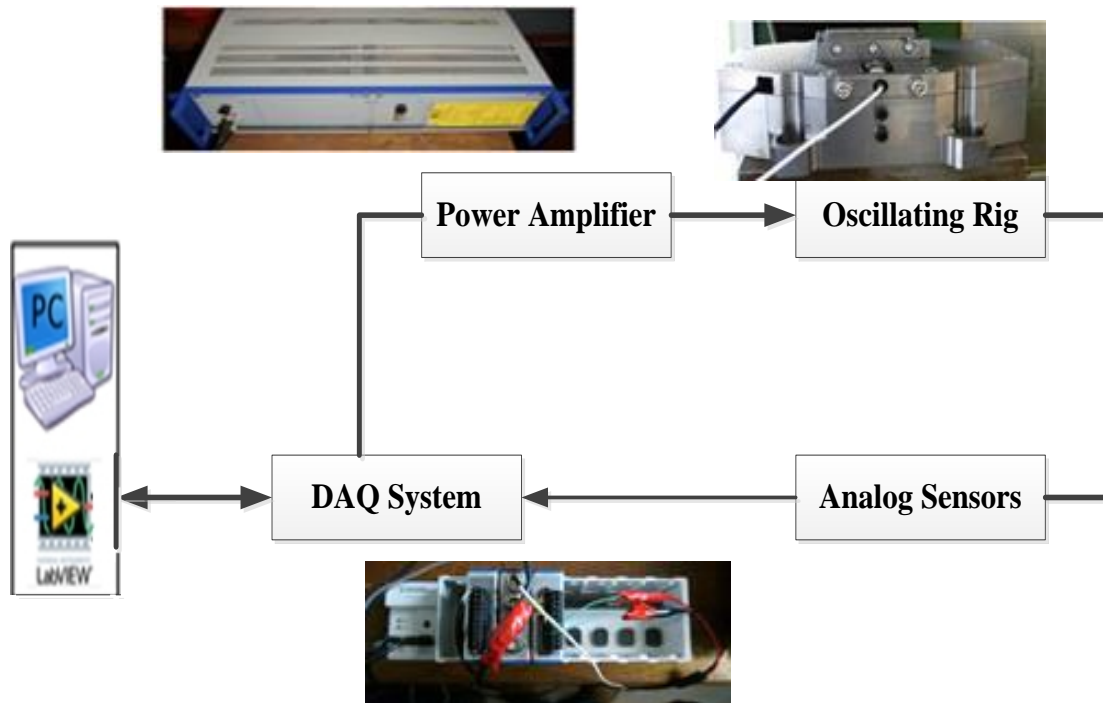


Figure 7.3: Experimental Configuration

7.3 Experimental Setup

In Figure 7.3 the signals from the accelerometer and the dynamometer were recorded using Labview DAQ and stored on a PC for further analysis. For the grinding tests the Abwood machine in Figure 4.1 was used and the depth of cut was set at 10, 15, 20, 25 and 30 μm . Two different materials were used namely, hard steel (EN31-64HRC) and a mild Steel (BS970 080440). In this experiment, the following frequencies 100,150,200,250 Hz were employed.

The Kistler dynamometer type 9257A was mounted under the self-contained oscillating jig to record the normal force (F_n), tangential force (F_t) and the force across wheel width (F_a) during the grinding process. The wheel speed was 35 m/s and the grinding process was dry cutting. The Figure 7.4 shows actual experimental setup where a laptop with Labview is used to drive the oscillating jig and to record the data in real time during the experiment.

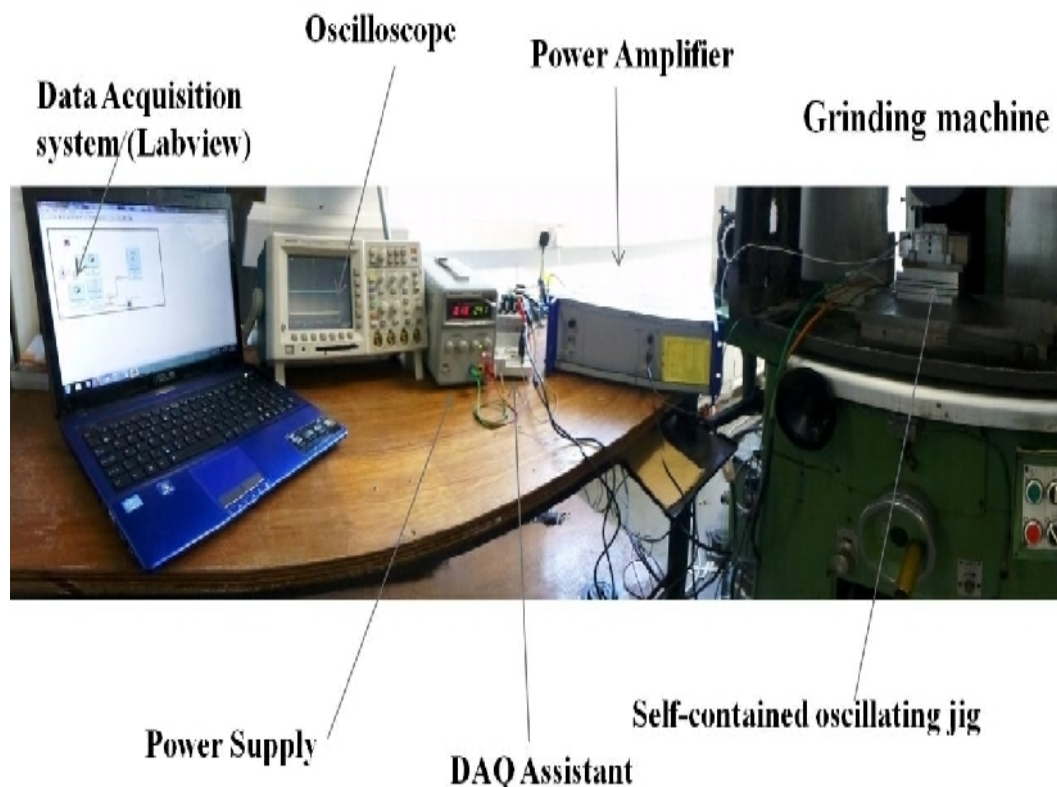


Figure 7.4: Actual Experimental Setup

Chapter 7. Preliminary Studies

Figure 7.5 illustrates a complete grinding cycle. No forces are present from the first few seconds of the grinding cycle due to no contact being made between the workpiece and the grinding wheel. The force rises when the wheel reaches face of the workpiece (Point A); and remain until the actual grinding is finished (Point B) the time span between point A and B determines the actual grinding time, in this case 0.76 seconds. This time was used to calculate the table speed, knowing the length of the workpiece (70 mm).

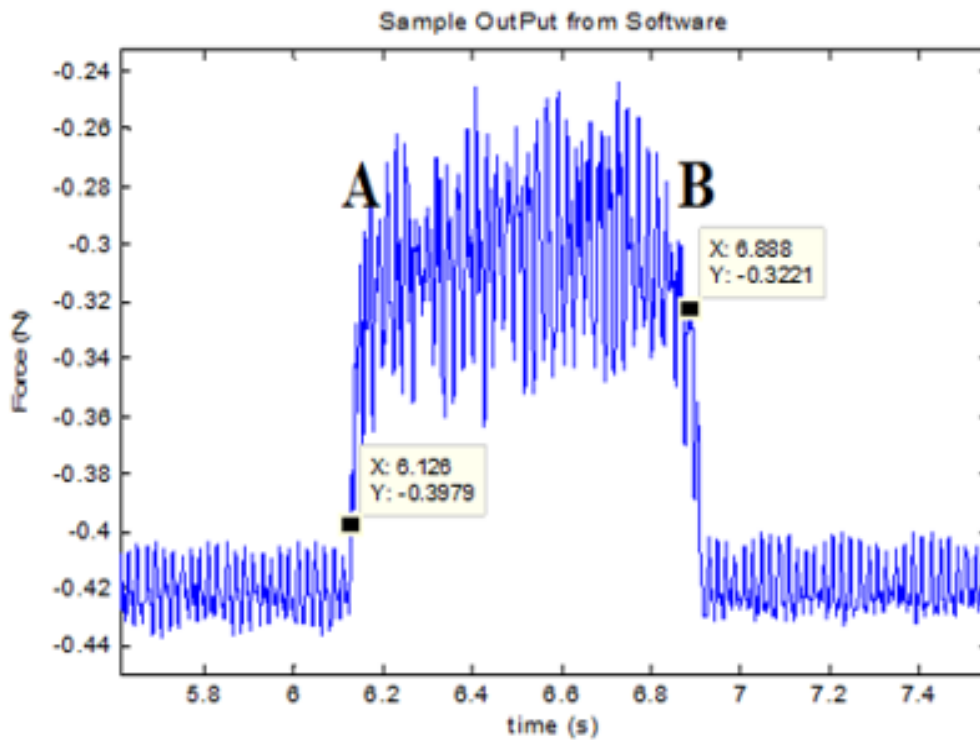


Figure 7.5: Typical Cutting Forces

Table 7.1: Grinding Parameters for Experimental Studies

Grinding Parameter	Value
Grinding Wheel Type	Al ₂ O ₃ (OVU33 A602HH 10VB)
Wheel Diameter	195 mm
Wheel Width	20 mm
Wheel Speed (V_s)	35m/s
Work Speed (V_w)	92 mm/s
Grinding Condition	Dry
Workpiece Materials	(EN31-64HRC) and (BS970 080440)
Cut Type	Up -Grinding,
Dressing	Fine, Single Point Diamond (10 μ m)
Wheel Feed	Traverse
Vibration Frequency	100Hz
Sine wave Amplitude	4 mV (Peak)
Applied Depth Of Cut	10 - 30 μ m

7.4 Results

In this study a range of frequencies were used to quantify the effect of the vibration on the forces generated during grinding. Large data were recorded; however, to reduce the number of graphs, results are presented in a 3D format and individual graphs are given in appendix -A.

7.5 Process Performance as Function of Frequency

A set of grinding tests were made to quantify the effect of frequencies on the actual achievable depth of cut. Figure 7.6 illustrates the achieved actual depth of cut against applied depth and the frequency variation. Here, it is seen that in conventional grinding i.e. no vibration, the depth of cut is very low. The vibration at 50 Hz was used as previous investigations showed no great benefits. Therefore 100 Hz and above was investigated. It is observed that with the increase in frequency, the actual achieved depth of cut increases. This result shows a clear benefit in applying vibration in axial direction.

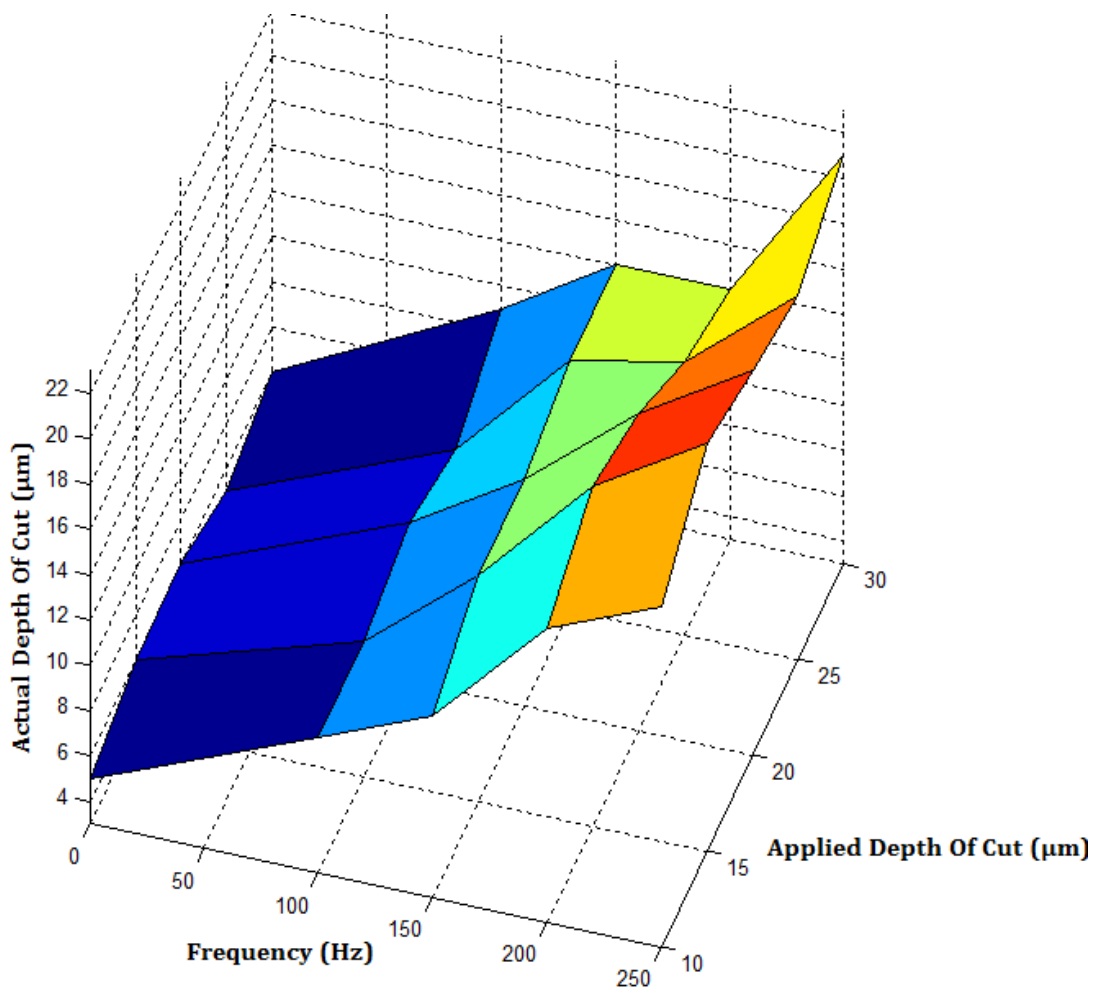


Figure 7.6: Actual depth of Cut as A Function of Applied Depth of Cut and Frequency

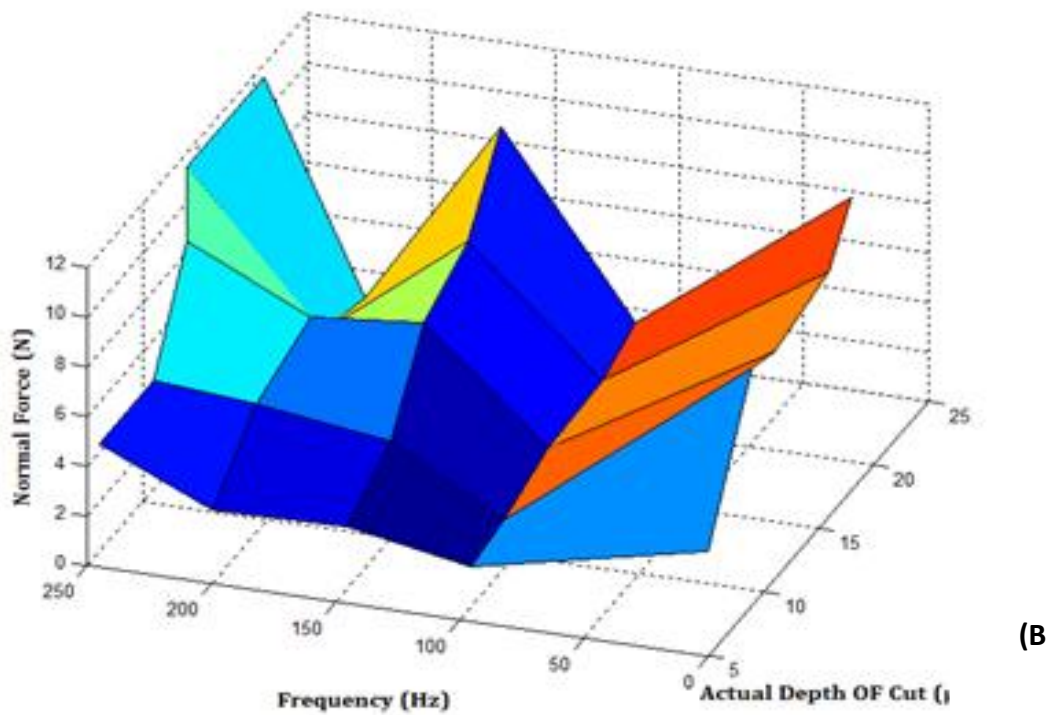
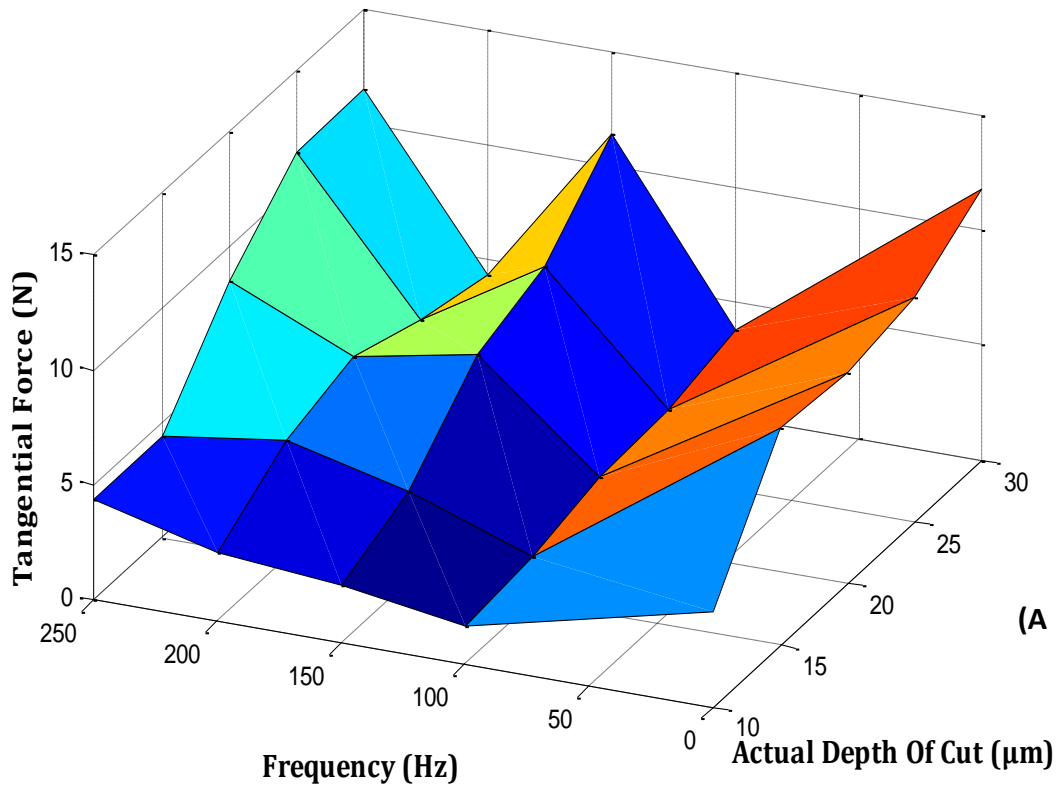


Figure 7.7: Cutting Forces as a Function of Actual Depth of Cut and Frequencies
A) Tangential (F_t); b) Normal (F_n)

Chapter 7. Preliminary Studies

Figure 7.7 shows the tangential forces as a function of actual achieved depth of and the frequencies. As illustrated, the cutting forces drop sharply from no vibration (conventional grinding) down to few Newton at 100 Hz. However, around 150 Hz the cutting forces slightly increased because the natural frequency of the machine tool spindle is 127 Hz. This means that the spindle at around 150Hz is compliant leading to higher forces. However, at 200 Hz, the grinding forces drop slightly at 20 μm depth but at 250 Hz the forces increase sharply. It is seen that 100 Hz secured the lowest grinding forces.

In this investigation of vibration assisted grinding, the hypothesis was to achieve maximum oscillation amplitude of 130 μm .

Referring to Table 4.11, a combination of driving voltage and frequency was used to define optimal output amplitude. However, examining data in the aforementioned table the desired amplitude was reached at 100 Hz with the lowest driving voltage. Therefore, this was considered as the economic way to drive the system with power input, yet achieving the required output. Consequently, the remaining study was carried out using 100Hz, and 4V peak to peak at the signal generator. The finding in Figure 8.1 supports this decision where the lowest grinding forces were achieved at 100 Hz

7.6 Conventional Grinding and Vibration Assistance

The Figure 7.8a and Figure 7.8b presents the relationship between the three forces involved in axial vibration assisted grinding, namely, normal force (F_n), tangential force (F_t) and the axial force across wheel width (F_a). The cutting forces were measured during the grinding of hard steel and soft steel, repeating the experiment twice, and the results were averaged over the grinding process.

It is observed that the cutting forces increase with the increase in depth of cut. However, in conventional grinding i.e. without vibration, the cutting forces are almost the double those recorded for grinding with vibration assistance.

Figure 7.8a and Figure 7.8b shows that the axial force across the wheel (F_a), stayed invariant with the increase in depth of cut. In Figure 7.8a and Figure 7.8b the

Chapter 7. Preliminary Studies

negligible force exerted in the axial direction (F_a) is caused by the free motion of the oscillating workpiece holder in the axial direction.

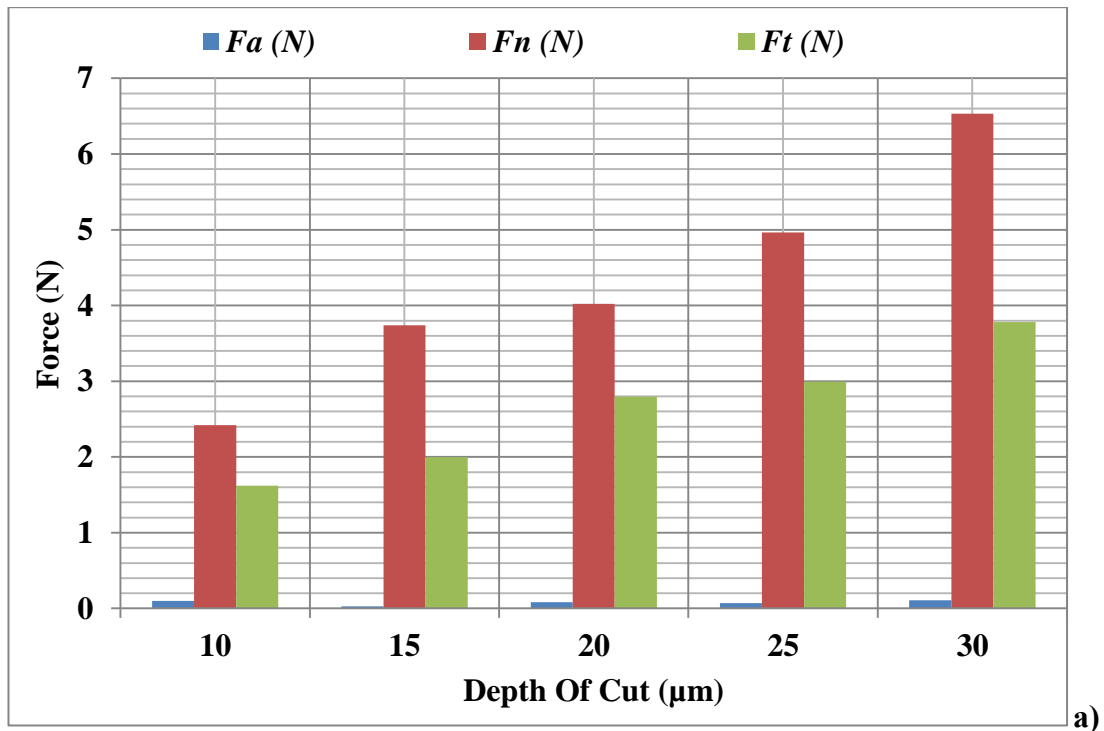


Figure 7.8a: Tangential, Normal and Axial Forces for Hard Steel as a Function of Depth of Cut at 100Hz

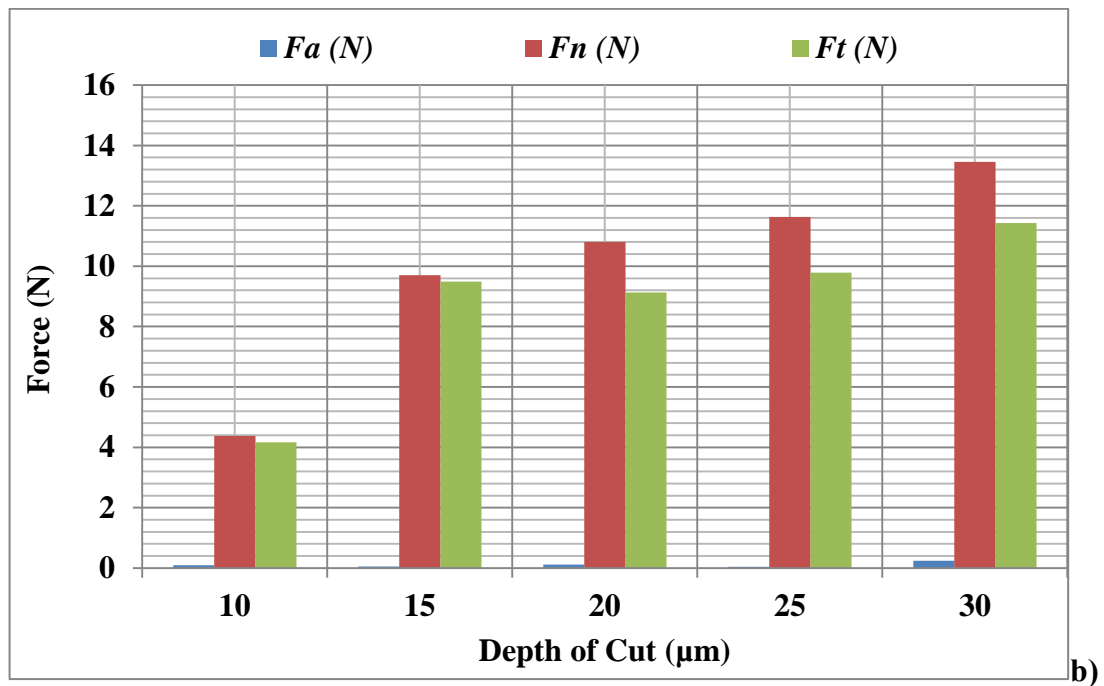


Figure 7.8b: Tangential, Normal and Axial Forces for Hard Steel as a Function of Depth of Cut with No Vibration

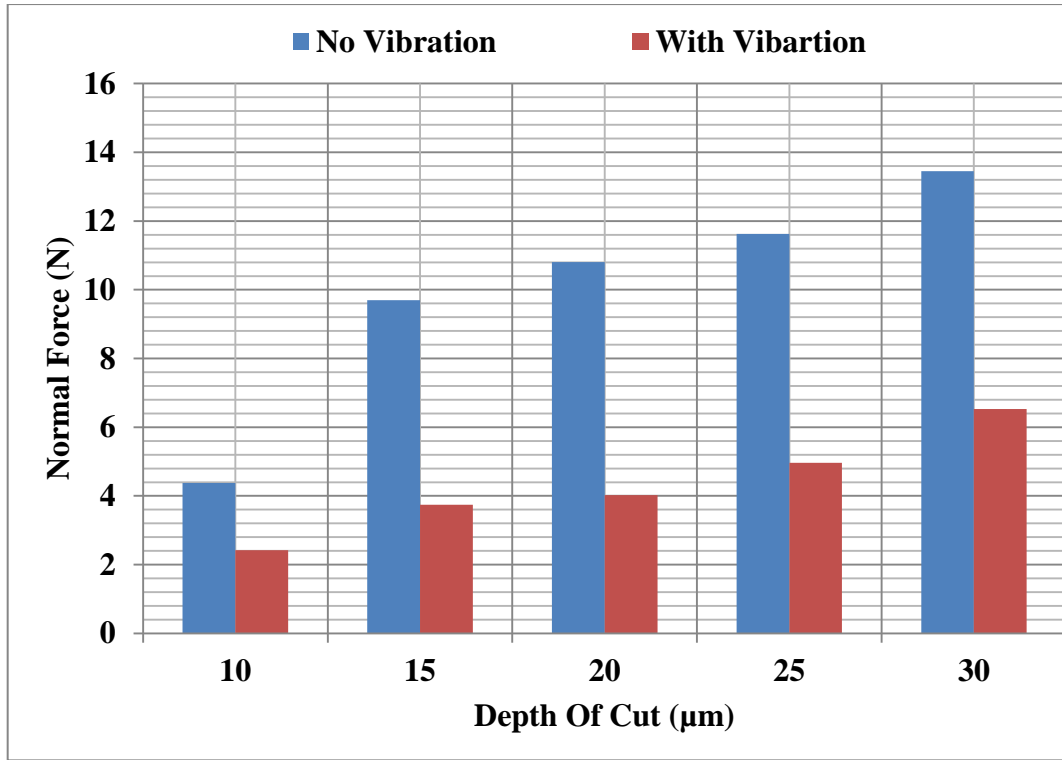


Figure 7.9a: Grinding Forces in Different Depth of Cut for Normal Forces

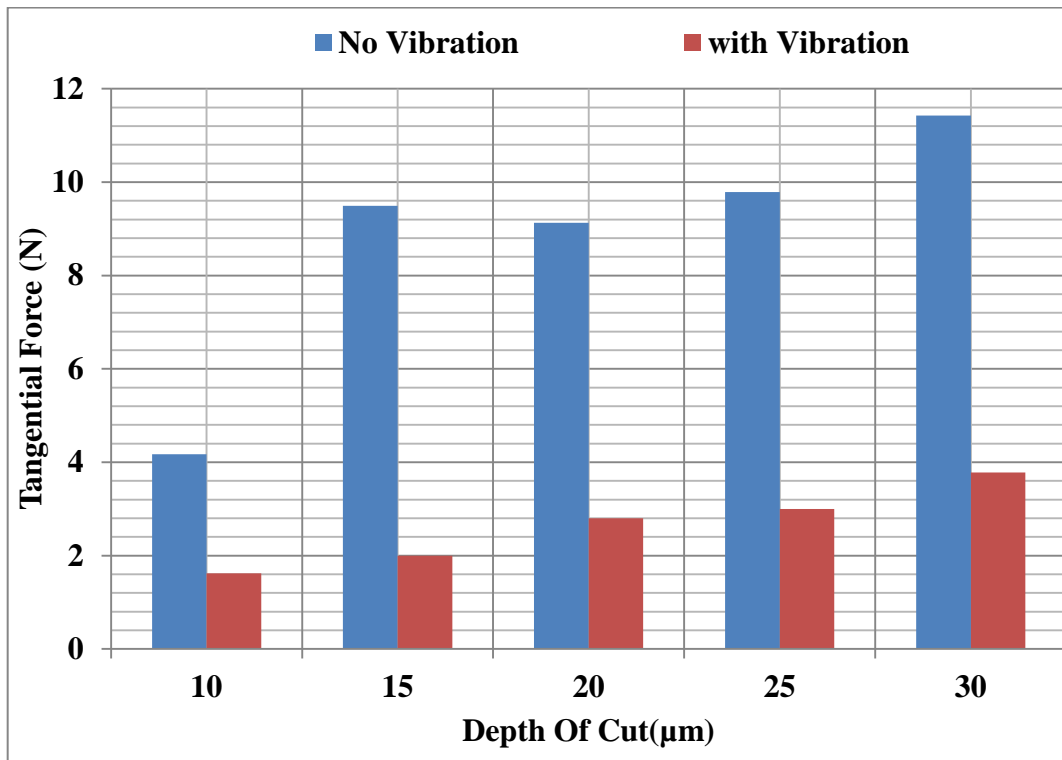


Figure 7.9b: Grinding Forces in Different Depth of Cut for Tangential Forces

Chapter 7. Preliminary Studies

Figure 7.9a and Figure 7.9b puts side by side the performance of grinding with vibration assistance and conventional grinding. It is seen that the normal forces in vibration assisted grinding is on average 43% of those generated by conventional grinding, and the tangential forces are about 26% of those without vibration. It is observed in Figure 7.10 that in vibration assisted grinding, the specific forces (F_n' , F_t') are below 1 N whereas, in conventional grinding (without vibration) the specific forces range above 1 N up to 2 N.

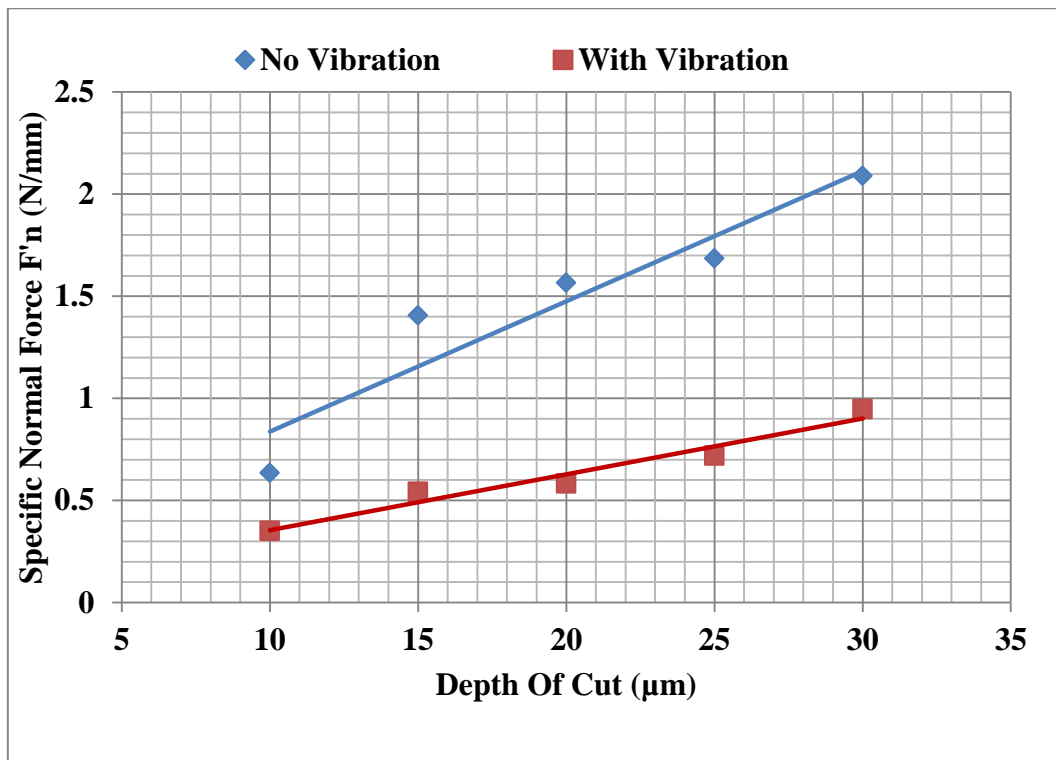


Figure 7.10a: Specific Normal Force

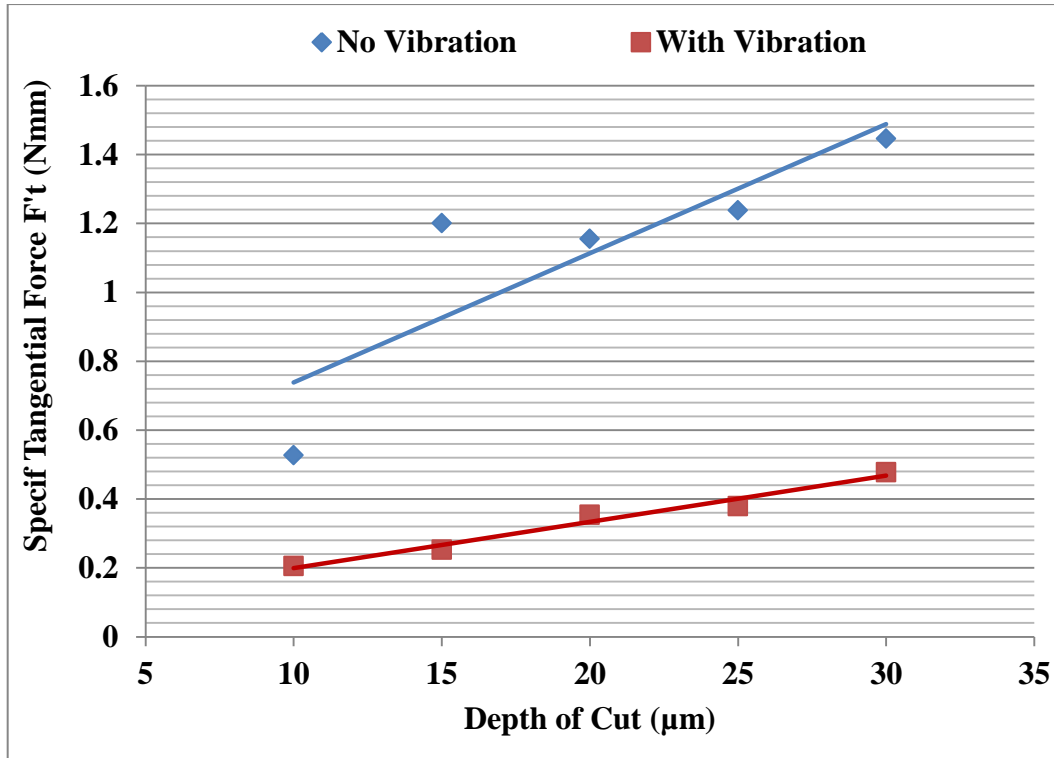


Figure 7.10b: Specific Tangential Force

7.7 Grinding Force Ratio

Force ratio defined as $\mu = F_t / F_n$, is an important parameter that give the indirect information about the efficiency of grinding (Rowe, 2014). The Figure 7.11 below presents the grinding force ratio with vibration at 100 Hz and without Vibration for the same grinding conditions. It is observed that grinding with vibration provided a stable process as the force ratio stayed almost constant with the increase in depth of cut. However, in conventional grinding the force ratio decreased as the depth of cut increased. This means that with vibration assistance the grinding process is more stable in terms of forces that affect the wheel life.

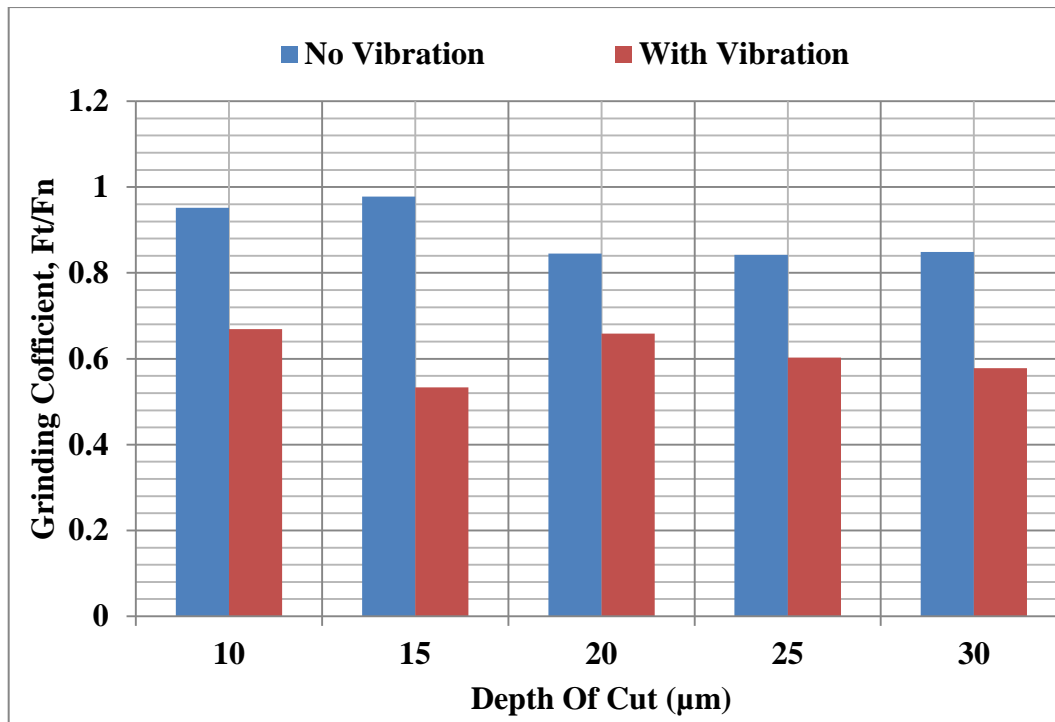


Figure 7.11: Grinding Force Ratio

7.8 Surface Roughness

The surface roughness of ground samples were measured using the Brukker GTK surface texture system. Here, three measurements were taken for each workpiece and the average was used as final result.

The surface roughness for hard steel (EN31-64HRC) is presented in Figure 7.12 where a better surface roughness was secured by applying vibration, a better quality where, on average an improvement of 29 % of the workpiece surface finish was achieved using vibration assisted grinding.

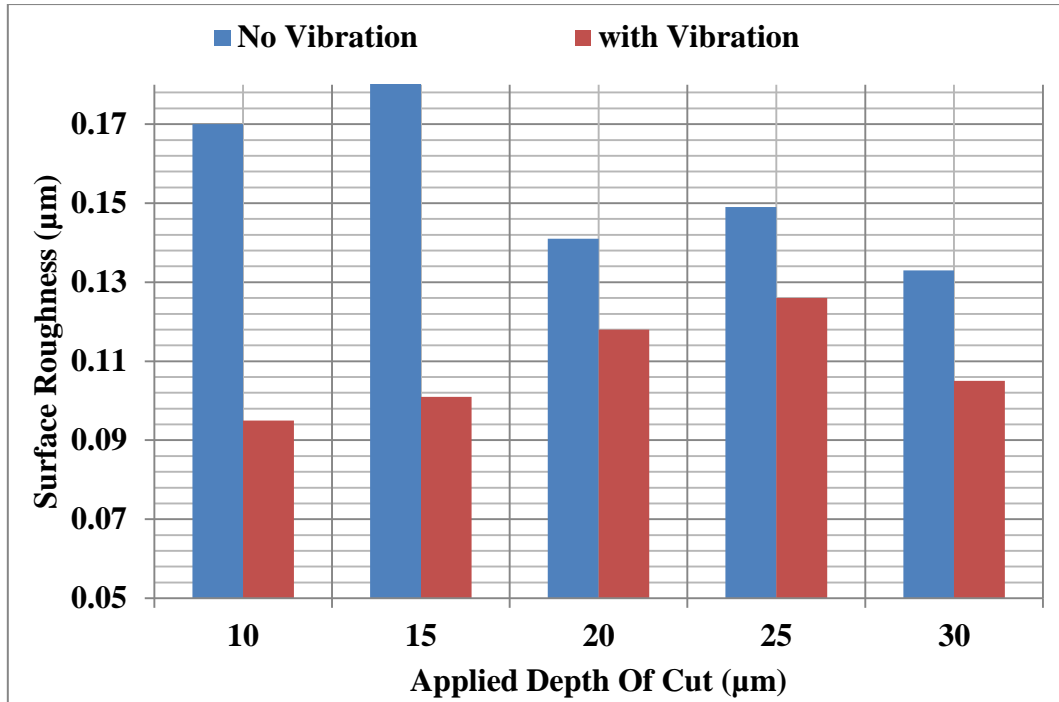


Figure 7.12: Surface Roughness

In grinding as in all processes, power consumption is important and it can be calculated as follows

$$P = Ft \cdot Vs \quad (7-1)$$

Where **P** is Power, **Ft** Normal force, and **Vs** is the wheel speed.

Figure 7.13 presents the grinding power for grinding with and without vibration. This result shows that grinding with vibration assistance reduced the power consumption on average by 25% compared to the grinding without vibration.

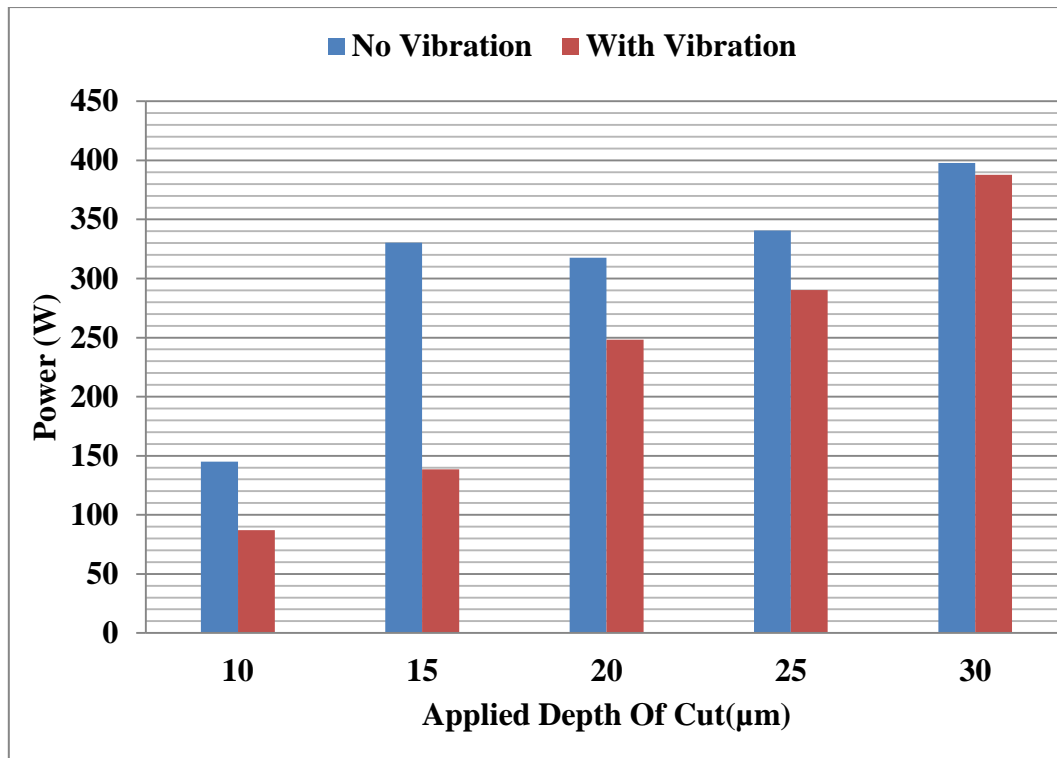


Figure 7.13: Power Consumption- Preliminary Studies

For the tests conducted in this study, the material removal rate with vibration assistance was always higher by 10% than the removal rate without vibration. (EN-31-64HRC)

7.9 Specific Grinding Energy

The fundamental parameter for machining process efficiency is the specific energy that is defined as energy per unit volume of material removed, which is expressed as follows.

$$e_c = P/Q \quad (7-2)$$

Where e_c is specific energy, P is power and Q is removal rate.

Figure 7.14 shows the specific grinding energy using the grinding wheel type (VU33 A602HH 10VB) to grind the hard steel (EN31-64HRC). It is seen that grinding with vibration produced the lowest specific energy. However, as the material removal rate increases, the efficiency of both methods seems to equalise.

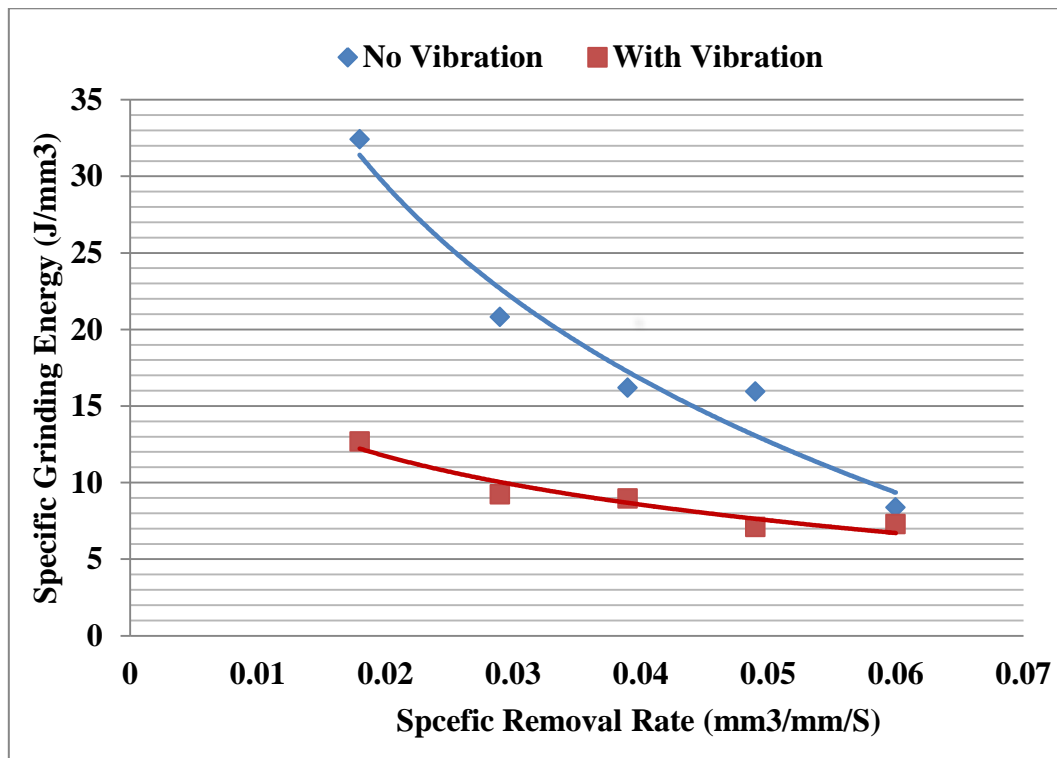


Figure 7.14: Specific Grinding Energies.

7.10 Remarks

The results obtained from the preliminary study led to the following observations:

- The superimposition of vibration in axial direction secured better process outcomes in terms of grinding forces (average 25% improvement), surface finish quality and power consumption.
- At depth of cut greater than 25 μm , the grinding with vibration assistance did not provide a net advantage over conventional grinding in terms of forces and surface roughness. This is a key observation suggesting that axial vibration is highly efficient for low depth cut i.e. less than 25 μm .
- In terms of frequencies it was identified that superimposing vibration at 100 Hz in this study provided the lowest forces. Also it was shown that at 100 Hz the desired amplitude of oscillation was achieved at the lowest driving voltage, i.e. 4V.

**Chapter 8: EFFECT OF VIBRATION ON GRINDING
PROCESS**

8.1 Introduction

The experimental work proceeded with the same arrangement as described in the previous chapter. However, in this experiment the frequency and the amplitude of the vibration were specified in a closed-loop. A PID controller using the signal from the accelerometer controlled the performance of the system by keeping the amplitude of oscillation at a set value.

Table 8.1: Grinding Parameter for Experimental Studies

Grinding Parameter	Value
Grinding Wheel Type	Al ₂ O ₃ (OVU33 A602HH 10VB)
Wheel Diameter	195 mm
Wheel Width	20 mm
Wheel Speed (V_s)	35m/s
Work Speed (V_w)	92 mm/s
Grinding Condition	Wet
Cut Type	Up -Grinding,
Depth of Dressing	Fine, Single Point Diamond (10 μ m)
Workpiece Materials	(EN31-64HNC) , (BS970 080440)
Wheel Feed	Traverse
Vibration Frequency	100Hz
Vibration Amplitude	130 μ m
Applied Depth Of Cut for hard steel and soft steel	(10, 15, 20, 25, 30) μ m
Applied Depth Of Cut for Titanium	(10, 20, 30 , 40) μ m

8.2 Vibration Frequency Effect

This set of experimental work was conducted on the Abwood machine 5025 surface grinding machine in wet condition using coolant at 5-10 % Castrol Hysol oil mix at a flood rate. The experiment was done with grinding wheel type Al₂O₃ (OVU33 A602HH 10VB), and the parameter of the test as shown in table 10.1 and the materials was used was hard steel.

The four vibration frequencies were 100Hz, 150Hz, 200Hz and 250Hz. The results are shown in Figure 8.1a and 8.1b. In order to confirm these results another material was used which was the mild steel with the same type of grinding wheel, and same grinding conditions.

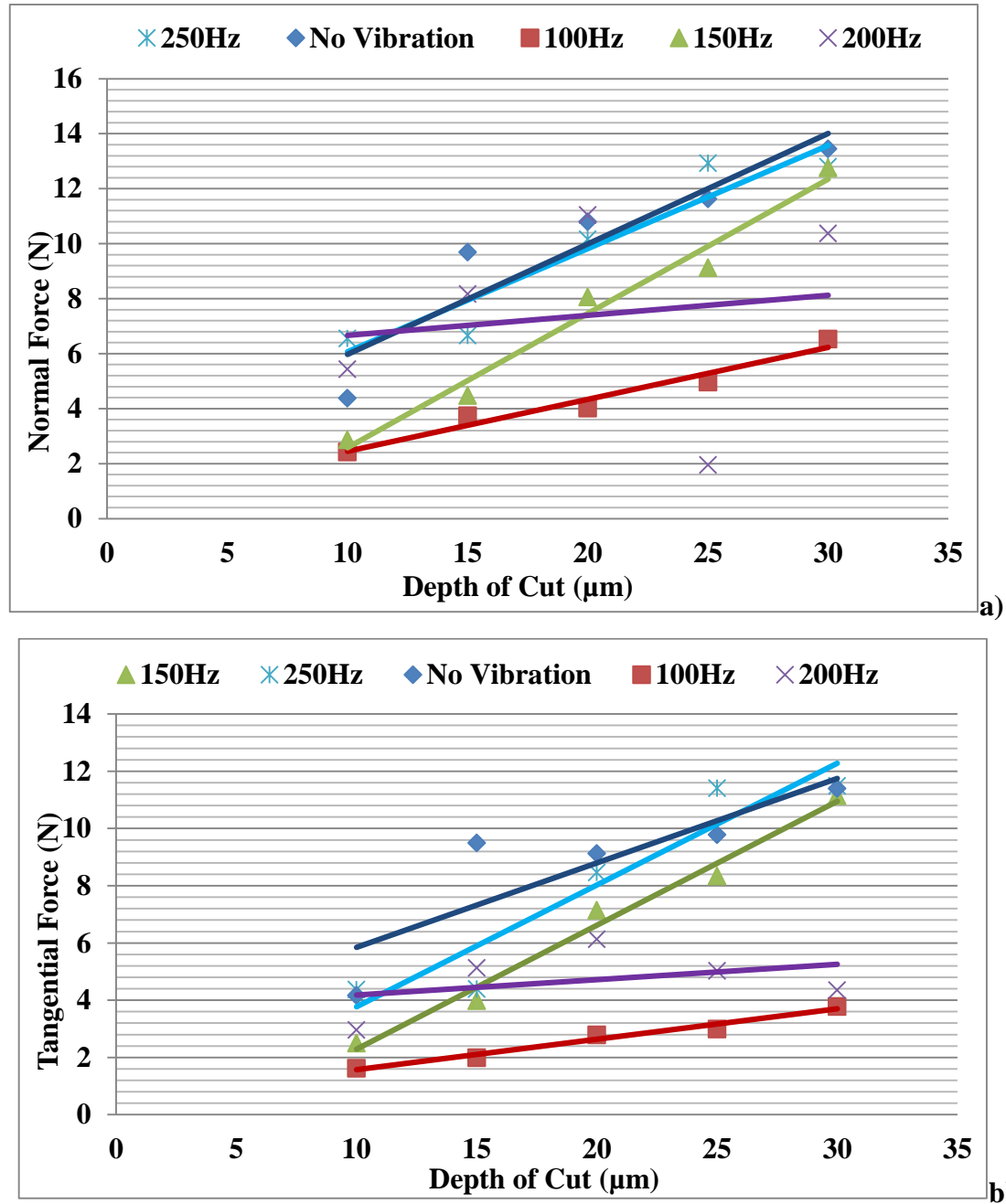


Figure 8.1: Vibration Frequency Effect: a) -Normal; b) – Tangential

For the vibration assisted grinding, the piezoelectric actuator was driven at a frequency of 100Hz and 4 V, which provided a displacement of 130 μm. The aim was to understand the impact of process conditions on the grinding performance of hard steel, soft steel and titanium. The input parameters are presented in Table 8.1.

8.3 Result of all Forces

The grinding forces were measured in three directions i.e. normal force (F_n), tangential force (F_t) and force across wheel width (F_a). Figures 8.3 and 8.4 present the grinding forces for soft and hard steel with coolant with and without vibration. It is observed that the application of coolant has decreased the cutting forces with reference to dry grinding presented in chapter 7. Furthermore, the superimposed vibration also leads to reduced cutting forces in all tests. Figure 8.2 illustrates the grinding performance in vibratory mode. Here it is seen that, though the vibration was applied in the axial direction, the axial forces (F_a) are negligible. This shows that there is no actual cutting performed in the axial direction, but only elastic indentation of the grits into the workpiece material. This is because, single grits perform a sine wave motion over the contact length. This is schematically illustrated in Figure 8.2c, where it is assumed the grit performs only oscillatory motion while the workpiece translates under the grit. However, in actual cutting the grit moves at the speed of the grinding wheel, therefore, it performs only a portion of the theoretical sine wave over the contact length.

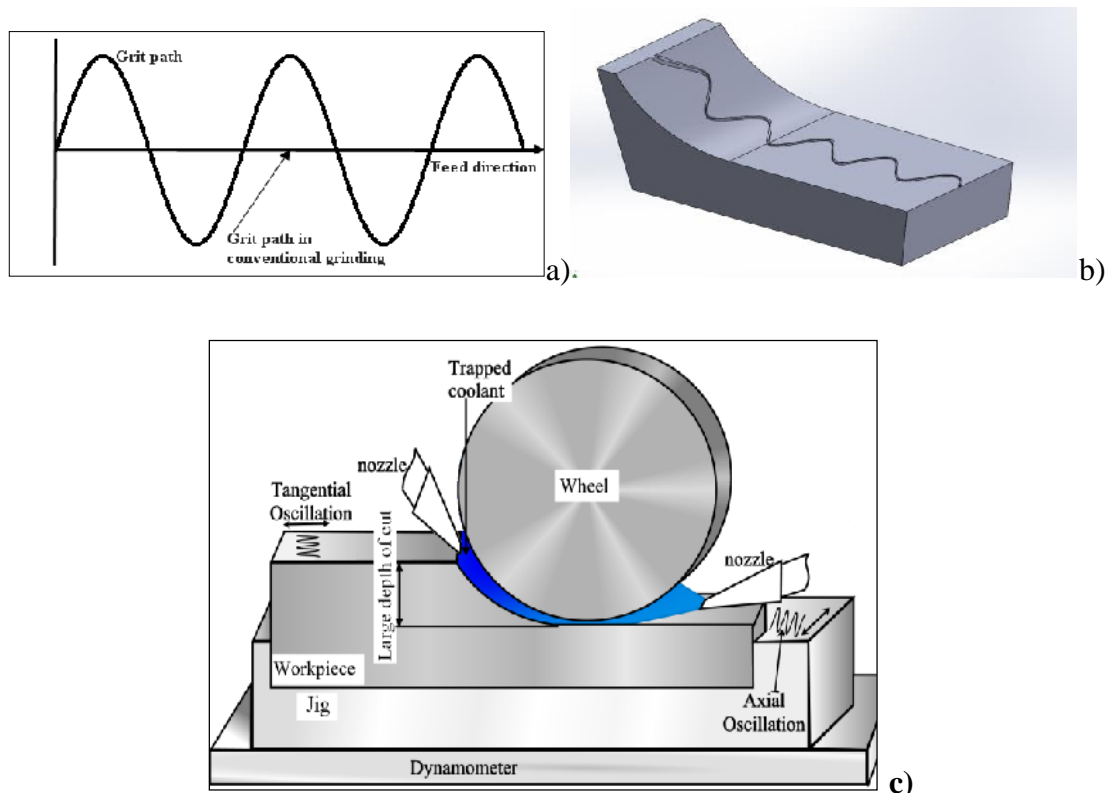


Figure 8.2: Schematic Representation of Grit Motion, (Batako Andre D.L., et al (2012))

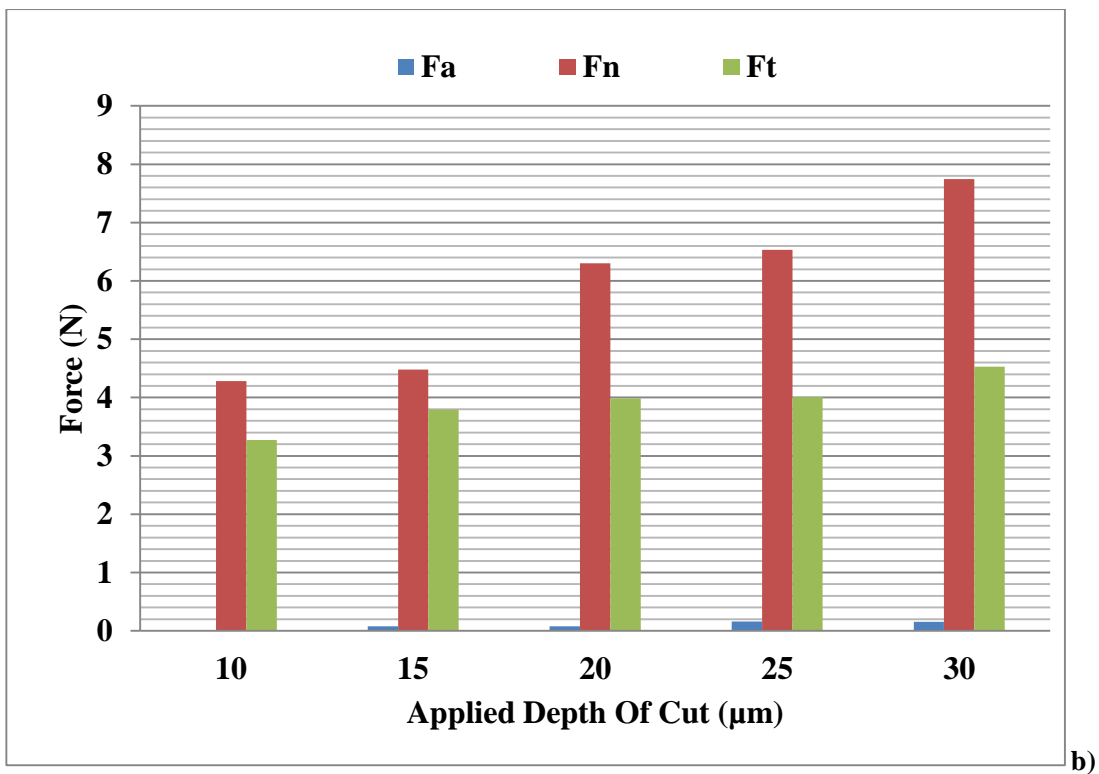
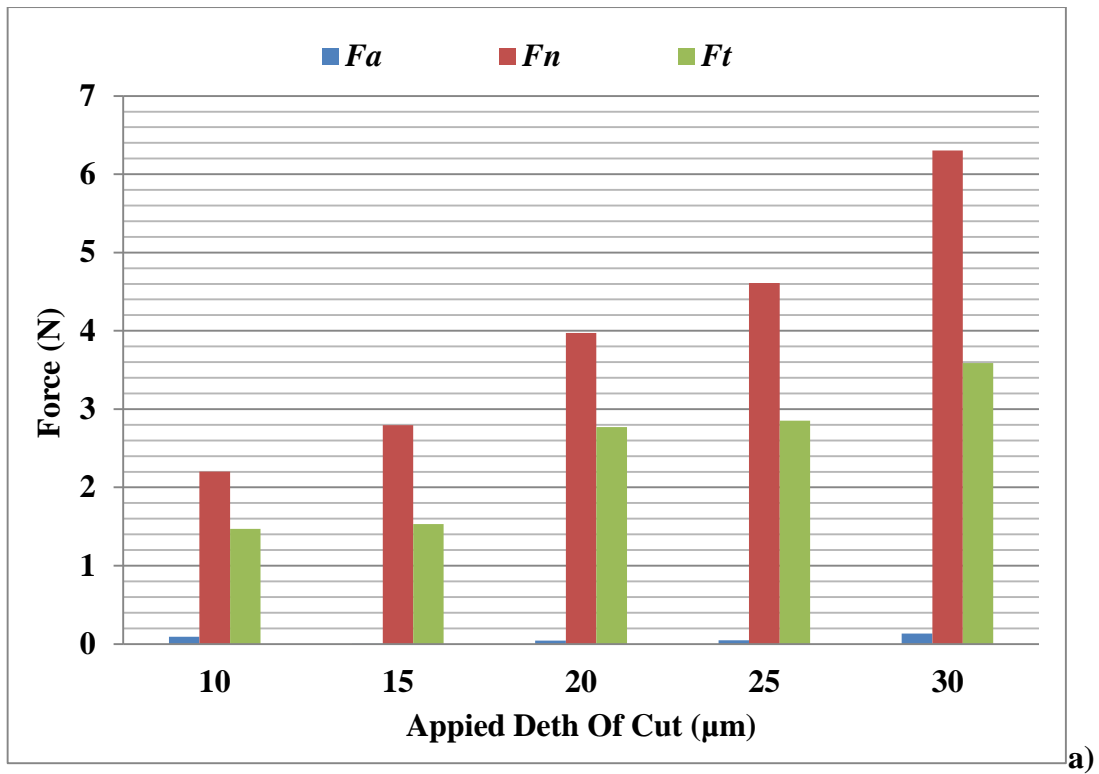


Figure 8.3: Grinding Forces for Hard Steel: (a) - With Vibration; (b) - No Vibration

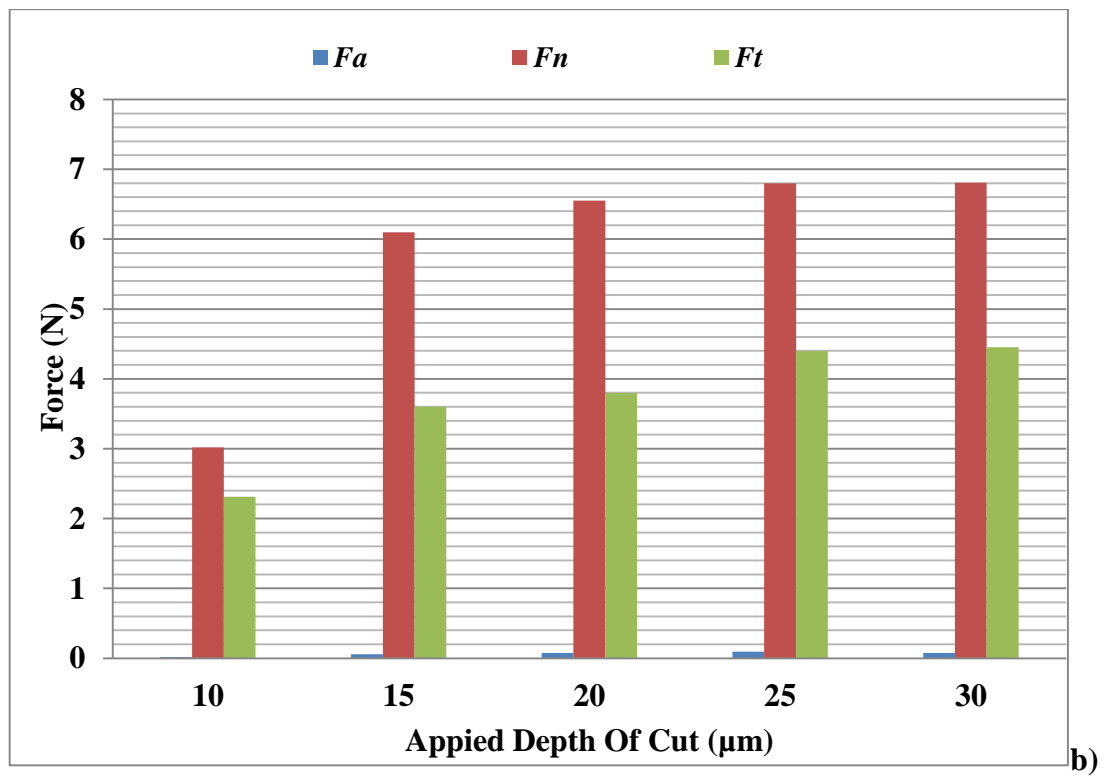
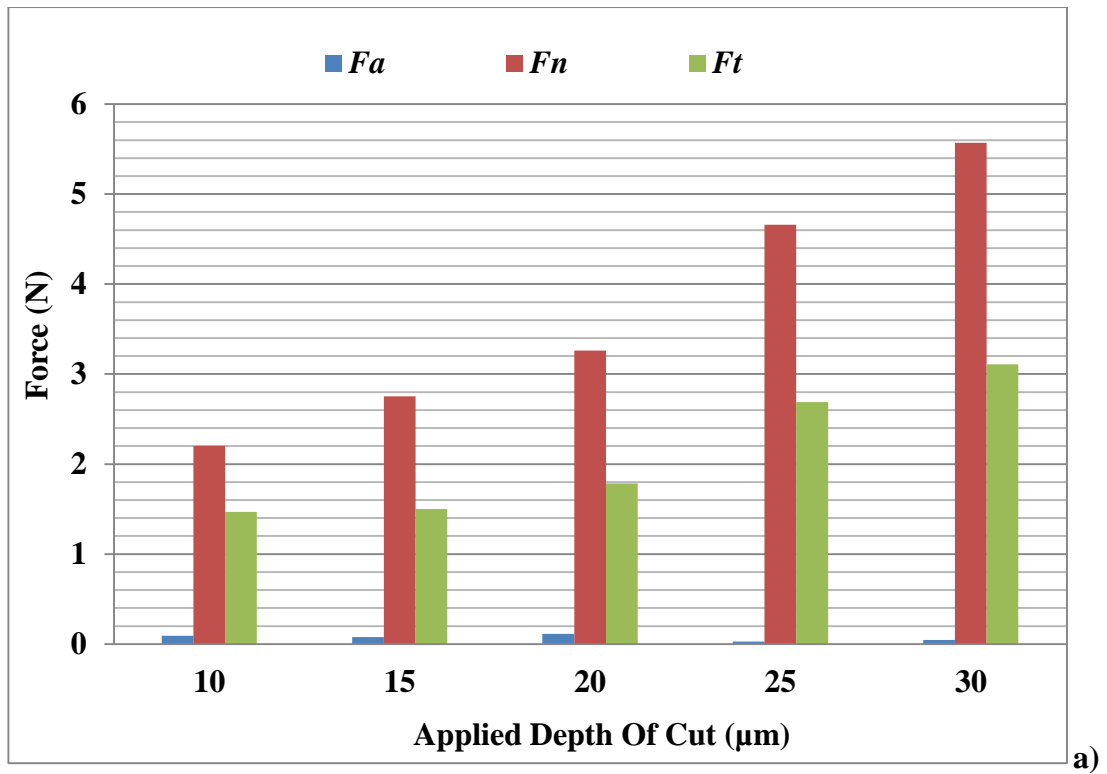


Figure 8.4: Grinding Forces for Soft Steel: (a) - With Vibration; (b) - No Vibration

For estimation, the geometric contact length;

$$l_g = \sqrt{a_e d_e} \quad (8.1)$$

Where a_e is the real depth of cut and d_e is diameter of wheel which is 195 mm.

Taking one of the actual depths of cut a_e say 21 μm , the contact length l_g is calculated as;

$$l_g = \sqrt{0.021 * 195} = 2.023 \text{ mm}$$

The total relative speed is

$$V_t = V_s + V_w \quad (8.2)$$

Where V_s is the wheel speed and V_w is the work speed. However, since the work speed is very small in comparison to the wheel speed it has been neglected.

Therefore the contact time can be given as follow:

$$\text{Contact Time} = \frac{L_g}{V_s} = \quad (8.3)$$

$$\frac{2.02}{35000} = 0.00006s$$

Nevertheless, it has been observed from the experiment that the contact length is proportional with the depth of cut.

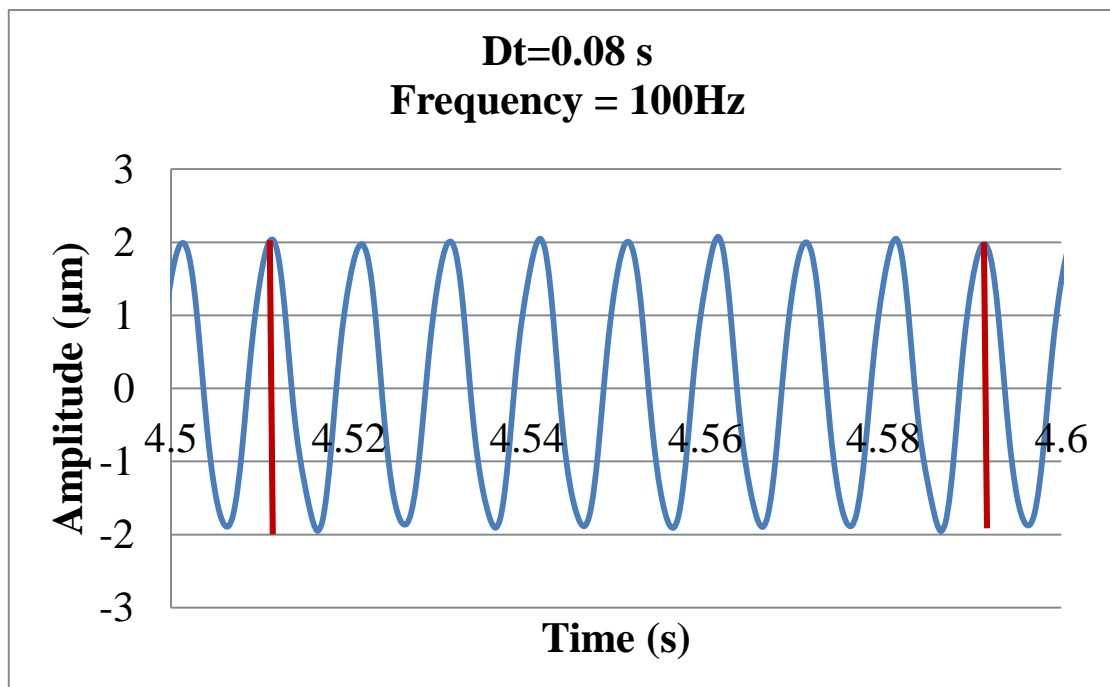


Figure 8.5: System Response under Actual Grinding

A number of cycles (waves) over the contact time in the grinding process can be estimated by determining the actual grinding time within a specific frequency, through which the cycles can be specified, (see Figure 8.5, eg 8 cycles per 0.08 second).

However, Figure 8.5 illustrates the response of the vibrating jig under grinding operation at full machine load. In addition to that, the figure also gives the frequency response behaviour of the jig in a closed loop control system of (100Hz).

It is concluded that the grits in axial vibratory grinding cut on their front and side faces. However, a net axial cutting is fully achieved by grits located in the middle of the workpiece. Actual chipping is performed by a small number of grits located at the edge of the workpiece.

Figure 8.2b depicts the cutting forces without vibration but the application of coolant led to a reduction of forces. This is explained by the lubrication effect that drastically reduces the friction between the wheel and the workpiece. In general coolant is used in all manufacturing processes. However, it accounts for up to 17% of total manufacturing cost Brinksmeier, (1998). Coolant application has a direct impact on the environment; this is why the preliminary study was carried out in dry conditions in order to see if grinding dry would bring some advantages. Figure 8.4 gives the results for grinding soft steel with and without vibration in wet conditions. It can be observed in Figure 8.3b and 8.4b in conventional grinding without vibration that there is an axial force component (less 0.1N) which is caused by the free motion of the workpiece holder in the axial direction. The workpiece holder is designed such a way that it sits freely on two guide ways that allow for the piezo to drive the system. Therefore during grinding the sub-assembly holder-workpiece can slide slightly in the axial direction causing the force sensor.

8.4 Normal and Tangential Forces

Figure 8.6 and Figure 8.7 show the performance of the grinding in terms of normal and tangential force for conventional and vibration for two materials. The normal forces in hard steel decreased around 42.4 % and tangential forces decreased about 38% when the vibration was applied to the process. In soft steel, grinding with superimposed vibration led to 38% decrease in the normal force and a reduction of 43% in tangential force.

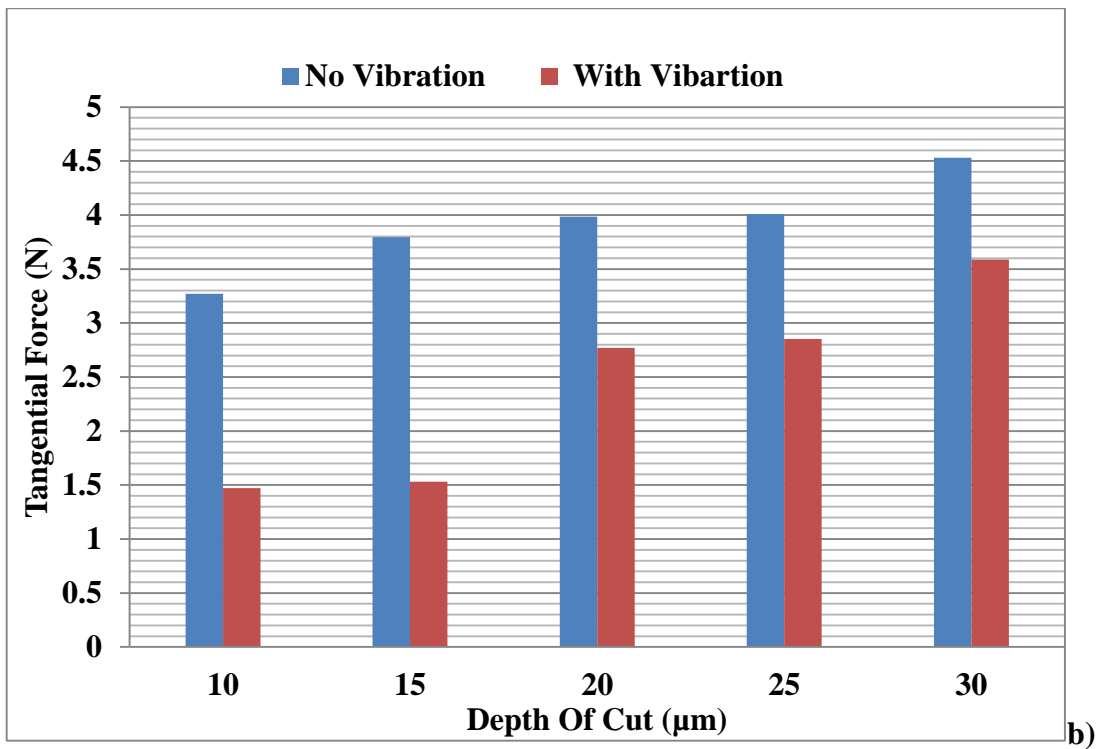
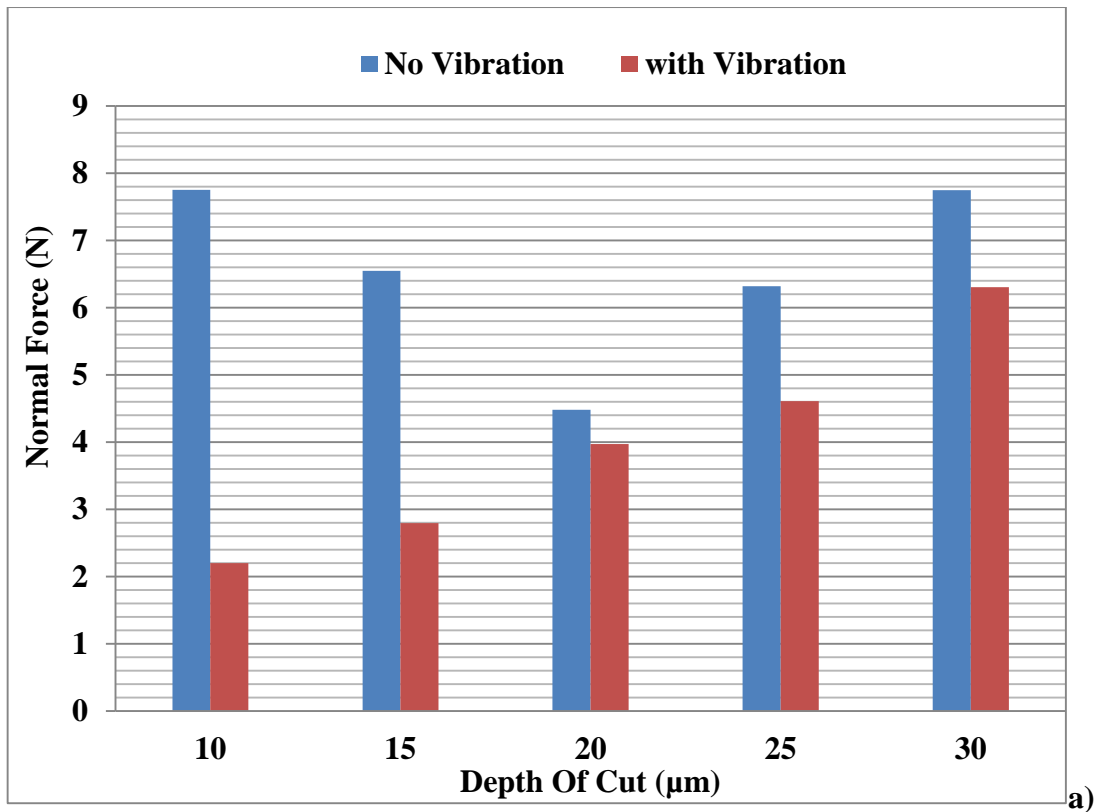


Figure 8.6: Grinding Force for Hard Steel: a) -Normal; b) – Tangential

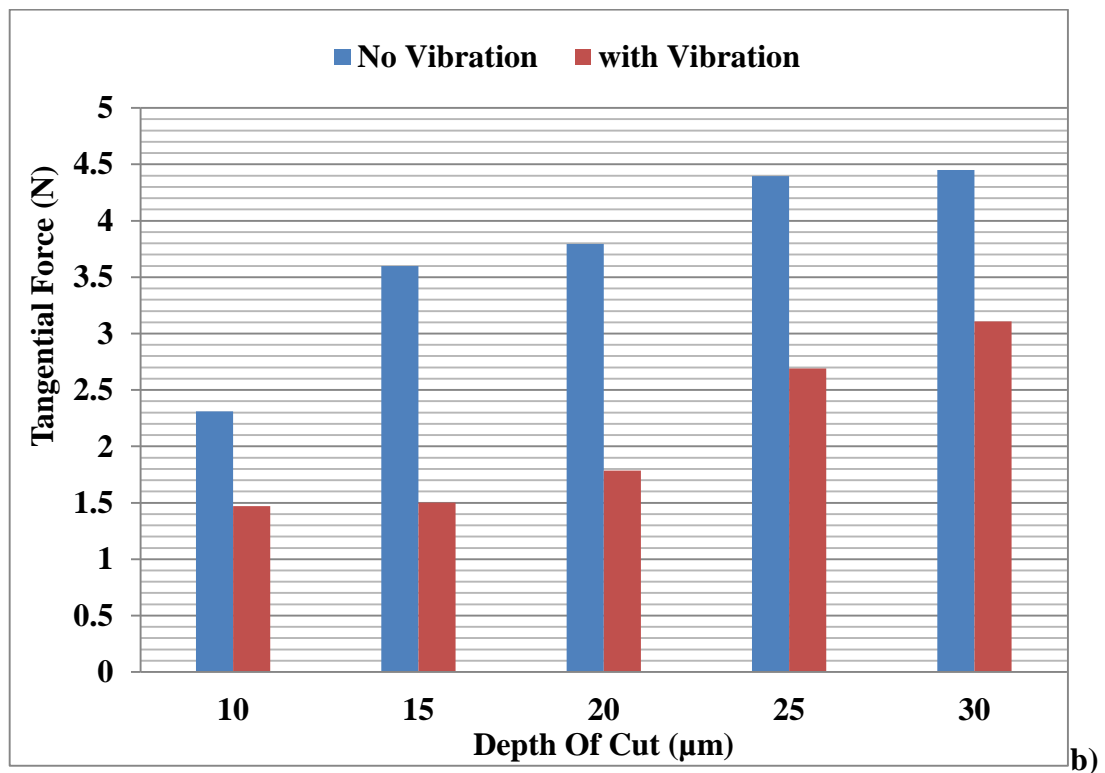
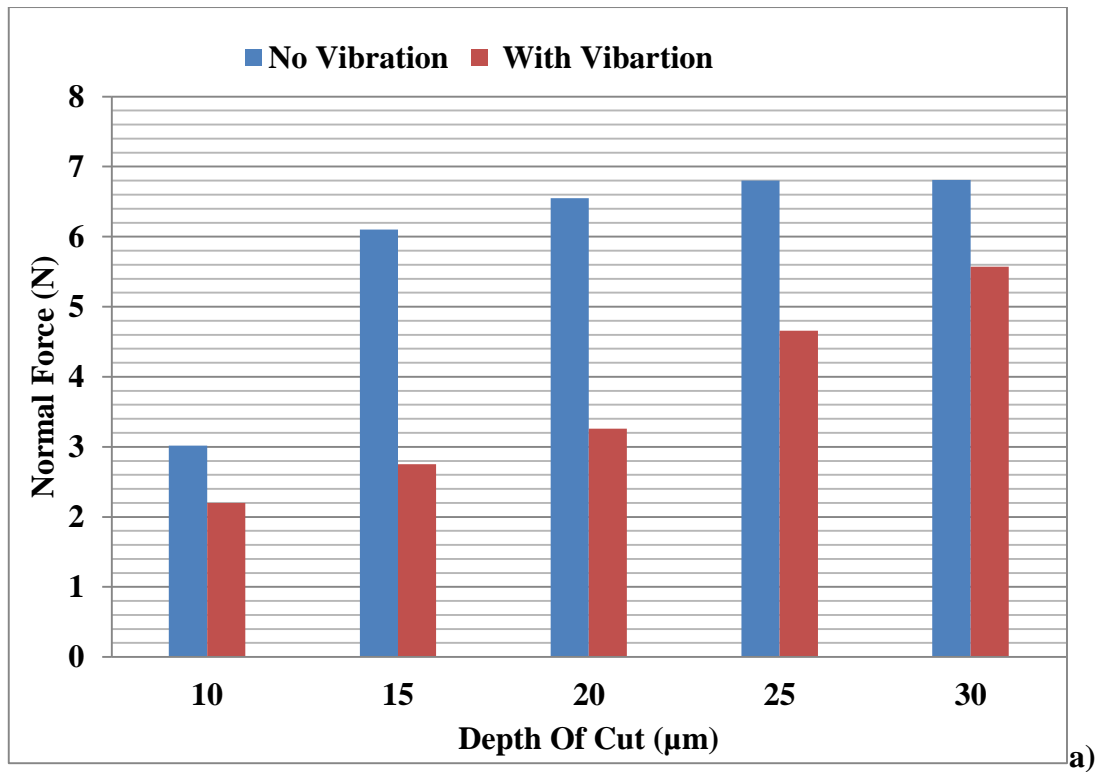


Figure 8.7: Grinding Forces for Soft Steel: a) -Normal; b) – Tangential.

8.5 Grinding Power

Figure 8.8 shows the power consumption during the grinding. It is observed that the application of vibration secured less process power compared to conventional grinding. An average decrease of 38% was achieved with vibratory grinding of hard steel and 43% in soft steel.

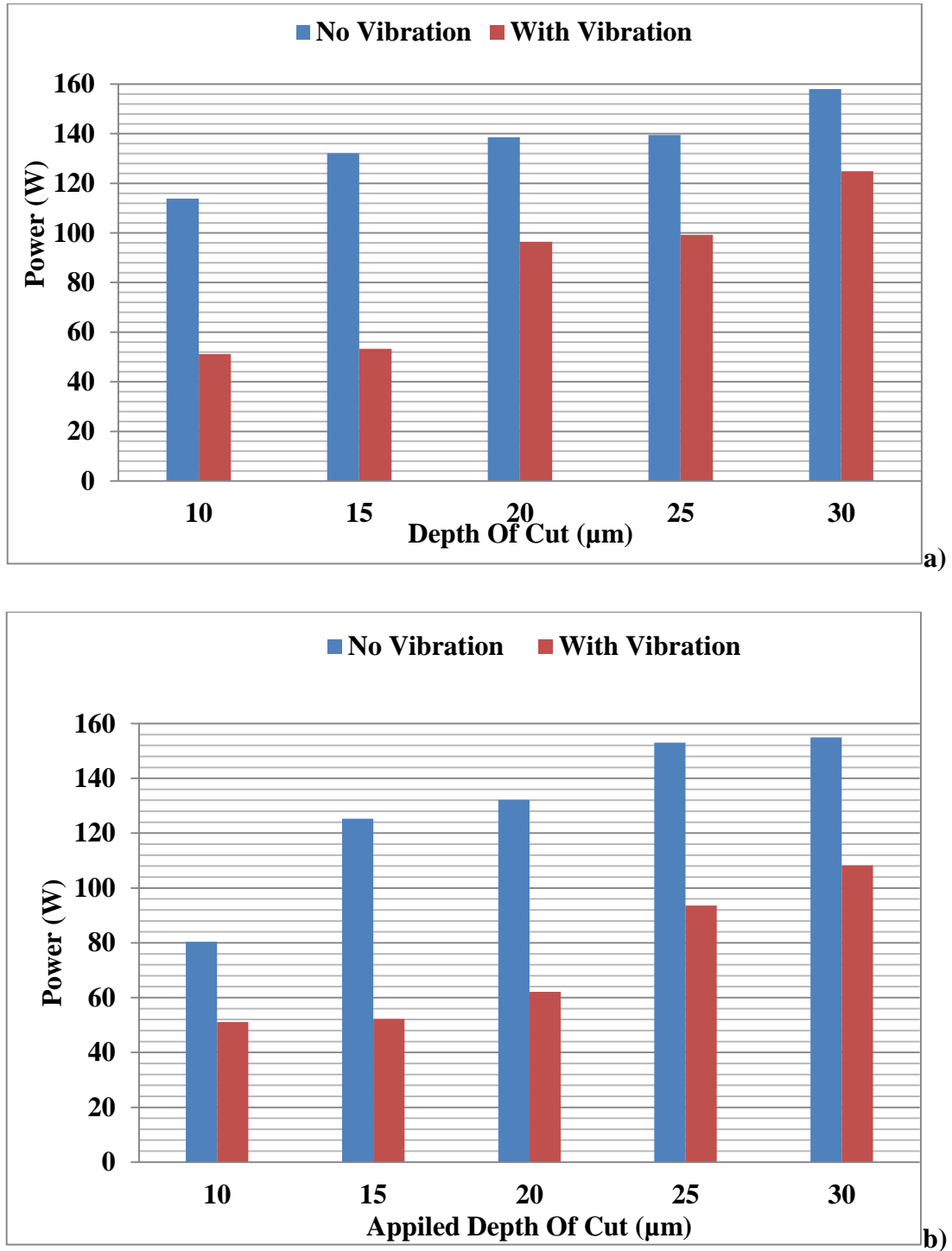


Figure 8.8: Power Consumption: a) – Hard Steel; b) – Soft Steel

8.6 Specific Grinding Energy

Figure 8.9 shows the relationship between specific grinding energy versus specific removal Rate. As in the figures depicting the power, the specific energy expresses the energy spent to remove unit volume of material. The application of vibration to the grinding process reduced the energy requirement with reference to conventional grinding. However, it is observed that as the material removal rate increases, the specific energy for conventional grinding converges towards vibro-grinding. Grinding soft steel required more energy in both processes especially for small depth of cut. This is because soft material loaded the grinding wheel very fast, and this led to increased rubbing and frictional forces, which increase the power consumption.

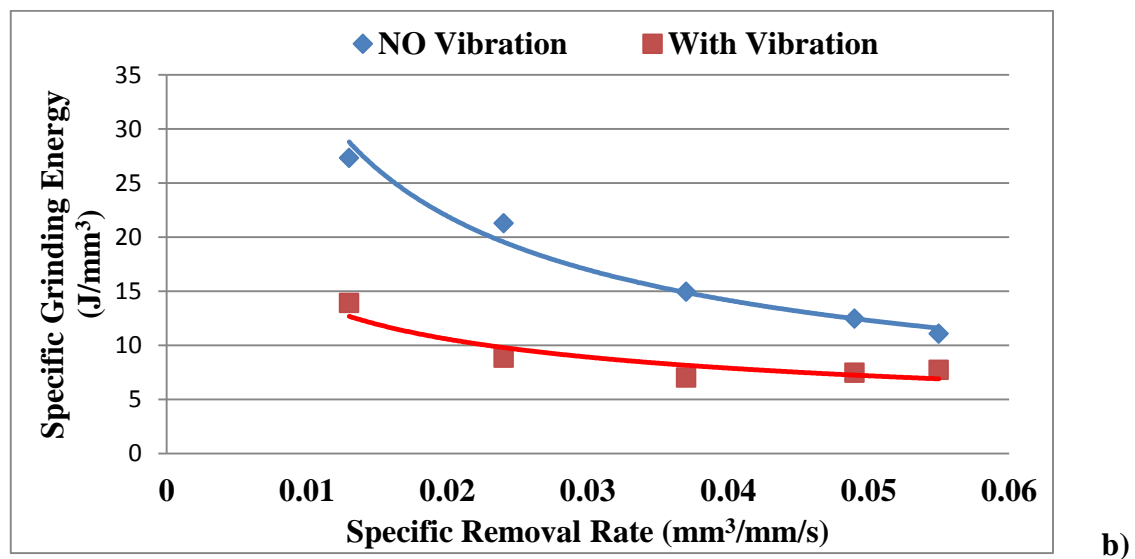
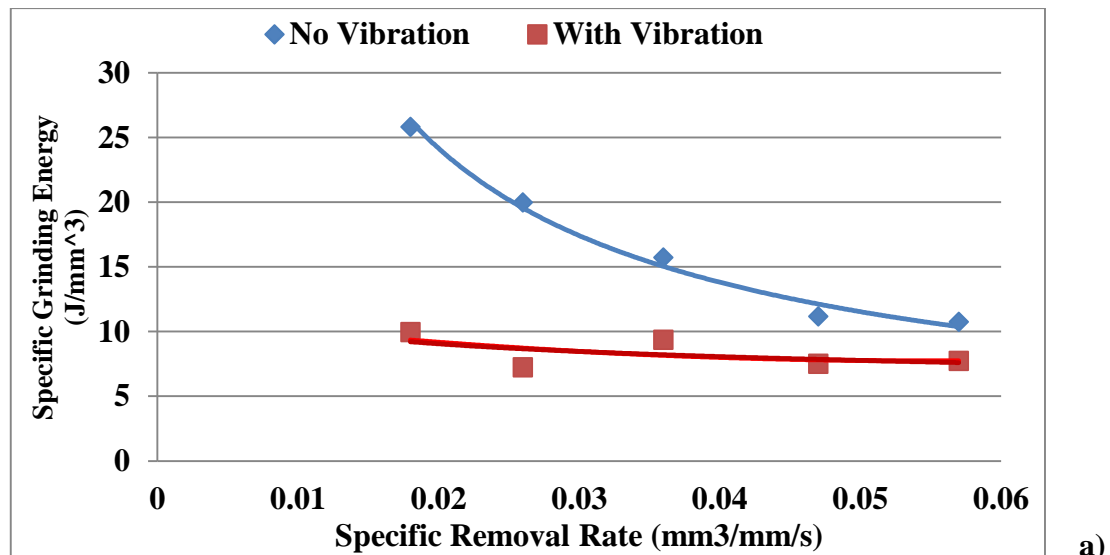


Figure 8.9: Specific Grinding Energy: a) – Hard Steel; b) – Soft Steel

8.7 Surface Roughness

Results in Figure 8.10 show the effect of depth of cut on grinding surface quality. It indicates that at low depth of cut the surface quality is relatively good. For the applied vibration, the surface finish in hard steel (0.11) is much better than in soft steel (0.14) on average. It can be seen that when depth of cut is larger, the surface quality becomes rougher than for smaller depth of cut. It can be seen that when vibration in applied in both materials a better surface roughness was obtained.

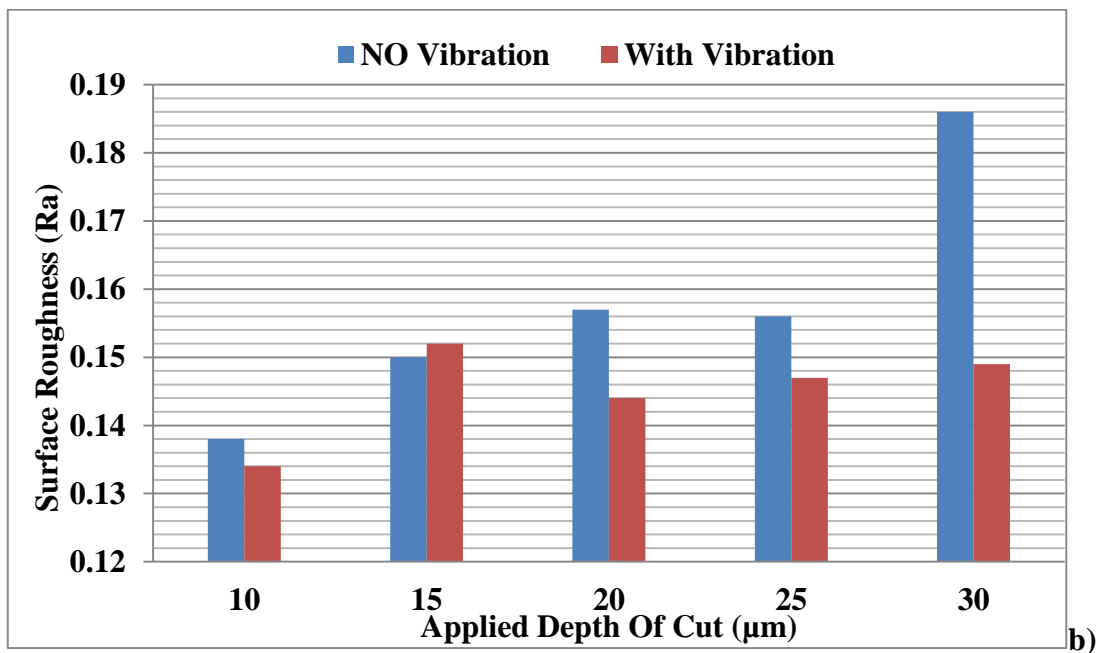
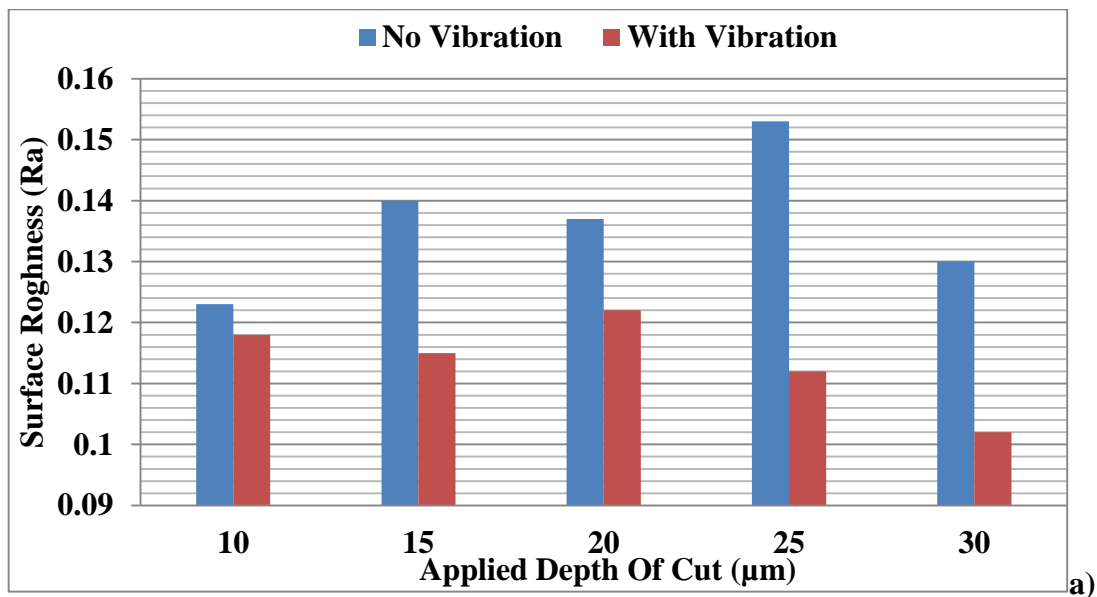
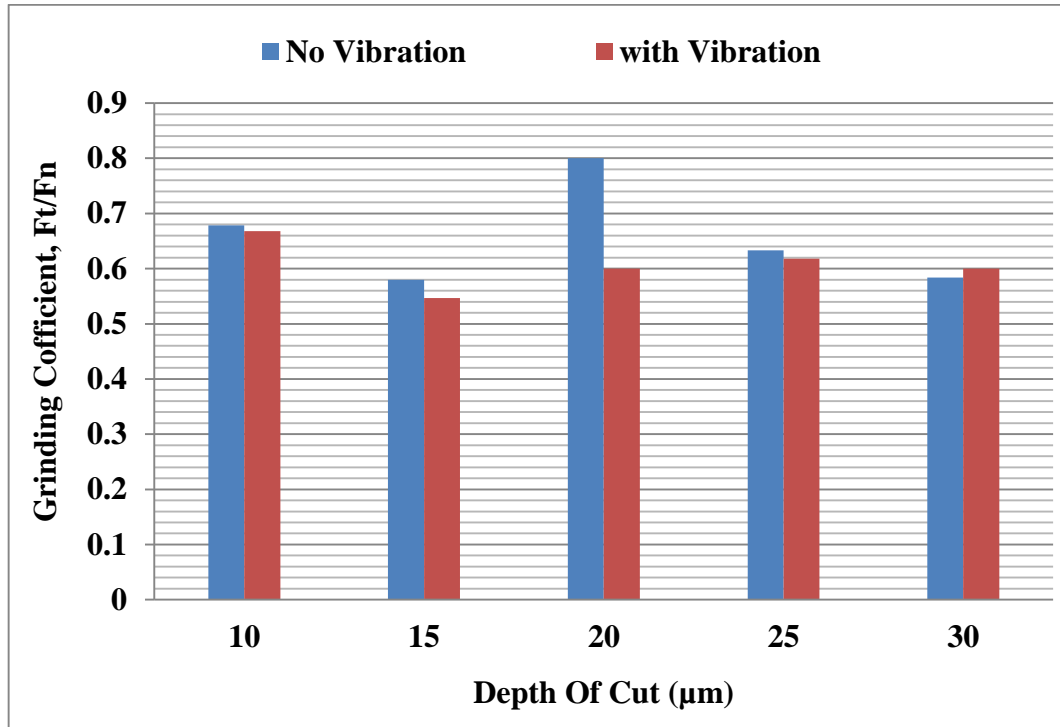


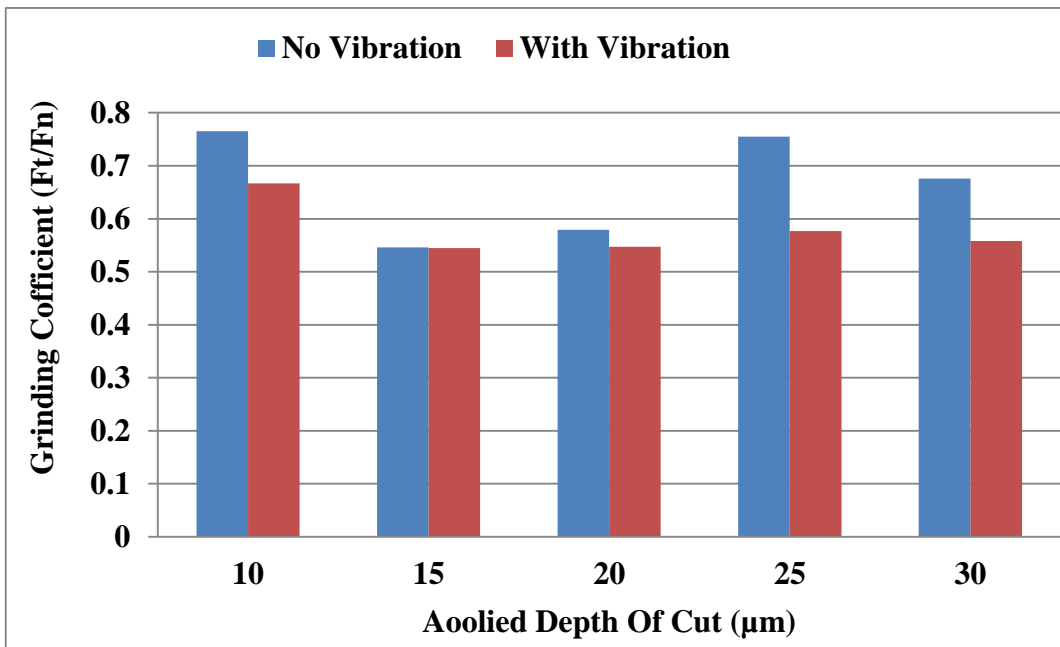
Figure 8.10: Surface Roughness:a)- Hard Steel; b) – Soft Steel

8.8 Grinding Coefficient

Figure 8.11 shows the grinding coefficient, it can be seen that at 15 and 20µm the grinding coefficient is low, generally in all cases the grinding coefficient with vibration is much better than without vibration.



a)



B)

Figure 8.11: Grinding Force Ratio: a) – Hard Steel; b) – Soft Steel

8.9 Remarks

The overall results of this chapter can be summarised as follows:

- In terms of forces as a function of frequency and depth of cut $f(freq, depth)$ it was identified that 100 Hz outperformed other frequencies. This is a key finding for low frequency application of vibration in grinding.
- Applying the vibration to the process allowed reducing the forces, power and improving the surface quality.
- It is observed that a small depth of cut grinding with vibration gave better result than grinding with a high depth of cut.

Chapter 9: Performance of The Developed Controller

9.1 Introduction

This chapter presents the influence of the developed controller on grinding process performance. Here a comparative study of conventional, and vibratory grinding is given. A contrast is made between open and closed loop controllers. The performance of the newly designed and implemented closed loop controller is emphasised by putting side by side the results of open loop and closed loop.

The performance of grinding with vibration in two independent directions i.e. axial and tangential is given here. The data for grinding with tangential vibration were obtained from previous studies which investigated extensively into the performance of the process, (Tsiakoumis, 2011).

Therefore this current work focused on the application of vibration in Axial direction to provide a complete understanding the effect of superimposed vibration on grinding process.

The aim of this is to study and compare the performance of vibration in two directions with the hardened steel EN31 (64 HRC). The tangential and normal forces and surface roughness were measured for conventional grinding, dry grinding and wet grinding. The real depth of cut was measured for all grinding trials which allowed calculating the power and the grinding energy. The experiment parameters are given in Table 9.1.

Table 9.1 Preliminary Experiment-Grinding Parameters

Grinding Parameter	Value
Grinding Wheel Type	Al2O3 (OVU33 A602HH 10VB)
Wheel Diameter	195 mm
Wheel Width	20 mm
Wheel Speed (V_s)	35m/s
Work Speed (V_w)	92 mm/s
Grinding Condition	Dry
Workpiece Materials	Hard steel (EN31-64HRC)
Wheel Feed	Traverse
Vibration Frequency	200Hz
Sine wave Amplitude	4 V (Peak)
Applied Depth Of Cut	10 – 30 μ m

9.2 Grinding Forces

Figure 9.1 presents the normal forces in two different axes which are (Tangential, Axial). In this set of tests, the oscillation was applied in open loop. Figure 9.1 compares the normal forces in axial and tangential vibration, the blue and red has been adopted by Tsiakoumis where it is observed that the forces in axial vibration are very low. The normal forces in axial vibration are around 30% of those recorded in tangential vibration. The experiments were carried out on the same machine tool, with the same process parameters, examination of the raw signal records showed that there was a lot of noise in the signal of tangential vibration. Therefore, poor signal to noise ratio might have led to reading higher force averages. Another reason could be the modification of the vibrating jig and workpiece holder to improve its performance. However, this sharp decrease in cutting forces may be explained by the cutting path performed by the grits. In axial oscillation each grit performs a sine wave motion over the contact length.

Chapter 9: Performance of The Developed Controller

This allows the grits to cut both sides (right and left) and front edges. The rear edge does not engage in cutting because there is no backward motion as in tangential vibration. In tangential vibration, grits do not actually cut but rather remove material from residual elastic deformation when the grits move back in each cycle. This is not the case in axial vibration where grits are continuously cutting with alternating edges, which induces an efficient cutting performance.

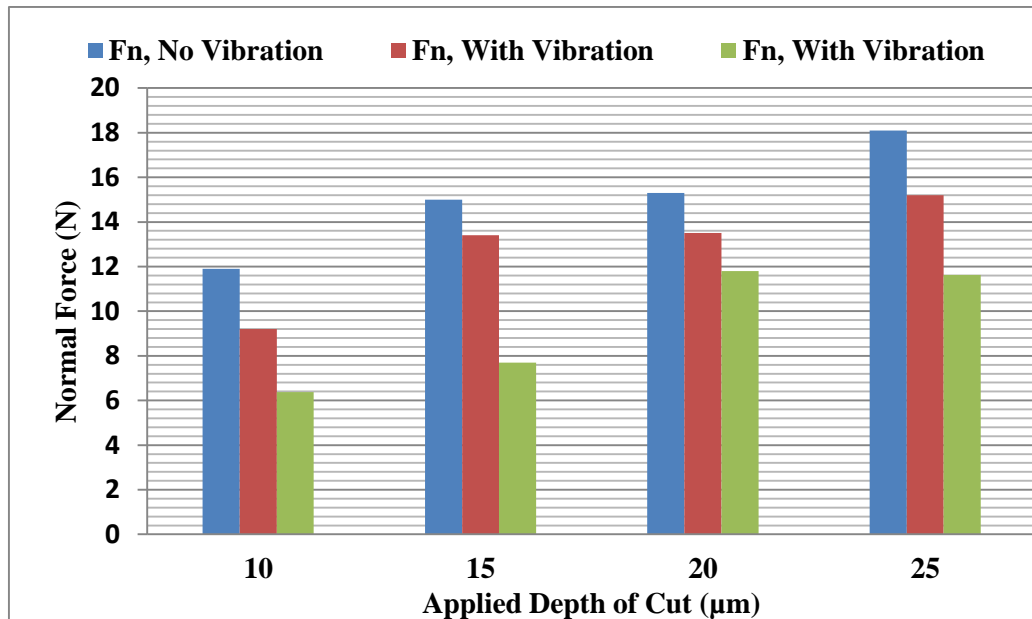


Figure 9.1: Normal Forces in Axial and Tangential

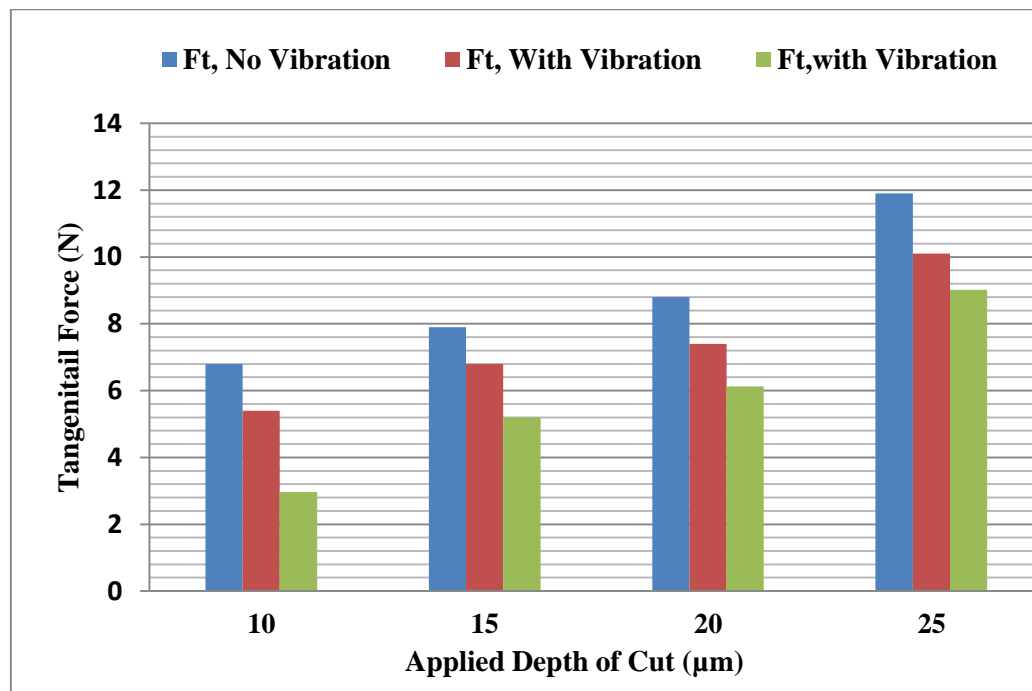


Figure 9.2: Tangential Forces in Axial and Tangential

Chapter 9: Performance of The Developed Controller

Therefore, in Figures 9.1 and 9.2, 60-70% reduction in cutting forces is observed in axial vibration with reference to tangential vibration. Tangential oscillation secured 23% improvement with reference to conventional grinding, whereas axial vibration provided 32% improvement, which is an extra 9% improvement over tangential oscillation.

Figure 9.3 gives the actual depth of cut for conventional, tangential and axial vibration. It shows that, the application of vibration gives a better cutting efficiency and, the improvement reached 12% in tangential oscillation, and 28% in axial vibration. Therefore, the oscillating in axial direction outperformed the tangential by 16% in actual depth of cut, meaning that, axial vibration secured cutting depth close to the target which is good in size holding, but not ideal. It can be noted that the axial vibration providing higher actual depth of cut also secured low cutting forces. The difference in force reading may be due to the signal to noise ratio in Tsiakoumis (2011) and the averaging method used in this study.

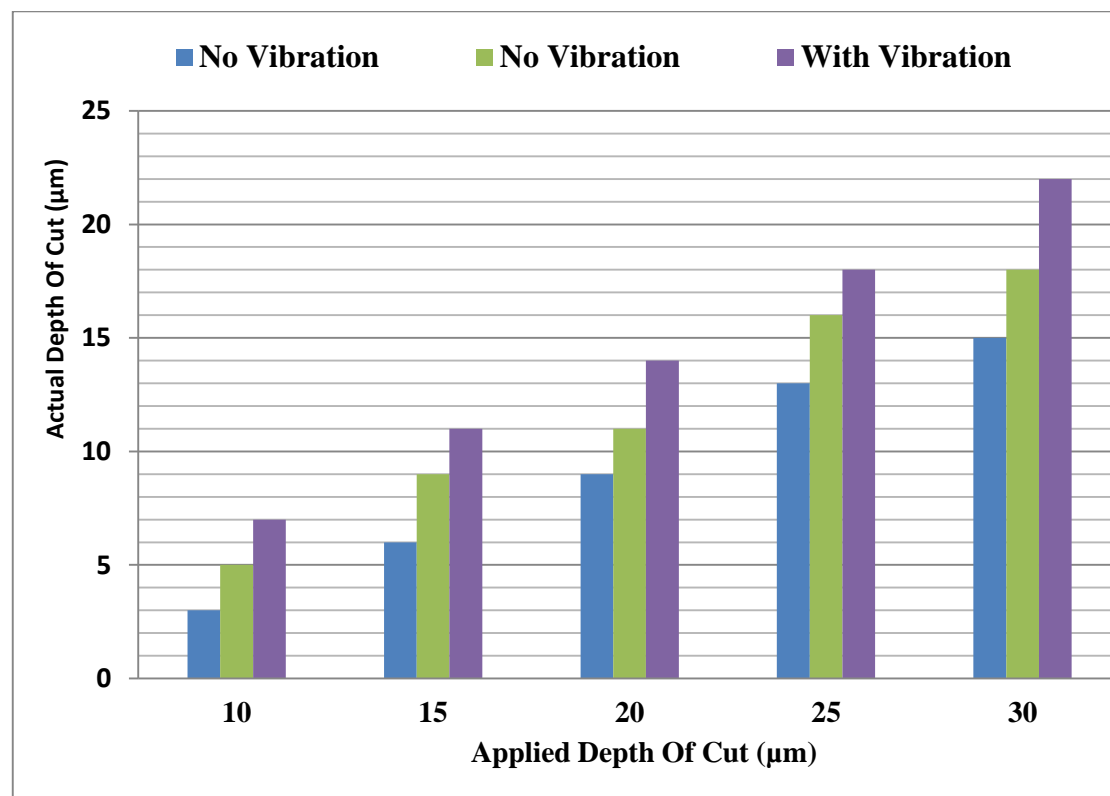


Figure 9.3: Preliminary Experiment Actual Depth of Cut

9.3 Surface Roughness

Figure 9.4 presents the surface roughness for conventional grinding and vibratory grinding with oscillation in axial and tangential direction. As in previous graphs a sharp improvement in roughness is observed, and this is explained by the dressing accuracy. It seems that during the grinding with tangential vibration, the dressing was coarse, whilst in axial oscillation the dressing was fine. Though, the dressing depth was set to identical 10 μm but the lead might have been different as it was manually driven by the operator.

Though surface roughness was about 20% better than conventional grinding, it is hard to conclude whether tangential or axial vibration is better. In addition, the surface measurement was undertaken in Tsiakoumis, (2011) using a physical stylus (TalySurf) that runs in contact with the surface, however in this work an optical measurement system (Bruker) was used. These two measurement systems provide readings in slightly different ways that might affect the results presented here.

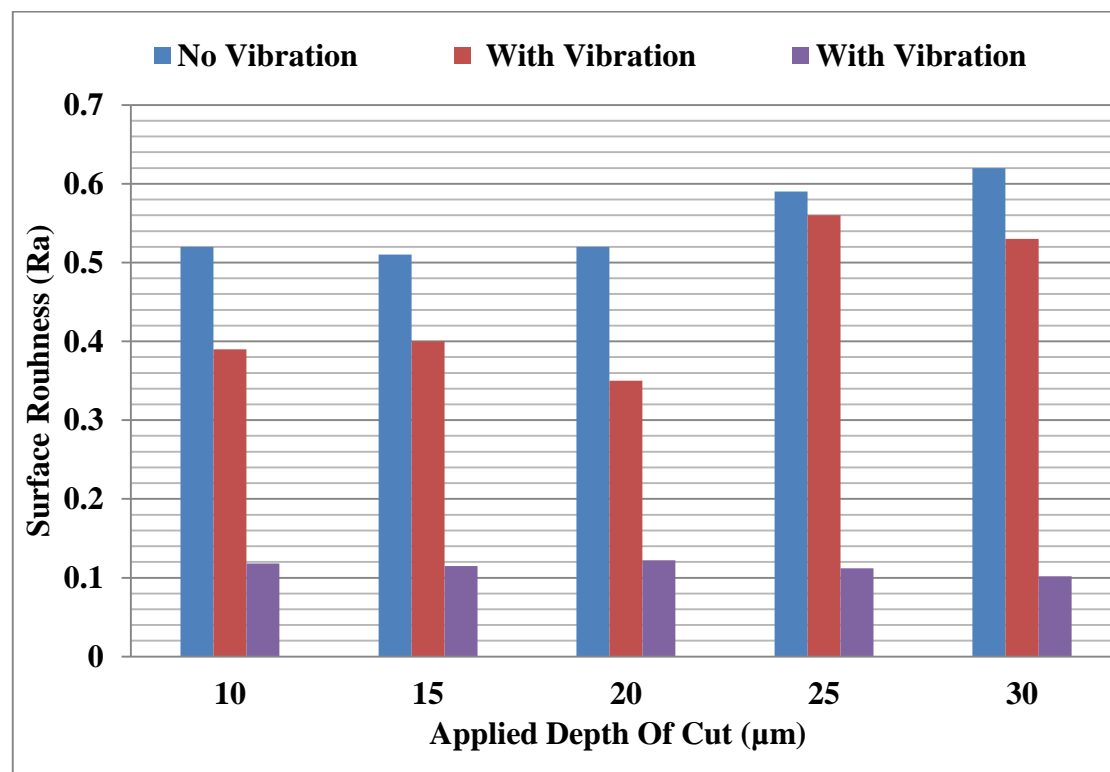


Figure 9.4: Surface Roughness for Mild Steel in Open Loop

9.4 Performance of the Developed Controller

Chapter 6 presented the design and implementation of the controller that used the accelerations of the workpiece holder to control the amplitude of oscillation. In this section this controller was used in actual grinding to quantify its effect on process performance. Figures 9.5 and 9.6 present the outputs of two control strategies i.e. open loop and closed loop control system with reference to conventional grinding.

In Figure 9.5 a decrease of 48% is observed in normal forces for the open loop, and 54% for the closed loop control system.

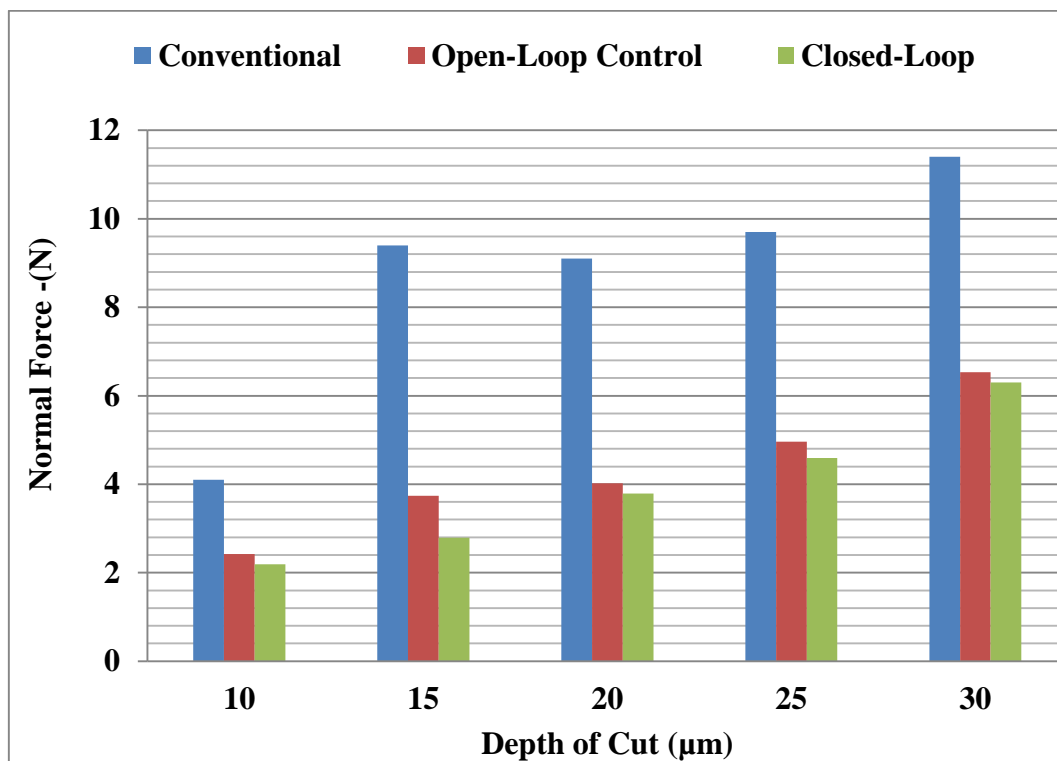


Figure 9.5: Normal Force for Hard Steel

In Figure 9.6 the reduction in tangential forces is about 33% with open loop and 38 % in closed loop control. Across all grinding trials the closed loop control secured on average an additional 6 % reduction in grinding forces.

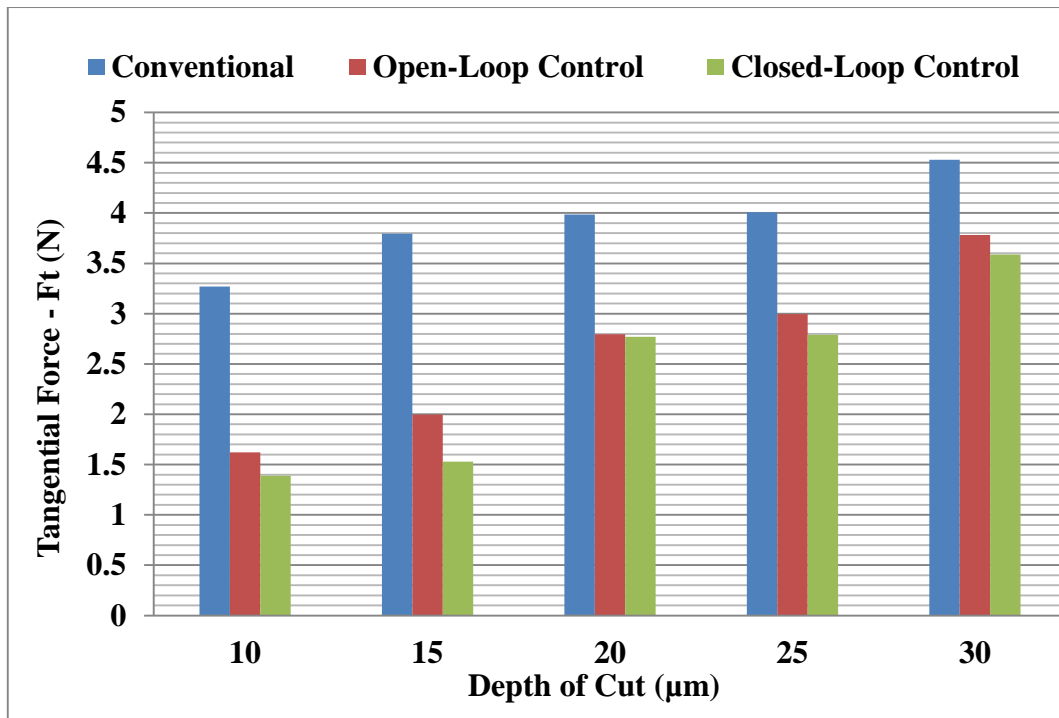


Figure 9.6: Tangential Force for Hard Steel

Figure 9.7 presents, the grinding performance in terms of surface roughness achieved by conventional and axial vibration assisted grinding with open loop and closed loop control. The results indicate that the application of vibration produced better surface roughness in both open and closed loop control technique.

Moreover, the vibration in closed loop control provided a small improvement in surface roughness over the open loop.

However, Tsiakoumis, (2011) reported that the performance of open and closed loop control vibration depends on process configuration, i.e. material (soft or hard), wheel type (close, open, soft, hard, grit size, etc.)

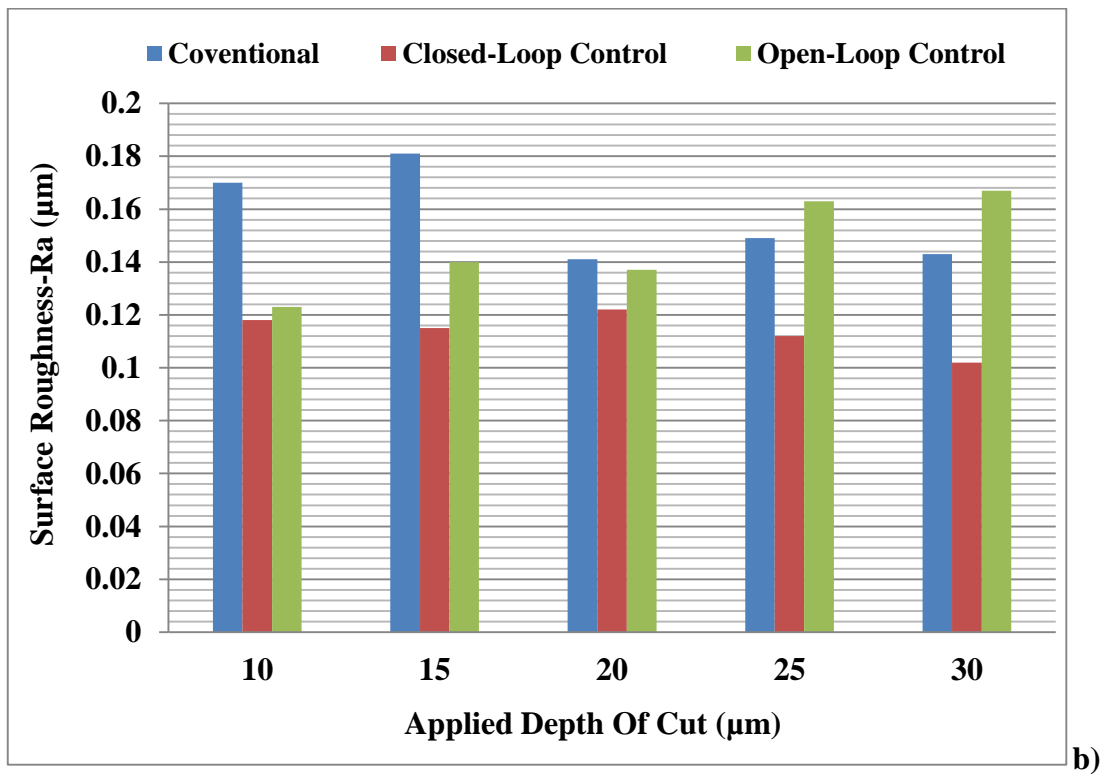
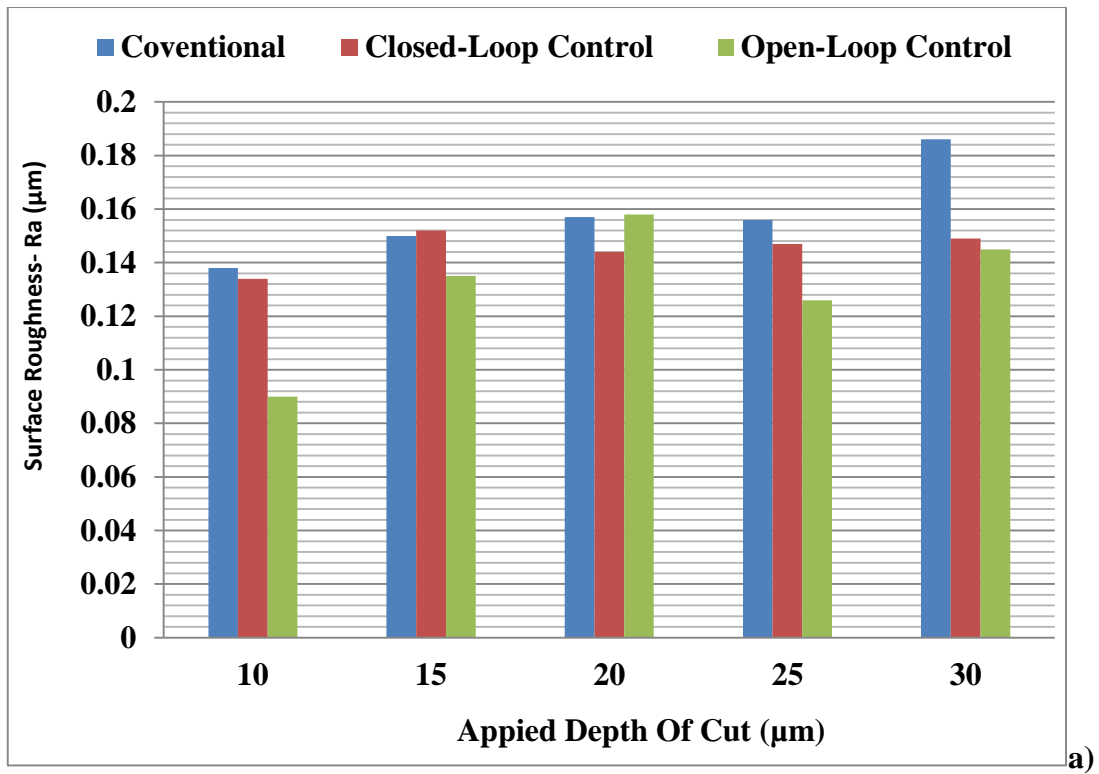


Figure 9.7: Surface Roughness a) Mild Steel b) Hard Steel

9.5 Specific Energy

Specific grinding energy is indicative of the energy spent to remove a unit volume of material and it is often used in the industry as a process efficiency factor. Figure 9.8 shows the grinding energies in conventional grinding with coolant and dry conditions. It illustrates the need for applying coolant, to reduce the friction and thus cutting forces and the surface finish. The process performance in hardened steel is given in Figure 9.8a and Figure 9.8b shows the results for mild (soft) steel.

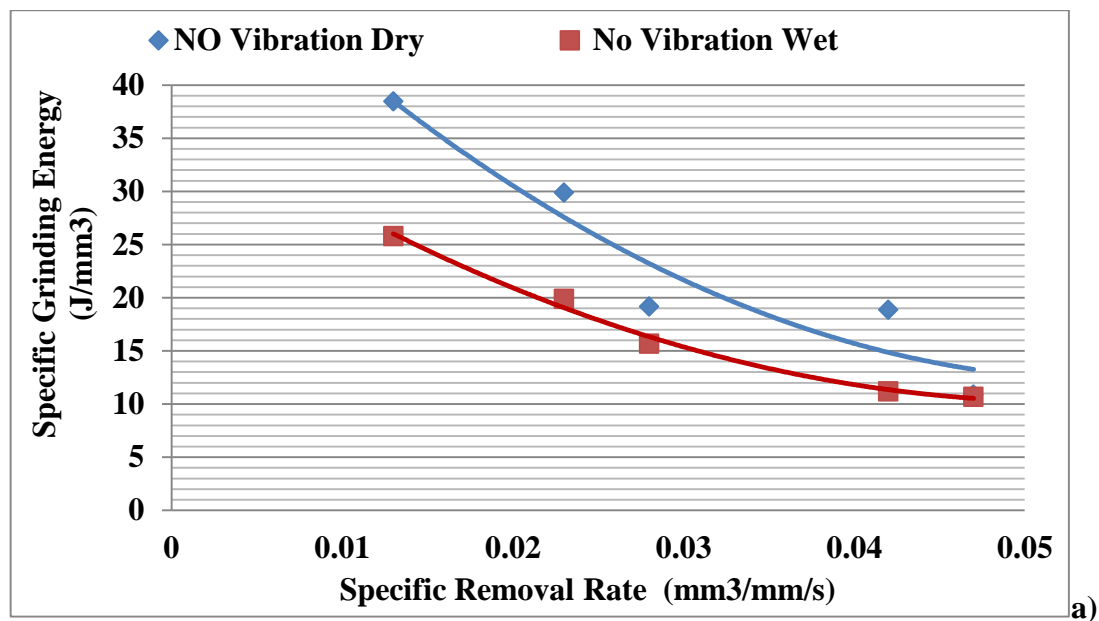


Figure 9.8a: Specific Energy in Hard Steel

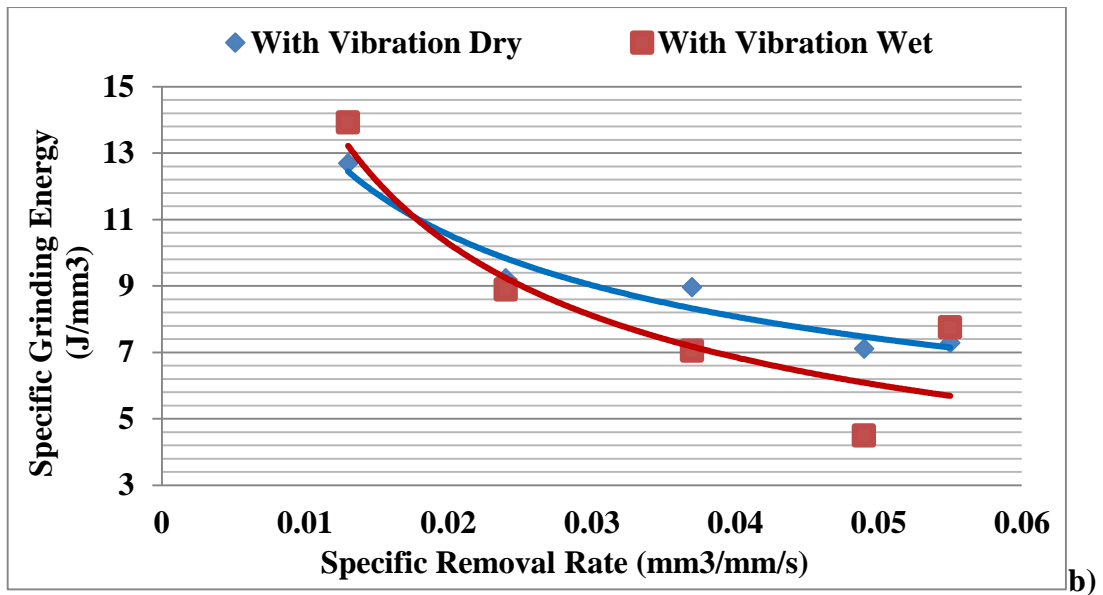


Figure 9.8b: Specific Energy in Mild Steel

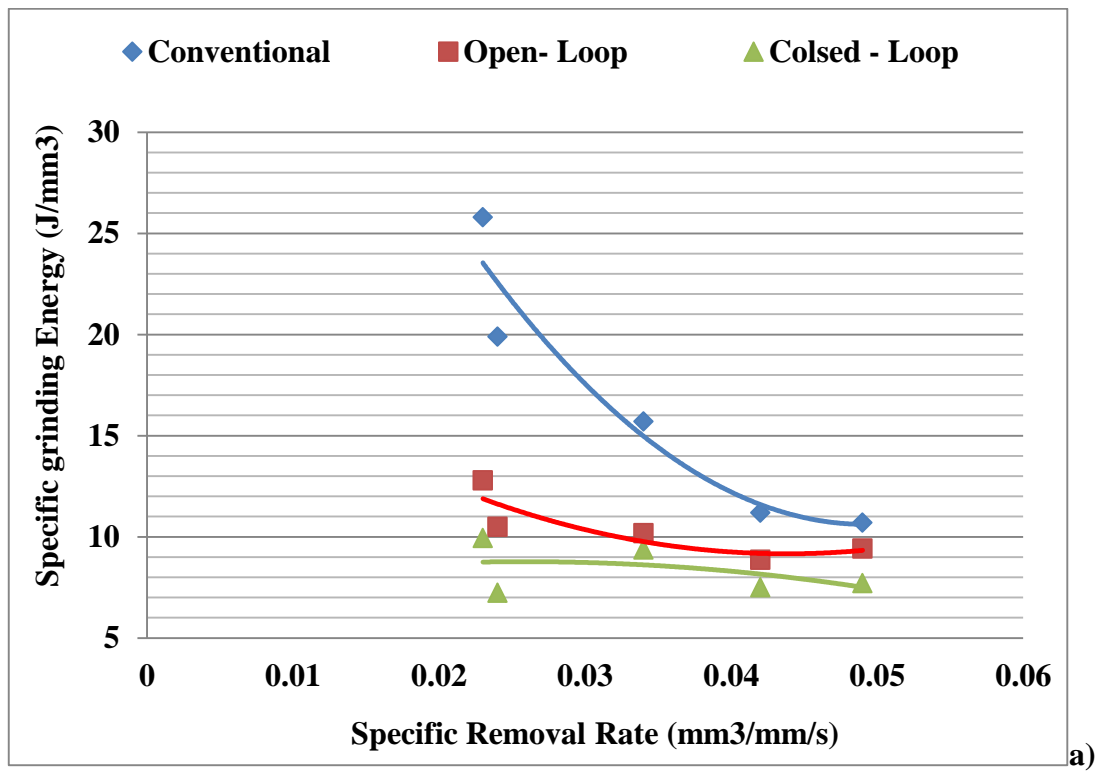


Figure 9.9a: Specific Energy in Mild Steel

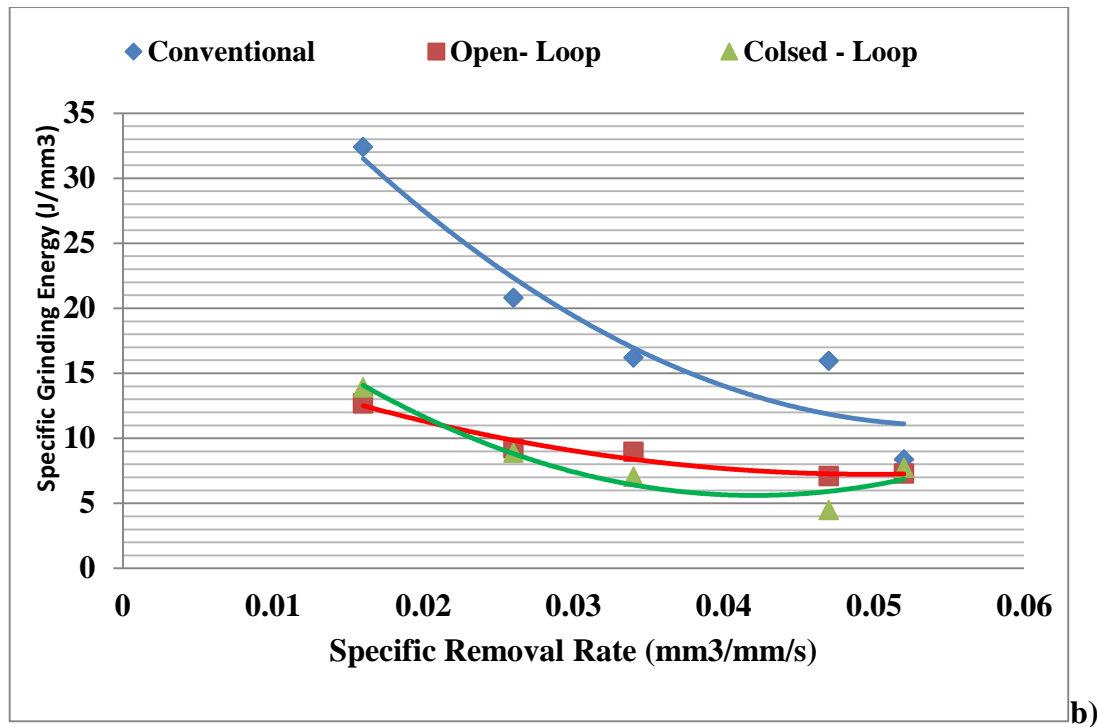


Figure 9.9b: Specific Energy in Hard Steel

Figure 9.9 presents the specific grinding energy requirements of the process by putting side by side conventional, vibratory grinding in open and closed loop control with flood cooling. It is observed in all cases that the superimposed vibration is superior to conventional grinding. In addition, the closed loop control brought in a further 8% reduction in energy consumption.

9.6 Remarks

- This study has revealed and supported that the application of vibration has a positive effect on grinding process performance both in dry and wet conditions. The application of controlled vibration using feedback reduced the grinding forces by 38% with reference to conventional grinding.
- In general the grinding which was vibration assisted secured a higher actual depth of cut, moreover the oscillation in axial direction led to an additional 16 % in actual depth of cut.
- The cutting forces in grinding with axial vibration were about 30% of those recorded in tangential vibration. However there were difficulties in making decisive conclusion on the superiority of axial vibration due to the slight difference in dressing strategy which was done manually thus not repeatable.

Chapter10: DISCUSSION & CONCLUSIONS

10.1 Discussion

The key target of the study was to design a controller to gauge the amplitude of the vibration during the grinding process. Labview and Matlab were used, and a number of different experiments were conducted with varying conditions of machining.

The normal and tangential force was measured using Kilter model 9257 piezoelectric dynamometer, mounted under the self-contained oscillating jig to record the normal force (F_n), tangential force (F_t) and the axial force across wheel width (F_a) during the grinding process.

The self-contained device that vibrates the workpiece during the grinding operation in order to improve wheel life, reduced cutting forces, improved surface roughness, reduced of the load per grain and therefore reduced wheel wear, amount of fluid used for cooling and improved heat removal from the grinding.

A novel model developed in this thesis has supported the experimental work and the elaboration of the controller to improve the process of superimposed vibration. The model parameters were selected to represent typical vibration grinding process. The model was used, in Matlab in conjunction with Labview, to develop the control technique which is presented in this thesis.

A novel approach to quantify the effect of frequencies on the actual achievable depth of cut was elaborated. The vibration at 50 Hz was used as previous investigations showed no great benefits. Therefore 100 Hz and above was investigated. It was observed that with the increase in frequency, the actual achieved depth of cut increases. This result shows a clear benefit in applying vibration in axial direction.

It was identified that superimposing vibration at 100 Hz in this study provided the lowest forces. Also it was shown that at 100 Hz the desired amplitude of oscillation was achieved at the lowest driving voltage, i.e. 4V.

In vibration assisted grinding, a higher value of actual depth of cut was achieved in all cases and the specific removal rates were improved. the grinding with vibration assistance did not provide a net advantage over conventional grinding in terms of forces and surface roughness at applied depth of cut greater than 25 μm .

Chapter 10: Discussion-Conclusion

This was due to the low stiffness of the grinding which had a large deflection at higher depth of cut. In general the grinding which was vibration assisted gave higher actual depth of cut, and the oscillating in axial direction secured an additional 16.3% in actual depth of cut.

The application of oscillation in axial direction showed that a significant improvement of workpiece quality could be achieved. Comparing oscillating in axial direction and tangential direction, axial vibration gave an additional reduction of 9% in normal grinding forces. Equally the superimposition of vibration in axial direction provided on average 25% improvement in tangential grinding forces, surface finish quality and power consumption.

The surface roughness of ground samples were measured using the Brukker GTK surface texture system. In hard steel (EN31-64HNC) vibratory grinding gave a better surface roughness with an average improvement of 29%. The improvement of surface roughness quality tended to worsen with the increasing depth of cut and this is true for both conventional and vibro-grinding.

With reference to conventional grinding, the reductions of surface roughness reached 19 % in tangential oscillation, (Tsiakoumis, 2011) and 20 % in axial direction for the same grinding condition and the same workpiece material.

It is seen that the normal forces in vibration assisted grinding are on average 43% of those generated by conventional grinding, and the tangential forces are about 26% of those without vibration. These results show that grinding with vibration assistance reduced the power consumption on average by 25% compared to the grinding without vibration.

Using the results obtained in a previous study (Tsiakoumis, 2011) where vibration was applied in tangential direction it is observed that the application of oscillation in axial direction secured an overall 32% improvement in tangential forces and 23% in normal forces over conventional grinding. Axial vibration outperformed tangential oscillation by 9%. Similarly, it was observed that, oscillation in tangential direction provided a gain of 12% whereas axial direction gave a 28% increase in actual achievable depth of cut. The net gain between axial and tangential oscillation is 16%.

The application of vibration in open loop decreased normal grinding forces by 48% whereas the developed closed loop control system brought an additional 6% in reduction of normal grinding forces.

Grinding in open loop with vibration gave 32% reduction in tangential force and the application of controlled vibration in closed loop provided an additional 6% gain.

With reference to surface roughness the results indicate that the application of vibration gave better surface roughness in both control techniques (open and closed loop). It was noticed that the vibration in closed loop control outperformed both conventional and open loop control.

In assessing the specific grinding energy as a function of specific removal rate in vibratory grinding with open loop and closed Loop control a series of tests were conducted in dry and wet conditions. The results show that vibration in closed loop with wet condition had the lowest specific energies as it removed more material than the other two grinding processes. The vibro-grinding in wet condition secured higher material removal rate than dry condition with about 8% less grinding energy than open loop control with dry condition.

In general the grinding with vibration assistance gave excellent depth of cut. The oscillating in axial direction provided an additional 16 % in actual achieved depth of cut.

10.2 Conclusions

This investigation has brought forward a fundamental understanding of axial vibration in grinding including:

- The derivation of a mathematical model describing the mechanical response of the driving self-contained oscillating stage under working conditions;
- The development of a complex of Labview programme codes that allow running the experiment, collecting data and controlling the system;
- The development of Matlab/Simulink code for solving and identifying system parameters

- The development of a control system that allowed for a closed feedback loop from the actual grinding zone to the controller. To the knowledge of the author this is first time this has been done in grinding where the actual amplitude of oscillation in the grinding contact zone is monitored and controlled.

The frequency- amplitude characteristics of the self-contained oscillation jig was defined in order to select the best performing displacement sensor. The sensor of choice was the Eddy-current sensor due to its noise-free output and its small size.

The grinding tests were conducted with and without coolant, with vibration and without vibration, and in open and closed loop control. The results showed that it is possible to positively affect the performance of the process using relatively low frequency vibration. It was revealed that the application of oscillation in axial direction (across wheel width) was better than in tangential direction (along table feed). This is because the superimposed oscillation extended the cutting path of the grit and allowed the grit to cut with two additional edges (left and right). Moreover, the grit keeps cutting on both directions of the oscillation, which is not the case in tangential vibration where grits may be disengaged from the workpiece.

The fact that axial oscillation outperformed tangential vibration at low frequency is new because the mass of research is focused on high frequency in the ultrasound range. The concept of controlling the actual amplitude of oscillation is new as in literature most work indicate only the set amplitude at the actuator, but not the real achieved amplitude in the cutting zone.

The comparative study of conventional grinding with open loop and closed loop control grinding showed the net advantage of closed loop grinding over conventional process. This is key finding as it is in line with the finding reported by Tsiakoumis (2011) where tangential vibration in closed loop gives better performance in surface quality. This work has shown that it is possible to achieve improvement in performance at any desired frequency as opposed to ultrasonic devices that must be run at resonance frequency. This is a major finding and this is supported by the results of this work where the driving frequency is not the resonance frequency (240 Hz) of the oscillating jig, but the frequency of the desired amplitude. Therefore one could run the process at any frequency depending on the target amplitude.

However for the oscillating jig used in this study, a major finding in this study was the identification of 100 Hz as the best performing frequency in this low range as opposed to a high frequency range.

It was shown that the application of vibration led to the reduction of cutting forces, to the increase in material removal rate and to the improvement of surface quality. This is a specific gain for the manufacturing industry to attain higher productivity with no modification of the existing machine tools by adding-on the oscillating jig. It also gives room to grind slender workpiece without excessive forces.

It was also proven that the superimposed vibration allowed grinding soft and gummy materials (mild steel, nickel and titanium; result of nickel and titanium were not given here due to confidentiality), which traditionally are difficult to grind.

10.3 Recommendation for Future work

In the frame of one single programme of work it is difficult to cover all aspects of the topic introduced in this thesis. Therefore there is a wide scope for studies to be done in order to take the work presented here to a new level with better functionality.

This will include but not only.

- Direct functional correlation of tangential and axial vibration and device an oscillating jig to operate simultaneously in two axes.
- Develop a 2D controller that would allow manipulating both axes in order to introduce elliptical motion.
- Investigate into functional surface in terms of designing and prescribing specific pattern on the finished surface.
- Undertake a full factorial study of oriented elliptical displacement of the workpiece, to characterise this new process.
- Study a wide range of work materials, in combination with a wide range of grinding wheels in order to derive the working envelope of 2D oriented vibration.

REFERENCES

References

- Ackermann J. (2002), Robust control: the parameter space Approach, Springer- Verlag, London, UK.
- Ackermann. J and D. Kaesbaure. (2001), Design of robust PID controllers, European control conference, pp. 522-527.
- Adachi, K., Arai, N., Harada, S., Okita, K. (1997), and Wakisaka, S. “A study on burr in low frequency vibratory drilling of aluminium”. Surface metrology, Measurement Science and Technology, Vol. 8, pp. 955-972.
- Albizuria, J., Fernandesb, M.H., Garitaonandiab, I., Sabalzac, X., Uribe-Etxeberriac, R., Hernandez, J.M. (2006) ‘An active system of reduction of vibrations in a centreless grinding machine using piezoelectric actuators’ International Journal of Machine Tools & Manufacture.
- Astrom. K and T. hagglund. (1995), PID Controllers: theory, Design, and Tuning, Instrum. Soc. America, Research Triangle Park, NC.
- Astrom. K, p. Albertos, and J. Quevedo. (2001), PID Control, Control Engineering Practice, pp. 1159-1161.
- Atkinson, A. (1992). Optimum Experimental designs. Clarendon, Oxford.
- Babitsky, V.I., Kalashnikov, A.N., Meadows, A., Wijesundara, A.A.H.P. (2003) ‘Ultrasonically assisted turning of aviation materials’ Journal of Materials Processing Technology v132 pp157–167.
- Babitsky, V.I., Mitrofanov, A.V., and Silberschmidt, V.V. (2004), ultrasonically assisted turning of aviation materials: simulations and experimental study, Ultrasonic, 42(1–9), pp.81-86.
- Batako Andre. D.L, Morgan M. N. and Rowe W Brian, (2012), high efficiency Deep Grinding with very high Removal Rates, International Advance Manufacturing Technology., pp.1- 11

References

- Batako, A. D., Rowe, W. B., Morgan, M. N. (2005) ‘Temperature measurement in high efficiency deep grinding’ *International Journal of Machine Tools & Manufacture*, 45 pp1231–1245.
- Bianchi, E. Fernandes, O., Valarelli, I., Silva, E., Spinelli. (1999) “Contribicao dos Rebolos Superabrasivos com ligantes Resinoide e Vitrificado”.
- Billing. S.A and Zhu Q. M. (1994). A structure detection algorithm for nonlinear dynamic rational models. *International Jornal*, pp. 1439-1463.
- Bonifacio, M. and Diniz, E., (1994) “ Correlating tool wear, tool life, surface roughness and tool vibration in finish turning with coated carbide tools”. Vol. 173, pp. 137-144.
- Brehl, D. (2008) “Review of vibration assisted machining”. *Precision Engineering*, Vol. 32, pp. 153-173.
- Brehl, E., Dow, A., Garrad, K., and Sohn, A. (2006) “Microstructure fabrication using elliptical vibration-assisted machining”. *Proceedings of ASPE*, Vol. 39, pp. 511-514.
- Cerniway. (2005) M. Elliptical Diamond Milling: Kinematics, Force and Tool. MSc Dissertation Graduate Faculty, North Carolina State University.
- Cheng, C.H., Tony, L. Schmitz, G. Scott, D. (2007)‘Rotating Tool Point Frequency Response Prediction Using RCSA’ *Machining Science and Technology*.
- Chern, G. L. & Chang Y-C. (2005) ‘Using two-dimensional vibration cutting for micro-milling’ *International Journal of Machine Tools & Manufacture* v46, pp. 659–666.
- Chern, L., and Chang, C. (2006). “using two-dimensional cutting for micro-milling”. *International journal of machine Tools & Manufacture*, Vol. 46, pp. 659-666.

References

- Chiu, N. & Malkin S. (1993) 'Computer simulation for cylindrical plunge grinding' University of Massachusetts-USA.
- Clerc, M. (1999) the swarm and coon G.A., theoretical consideration of regarded control, Trans. ASME, vol. 75, pp.827-834.
- Cohen G, and Coon G. (1953) "Theoretical consideration of control", Trans. ASME, Vol 75, pp. 827-834.
- D'Azzo, J.J., C. H. Houpis. (1966) Feedback Control System Analysis and Synthesis," McGraw-Hill Book Company.
- Datta. A, M.T. ho, and S.P. (2001) Bhattacharyya, structure and Synthesis of PID Controllers, Springer-Verlag, London, UK.
- Delansky. J.F. and Bose. N.K. (1989), Schur stability and stability domain construction, Int. J. Control, Vol.49, No. 4, pp, 1175-1183.
- Endo, T., Tsujimoto, T., and Mitsui, K. (2008). "Study of Vibration-assisted micro-EDM: the effect of vibration on machining time and stability of discharge", precision engineering, vol. 32, pp. 269-277.
- Filiz, S., Cheng, C.H., Powell, K.B., Schmitz, T.L., Ozdoganlar, O. B. (2009) 'An Improved Tool-Holder Model for RCSA Tool-Point Frequency Response Prediction' Precision Engineering 33 pp. 26-36.
- Gaing, Z.L. (2004) Aparticle swarm optimization approach for optimum design of PID controller in AVR system. IEEE transaction on Energy Conversion, pp. 384-391.
- Gallemaers J P, Yegenoglu K, Vatovez C. (1986); Optimizing Grinding Efficiency with Large Diameter CBN Wheels; Int. Grind. Conf. Philadelphia.
- Garcia-Gardea, E., Kapoor, S.G., Wu, S.M. (1980) 'Analysis of Grinding Dynamics by Dynamic Data System Methodology' International Journal of Machine Tool Design and Research, v.21 No.2 pp.99-108

References

- Giordano, F, Fox W, Horton S and Weir M (2008) First course in mathematical Modelling Belmont. Belmont, CA, United State of America: Cengage Learning.
- Goodwin. C, Graebe. F and E. Salgado. M. (2001) Control System Design, Prentice-Hall, Upper Saddle River, NJ.
- Goodwin. G. C, Graebe. S.F and Salgado. M.E. (2001) Control System Design, Prentice-Hall, Upper Saddle River, NJ.
- Grumble. M.J. (2001) industrial Control Systems Design, John Wiley& Sons, Manchester, UK.
- Gryazina. E. N, and Polyak. B. T. (2006) Stability regions in the parameter space: D-decomposition revisited, Automatica, vol. 42, pp. 13-26.
- Harris C. M and Piersol A. G. (2002) Harris' Shock and vibration Handbook. 5th Edition. New York. NY Mcgrwa-Hill.
- Haykin, S. (1994) Neural Networks: A comprehensive Foundation. Macmillan College Publishing Company, 866 Third Avenue, NY.
- Hendricks. E and Sorenson S. (1990) Mean value modelling of spark ignition engines. SAE Technical papers.
- Ho. M.T, and Lin. C.Y. (2003) PID Controller Design for robust performance, IEEE. Trance Automatic control, Vol. 48, pp. 1404-1409.
- ID Grinding, 2011, [Online] available:<http://www.fvht.com/gallmar/i.d-grinding>. (accessed on 3rd November 2012).
- Ikawa, N., Donadson, R., Komanduri, R., Konig, W., McKeown, P., Moriwaki, T., Stowers, I. (1991) "Ultraprecision Metal Cutting – The Past, the Present and the Future", Annals of the CIRP, Vol. 40, part 2, pp. 587-597.
- Isaac Horowitz. (1991) Survey of quantitative feedback theory (qft), International Journal of Control, vol. 53, PP. 255-291.

References

- Jenkins, E. H., Kurfess, R. T. (1996) 'Dynamic Stiffness Implications for a Multi-Axis Grinding System' *Journal of Vibrations and Control*, v.3 pp.297-313.
- Jenksin, E. H., Kurfess, R.T. (1996) 'dynamic stiffness implication for a multi-Axis Grinding system.
- Jiang, Y.X., Tang, W.X., Zhang, G.L., Song, Q.H., Li, B.B., Du, B. (2007) 'An Experiment Investigation for Dynamics Characteristics of Grinding Machine' *Key engineering materials* Vol. 329 pp.767-772.
- Jung-Hwan, A., Han-Seok, L., Seong-Min, S. (1999) "Improvement of Micro-machining Accuracy by 2-Dimensional Vibration Cutting", *American Society of Precision Engineers Conference Proceedings*, Vol. 20, pp. 150-153.
- Jury. E. I, and Blanchard. J. (1961) "Stability test for linear discrete systems in table form".
- Kang, Y., Chang, Y.P. Tsai, J.W., Chen, S.C., Yang, L.K. (2001) 'Integrated CAE Strategies for the Design of Machine Tool Spindle-Bearing Systems. *Finite Elements in Analysis and Design* 37 pp.485-511.
- Keel. H, Rego. J, and Bhattacharyya S. (2003), A new approach to digital PID controller design, *IEEE Trans. Automatic control*, Vol. 48, No4.
- Keel. L. H, Rego. J. I and Bhattacharyya. S.P. (2003) a new approach to digital PID controller design, *IEEE Trans. Automatic control*, Vol. 48, No4.
- Kim, J.-D and Choi, I.-H. (1997) Micro surface phenomenon of ductile cutting in the Ultrasonic vibration cutting of optical plastics, *Journal of Materials Processing Technology*, 68(1), pp.89-98.
- Kirpitchenko, I., Zhang, N., Tchernykh, S., Liu, D.K. (2002) 'Dynamics and Control of Grinding Machines' *6th International Conference on Motion and Vibration Control' Part 2*, pp 1039-44.

References

- Klocke, F., Rubenach, O. (1998) “Ultrasonic Assisted Diamond Turning of Steel and Glass”, American Society of Precision Engineers Conference Proceedings, Vol. 19, pp. 179-190.
- Krishna Kumar. K and Goldberg D.E, (1992) control system optimization using Genetic Algorithms, Journal of Guidance, control and Dynamics, pp. 735-740.
- Krohling R, Rey J., (2001) Design of optimal disturbance rejection PID controllers using genetic algorithm. IEEE pp. 78-82.
- Kuriyagawa, T., Shirosawa, T., Saitoh, O., Syoji, K. (2002) ‘Development of Micro Ultrasonic Abrasive Machining System’ JSME International Journal Vol. 45, No 2.
- Lee, H. S. & Furukawa, Y. (1988) ‘On the Method to Determine the Stiffness of Grinding Machines’ Bull. Japan Soc. Of Prec. Engineering Vol.22 No.2.
- Liang, Z., Wu, Y., Wang, X., Zhano, W. (2010) ‘A new two dimensional ultrasonic assisted grinding (2D- UAG) method and its fundamental performance in monocrystal silicon machining’ International journal of Machine Tools & Manufacture, pp. 728-736.
- Liu, C.S., Zhao, B., Gao, G.F., Jiao, F. (2002) Research on the characteristics of the cutting force in the vibration cutting of a particle-reinforced metal matrix composites SiCp/Al, Journal of Materials Processing Technology, 129(1-3), pp.196-199.
- Ljung L. (1999) System identification, theory for the user. Prentice Hall PTR, New Jersey, USA.
- Ljung L. (2007) system Identification Toolbox 7 User Guide. The math work, Inc.
- Ljung. L, (2010) System identification toolbox, getting started Guide. The math works, Inc., 3 Apple Hill drive.

References

- Mahmud Iwan Solihin. (2011) Lee fook Tack and Moey leap Kean, Tuning of PID Controller using Practicale swarm optimization, processing of the international conference on advanced science.
- Malkin, Stephen (1989) Grinding Technology: Theory and Applications of Machining with Abrasives, Society of Manufacturing Engineers, Dearborn, and Michigan.
- Mannan, M. (1999) “Detection and location of structural cracks using FRF measurements”. IMAC VIII.
- Marinescu, I. D., Hitchiner, M., Uhlmann, E., Rowe, B. W., Inasaki, I. (2007) ‘Handbook of Machining with Grinding Wheels’ CRC Press, Taylor and Francis Group LLC, New York USA.
- Matsumura, T. (2005) Glass machining with micro-end mill. Japan Society of Mechanical Engineers (JSME), Vol. 1, pp. 139-158.
- Maziah Mohamad. (2004) vibration control of mechanical suspension system using AFC (Active Force Control).
- Milos, G., and Milutinovic, D. (2009) “Desktop 3- parallel kinematic milling machine”. International of advance manufacturing Technology, Vol. 46, pp. 51-60.
- Mitrofanov, A.V., Babitsky, V.I., Silberschmidt, V.V. (2003) ‘Finite element simulations of ultrasonically assisted turning’ Computational Materials Science v28 pp 645–653.
- Mohony T.O, C J Downing and K Fatla (2000) Genetic Alogrithm for PID parameters optimization: minimizing error criteria, process control and instrumentation, pp. 148-153.
- Moriwaki, T, and Shamoto, E (1991) Ultraprecision Diamond Turning of stainless steel by applying ultrasonic vibration. Annals of the CIRP, Vol. 40, pp. 559-562.

References

- Musa. M, and Hewit J. (1996) Active Force Control Applied to A rigid Robot Arm.
- Oberg, E., Jones, Franklin D., Horton, Holbrook L., and Ryffel, Henry H.(2000) Machinery's Handbook, Industrial Press Inc., New York, p.1190.
- Ogata. K, (1987) Modern control systems, university of Minnesota, Prentice Hall.
- Ogata. K. (1994) Discrete Time Control System, presentic-Hall, Englewood Cliffs, NJ.
- Ogata.K, (2005) Modern Engineering (fifth edition), university of Minnesota Prentice Hall.
- Orynski, F. & Bechcinski, G. (2003) ‘Experimental research on the vibration surface grinding’ XXVI Naukowa Szcola Obrobki Sciernej.
- Orynski, F., Pawlowski, W. (2002) ‘The mathematical description of dynamics of the cylindrical grinder’ International Journal of Machine Tools & Manufacture 42 pp.773–780.
- Outer- Diameter. (2011) [Online] available:<http://www.fvht.com/gallmar/i.d-grinding>. (accessed on 12 September 2012).
- Palanna, R, and Bukapatanam, S, (2002) “The concept of model-based tampering for improving process performance: An illustrative application to turning process,” International Journal of Machining Science and Technology, P. 263-282.
- Piezoelectric Actuator. (2012) [Online] available: <http://www.piceramic.com/products.html> (11March2012).
- Pillay. N, and Govender P. (2007) a particle swarm optimization Approach for model independent Tuning of PID control Loop.

References

- Rosen, A (1956), “ceramic Transformer and filters, ” Proc. Electronic Comp. p. 205-211.
- Rubenach O. (2003) from process innovation to product innovation—ultrasonic assisted diamond turning of optical glass. In Diamond Rev 41–7.
- Shamoto E, Moriwaki T, (1999) ultraprecision diamond cutting of hardened steel by applying elliptical vibration cutting. CIRP Ann; 48:441–4.
- Shamoto E, Suzuki N, Tsuchiya E, Hori Y, Inagaki H, Yoshino K, (2005) Development of 3-DOF ultrasonic vibration tool for elliptical vibration cutting of sculptured surfaces. CIRP Ann 54:321-4.
- Shamoto, E., Hirokazu, M., and Moriwaki, T. (2006) “Ultraprecision 6- Axis table driven by means of walking drive”. Department of Mechanical Engineering, Kobe University, pp. 299-302.
- Shamoto, E., Moriwaki, T. and Matsuo, M. (1997) Ultraprecision diamond cutting of die steel by applying ultrasonic elliptical vibration cutting, International Conference and Exhibition on Design and Production of Dies and molds, Istanbul, Turkey, pp.105-110.
- Sjoberg J., Zhang Q., Ljung L., Benveniste A., Delyon B, Glorennec P., Hjalmarsson H., Juditsky A, (1995) Nonlinear black box modelling in system identification: pp. 1691-1724.
- Skelton, C. (1968) “Turning with an oscillating tool” International of journal Machine Tool Des. & Res., Vol. 8, pp. 239-259.
- Soderstrom. T, and Stoica. P, (1989) System identification. Prentice-Hall.
- Solihin, M. (2011) Tuning of PID Controller using particle Swarm Optimization (PSO), Proceeding of the International Conference on Advanced Science.
- Soylemez. M. T, N. Munro and H. Naki (2003) fast calculation of stabilization PID controllers, Automatica, pp. 121-126.

References

- Surface Grinding (2011) [Online] available: <http://www.dkprecision.co.uk> (accessed on 12 September 2012).
- Suzuki, N., Haritani, M., Yang, J., Hino, R. and Shamoto, E. (2007) Elliptical vibration cutting of tungsten alloy molds for optical glass parts, *CIRP Annals – Manufacturing Technology*, 56(1), pp.127-130.
- Syoji, K. (1999) ‘Evolution in Grinding: Aiming for the maximum limits in efficiency and precision-from micron to Nano, and from high speed to ultra-high speed.’ *Journal of the Japan Society for Precision Engineering*, 65:31.
- Tawakoli, T. (1993) ‘High Efficiency Deep Grinding’ VDI-Verlag GmbH, Mechanical Engineering Publications, London.
- Tawakoli, T. and Azahoushang, B. (2008) ‘Influence of ultrasonic vibrations on dry grinding of soft steel’ *International Journal of Machine Tool & Manufacture*. Pp 1585-1591.
- Triantos. G and Shenon. A. T, (2004) NARMAX Structure selection for powertrain control. *Proceeding IFAC symposium on: Advance in Automatic Control*, Salerno, PP. 1-4.
- Tsiakoumis V. I, (2011) an investigation into Vibration assisted Machining – Application to surface grinding Processes PhD thesis LJMU.
- Visioli A. (2001) Tuning of PID controllers with fuzzy logic. *Proc Inst Elect control theory*, pp.1-8.
- Walsh, A., Baliga, B., Hodgson, A., (2004) Force modelling of the crankshaft pin grinding process. *Processing of the institution of Mechanical Engineers, Journal of Automobile Engineering*, p219-1-5.
- Wang, X., Zhou M., Gan K., and Ngoi, B. (2002) “Theoretical and experimental studies of ultraprecision machining of brittle materials with ultrasonic vibration”. *International Journal of Advanced Manufacturing Technology*. Vol. 20, pp. 99-102.

References

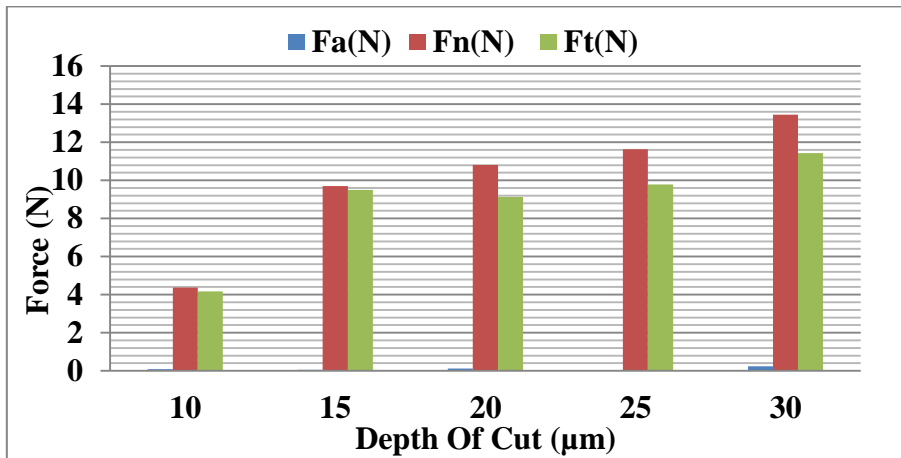
- Wang, Q, P Spronck and R Tracht (2003) an overview of genetic algorithms applied to control engineering problems. Proceeding of the second international conference on machine learning and cybernetics.
- Weber H, Herberger J, Pilz R. (1984) Turning of Machin able glass ceramics with an ultrasonically vibrated tool. CIRP Ann; 33:85–7.
- Wellstead, P. E. (1979) Introduction to physical system modelling. Academic press, London.
- Wok, D.P., Leung. T. P and F. sheng. (1993) Genetic algorithm for optimal dynamic control robot arms. Proceedings of the international conference on industrial Electronics, control and instrumentation.
- Wu, Y., and Fan, Y. (2003) “Develop an ultrasonic elliptical vibration shoe centreless technique”. Journal of Materials Processing Technology, pp. 155-159.
- Xiao, G., Malkin, S. & Danai, K. (1992) ‘Intelligent Control for Cylindrical Plunge Grinding’ Proc. of American control conference. Chicago: 391.
- Xiao, M., and Sato, K (2003) “the effect of tool nose radius ultrasonic vibration cutting of hard material”. International Journal of Machine Tool & Manufacuring, Vol, 43, pp. 1375-1382.
- Xu, A. Data and S.P. (2001) Bahattyya, Computation of all stabizing PID gains for Digital control system, IEEE Trans. Automatic control, vol.46, No.4.
- Zaruba, Z. (2005) ‘Development of Grinding Strategy Incorporating Novel Methods for Controlling Wave shift and Wheel Run-Out’ (Doctoral Dissertation) Faculty of computing, Engineering and mathematical Sciences, University of Bristol.
- Zhang, B., & Meng, J. (2003) ‘Grinding damage in fine Ceramics’ Journal of Nanotechnology and Precision Engineering. (1): pp25-30.

References

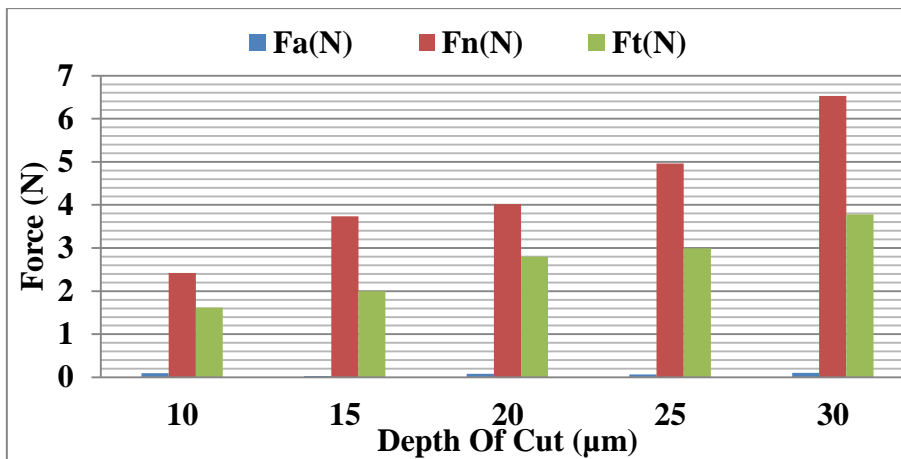
- Zhang, B., Hu, Z., Luo, H., Deng, Z. (2006) ‘Vibration-Assisted Grinding Piezo table Design and Fabrication’ *Nanotechnology and Precision Engineering* Vol.4 No.4.
- Zhang, M., Kirpitchenko, I., Liu, D.K. (2005) ‘Dynamic Model of Grinding Process’ *Journal of Sound and Vibration*, 280 pp.425–432.
- Zhang, P. & Miller, H. M. (2003) ‘Grinding wheel loading with and without Vibration assistance’ *Proc. of the ASPE Annual Meeting* pp 455-458 Michigan Technological University, Houghton, MI.
- Zhao, Z.Y. (1993) Fuzzy gain scheduling of PID controllers. *IEEE Transaction System, Man and Cybernetics*.
- Zhong, Z. W., Yang, H. B. (2004) ‘Development of a vibration Device for Grinding with Micro vibration.’ *Materials and Manufacturing Processes* 19:6, pp: 1121-1132.
- Zhou, M., Eow, Y., Ngoi, B., Lim, E. (2003) ‘‘Vibration – assisted precision Machining of steel with PCD tools’’. *Material Manufacturing Process*, pp. 825-834.
- Ziegler J, and Nichols B (1942) optimum setting for automatic controller, *Trans. ASME* 64, p. 759-768.

A-1 Hard Steel All Forces

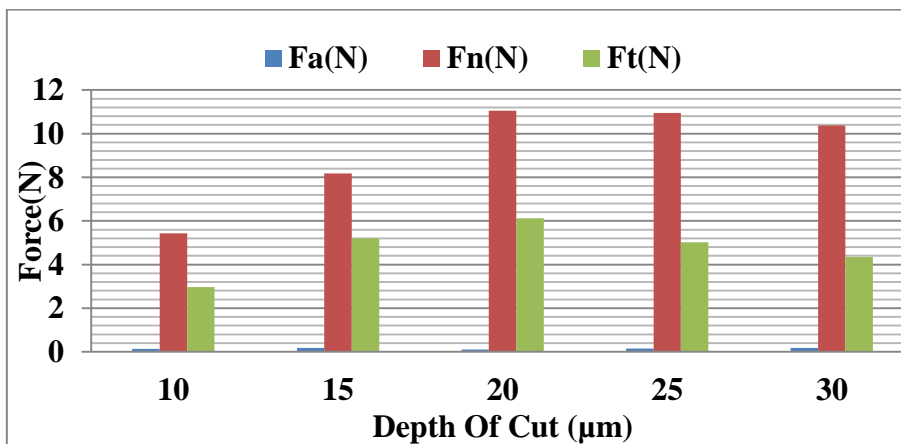
No vibration



With Vibration 100Hz

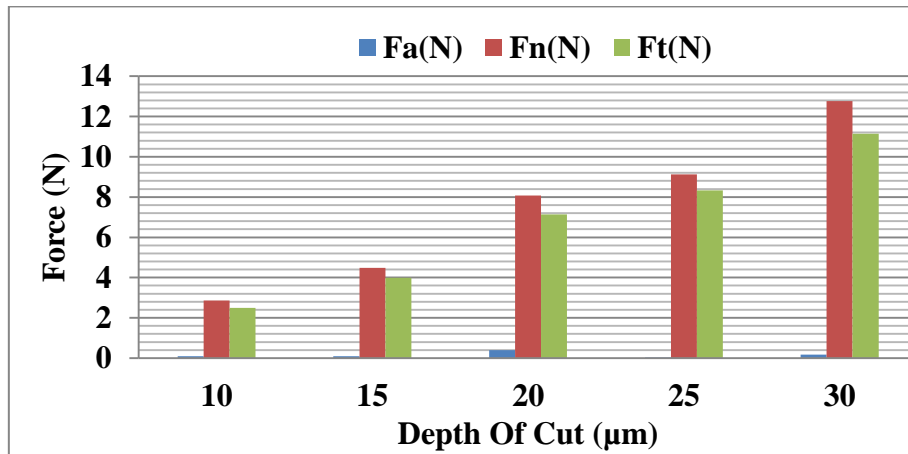


With Vibration 150Hz

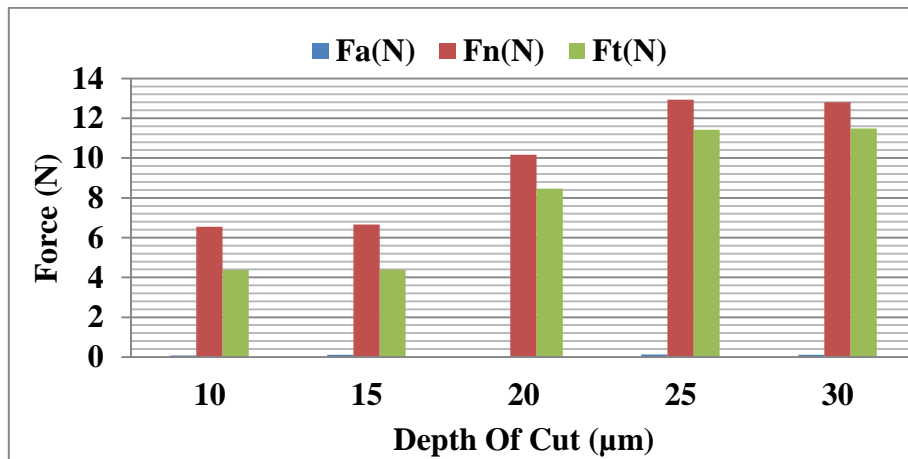


Appendices

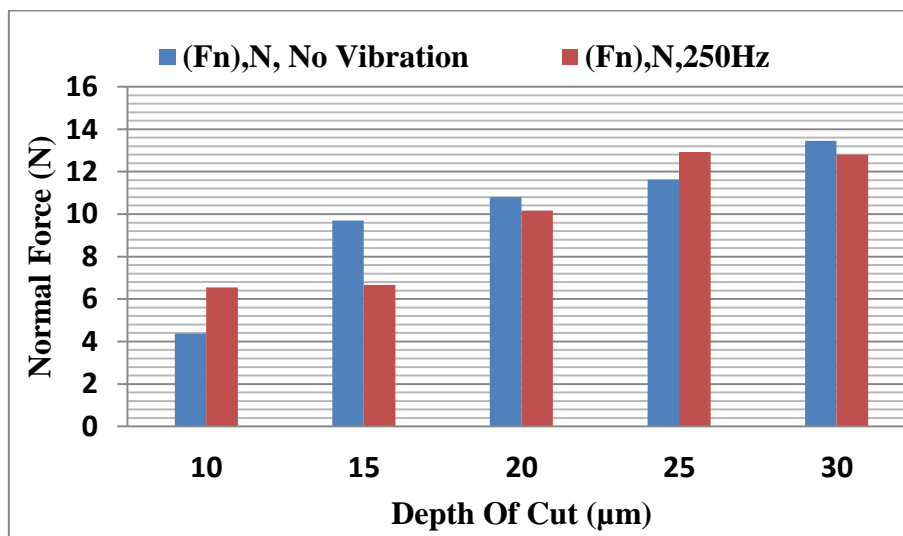
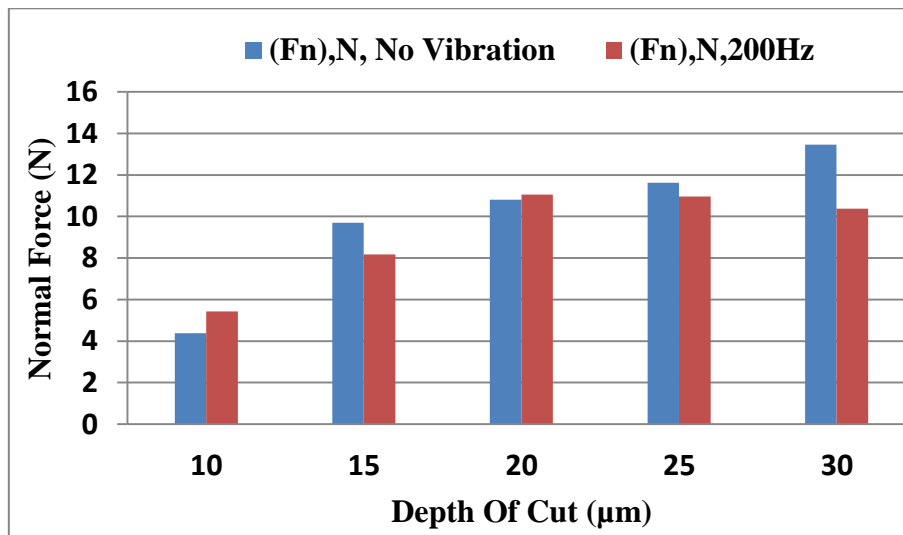
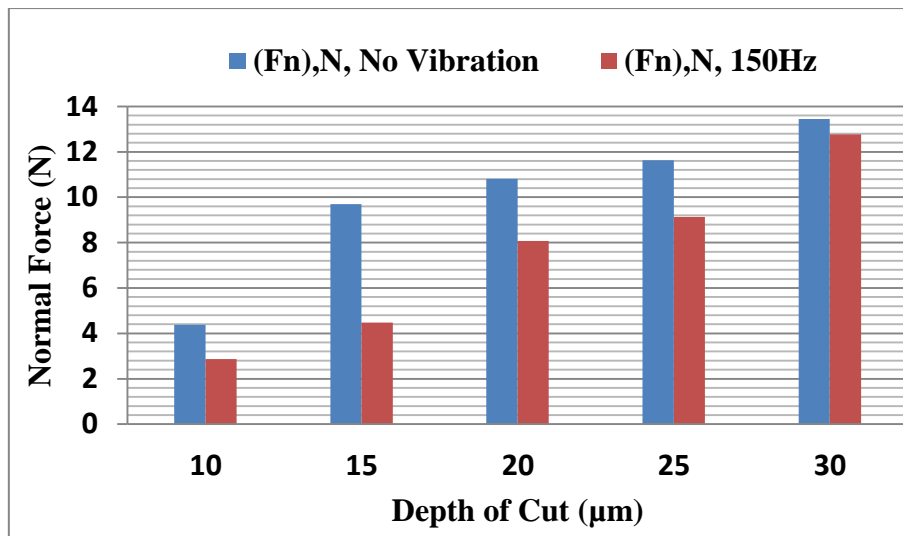
With Vibration 200Hz



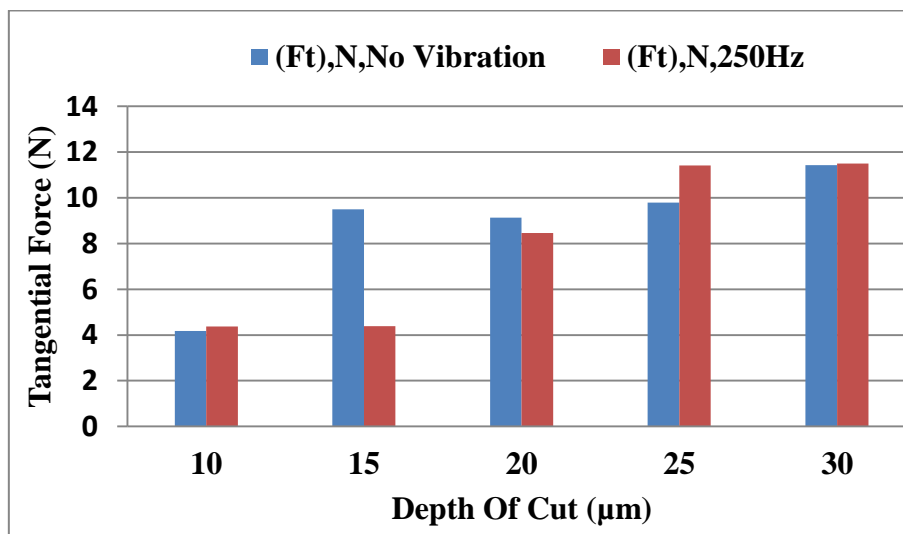
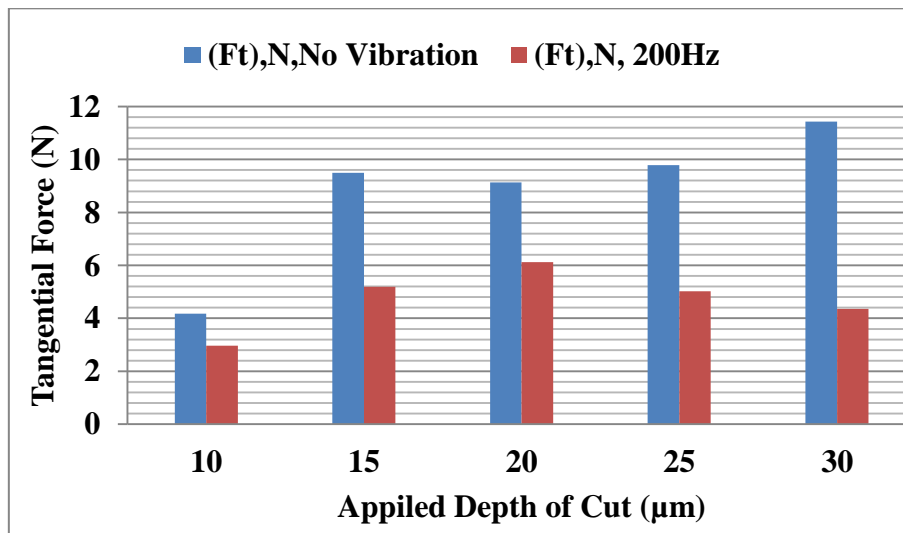
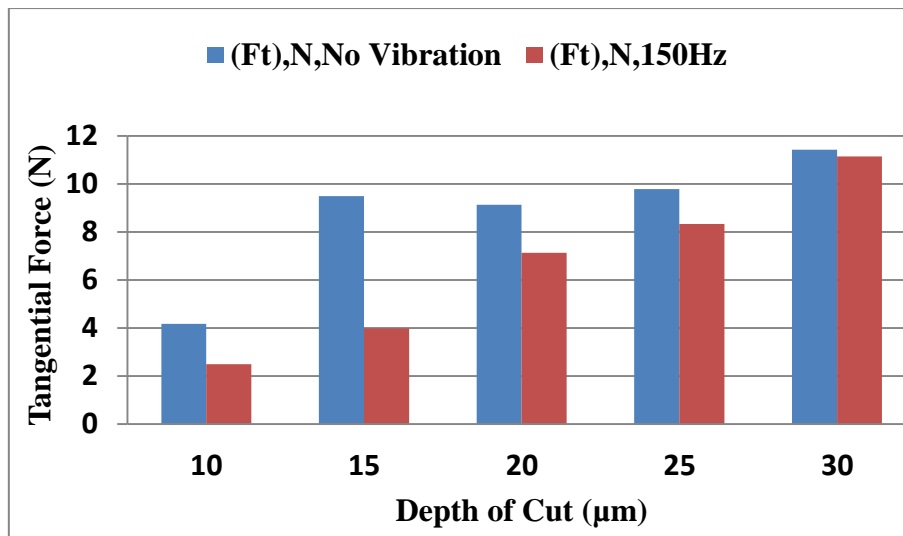
With Vibration 250Hz



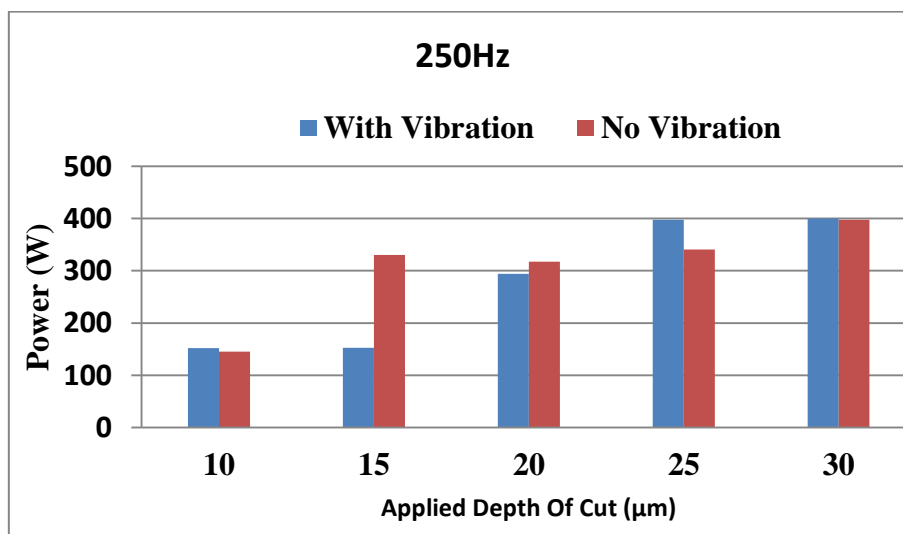
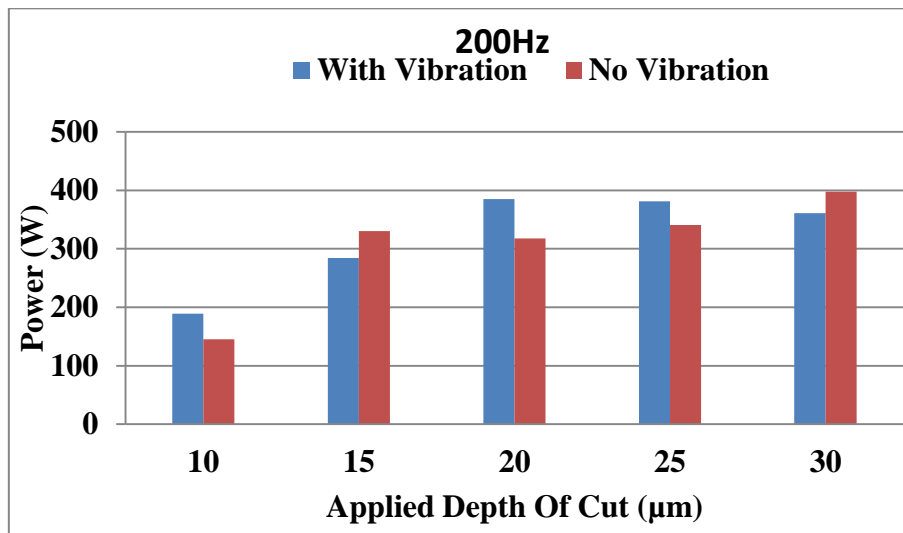
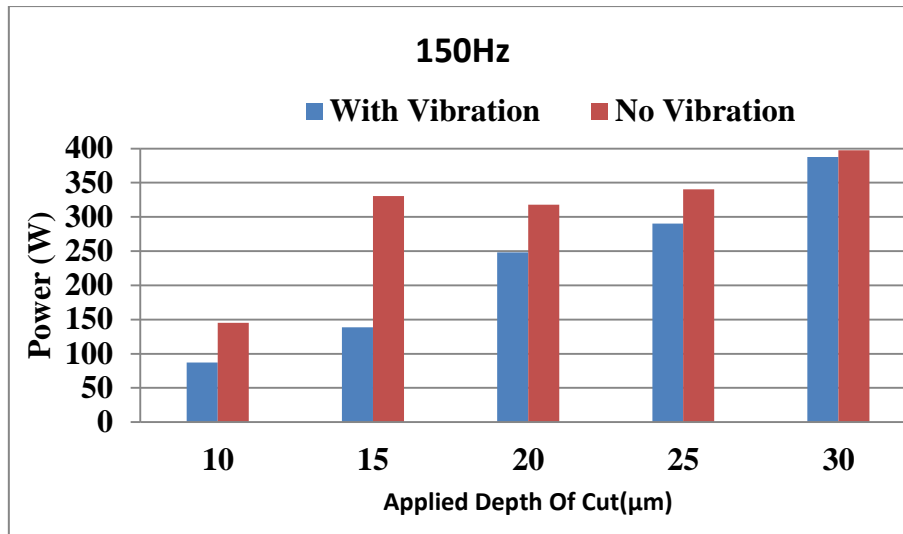
A-2 Hard Steel Normal Forces



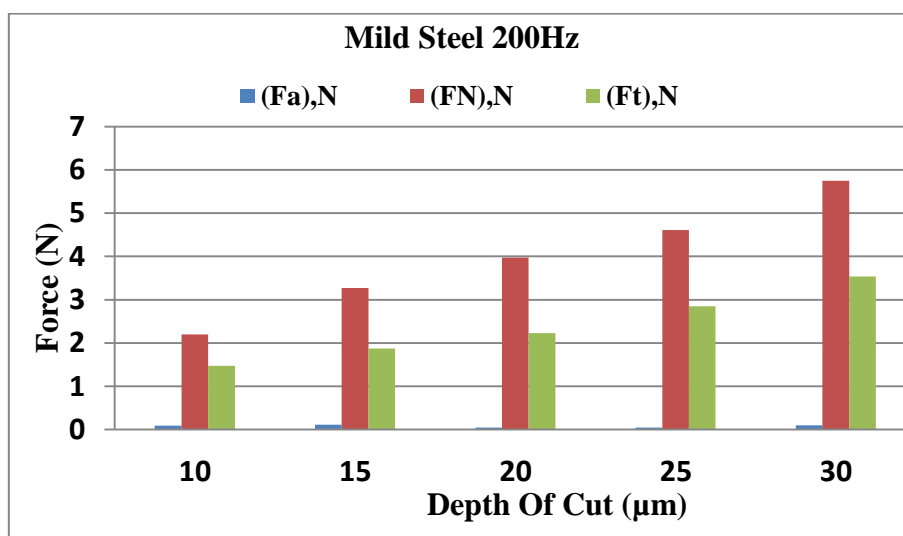
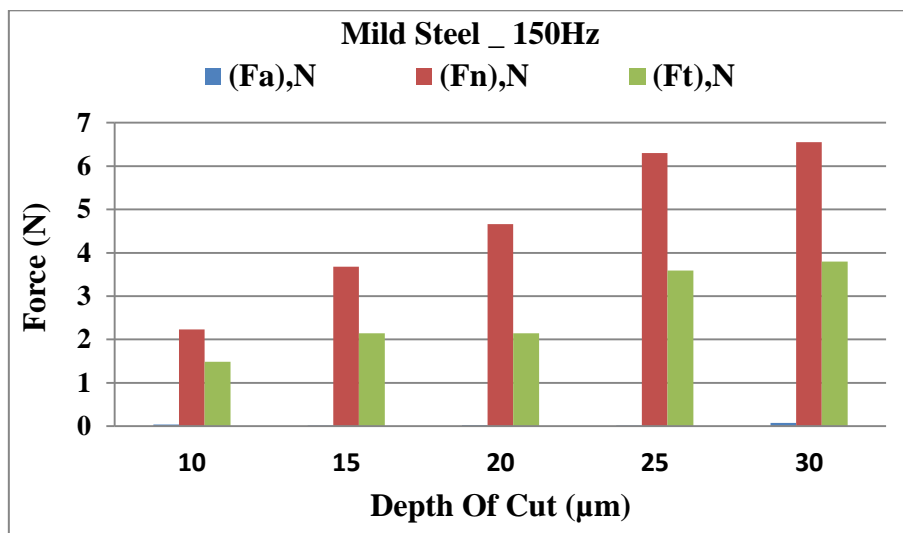
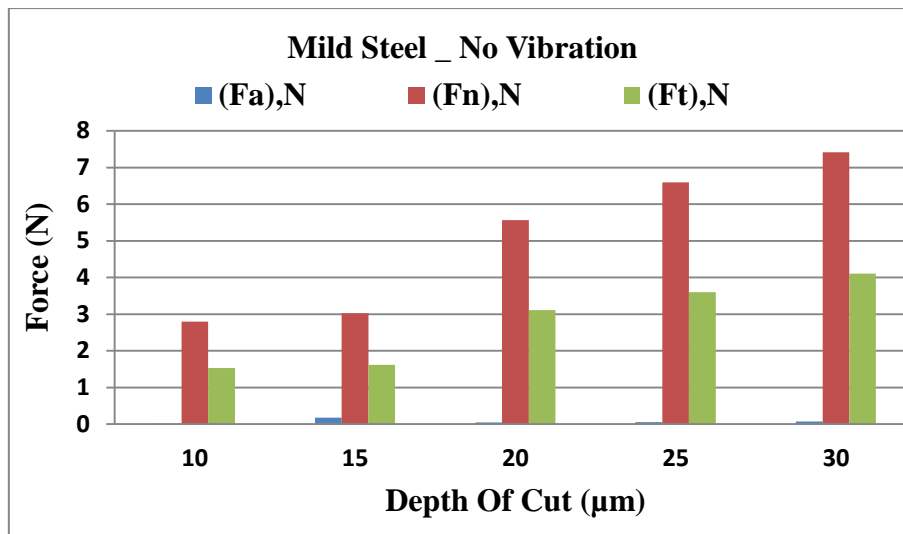
A-3 Hard Steel Tangential Forces



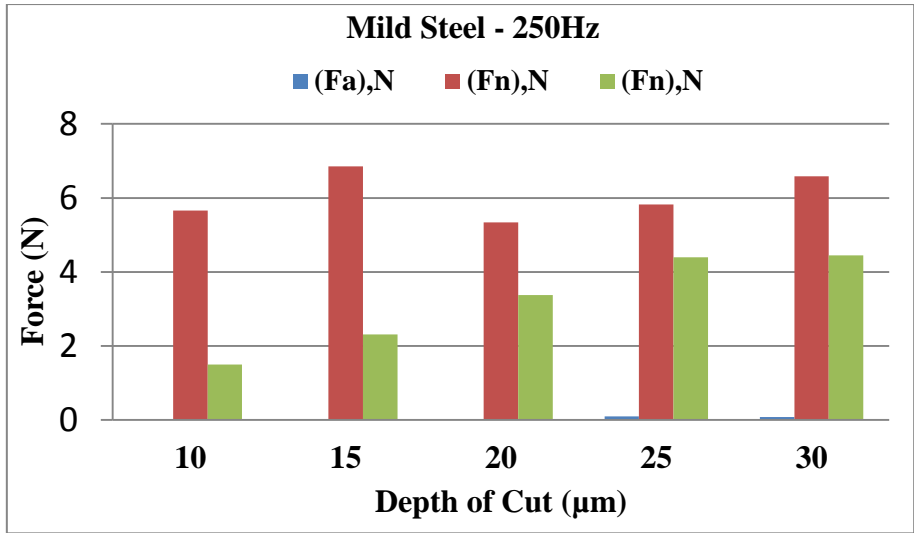
A-4 Hard Steel Power



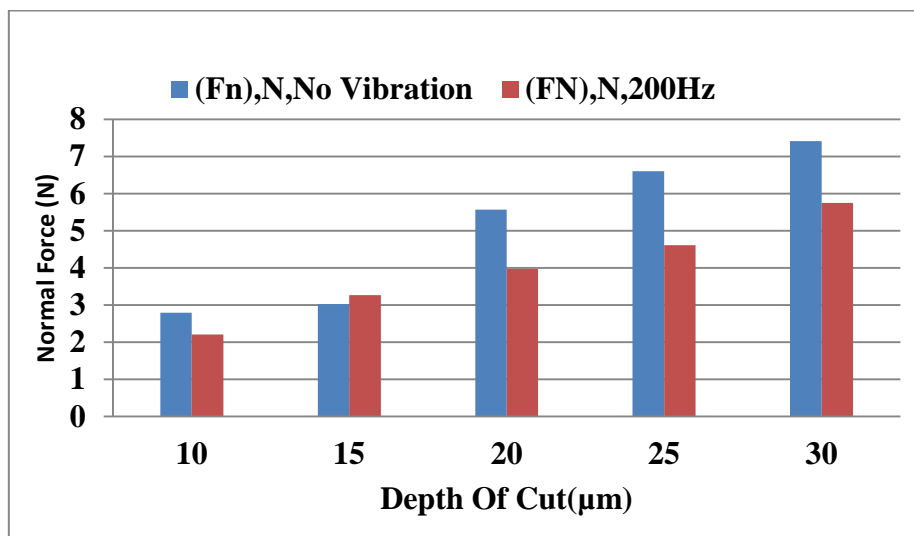
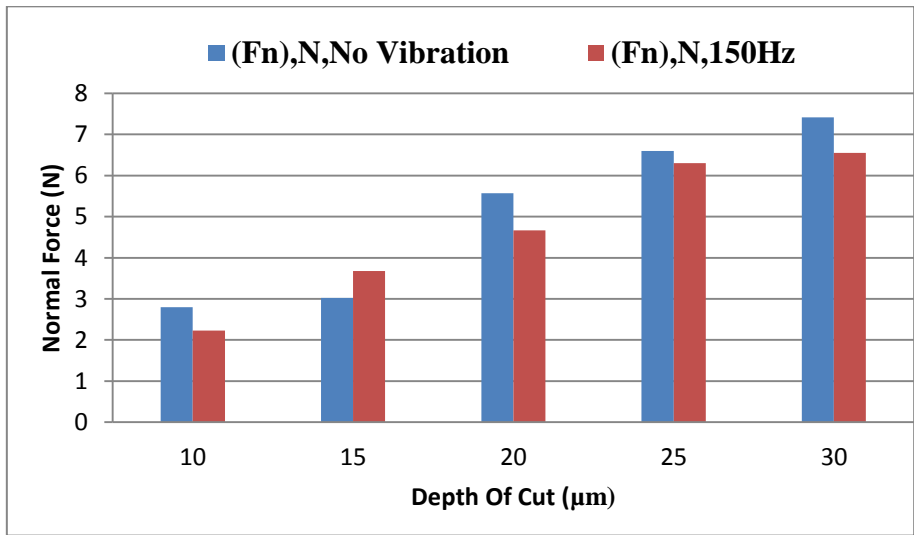
B-1 Mild Steel All Forces



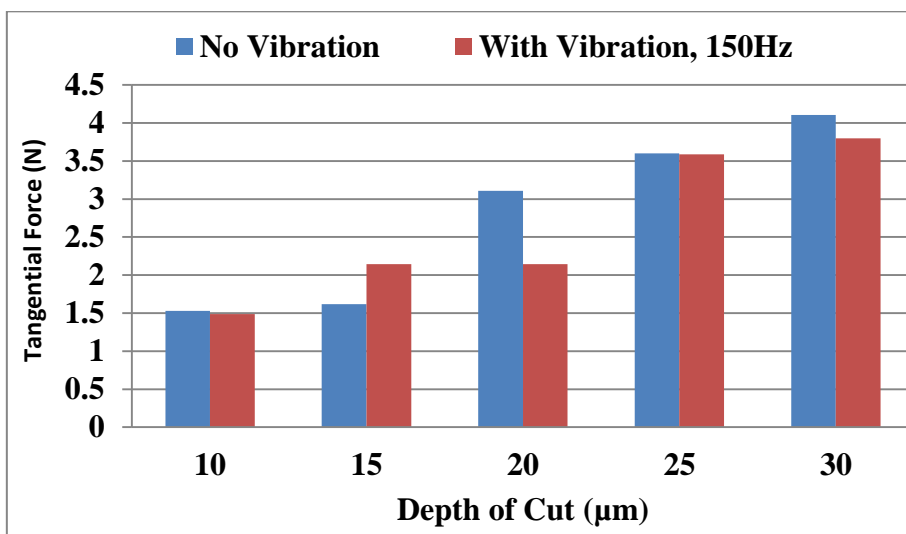
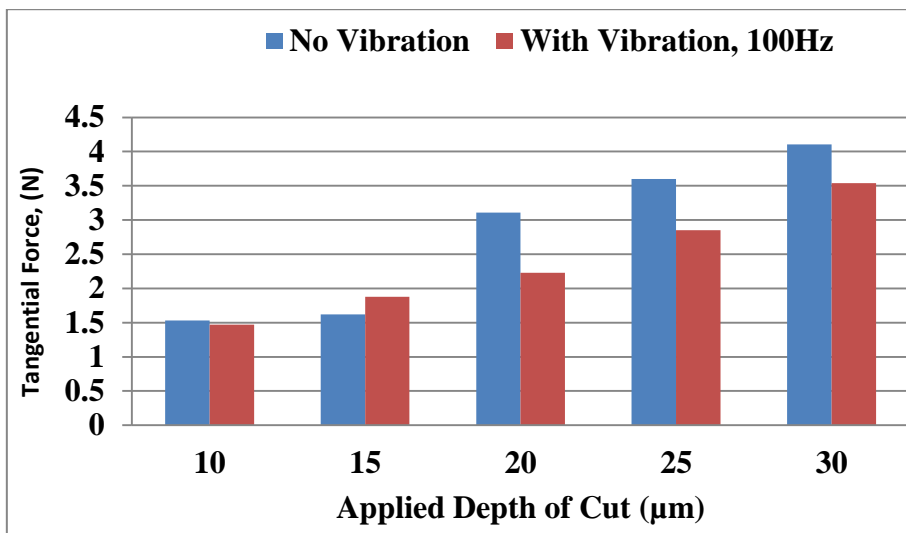
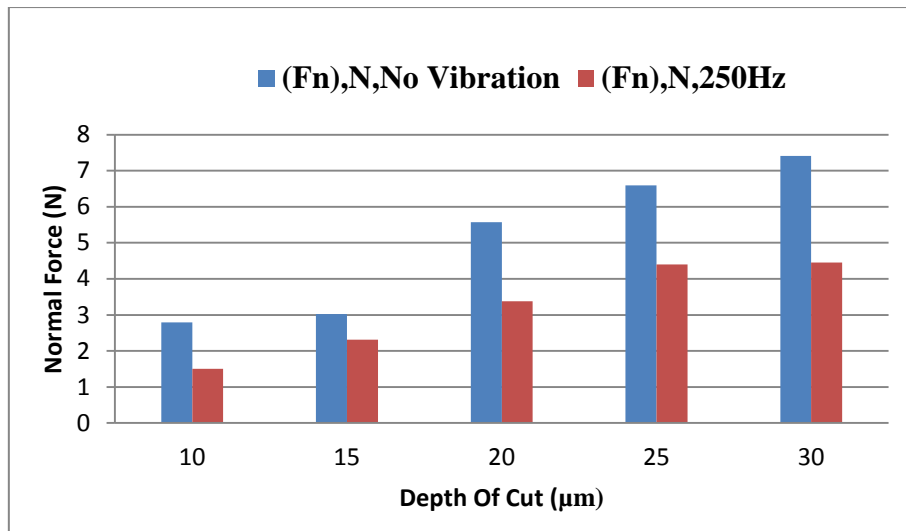
Appendices



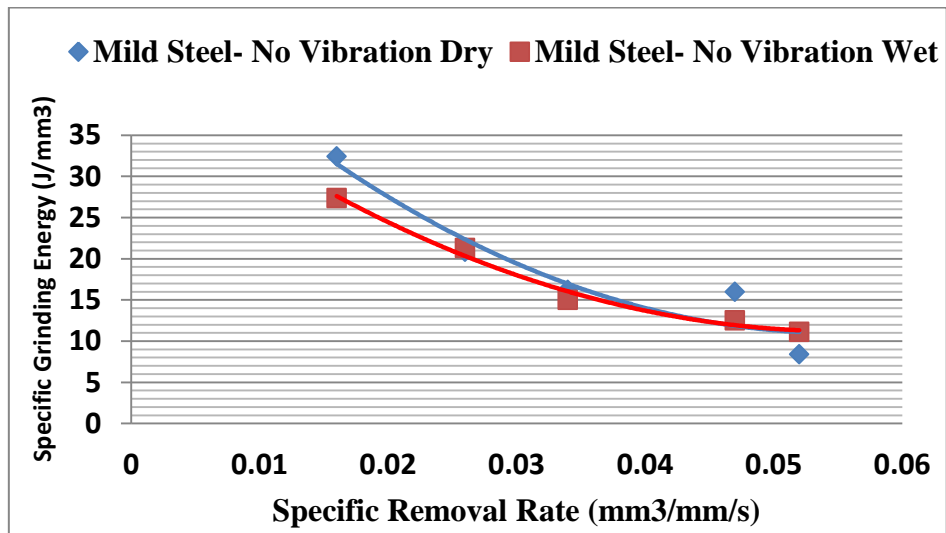
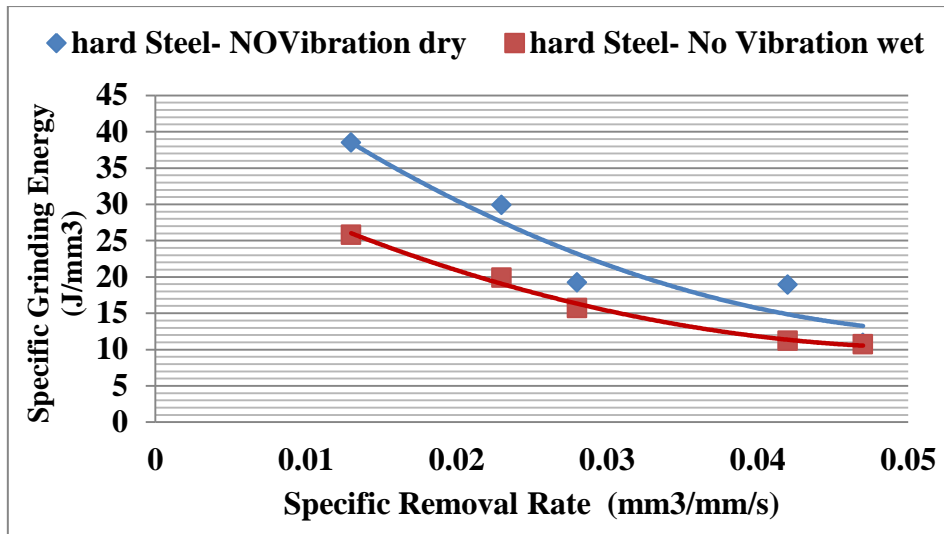
B-2 Mild Steel Normal Forces



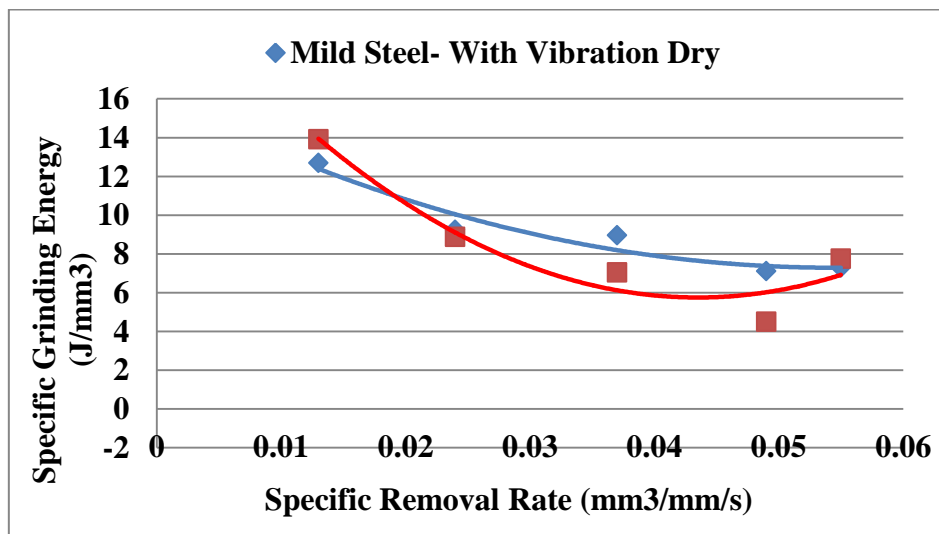
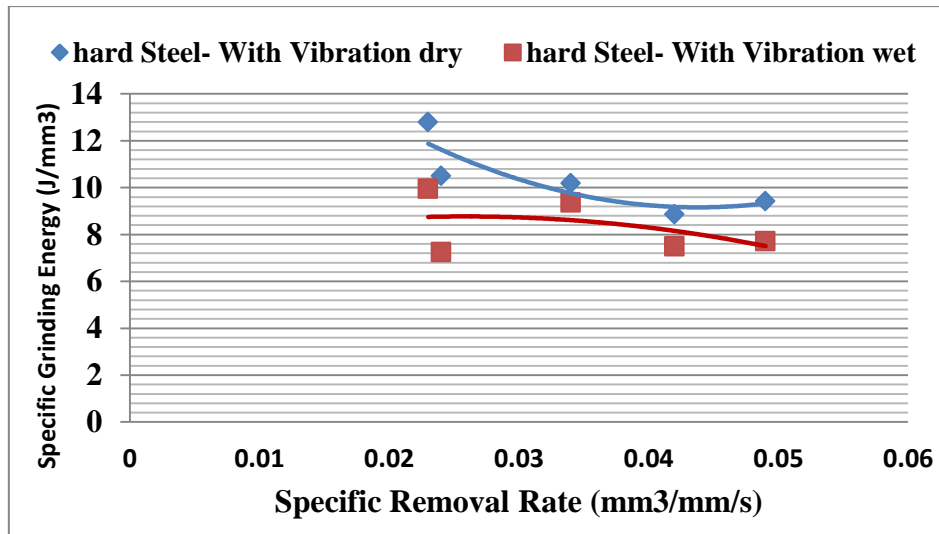
Appendices



C-1 Specific Grinding Energy Soft Steel

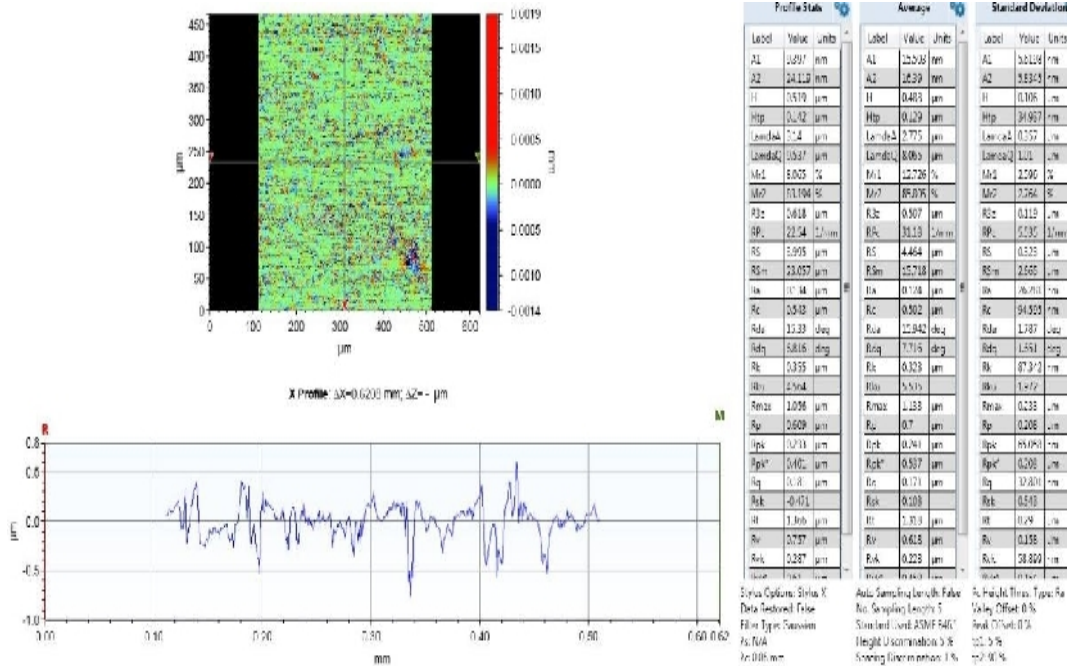


C-2 Specific Grinding Energy Soft Steel

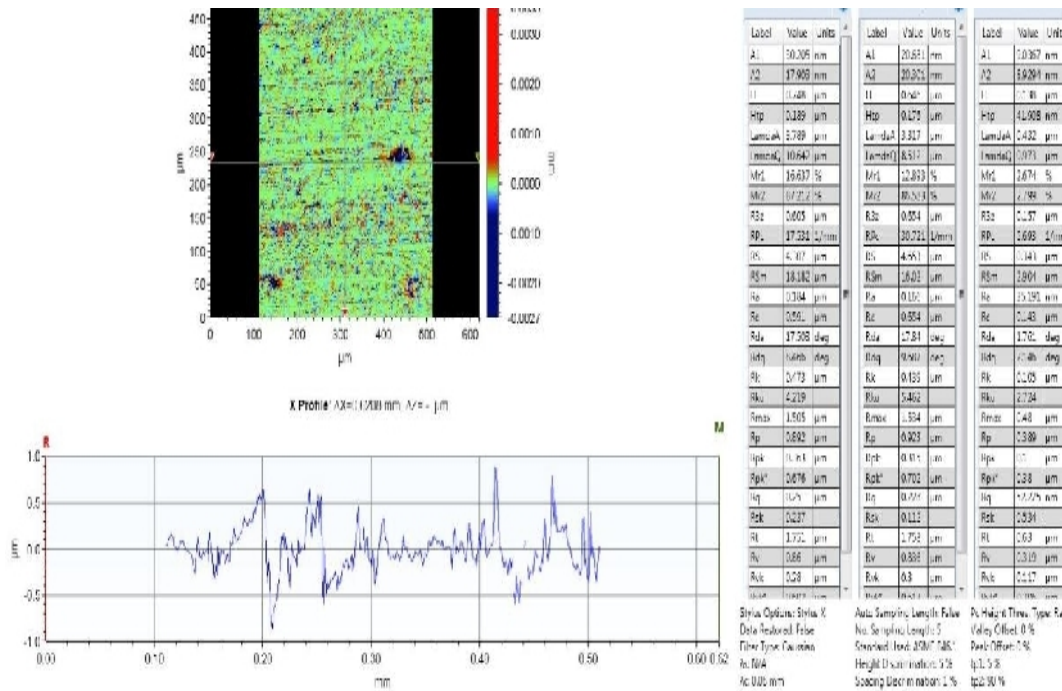


Appendices

A-1 10µm hard steel No Vibration

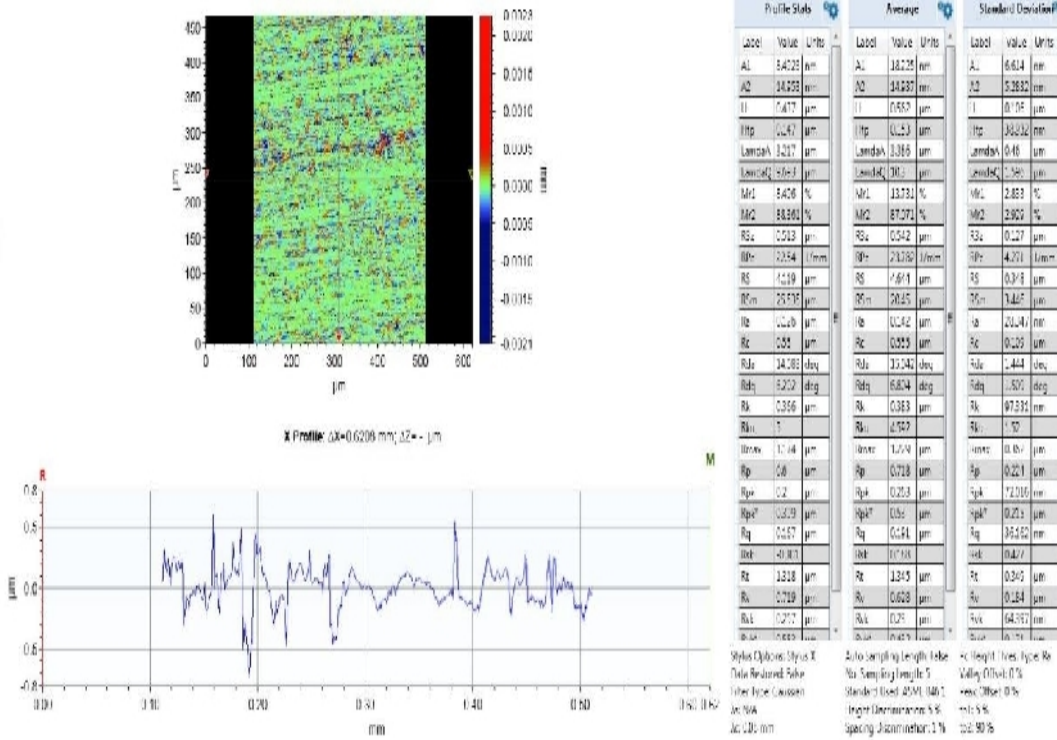


15 µm hard steel No Vibration

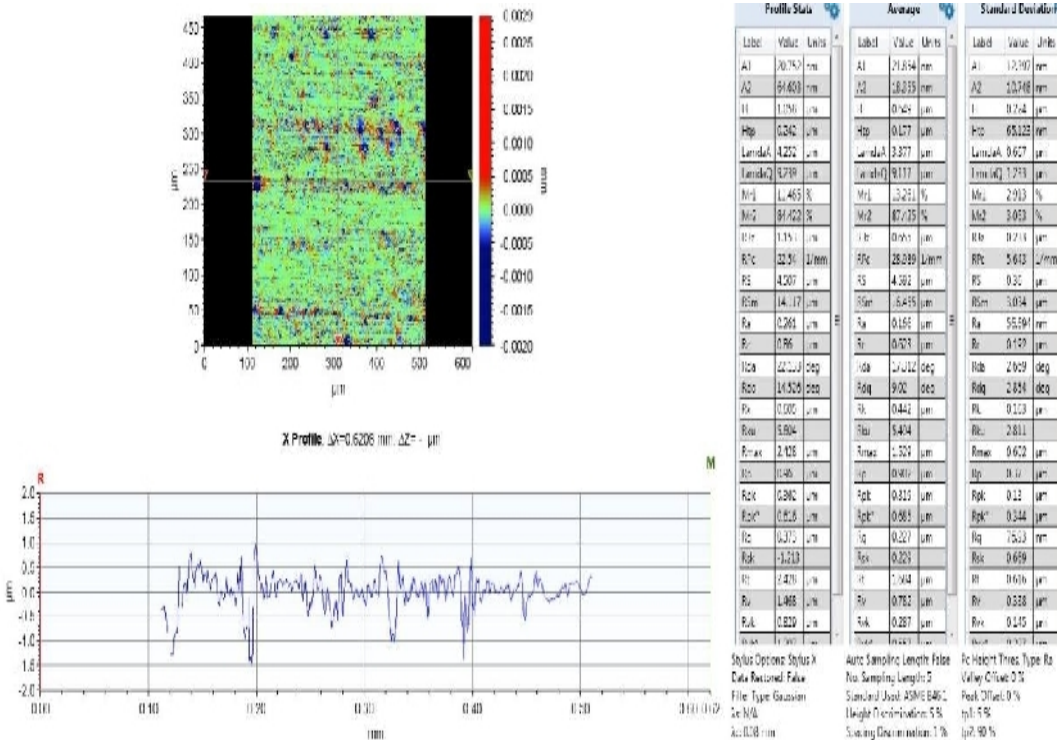


Appendices

20µm hard steel No Vibration

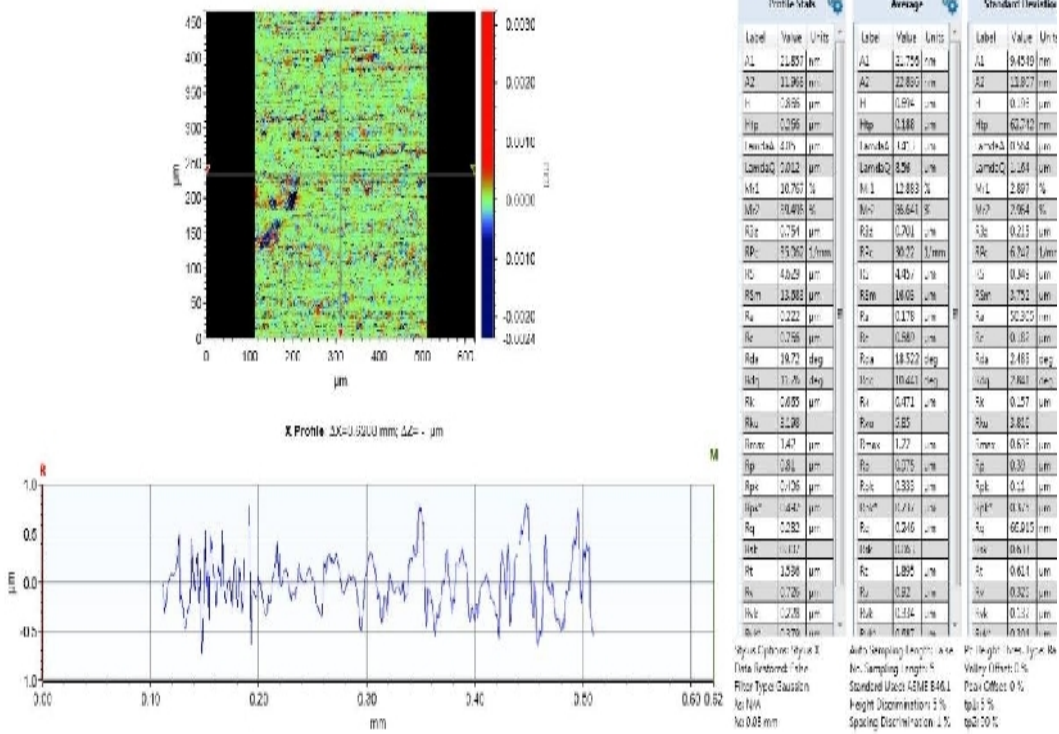


20µm hard steel No Vibration

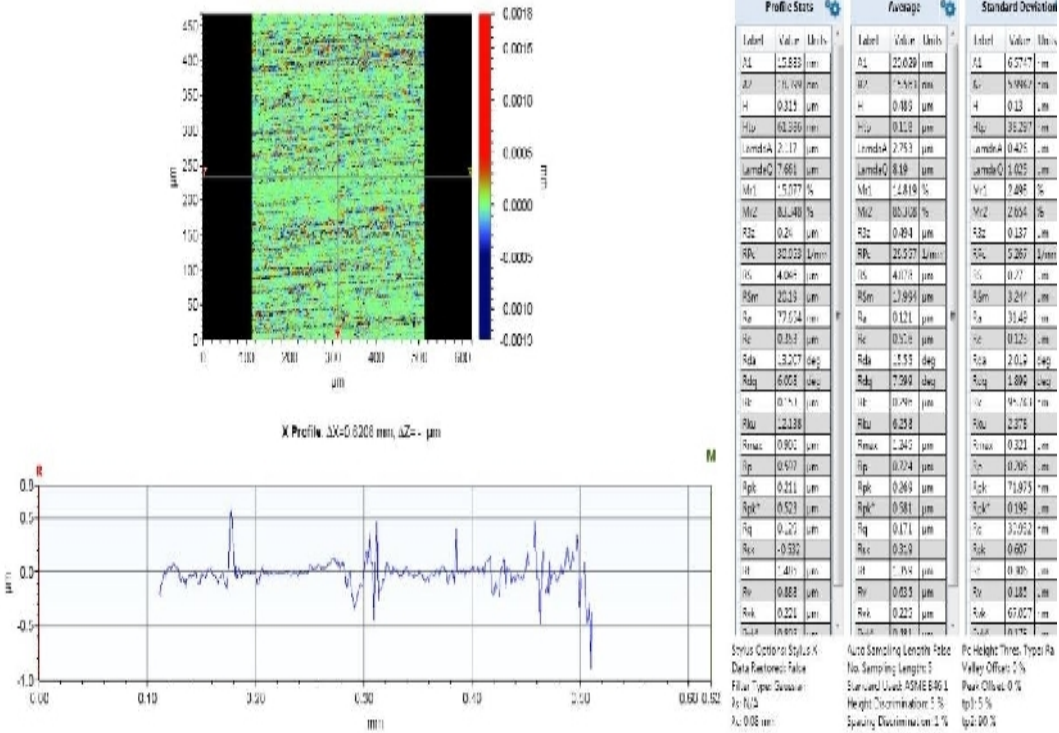


Appendices

30µm hard steel No Vibration

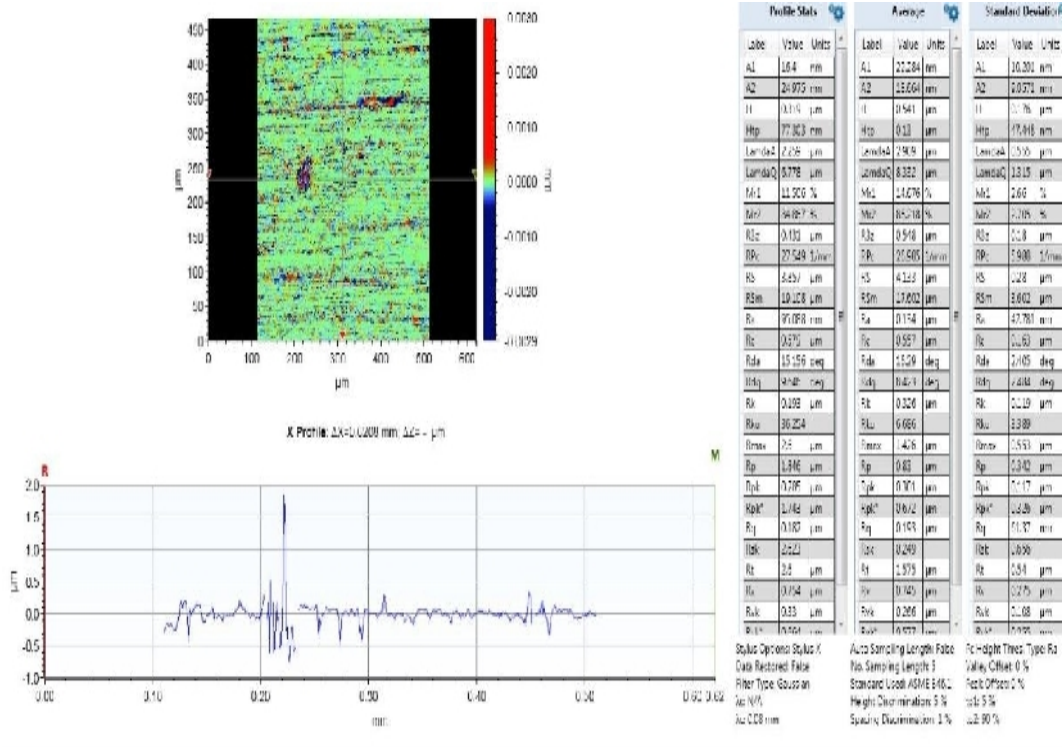


A-2 10 µm soft steel No Vibration

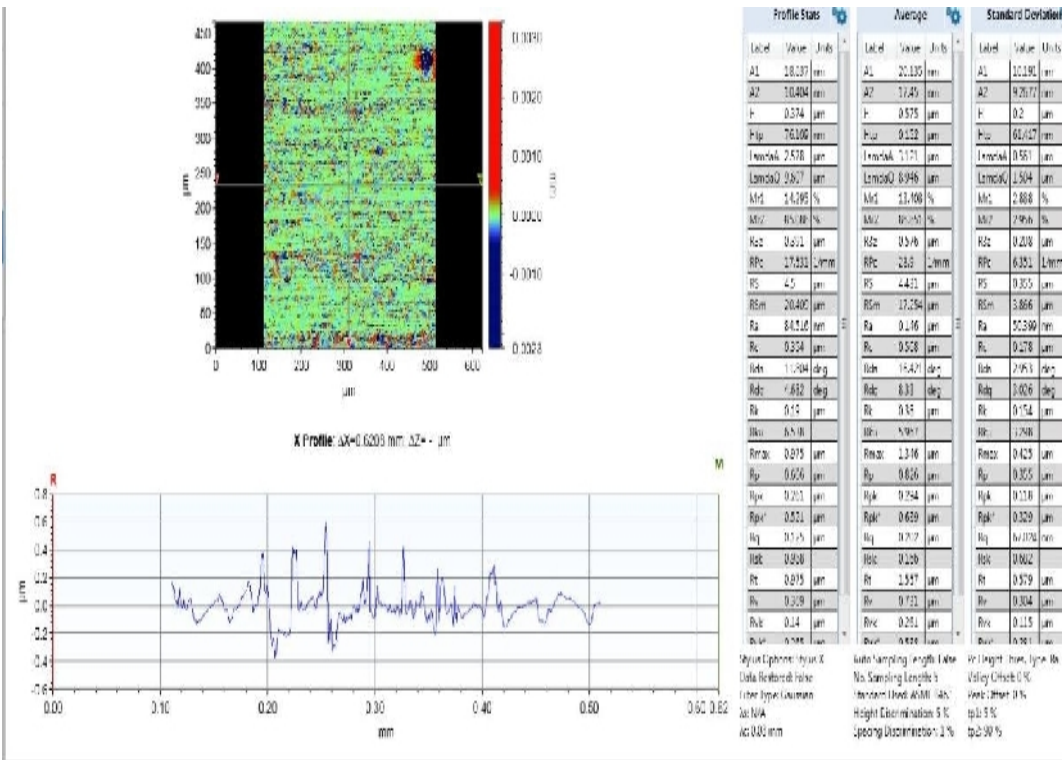


Appendices

15µm soft steel No Vibration

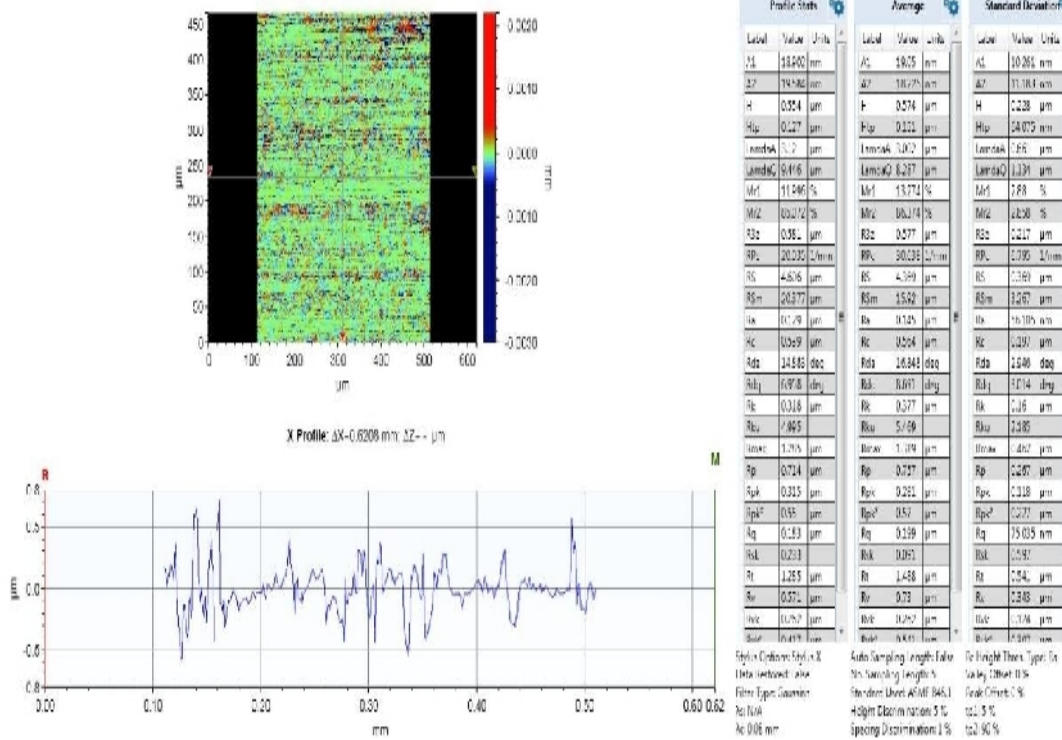


20µm soft steel No Vibration

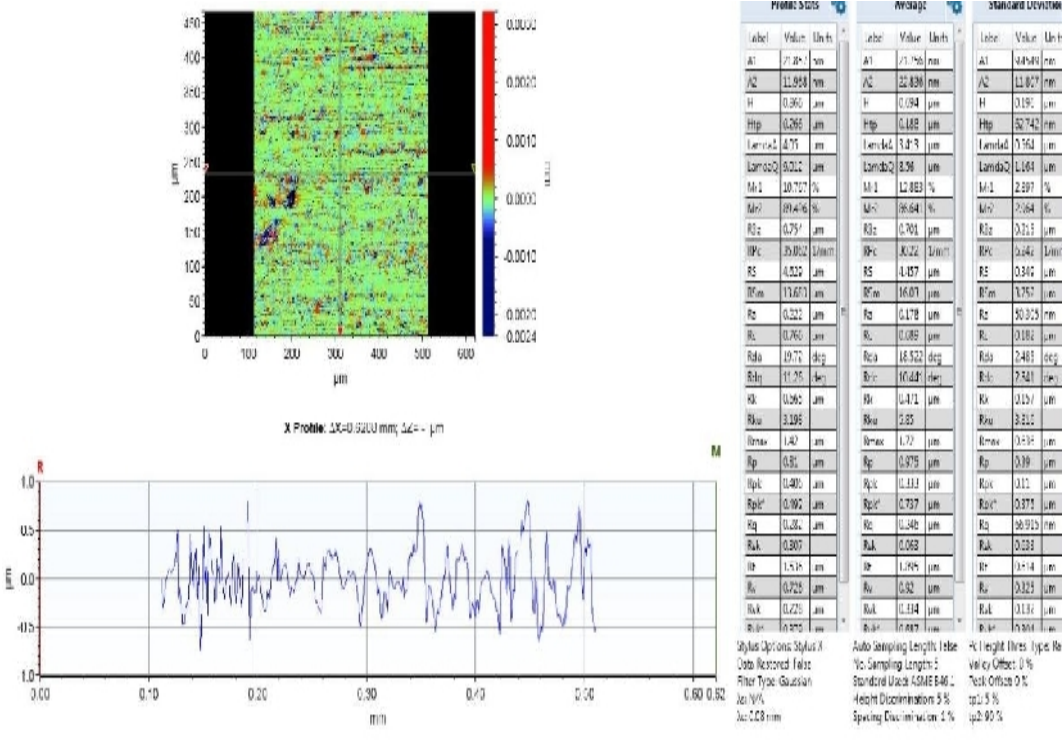


Appendices

25 µm soft steel No Vibration

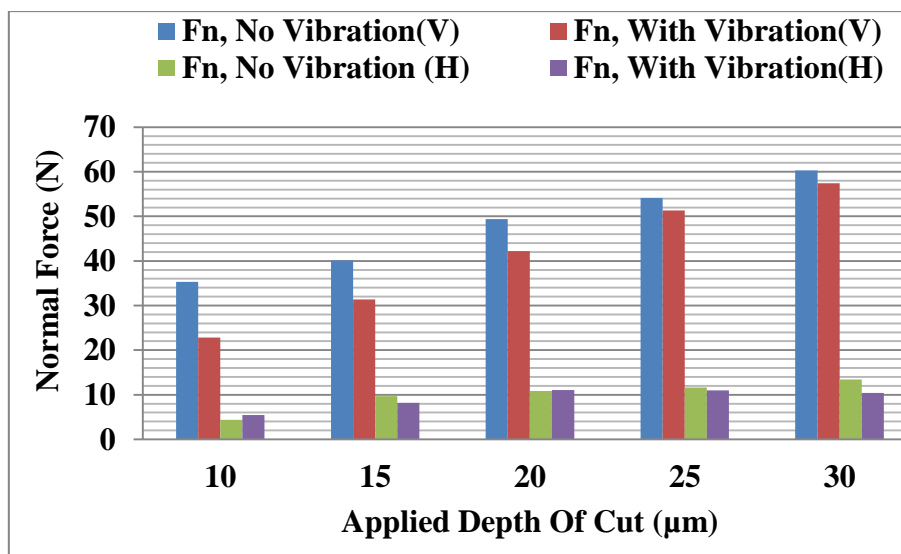
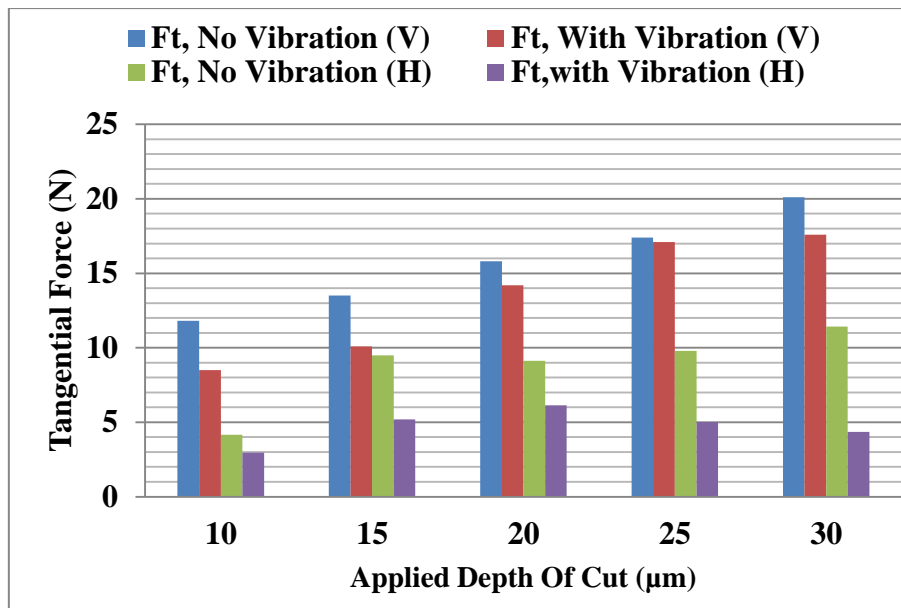


30µm soft steel No Vibration

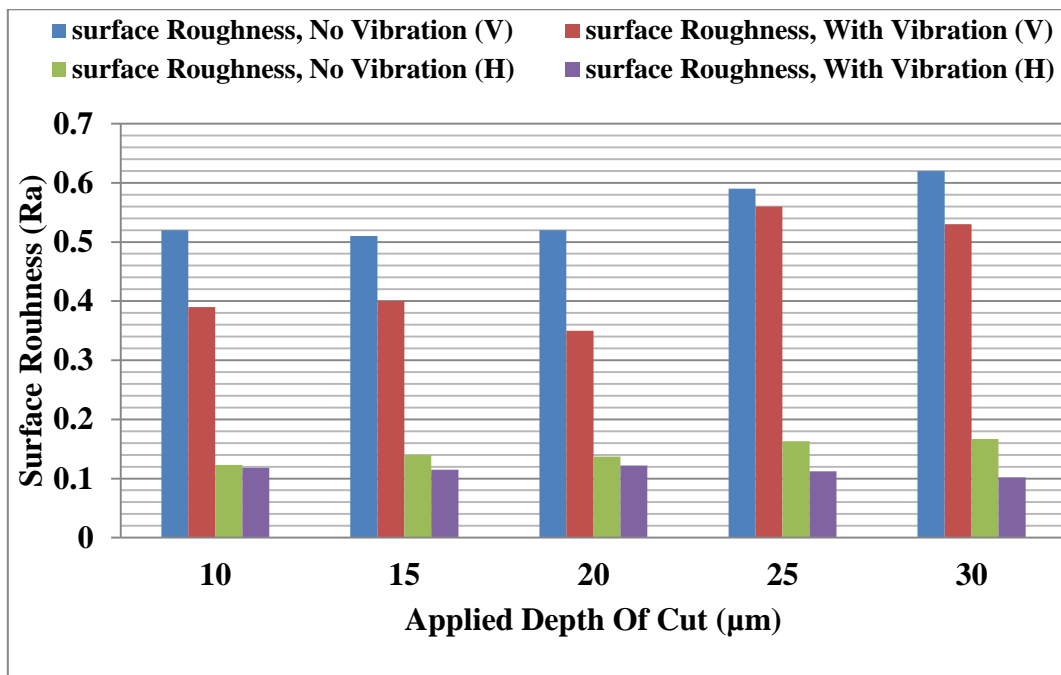
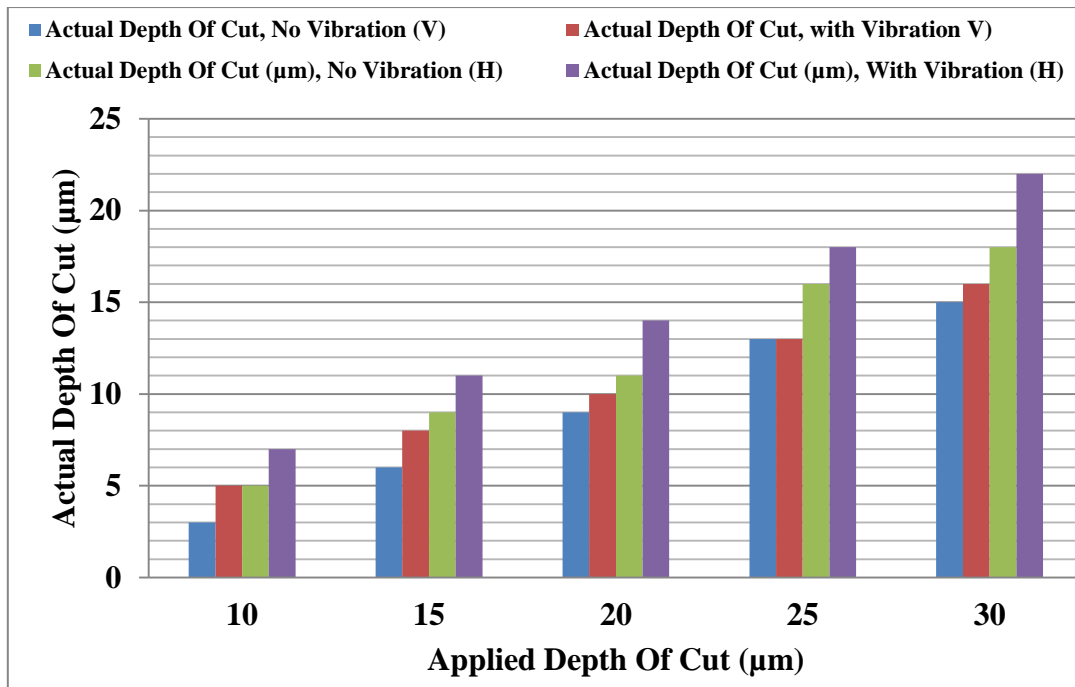


Appendices

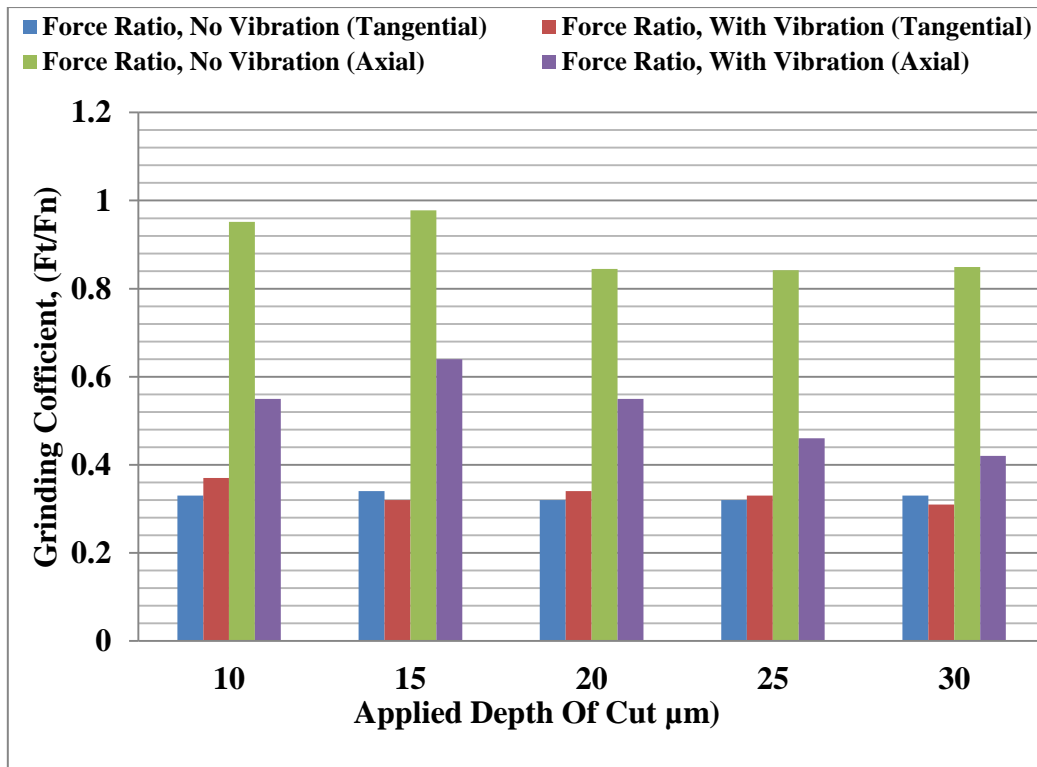
E-1 Comparing result (Tangential direction and axial direction)



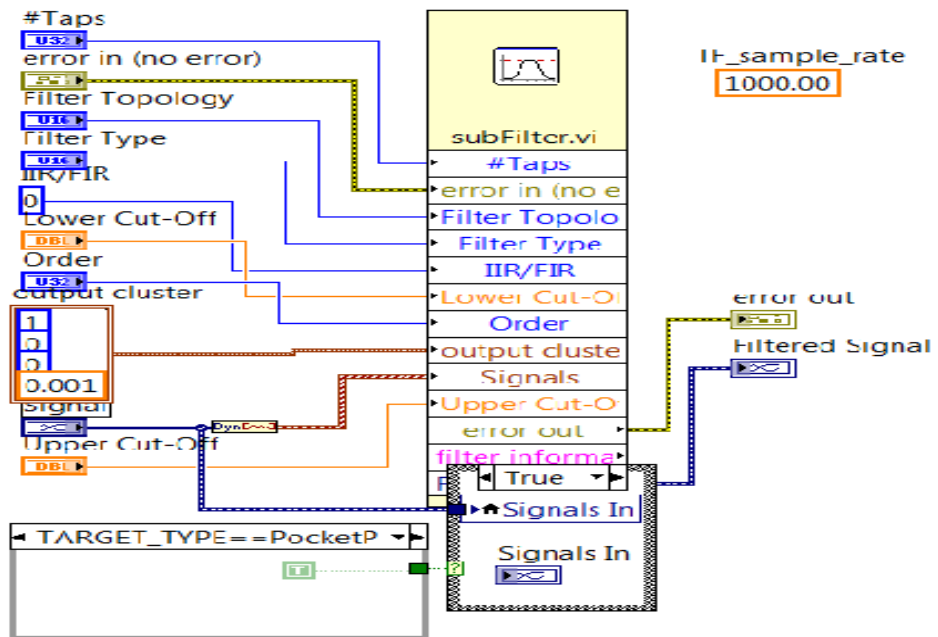
Appendices



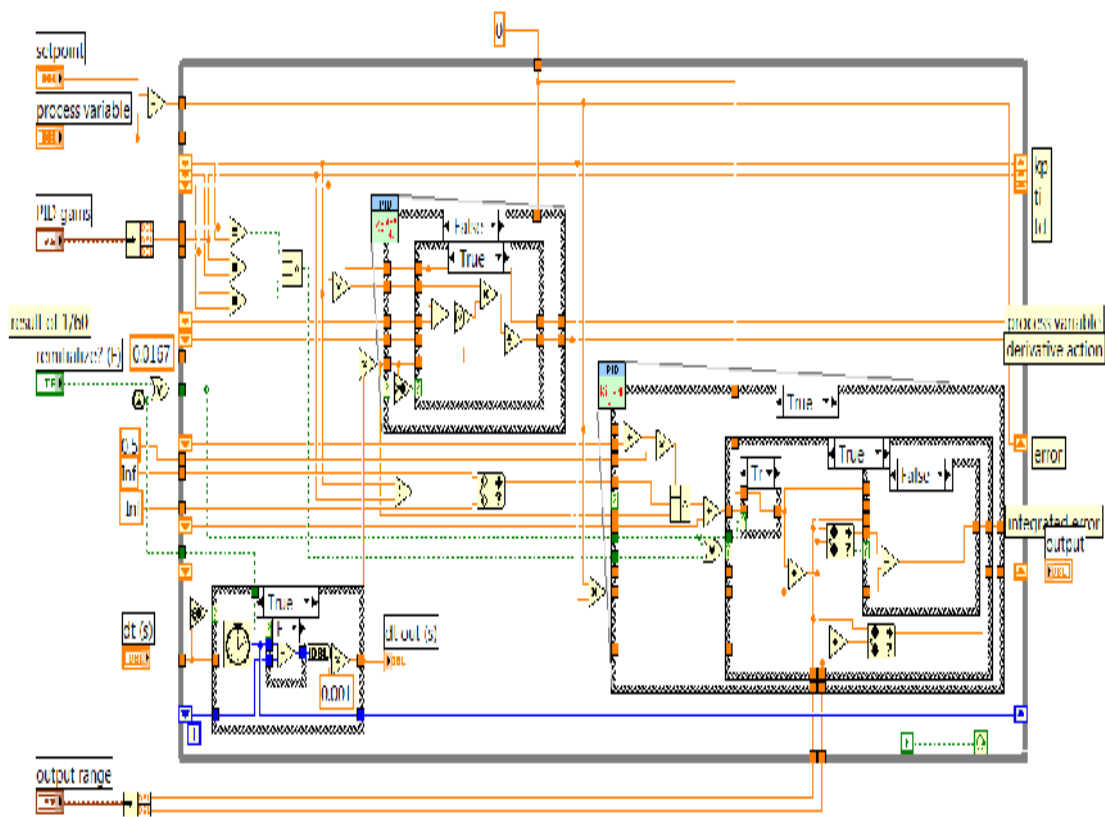
Appendices



F-3 Filter



F-4 PID Controller



Matlab Code

How to get the K_i and K_p from transfer function through the code:

```
clear all; close all; clc

% data = iddata(y,u,Ts);

% G = spa(data,[],w);

w = logspace(-1,1,100);w = w';

s = tf('s');

G = G=((-0.217*s)*(-5.656*s+38.86))/(s^2+992.5*s+3048); % change this to your
TF

[a b] = nyquist(G,w);

a = squeeze(a);

b = squeeze(b);

Gc = a+1j*b;

%w = squeeze(w);

%% ----- Parameter Space [choosing gain and
phase]

% -----Gain-----

gm = 10; %dB

M = -1/10^(gm/20);

phm = 0; %degree

Ph = (-180+phm); %Phase

A = sqrt(M^2/(1+(tand(Ph))^2));

B = A*tand(Ph);

C = A+1j*B;

%% ----- Gn Parameter Space

Kp = -real(C./Gc);
```

Appendices

```

Ki = w.*imag(C./Gc);

figure(1)

plot(Ki,Kp,'-o'); hold on

xlim([0 3])

ylim([0 6])

xlabel('ki')

ylabel('kp')

```

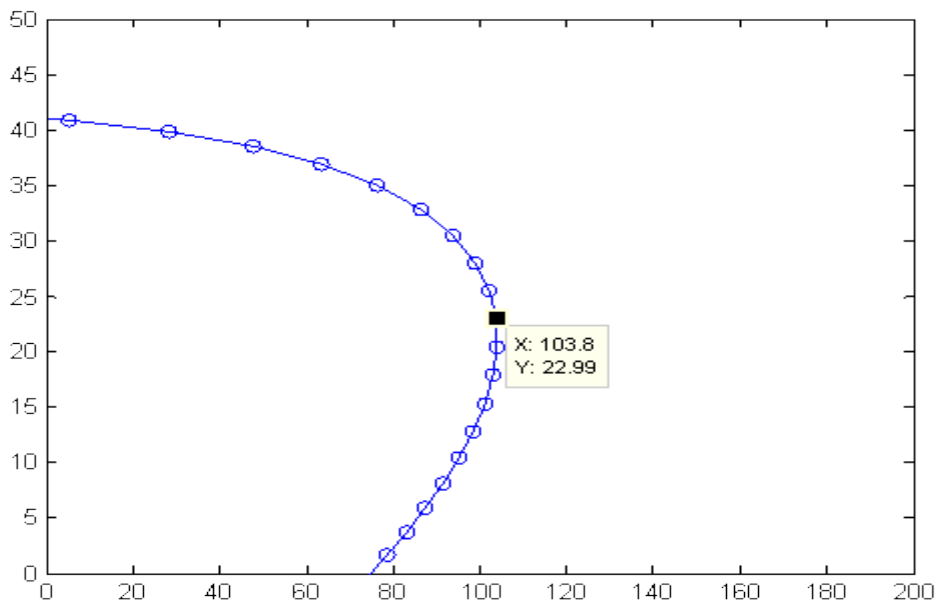
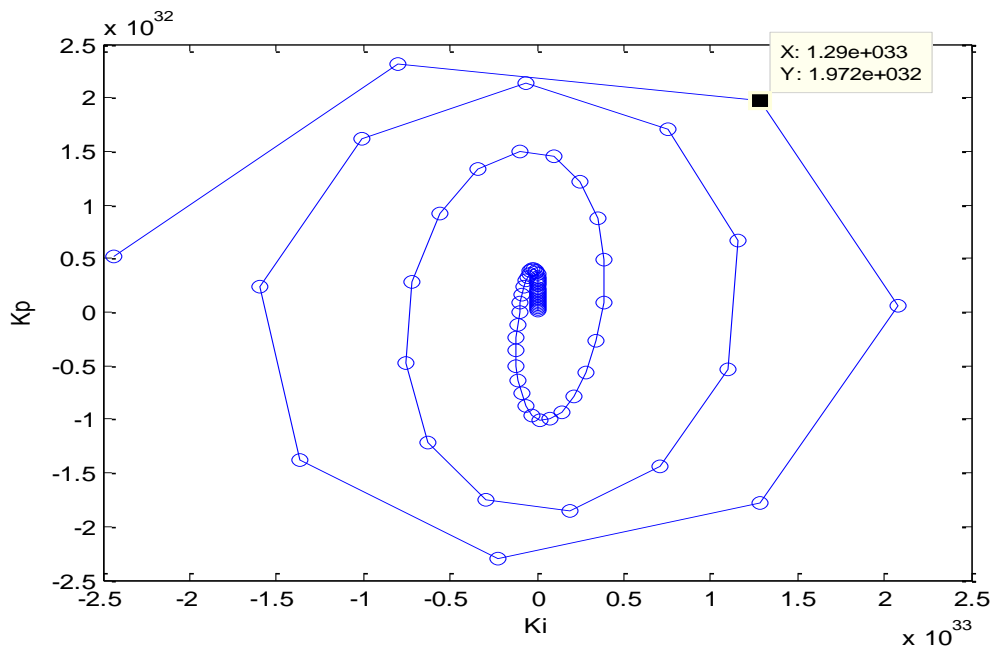
Nominator				dominator		
no	exp	S	Constant	S ²	S	Constant
1	-0.217	-5.656	38.86	1	992.5	3048
2	-2.49	25.13	0.1186	1	1004	3905
3	-3	0.05859	4.688 ⁻⁰⁰⁶	1	16.44	0.0006652
4	-0.286	3.728	0.3116	1	237.5	25.63
5	-0.228	0.6623	3.018	1	32.24	259.9
6	-1.98	31.77	2.019 ^{-e007}	1	1000	3.418 ^{e-005}
7	-0.28	-0.8758	372.4	1	761.1	3.973 ^{e004}
8	-0.288	3.272	1.656	1	349.1	127.7
9	-1.02	11.53	10.84	1	185.7	1702
10	-0.228	0.6623	3.018	1	32.24	259.9
11	-0.0871	0.4548	17.04	1	153.4	453.1
12	-0.0438	0.7199	116	1	174.5	6878
13	-2.9	19.62	-1.856	1	1000	0.09177
14	-18.87	0.655	0.1059	1	35.47	27.64

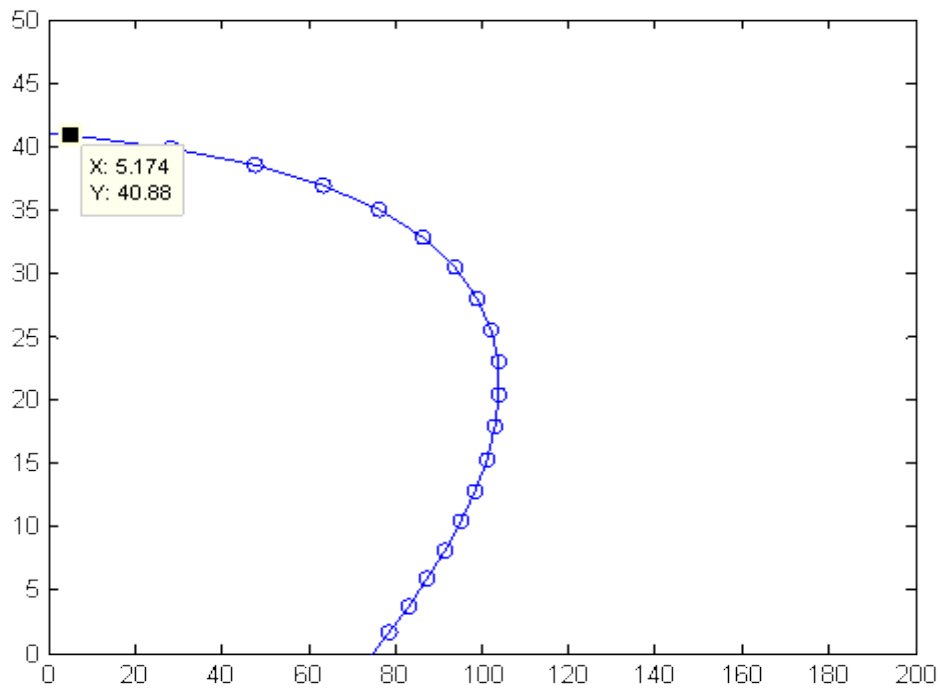
Appendices

Nominator

dominator

	Exp	S	Constant	S ²	S	Constant
Min	-18.87	-5.656	-1.856	1	16.44	0.30000418
mean	-2.28	6.517	40.108	1	42.672.8	4.679.5
Max	-0.0438	31.77	372.4	1	1004	3905





How to get the parameters for the controller from the phase margin and gain margin:

```
clear all; close all; clc

filename = '200hz_40m_soft_steel.xls';

u = xlsread(filename,1,'E3:E18002');
y = xlsread(filename,1,'F3:F18002');
t = xlsread(filename,1,'A3:A18002');

F = 100; % Hz

figure(1)

plot(t(1:100),u(1:100));

hold on

plot(t(1:100),y(1:100),'r')

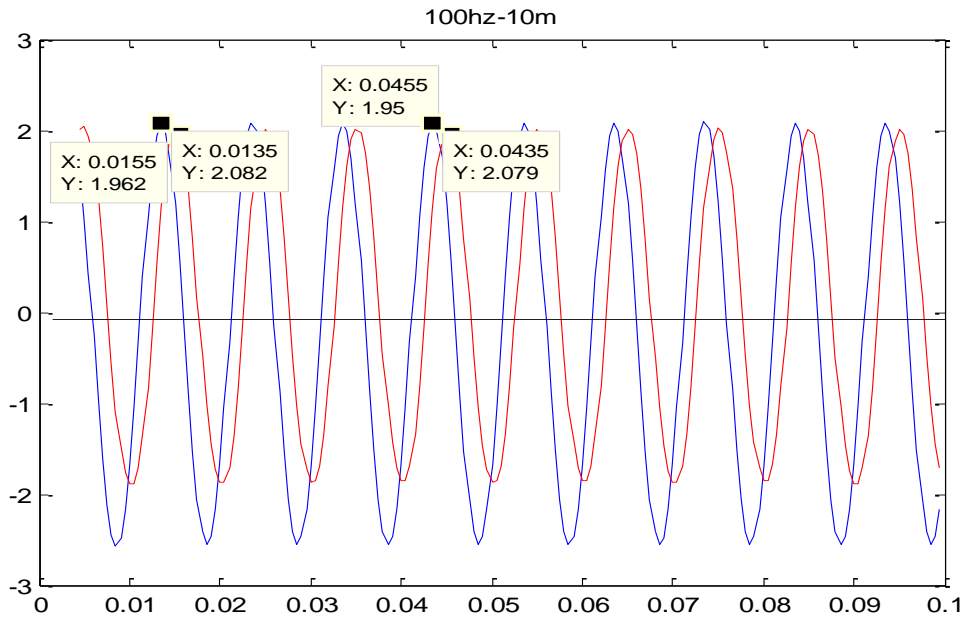
A = max(abs(y(1:100)))/max(abs(u(1:100)));

[~,Ity] = findpeaks(y(1:100));

[~,Itu] = findpeaks(u(1:100));

ph = F*mean(diff(t(Ity))) - mean(diff(t(Itu))); % rad
```

Appendices



Data Number	Phase value	Amp Value	Phase man
100hz10m	0.99	0.7916	0.0015
100hz15m	0.99	0.7813	0.0015
100hz20m	0.9775	0.8079	0.0015
100hz25m	1.0026	0.8006	0.0015
100hz30m	0.9901	0.7948	0.0015

```

close all; clear all; clc

t = 0:0.01:5;

w = 5;

ph = pi/2;

A1 = 1;

A2 = 2;

S1 = A1*sin(w*t);

S2 = A2*sin(w*t+ph);

plot(t,S1,'linewidth',2); hold on

plot(t,S2,'r','linewidth',2)

xlabel('x')

ylabel('y')

```

Appendices

Amp	Phase (s)	Phase (Degree)
100 Hz		
0.7916	-0.0016	-57.6
0.7813	-0.0016	-57.6
0.8079	-0.0016	-57.6
0.8006	-0.0016	-57.6
0.7993	-0.0016	-57.6
150 Hz		
Amp	Phase (s)	Phase (Degree)
13.5539	-0.0271	-(1463.4) = -23.4
19.54	-0.0391	-(2111.4) = -311.4
20.6742	-0.093	-(5022) = -342
21.1377	-0.0211	-(1139.4) = -59.4
22.0908	-0.0221	-(1193.4) = -113.4
250 Hz		
Amp	Phase (s)	Phase (Degree)
7.2874	-0.0291	-(2619) = -99
7.9494	-0.0318	-(2862) = -18
7.3181	-0.0293	-(2637) = -117
7.2874	-0.0291	-(2619) = -99

Appendices

```
close all; clear all; clc

ph1 = 2*pi*100.*[-0.0016; -0.0016; -0.0016; -0.0016; -0.0016];% rad
ph2 = 2*pi*150.*[-0.0271; -0.0391; -0.093; -0.0211; -0.0221];
ph3 = 2*pi*250.*[-0.0291; -0.0318; -0.0293; -0.0291];

A1 = [0.7916; 0.7813; 0.8079; 0.8006; 0.7993];
A2 = [13.5539; 19.54; 20.6742; 21.1377; 22.0908];
A3 = [7.2874; 7.9494; 7.3181; 7.2874];

r1 = A1.*exp(1j*ph1);
r2 = A2.*exp(1j*ph2);
r3 = A3.*exp(1j*ph3);

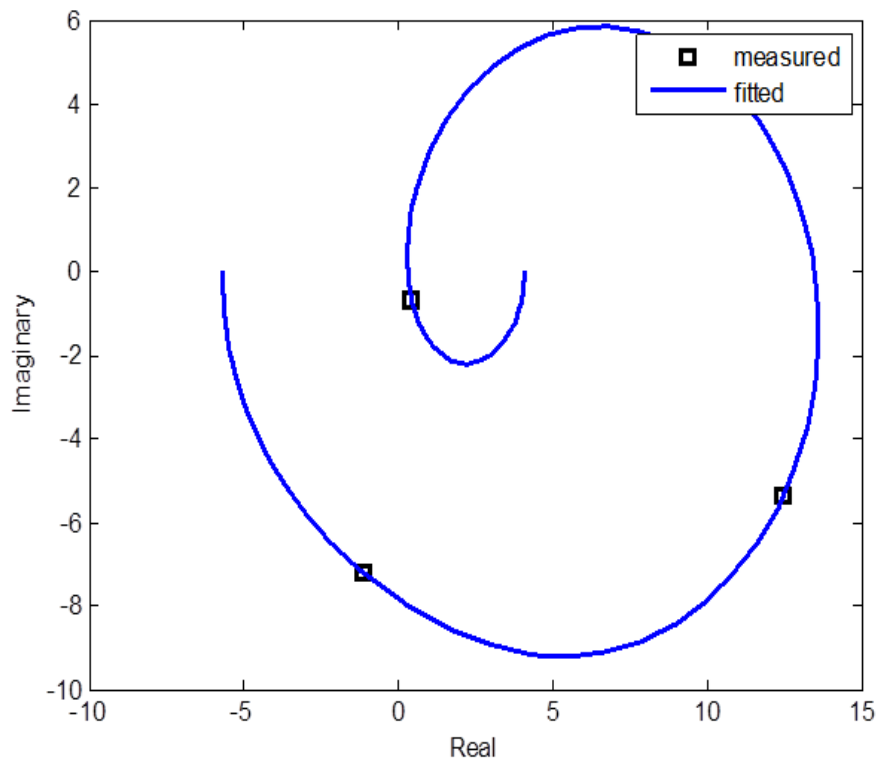
C1 = [r1(1);r2(1);r3(1)];
C2 = [r1(2);r2(2);r3(2)];
C3 = [r1(3);r2(3);r3(3)];

w = 2*pi.*[100; 150; 250];
[b1,a1] = invfreqs(C1,w,3,3,[],100);
G1 = tf(b1,a1);

[reG1, imG1] = nyquist(G1);
reG1 = squeeze(reG1);
imG1 = squeeze(imG1);
```

Appendices

```
figure(1)
plot(real(C1),imag(C1),'ks','Linewidth',2); hold on
plot(reG1,imG1,'-','Linewidth',2)
xlabel('Real')
ylabel('Imaginary')
legend('measured','fitted')
```



Equipment's

I. Power Amplifier E-472.2

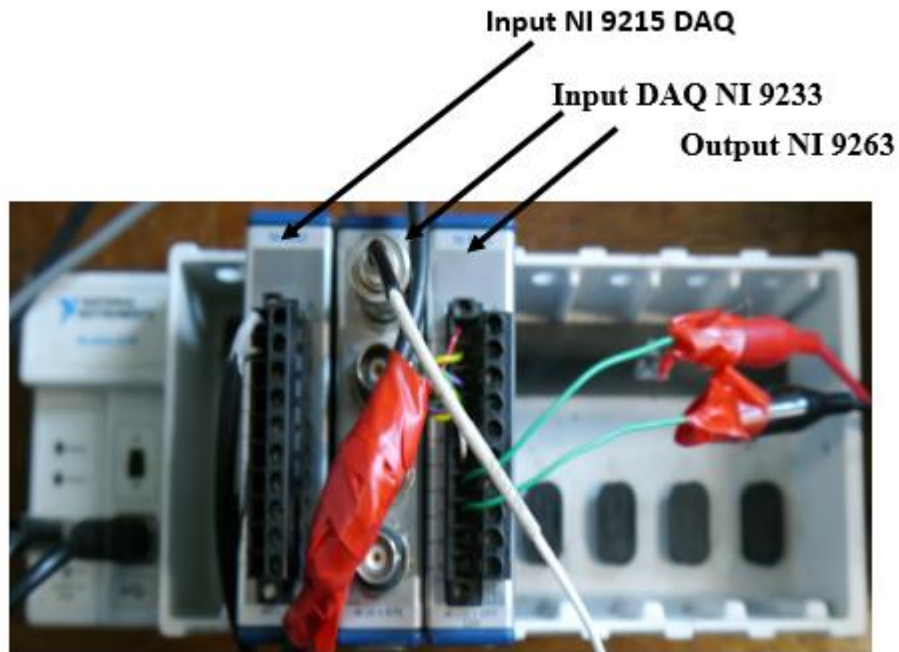


II. The Accelerometer A kistler 8704B100



Appendices

III. Input NI 9215 DAQ, Input DAQ NI 9233 and Output NI 9263 DAQ



IV. 3-axis Kistler 9257A Dynamometer



V. Kistler Charge Amplifier Type 5073



VI. Grinding Wheel



VII. Function Generators



VIII. Oscilloscope



IX. Bruker GTK surface texture system

